

STRATEGIES TO IMPROVE CARDIAC RESYNCHRONIZATION THERAPY

Wouter Maria van Everdingen

COLOFON

Financial support by the Dutch Heart Foundation (Hartstichting) and the Heart & Lung Foundation Utrecht for the publication of this thesis is gratefully acknowledged.

Moreover, financial support by CART-Tech B.V., Pfizer B.V., Abbott B.V., ChipSoft, Servier Nederland Farma B.V., CD Leycom / Cardiodynamics B.V., and Biotronik Nederland B.V. for the publication of this thesis is gratefully acknowledged.

Author:	Wouter Maria van Everdingen
Cover design and lay-out:	Miranda Dood, Mirakels Ontwerp
Printing:	Gildeprint – The Netherlands
ISBN:	978-90-9030775-6

A catalogue record is available from the Universiteit Utrecht.

© Wouter Maria van Everdingen, Utrecht, The Netherlands, 2018.

All rights reserved. No parts of this publication may be reproduced or transmitted in any form by any means, without permission of the author.

STRATEGIES TO IMPROVE CARDIAC RESYNCHRONIZATION THERAPY

STRATEGIEËN VOOR VERBETERING VAN
CARDIALE RESYNCHRONISATIE THERAPIE
(met een samenvatting in het Nederlands)

PROEFSCHRIFT

ter verkrijging van de graad van doctor aan
de Universiteit Utrecht op gezag van de rector magnificus,
prof. dr. G.J. van der Zwaan, ingevolge het besluit van het college
voor promoties in het openbaar te verdedigen op donderdag
15 februari 2018 des middags te 4.15 uur

door

Wouter Maria van Everdingen

geboren op 9 mei 1987 te Zevenaar

PROMOTOREN:

Prof. dr. P.A.F.M. Doevendans

Prof. dr. F.W. Prinzen

COPROMOTOREN:

Dr. M. Meine

Dr. M.J.M. Cramer

“Medical technology is like a racing bike, you need to fully understand its possibilities and limitations to climb a mountain without crashing.”

TABLE OF CONTENTS

CHAPTER 1 General introduction and outline of the thesis p.08

PART I MECHANICAL DYSSYNCHRONY

CHAPTER 2 Echocardiography and cardiac resynchronisation therapy, friends or foes? p.26

CHAPTER 3 Comparison of septal strain patterns in dyssynchronous heart failure between speckle tracking echocardiography vendor systems p.50

CHAPTER 4 Comparison of strain parameters in dyssynchronous heart failure between speckle tracking echocardiography vendor systems p.72

CHAPTER 5 Comparison of strain imaging techniques in CRT candidates: CMR tagging, CMR feature tracking and speckle tracking echocardiography p.106

CHAPTER 6 End-systolic septum strain: a multi-modality parameter that accurately predicts response in cardiac resynchronization therapy p.136

PART II RIGHT VENTRICULAR FUNCTION

CHAPTER 7 Combining computer modelling and cardiac imaging to understand right ventricular pump function p.172

CHAPTER 8 Echocardiographic prediction of cardiac resynchronization therapy response requires analysis of both mechanical dyssynchrony and right ventricular function p.192

PART III QUADRIPOLAR LEFT VENTRICULAR LEADS

CHAPTER 9	Quadripolar leads in cardiac resynchronization therapy – a review.	p.220
CHAPTER 10	Anodal capture with a quadripolar left ventricular lead	p.246
CHAPTER 11	Can we use the intrinsic left ventricular delay (QLV) to optimize the pacing configuration for cardiac resynchronization therapy with a quadripolar left ventricular lead?	p.252
CHAPTER 12	Pressure-volume loop analysis of multi-point pacing with a quadripolar left ventricular Lead in cardiac resynchronization therapy	p.278
CHAPTER 13	Optimization of the atrioventricular delay in CRT with quadripolar leads: should we optimize every LV pacing configuration and multi-point pacing?	p.300
CHAPTER 14	General discussion	p.318

APPENDIX

I	Nederlandse samenvatting	p.342
II	List of abbreviations	p.352
III	List of publications	p.356
IV	Dankwoord	p.358
V	Curriculum vitae	p.365



General introduction and outline of the thesis

1 GENERAL INTRODUCTION AND OUTLINE OF THE THESIS

In the current time frame, the development of (medical) technology exceeds the human mind. Medical technology has advanced our possibilities, but without proper knowledge of its function, its full potential cannot be utilized. A field of modern day medicine with technological developments at exhilarating rates is cardiology. This thesis focusses on the use cardiac resynchronization therapy (CRT) as a medical technology for patients with dyssynchronous heart failure. This thesis is meant to gain more insight in the possibilities to diagnose and treat patients with CRT. The first part focusses on quantification of mechanical dyssynchrony and discoordination observed in patients eligible for CRT. Furthermore, strategies to optimize CRT delivery are discussed, of which the relatively new quadripolar left ventricular (LV) leads has an important role in this thesis.

EPIDEMIOLOGY

Heart failure is a syndrome caused by abnormalities in cardiac structure and/or function. Heart failure is present in about 2-3% of the adult population, with an increasing prevalence in the population above 65 years.^{1, 2} Heart failure is also associated with significant mortality, morbidity, and healthcare expenditures, particularly in patients aged ≥ 65 years.² Although improving, survival estimates after diagnosis of heart failure are still 50% at 5 years and as low as 10% at 10 years,³ while LV dysfunction is associated with an increased risk of sudden death. In over a third of heart failure patients a conduction disorder may be present.⁴ Left bundle branch block (LBBB) and intraventricular conduction delay (IVCD) in particular are found in approximately 20-28% and 11-19% of patients respectively. LBBB and IVCD are more common with increasing age and are strong independent predictors of mortality.⁴ Conduction disorders like LBBB may develop due to heart failure or may even be causative to heart failure.⁵ New onset LBBB even has harmful effects on cardiac function and prognosis.⁶ LBBB is therefore an important therapeutic target in heart failure patients. This therapeutic target may be treated effectively with CRT.⁷ A considerable proportion of patients is found eligible for CRT, as a working group of the European Society of Cardiology recently estimated that at least 400 patients per million of the population might be suitable candidates for CRT.⁷

CARDIAC RESYNCHRONIZATION THERAPY

In LBBB, ventricular depolarization of the right ventricle (RV) occurs fast through the intact right bundle branch, while LV depolarization relies on slower myocardial cell-to-cell conduction. The delay in LV depolarization is largest in the LV free wall. The rapid activation of the RV and interventricular septum causes early contraction, which in combination with delayed LV free wall activation causes a dyssynchrony in myocardial contraction. Dyssynchrony is present between atria and ventricles (i.e. atrioventricular), between ventricles (i.e. interventricular) and within the LV (i.e. intraventricular). Dyssynchrony leads to an inefficient cardiac pump function and even to cardiac remodelling.⁸ Dyssynchrony may thereby cause heart failure or may worsen existing heart failure if developed later on. Dyssynchronous heart failure may be treated with CRT, an advanced device-based therapy for heart failure, with a pacemaker device (with or without a defibrillator function) connected to three implanted leads. Leads are implanted through the venous system, with one lead positioned in the right atrium, a second in the right ventricle and the latter on the LV free wall epicardium through a tributary vein of the cardiac venous system. The pacemaker device uses synchronized atrial and biventricular pacing to increase cardiac function of patients with LBBB. By resynchronizing electrical activation, CRT acutely improves cardiac function and may induce long-term reverse remodelling.⁹ Reverse remodelling is characterized as a gradual decrease of LV volume and improvement of LV function. The concept of CRT was first tested in 1994 and has since been thoroughly studied in large multicentre trials.¹⁰⁻¹² These multicentre trials have shown that CRT may induce reverse remodelling, improves exercise capacity, improves LV function, and reduces heart failure symptoms. Moreover, less hospitalizations for heart failure and an improvement in prognosis are seen in patients treated with CRT.^{10, 12} Despite these promising results, a considerable proportion (30-40%) of patients do not respond substantially.¹³ Non-response to CRT is seen on several levels, including no effect on hard outcome parameters such as morbidity, mortality, and hospitalizations, as well as in clinical outcome parameters such as absence of reverse remodelling or failure to improve in symptoms or NYHA-class. Non-response is multifactorial, due to selection of appropriate candidates, allocation of therapy, device implantation, device programming and patients' potential co-morbidities. Optimization of CRT may focus on three aspects: A) patient selection, B) device implantation, and C) device programming. All three aspects interact on the efficacy of CRT (figure 1).

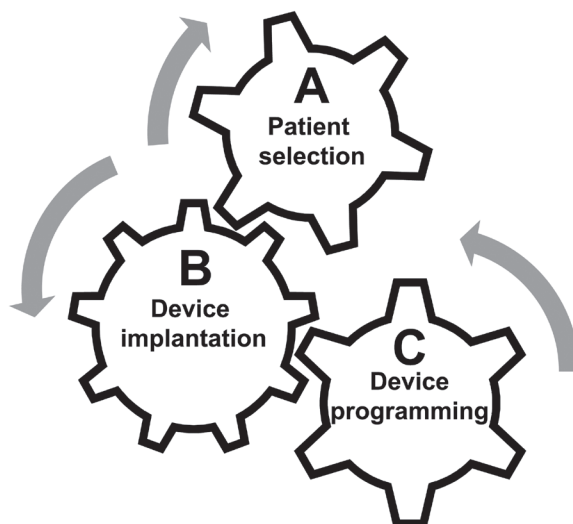


FIGURE 1. Interacting factors of response to cardiac resynchronization therapy

Interaction of factors influencing effectiveness of cardiac resynchronization therapy (CRT) are depicted. A) Patient selection, B) device implantation, and C) device programming all interact and are alterable factors to improve the therapeutic effect of CRT.

A) PATIENT SELECTION

Current international guidelines preclude CRT for patients with heart failure with symptoms according to New York Heart Association (NYHA) class II-IV, despite optimal pharmacological therapy.^{7, 14} The LV ejection fraction should be 35% or lower and QRS width ≥ 120 ms and preferably ≥ 150 ms with an LBBB.^{7, 14} While definition of a true LBBB is a topic of continuing debate,¹⁵ patients with LBBB benefit the most from CRT. Although patients with QRS-width ≥ 120 ms are still potential candidates, there is also a larger proportion of potential non-responders among them. Predicting response and non-response is therefore an area of interest. Prediction of response was the main aim of the MARC study, conducted in six medical centres in the Netherlands.¹⁶ The MARC study has recently proposed a score based on multiple patient characteristics to determine potential response to CRT.¹⁶ These patient characteristics included several criteria not yet included in the international guidelines, among which electrocardiographic (i.e. QRSarea) and echocardiographic criteria. The echocardiographic criteria are a continuing field of research in the UMC Utrecht, where echocardiographic parameters of dyssynchrony are thoroughly analysed.¹⁷⁻¹⁹

ASSESSMENT OF DYSSYNCHRONY AND DISCOORDINATION

As mentioned, the electrical substrate for CRT can be identified on the surface ECG, as an LBBB pattern or QRS width above 120ms. Although the electrical substrate is relative easily identified, cardiac mechanics are influenced by more than by electrical delay alone. Myocardial properties such as scar burden, contractility, LV dilatation and loading conditions, are relatively masked on an ECG. Some even suggest that these mechanical properties are as important as an electrical substrate.^{17, 20} Assessment of cardiac mechanics is still developing, with several indices as markers for mechanical dyssynchrony.²¹ The most promising parameters rely on myocardial deformation imaging. Deformation imaging is possible with several cardiac imaging modalities, such as echocardiography or magnetic resonance imaging (MRI). As no imaging based parameter has yet been incorporated in selection criteria for CRT, the search for the optimal deformation parameter continues.

DEFORMATION IMAGING

Myocardial deformation can be assessed using multiple parameters, which are based on either displacement, velocity or strain.²² The first two were used at the beginning of the era of deformation imaging, obtained from tissue Doppler recordings of myocardial contraction. Displacement and velocity of tissue does not directly translate to myocardial deformation, but assesses the motion caused by deformation. As both displacement and velocity may be affected by passive tethering or overall heart motion, they are not true deformation parameters. Displacement and velocity can however be used to measure strain and strain rate. Strain is the fractional change in length or thickness of a specific segment of myocardium, during a given time period. Strain is a dimensionless unit, expressed as the percentage of its original length. Strain is generally provided by the Lagrangian formula: $L_t = (L_t - L_0) / L_0$, in which L_0 is the length at onset and L_t the length at a given time point. Strain can be assessed with multiple techniques, including speckle tracking echocardiography, MRI tagging and MRI feature tracking. Three strain directions are commonly used; longitudinal (i.e. deformation from base to apex), circumferential (i.e. deformation in the short-axis plane) and radial strain (i.e. deformation caused by wall thickening). Specific parameters may be obtained from strain curves, of which longitudinal and circumferential strain curves were used in this thesis.

SPECKLE TRACKING ECHOCARDIOGRAPHY

Speckle tracking echocardiography uses the specific grey scale speckle pattern of standard B-mode images to detect myocardial deformation.²² The speckle pattern is caused by interference of local acoustic backscatter and is unique for each myocardial region. As the speckle pattern of small areas are fairly stable throughout the cardiac cycle, they can be 'tracked' during different cardiac phases. Specific speckle tracking software algorithms quantify the relative displacement between speckles and thereby quantify strain. Speckle tracking is relatively angle-independent and can be tracked in multiple directions on the two-dimensional imaging plane. Several software packages to quantify myocardial strain exist, which are specific to the manufacturer of the ultrasound machine

MRI TAGGING AND FEATURE TRACKING

MRI is a more comprehensive imaging technique compared to echocardiography, and is increasingly used in cardiology. Beside detailed information on viability through late gadolinium enhancement, cardiac dimensions, MRI may also lend information on cardiac deformation. Deformation may be obtained with specialized imaging protocols, which create tag lines across the myocardium.²³ Tag lines are created by modulation of the magnetization gradient, nulling the myocardium in a grid pattern prior to the onset of image acquisition. Contracting areas of myocardium causes the grid pattern to deform throughout the cardiac cycle. This deformation can be assessed with dedicated software algorithms to assess myocardial strain in multiple directions. Another MRI-based approach is feature tracking, which partly resembles speckle tracking echocardiography as it uses standard imaging acquisitions and tracks specific myocardial features for deformation analysis.²⁴ Feature tracking can be applied on routine cine images and relies on the recognition of specific patterns or 'features' in the image to be tracked and followed in the successive images. The deformation of specific features can be used to determine myocardial strain.

PARAMETERS OF MECHANICAL DYSSYNCHRONY AND DISCOORDINATION

The strain curves produced by the abovementioned imaging techniques may be analysed to quantify dyssynchrony or discoordination. Commonly, dyssynchrony is defined by differences in timing parameters while discoordination is based on percentage or fractions of inefficient stretching and shortening. Several dyssynchrony parameters, mainly obtained

with tissue Doppler imaging, were found unable to predict response to CRT in a large multi-centre trial, although positively tested in single centre studies.²⁵ Whether discoordination parameters may follow the same path remains to be seen, as single centre studies have so far been rather positive and a multicentre trial remains to be conducted.^{18, 26, 27} Discoordination is sensitive to myocardial viability and contractility, thereby incorporating important aspects of cardiac imaging. Whether these discoordination parameters remain (strong) predictors of CRT response when tested in combination with known (electrocardiographic) selection criteria for CRT, is an area of further research. The influence of the specific imaging technique and software package for strain analysis on these parameters of mechanical discoordination is also unknown. Multiple vendors have produced software packages capable of analysing myocardial strain. The influence of the vendor specific analysis on myocardial strain values is elucidated in the current thesis.

B) DEVICE IMPLANTATION

The effectiveness of cardiac resynchronization is influenced by the implantation of the CRT device and specifically its three leads. Especially the position of the LV lead is associated with response to CRT.^{28, 29} Using the conventional transvenous approach, LV lead positioning is limited by the coronary venous anatomy. The LV lead may be positioned in a tributary of the coronary sinus, overlying the LV epicardium. Its tip is wedged in a distal vein, and may be closer to the apex than desired, or positioned in or near myocardial fibrosis or close to the phrenic nerve. Pacing in or near myocardial fibrosis may lead to non-response,³⁰ while phrenic nerve capture leads to undesired chronic hiccups. Biventricular pacing with a suboptimal LV lead position may hamper successful resynchronization, as not all myocardial tissue is recruited to improve cardiac function. Unsuccessful resynchronization may therefore lead to non-response. Achieving an optimal LV lead position during CRT implantation is of importance. There are alternative implantation techniques to improve the LV lead position. The LV lead may be placed endocardial or epicardial with a transthoracic approach. A third option has become the new standard for LV lead placement, using a quadripolar LV lead. This type of lead has four electrodes on the distal end, spaced several centimetres, while conventional bipolar LV leads only have two electrodes positioned closely together at the tip of the lead. The additional electrodes offer more pacing sites than conventional bipolar LV leads. Additional electrodes may be positioned closer to the optimal pacing area, further from scar tissue and/or the phrenic nerve. The effect of implementing quadripolar leads on

1 success of CRT is of recent interest. Multiple studies have been performed with quadripolar leads and found positive hemodynamic and functional effects, which are elucidated in this thesis. Due to the inherent limitations of these studies, we have conducted a multicentre study to assess the optimization of CRT with a quadripolar lead: the Opticare-QLV study.

C) DEVICE PROGRAMMING

After implantation of the CRT device, resynchronization may be achieved by synchronized atrial sensing or pacing (dependent on the heart rhythm) followed by biventricular pacing. Resynchronization is achieved by implemented pacing delays between atrial and ventricular events; the atrioventricular (AV) delay, and between ventricular events: the interventricular (VV) delay. The AV delay should be early enough to guarantee biventricular pacing before depolarization by intrinsic conduction, while optimizing atrioventricular filling. The VV delay may be adjusted to facilitate optimal resynchronization and improve cardiac function. Both delays are known to influence acute hemodynamic response to CRT,³¹ while long-term effects of optimization are less clear.³² Besides optimization of the pacing delays, one may choose the specific pacing configuration of a quadripolar electrode. As mentioned, results of studies on CRT with quadripolar LV leads have been positive. However, a proficient tool to select the optimal configuration and pacing site is lacking. Another novelty for CRT with quadripolar LV leads is the possibility of multi-point pacing (MPP). The principle behind MPP is that two pacing stimuli may create a faster and more homogeneous depolarization wave front, which may be especially beneficial in patients with myocardial scarring or fibrosis. However, experimental work has shown that pacing at multiple sites is only beneficial if a single site is suboptimal.³³ Several manufacturers have implemented algorithms which facilitate two pacing stimuli from a single quadripolar lead. These stimuli may be delivered directly after each other (5ms), or with a programmable delay. Studies on MPP have so far been fairly positive, although patients may respond differently on the algorithm.³⁴⁻³⁶

ASSESSMENT OF CARDIAC FUNCTION

Increasing response to CRT, whether related to device implantation or device optimization, requires a reliable parameter indicating changes in effect. This effect may be measured acutely or after a period of potential reverse remodelling. While the coupling between the acute and long-term effect of CRT is relatively unknown, a study on assessment of cardiac

stroke work through invasive pressure-volume loops has shown a fair correlation with reverse remodelling measured by echocardiography.³⁷ Therefore, pressure-volume loops might be a good indicator for long-term benefit. Although previously used measurements of acute improvements, such as the maximal increase of pressure ($LV dp/dt_{max}$) are reproducible and relatively simple, they have no relation with long-term effect.^{38, 39} Pressure-volume loops give more physiological insight in the total cardiac cycle, and are moreover related with long-term response.³⁷ Pressure-volume loops require simultaneous recording of LV pressure and volume, which is possible with a dedicated conductance catheter with pressure sensor. The acquired data is plotted for the complete cardiac cycle, generating a loop without a time dimension on either axis. The pressure-volume relationship for a single cardiac cycle is divided into four basic phases: ventricular filling (a), isovolumetric contraction (b), ejection (c), and isovolumetric relaxation (d) (figure 2). The surface of the loop is used to calculate the stroke work of the cardiac cycle.

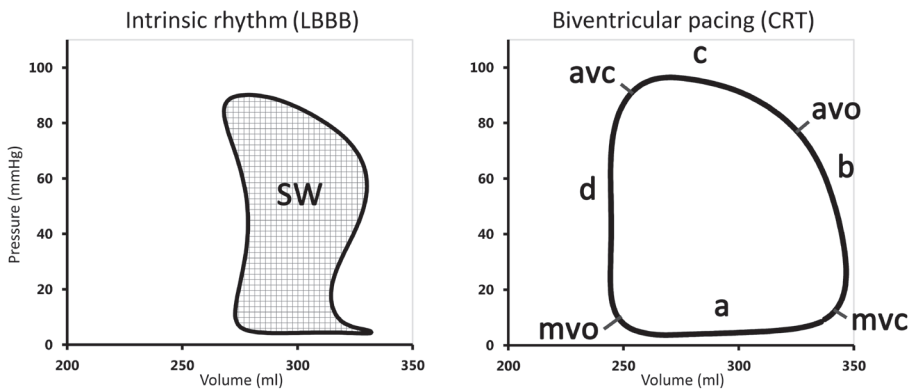


FIGURE 2. Examples of pressure-volume loops

Examples of pressure-volume (PV) loops, obtained in a patient with super response directly after cardiac resynchronization therapy device implantation. A PV loop during intrinsic rhythm is shown in the left panel, with the surface within the PV loop defined as stroke work (SW). During biventricular pacing (right panel) the PV loop size increases substantially. The four cardiac phases (a: ventricular filling, b: isovolumetric contraction, c: ejection, and d: isovolumetric relaxation) and valve states are depicted. CRT: cardiac resynchronization therapy, LBBB: left bundle branch block, SW: stroke work, avo: aortic valve opening, avc: aortic valve closure, mvo: mitral valve opening, mvc: mitral valve closure.

1

THESIS OUTLINE

Firstly, this thesis aims to improve our understanding of assessment of mechanical dyssynchrony and discoordination caused by an LBBB. Echocardiographic assessment plays an important role in CRT, however the incorporation of myocardial dyssynchrony and discoordination parameters in prediction of CRT remains challenging. The role of echocardiography in CRT is elucidated in **chapter 2**. **Chapter 3 and 4** encompass the comparison of different speckle tracking echocardiography software packages for assessment of dyssynchrony and discoordination. These software packages are used to analyse myocardial strain derived from echocardiographic images obtained of patients eligible for CRT. Different basic strain parameters as well as dyssynchrony and discoordination parameters are compared. We aim to improve our understanding in the effect of different software packages on assessment of mechanical dyssynchrony and discoordination in **chapter 3 and 4**. These parameters are also compared between strain analysis with speckle tracking echocardiography, MRI feature tracking and MRI tagging in **chapter 5**. The effect of the results of these techniques on CRT response prediction is investigated in **chapter 6**. These two chapters aim to compare mechanical dyssynchrony and discoordination parameters obtained with strain imaging techniques to gold-standard MRI tagging.

Secondly, the influence of the RV on mechanical dyssynchrony and CRT response is of interest. RV dysfunction is seen in a subgroup of CRT patients.⁴⁰ RV dysfunction may be caused by a primary RV disease, by backward failure or a combination of the two. Some studies suggest that RV dysfunction decreases response to CRT,^{41, 42} while a recent meta-analysis found no effect.⁴³ The RV is relatively difficult to image. The understanding of its anatomy, function and interaction with the LV may be improved by computer models. A review on the possibilities of computer models of the RV is given in **chapter 7**. One of these computer models, the CircAdapt model, is used to improve our understanding of RV dysfunction on mechanical dyssynchrony and CRT response in **chapter 8**. Using this computer model, we aimed to investigate the effect of RV dysfunction on the interaction and prediction of response to CRT with parameters of mechanical dyssynchrony.

The therapeutic options in for device implantation of CRT are constantly under development, with the recent introduction of quadripolar LV leads as an important milestone. Lastly, **chapter 9** of this thesis aims to extend our insights in the hemodynamic benefit of quadripolar LV leads in CRT. Potential benefits are mentioned, as well as available literature on the

benefits of these leads. An important phenomenon seen in other studies on LV pacing with a quadripolar LV lead is described in **chapter 10**, as anodal capture may complicate results of device optimization. In **chapter 11** we investigate the relation between (intra)ventricular conduction intervals and the hemodynamic effects of the four pacing sites of a quadripolar LV lead. The intrinsic LV conduction interval (“QLV”) is measured through simultaneous recording of the twelve-lead ECG and electrograms of the pacemaker leads. The aim of **chapter 11** was to associate the acute hemodynamic benefit analysed with pressure volume loops, measured with an invasive conductance catheter with QLV and the anatomical position of the electrodes of a quadripolar LV lead. Another optimization strategy for CRT arising from quadripolar LV leads is MPP. Although recent studies on MPP are rather positive, there are important limitations in the study designs. We aim to make a fair comparison of MPP with optimized biventricular pacing with a quadripolar LV lead in **chapter 12**. In order to do so, we compared all possible electrodes to multiple MPP settings, after optimization of the AV delay. The effect of MPP is also investigated in specific subgroups, to determine factors associated with benefit of MPP. In **chapter 13**, the effect of AV delay optimization in patients with CRT and a quadripolar LV lead is explored. There are several algorithms available to determine the optimal AV delay, however the physiologic basis is often lacking. We aim to associate parameters of atrioventricular conduction intervals with acute hemodynamic response measured by PV loops to determine the optimal AV delay.

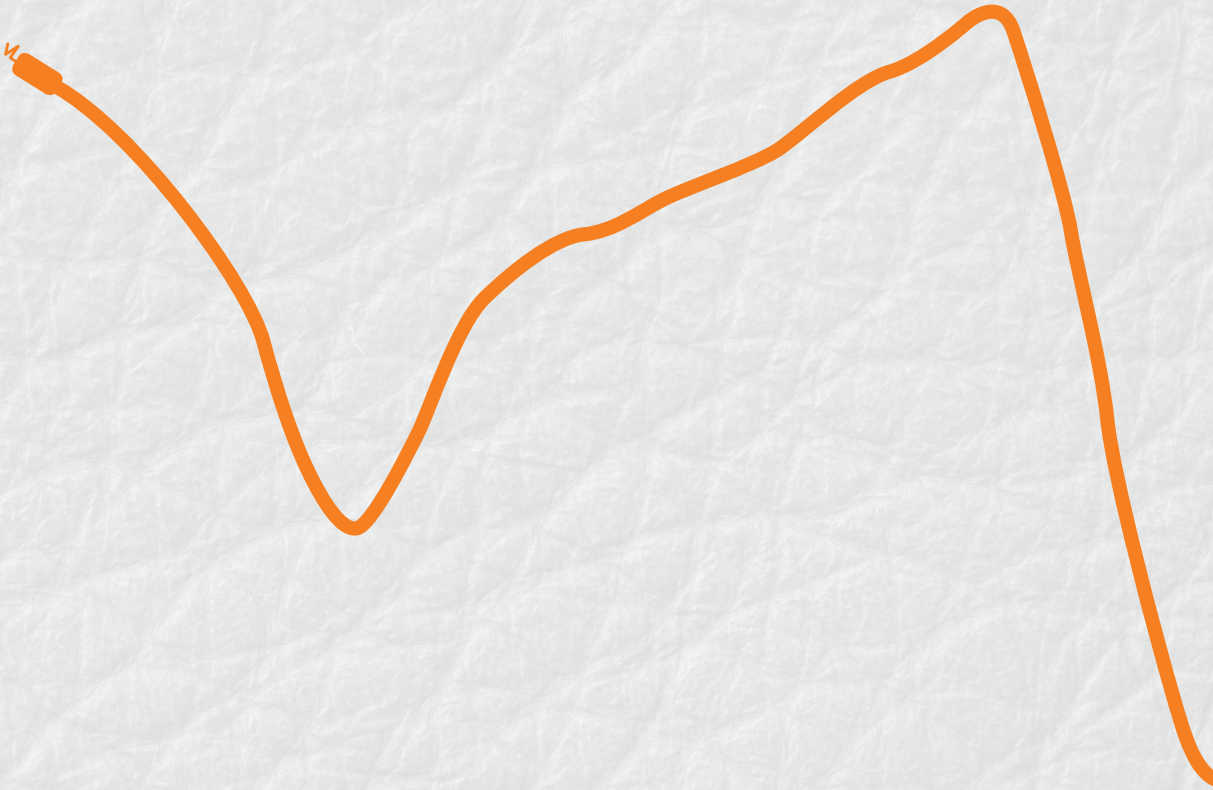
REFERENCES

1. van Riet EE, Hoes AW, Wagenaar KP, Limburg A, Landman MA, Rutten FH. Epidemiology of heart failure: the prevalence of heart failure and ventricular dysfunction in older adults over time. A systematic review. *Eur J Heart Fail.* 2016;18:242-52.
2. Roger VL. Epidemiology of heart failure. *Circulation research.* 2013;113:646-59.
3. Mosterd A, Cost B, Hoes AW, de Bruijne MC, Deckers JW, Hofman A, et al. The prognosis of heart failure in the general population: The Rotterdam Study. *Eur Heart J.* 2001;22:1318-27.
4. Lund LH, Benson L, Stahlberg M, Braunschweig F, Edner M, Dahlstrom U, et al. Age, prognostic impact of QRS prolongation and left bundle branch block, and utilization of cardiac resynchronization therapy: findings from 14,713 patients in the Swedish Heart Failure Registry. *Eur J Heart Fail.* 2014;16:1073-81.
5. Schneider JF, Thomas HE, Jr., Kreger BE, McNamara PM, Kannel WB. Newly acquired left bundle-branch block: the Framingham study. *Ann Intern Med.* 1979;90:303-10.
6. Regueiro A, Abdul-Jawad Altisent O, Del Trigo M, Campelo-Parada F, Puri R, Urena M, et al. Impact of New-Onset Left Bundle Branch Block and Periprocedural Permanent Pacemaker Implantation on Clinical Outcomes in Patients Undergoing Transcatheter Aortic Valve Replacement: A Systematic Review and Meta-Analysis. *Circ Cardiovasc Interv.* 2016;9:e003635.
7. Brignole M, Auricchio A, Baron-Esquivias G, Bordachar P, Boriani G, Breithardt OA, et al. 2013 ESC Guidelines on cardiac pacing and cardiac resynchronization therapy. *Eur Heart J.* 2013;34:2281-2329.
8. Prinzen FW, Vernooy K, De Boeck BW, Delhaas T. Mechano-energetics of the asynchronous and resynchronized heart. *Heart Fail Rev.* 2011;16:215-24.
9. Bakker PF, Meijburg HW, de Vries JW, Mower MM, Thomas AC, Hull ML, et al. Biventricular pacing in end-stage heart failure improves functional capacity and left ventricular function. *J Interv Card Electrophysiol.* 2000;4:395-404.
10. Ghio S, Freemantle N, Scelsi L, Serio A, Magrini G, Pasotti M, et al. Long-term left ventricular reverse remodelling with cardiac resynchronization therapy: results from the CARE-HF trial. *Eur J Heart Fail.* 2009;11:480-8.
11. Cleland JG, Daubert JC, Erdmann E, Freemantle N, Gras D, Kappenberger L, et al. The effect of cardiac resynchronization on morbidity and mortality in heart failure. *N Engl J Med.* 2005;352:1539-49.

12. Moss AJ, Hall WJ, Cannom DS, Klein H, Brown MW, Daubert JP, et al. Cardiac-resynchronization therapy for the prevention of heart-failure events. *N Engl J Med*. 2009;361:1329-38.
13. Daubert JC, Saxon L, Adamson PB, Auricchio A, Berger RD, Beshai JF, et al. 2012 EHRA/HRS expert consensus statement on cardiac resynchronization therapy in heart failure: implant and follow-up recommendations and management. *Europace*. 2012;14:1236-86.
14. Russo AM, Stainback RF, Bailey SR, Epstein AE, Heidenreich PA, Jessup M, et al. ACCF/HRS/AHA/ASE/HFSA/SCAI/SCCT/SCMR 2013 appropriate use criteria for implantable cardioverter-defibrillators and cardiac resynchronization therapy. *J Am Coll Cardiol*. 2013;61:1318-68.
15. Strauss DG, Selvester RH, Wagner GS. Defining left bundle branch block in the era of cardiac resynchronization therapy. *Am J Cardiol*. 2011;107:927-34.
16. Maass AH, Vernooy K, Wijers SC, van 't Sant J, Cramer MJ, Meine M, et al. Refining success of cardiac resynchronization therapy using a simple score predicting the amount of reverse ventricular remodelling: results from the Markers and Response to CRT (MARC) study. *Europace*. 2017.
17. Van't Sant J, Ter Horst IA, Wijers SC, Mast TP, Leenders GE, Doevendans PA, et al. Measurements of electrical and mechanical dyssynchrony are both essential to improve prediction of CRT response. *J Electrocardiol*. 2015;48:601-8.
18. Leenders GE, De Boeck BW, Teske AJ, Meine M, Bogaard MD, Prinzen FW, et al. Septal rebound stretch is a strong predictor of outcome after cardiac resynchronization therapy. *J Card Fail*. 2012;18:404-12.
19. De Boeck BW, Teske AJ, Meine M, Leenders GE, Cramer MJ, Prinzen FW, et al. Septal rebound stretch reflects the functional substrate to cardiac resynchronization therapy and predicts volumetric and neurohormonal response. *Eur J Heart Fail*. 2009;11:863-71.
20. Cleland J, Freemantle N, Ghio S, Fruhwald F, Shankar A, Marijanowski M, et al. Predicting the long-term effects of cardiac resynchronization therapy on mortality from baseline variables and the early response a report from the CARE-HF (Cardiac Resynchronization in Heart Failure) Trial. *J Am Coll Cardiol*. 2008;52:438-45.
21. Leenders GE, Cramer MJ, Bogaard MD, Meine M, Doevendans PA, De Boeck BW. Echocardiographic prediction of outcome after cardiac resynchronization therapy: conventional methods and recent developments. *Heart Fail Rev*. 2011;16:235-50.
22. Teske AJ, De Boeck BW, Melman PG, Sieswerda GT, Doevendans PA, Cramer MJ. Echocardiographic quantification of myocardial function using tissue deformation imaging, a guide to image acquisition and analysis using tissue Doppler and speckle tracking. *Cardiovasc Ultrasound*. 2007;5:27.

- 1
23. Prinzen FW, Hunter WC, Wyman BT, McVeigh ER. Mapping of regional myocardial strain and work during ventricular pacing: experimental study using magnetic resonance imaging tagging. *J Am Coll Cardiol.* 1999;33:1735-42.
 24. Pedrizzetti G, Claus P, Kilner PJ, Nagel E. Principles of cardiovascular magnetic resonance feature tracking and echocardiographic speckle tracking for informed clinical use. *J Cardiovasc Magn Reson.* 2016;18:51.
 25. Chung ES, Leon AR, Tavazzi L, Sun JP, Nihoyannopoulos P, Merlino J, et al. Results of the Predictors of Response to CRT (PROSPECT) trial. *Circulation.* 2008;117:2608-16.
 26. Leenders GE, Lumens J, Cramer MJ, De Boeck BW, Doevendans PA, Delhaas T, et al. Septal deformation patterns delineate mechanical dyssynchrony and regional differences in contractility: analysis of patient data using a computer model. *Circ Heart Fail.* 2012;5:87-96.
 27. Lumens J, Tayal B, Walmsley J, Delgado-Montero A, Huntjens PR, Schwartzman D, et al. Differentiating Electromechanical From Non-Electrical Substrates of Mechanical Discoordination to Identify Responders to Cardiac Resynchronization Therapy. *Circ Cardiovasc Imaging.* 2015;8:e003744.
 28. Kronborg MB, Johansen JB, Riahi S, Petersen HH, Haarbo J, Jorgensen OD, et al. An anterior left ventricular lead position is associated with increased mortality and non-response in cardiac resynchronization therapy. *Int J Cardiol.* 2016;222:157-62.
 29. Singh JP, Klein HU, Huang DT, Reek S, Kuniss M, Quesada A, et al. Left ventricular lead position and clinical outcome in the multicenter automatic defibrillator implantation trial-cardiac resynchronization therapy (MADIT-CRT) trial. *Circulation.* 2011;123:1159-66.
 30. Kydd AC, Khan FZ, Watson WD, Pugh PJ, Virdee MS, Dutka DP. Prognostic benefit of optimum left ventricular lead position in cardiac resynchronization therapy: follow-up of the TARGET Study Cohort (Targeted Left Ventricular Lead Placement to guide Cardiac Resynchronization Therapy). *JACC Heart Failure.* 2014;2:205-12.
 31. Bogaard MD, Meine M, Tuinenburg AE, Maskara B, Loh P, Doevendans PA. Cardiac resynchronization therapy beyond nominal settings: who needs individual programming of the atrioventricular and interventricular delay? *Europace.* 2012;14:1746-53.
 32. Auger D, Hoke U, Bax JJ, Boersma E, Delgado V. Effect of atrioventricular and ventriculoventricular delay optimization on clinical and echocardiographic outcomes of patients treated with cardiac resynchronization therapy: a meta-analysis. *Am Heart J.* 2013;166:20-9.

33. Ploux S, Strik M, van Hunnik A, van Middendorp L, Kuiper M, Prinzen FW. Acute electrical and hemodynamic effects of multisite left ventricular pacing for cardiac resynchronization therapy in the dyssynchronous canine heart. *Heart Rhythm*. 2014;11:119-25.
34. Sterlinski M, Sokal A, Lenarczyk R, Van Heuverswyn F, Rinaldi CA, Vanderheyden M, et al. In Heart Failure Patients with Left Bundle Branch Block Single Lead MultiSpot Left Ventricular Pacing Does Not Improve Acute Hemodynamic Response To Conventional Biventricular Pacing. A Multicenter Prospective, Interventional, Non-Randomized Study. *PloS one*. 2016;11:e0154024.
35. Zanon F, Baracca E, Pastore G, Marcantoni L, Fraccaro C, Lanza D, et al. Multipoint pacing by a left ventricular quadripolar lead improves the acute hemodynamic response to CRT compared with conventional biventricular pacing at any site. *Heart Rhythm*. 2015;12:975-81.
36. Thibault B, Dubuc M, Khairy P, Guerra PG, Macle L, Rivard L, et al. Acute haemodynamic comparison of multisite and biventricular pacing with a quadripolar left ventricular lead. *Europace*. 2013;15:984-91.
37. de Roest GJ, Allaart CP, Kleijn SA, Delnoy PP, Wu L, Hendriks ML, et al. Prediction of long-term outcome of cardiac resynchronization therapy by acute pressure-volume loop measurements. *Eur J Heart Fail*. 2013;15:299-307.
38. Duckett SG, Ginks M, Shetty AK, Bostock J, Gill JS, Hamid S, et al. Invasive acute hemodynamic response to guide left ventricular lead implantation predicts chronic remodeling in patients undergoing cardiac resynchronization therapy. *J Am Coll Cardiol*. 2011;58:1128-36.
39. Bogaard MD, Houthuijzen P, Bracke FA, Doevendans PA, Prinzen FW, Meine M, et al. Baseline left ventricular dP/dtmax rather than the acute improvement in dP/dtmax predicts clinical outcome in patients with cardiac resynchronization therapy. *Eur J Heart Fail*. 2011;13:1126-32.
40. Damy T, Ghio S, Rigby AS, Hittinger L, Jacobs S, Leyva F, et al. Interplay between right ventricular function and cardiac resynchronization therapy: an analysis of the CARE-HF trial (Cardiac Resynchronization-Heart Failure). *J Am Coll Cardiol*. 2013;61:2153-60.
41. Leong DP, Hoke U, Delgado V, Auger D, Witkowski T, Thijssen J, et al. Right ventricular function and survival following cardiac resynchronisation therapy. *Heart*. 2013;99:722-8.
42. Campbell P, Takeuchi M, Bourgoun M, Shah A, Foster E, Brown MW, et al. Right ventricular function, pulmonary pressure estimation, and clinical outcomes in cardiac resynchronization therapy. *Circ Heart Fail*. 2013;6:435-42.
43. Sharma A, Bax JJ, Vallakati A, Goel S, Lavie CJ, Kassotis J, et al. Meta-Analysis of the Relation of Baseline Right Ventricular Function to Response to Cardiac Resynchronization Therapy. *Am J Cardiol*. 2016;117:1315-21.



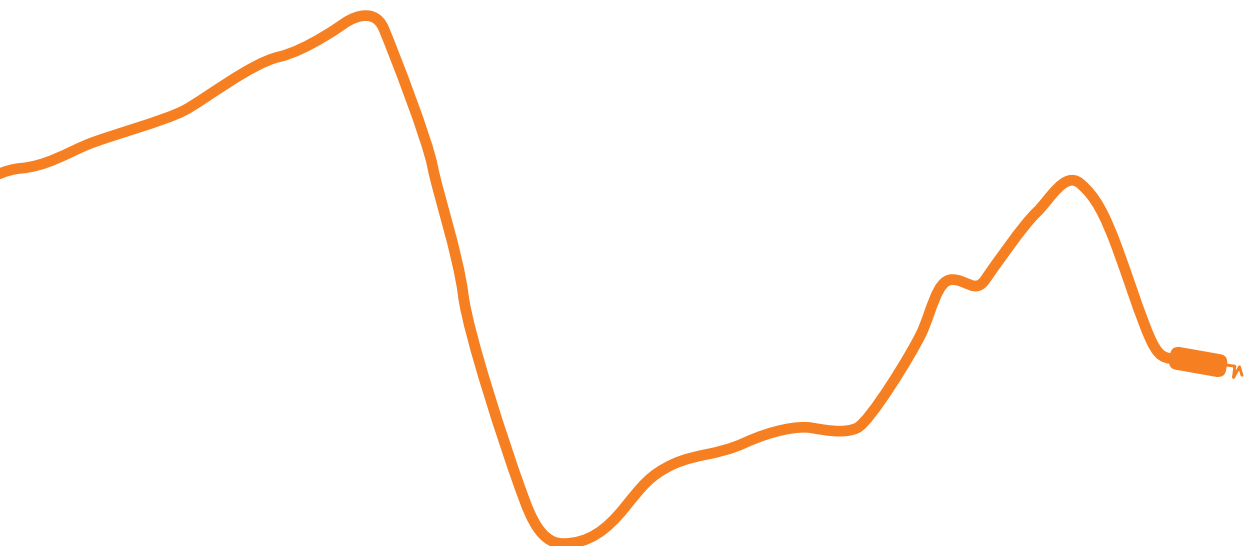
PART I

MECHANICAL DYSSYNCHRONY





Echocardiography and cardiac resynchronisation therapy: friends or foes?



Wouter M. van Everdingen (MD)¹, Jurjan C. Schippers (MD)¹,
Jetske van 't Sant (MD, PhD)¹, Karan Ramdat Misier¹,
Mathias Meine (MD PhD)¹, Maarten J. Cramer (MD, PhD)¹

¹ Department of Cardiology, University Medical Center Utrecht, Utrecht, The Netherlands

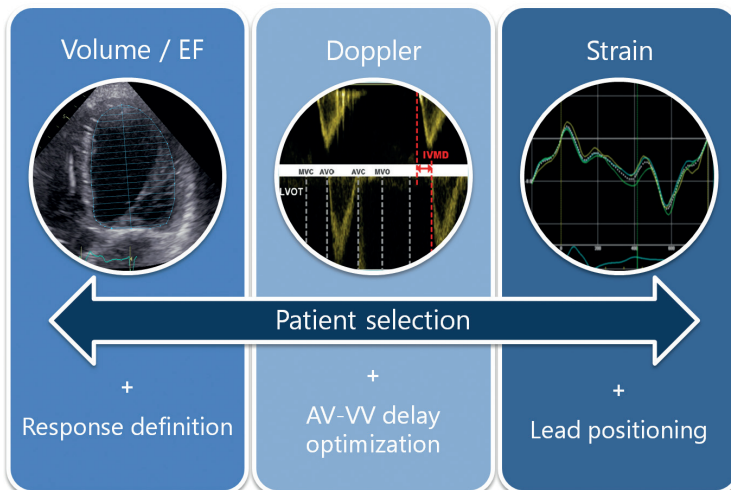
Netherlands Heart Journal, 2016 Jan;24(1):25-38

ABSTRACT

Echocardiography is used in cardiac resynchronisation therapy (CRT) to assess cardiac function, and in particular left ventricular (LV) volumetric status, and prediction of response. Despite its widespread applicability, LV volumes determined by echocardiography have inherent measurement errors, inter-observer and intra-observer variability, and discrepancies with the gold standard magnetic resonance imaging. Echocardiographic predictors of CRT response are based on mechanical dyssynchrony. However, parameters are mainly tested in single-centre studies or lack feasibility. Speckle tracking echocardiography can guide LV lead placement, improving volumetric response and clinical outcome by guiding lead positioning towards the latest contracting segment. Results on optimisation of CRT device settings using echocardiographic indices have so far been rather disappointing, as results suffer from noise. Defining response by echocardiography seems valid, although re-assessment after 6 months is advisable, as patients can show both continuous improvement as well as deterioration after the initial response. Three-dimensional echocardiography is interesting for future implications, as it can determine volume, dyssynchrony and viability in a single recording, although image quality needs to be adequate. Deformation patterns from the septum and the derived parameters are promising, although validation in a multicentre trial is required. We conclude that echocardiography has a pivotal role in CRT, although clinicians should know its shortcomings.

INTRODUCTION

Thus far, echocardiography has a pivotal role in cardiac resynchronisation therapy (CRT), underlined by the wide field of application, determining cardiac function and specifically left ventricular (LV) function and response due to desired reverse electro-mechanical remodelling. The range of tools, from brightness mode or Doppler imaging to deformation imaging, offers the possibility of patient selection and response prediction, lead placement optimisation strategies and optimisation of device configurations (central illustration).¹⁻³ Multiple single-centre studies have advocated the value of echocardiography in patient selection and determining prognosis.⁴⁻⁶ However, limitations are known, as the PROSPECT study showed a limited value regarding response prediction, and EchoCRT gave insight into the potential negative effects of echocardiographic parameters as selection criteria.^{3, 7} Moreover, echocardiography can have a relatively substantial measurement error and not every patient is suitable for adequate echocardiographic volume assessment, especially in non-expert hands.⁸ The question arises whether echocardiography is a useful imaging tool for evaluation of CRT patients, or are its shortcomings impeding clinical decision making? This review reflects on the role of echocardiography in the field of CRT, are they friends or foes?



CENTRAL ILLUSTRATION

Role of echocardiography in CRT. Echocardiography can be used to select patients by volume and subsequent ejection fraction assessment and by dyssynchrony parameters based on Doppler and/or strain analysis. Doppler can also optimise CRT settings, while strain analysis could support LV lead optimisation strategies.

PATIENT SELECTION

LEFT VENTRICULAR EJECTION FRACTION

Echocardiography gives insight into the cardiac anatomy and valvular dysfunction of CRT patients. Its main role in CRT is determining cardiac function and especially LV volumes and ejection fraction (LVEF). International guidelines on CRT define a cut-off for LVEF at $\leq 35\%$, independent of the imaging tool used.^{9,10} A meta-analysis of randomised trials on the effects of CRT on morbidity and mortality has underlined this cut-off. A reduced benefit or even adverse effect in patients with an LVEF above the cut-off was observed, although the large confidence interval might indicate that a subgroup of patients with LVEF $>35\%$ do benefit (hazard ratio for all-cause mortality: 0.28-2.00).¹¹ This could be due to an overestimation of LVEF by echocardiography. A sub-analysis of the PROSPECT study advocated the benefit of CRT in patients above the threshold.¹² The threshold for response to CRT is probably more a continuum than binary.

Although the biplane Simpson's method is the most robust method to determine LV volume and function for echocardiography, intraobserver and interobserver variability can be high, with reported differences in LVEF of up to 18% (Bland-Altman limits of agreement or two standard deviations).⁸ A study compared LVEF determined by a recruiting centre to an echocardiography core lab. The correlation coefficient was fair among 413 patients (R^2 : 0.69). A mean difference of 0.2% was found, although a wide confidence interval was observed (95% CI: -17.4-17.8%). Moreover, 20% of all patients would have been reclassified by another centre, using a cut-off for LVEF of 30%.¹³ These results underline the limitations of echocardiography for a strict cut-off, beside the need for core lab activities.

Volumes derived with echo are underestimated compared with 'gold standard' magnetic resonance imaging (MRI).^{14, 15} Nevertheless a meta-analysis found a mean difference between the two modalities of close to 0%, although a large spread and heterogeneity between studies was observed.⁸ Assessment of LVEF by MRI and echocardiography shows opposing results for CRT eligibility in 28% of patients, using the guideline cut-off. Compared with MRI, echocardiography underestimated both end-diastolic and end-systolic volume, while overestimating LVEF.¹⁵ As most large multicentre trials on the selection of patients for CRT used echocardiographic-derived volumes, cut-offs cannot be directly translated to other imaging techniques.

Averaging of several measured beats improves accuracy in general, and is applicable to all patients and specifically in atrial fibrillation. Contrast-enhanced echocardiography for volume assessment can further reduce intraobserver and interobserver variability.^{16, 17} An intravenous contrast agent can identify the endocardial borders more precisely. When used in either two- or three-dimensional echocardiography, LV volumes determined by contrast are also more similar (less underestimated) to MRI.¹⁶ Results on LVEF are conflicting, as both similar and improved correlations to MRI are reported using contrast-enhanced volumes compared with conventional echocardiography.¹⁶⁻¹⁸

Based on these findings, the cut-off for selection of patients eligible for CRT should depend on the imaging tool. Moreover, subgroups for LVEF 30–40% might be incorporated in future guidelines.¹² Patients with LVEF above the current cut-off, but with a true left bundle branch block (LBBB), might benefit from CRT. Implementation of subgroups, in concordance with the role of QRS width in current guidelines, may reflect the role of LVEF in CRT more appropriately. However, evidence supporting CRT in subgroups based on LVEF needs to be further established.

DYSSYNCHRONY

Selection criteria for patients eligible for CRT based on electrical or mechanical dyssynchrony show a preference for an electrical substrate.⁹ Correcting mechanical dyssynchrony without an electrical substrate has proven to be ineffective, as has been shown in large trials such as Echo CRT.⁷ Moreover, after PROSPECT, it remains debated whether mechanical dyssynchrony is warranted as an indicator for response to CRT, as the study design and applied dyssynchrony parameters are disputed.¹⁹ Guidelines have so far been restricted to clinical and electrocardiographic selection criteria (i.e. QRS width and LBBB morphology). As previously mentioned, imaging tools are strictly necessary to determine LVEF. Mechanical dyssynchrony proven by any echocardiographic parameter are not included in current guidelines. Patients with a class I indication (i.e. LBBB) will most certainly have a form of mechanical dyssynchrony when assessed by echo. Patients with a class III indication (i.e. QRS <120 ms) and with proven dyssynchrony are no better or even worse with CRT.^{7,20} The additional value of dyssynchrony parameters might be in the class IIa or b groups. In these groups, with prolonged QRS width (≥ 120 or ≥ 150 ms) and non-LBBB, visualised mechanical dyssynchrony could indicate a treatable substrate.

Mechanical dyssynchrony parameters (Table 1) should be based on a physiological principle, where early septal and delayed activation of the LV free wall causes disturbed LV intraventricular and interventricular interaction. An ideal parameter indicates a substrate that can be corrected by biventricular pacing. Prediction models for volumetric response (>15% decrease in end-systolic volume) advocate the use of mechanical dyssynchrony parameters, on top of existing criteria.^{21, 22} However, multicentre trials and meta-analysis have failed to show an added value of several dyssynchrony indices, although interventricular mechanical dyssynchrony (IVMD) was associated with increased survival in the CARE-HF study.^{3, 23, 24} Other parameters (systolic rebound stretch of the septum (SRS_{sept}), septal flash and apical rocking) are only proven in single-centre studies.^{4, 25, 26}

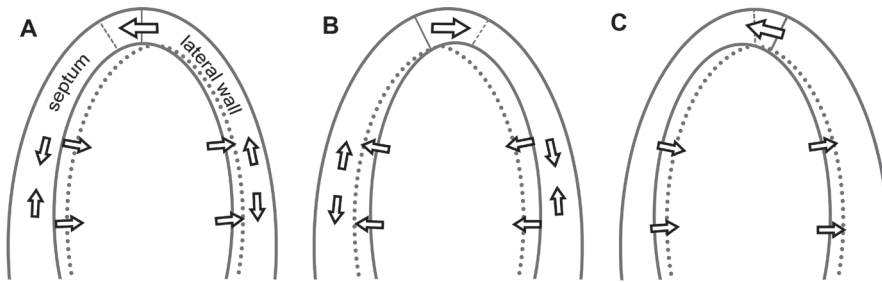


FIGURE 1. Schematic representation of apical rocking and septal flash

Schematic representation of the left ventricle in echocardiographic apical four-chamber view, showing both septal flash and apical rocking due to left bundle branch block induced mechanical dyssynchrony. A: Early septal contraction stretches the lateral wall and rocks the apex to the left, while the septum thickens and moves inwards. B: Late lateral wall contraction stretches the septum and rocks the apex to the right. C: Relaxation of the lateral wall with continuing septal contraction, while the apex moves to its original position.

Visual assessment or ‘eye-balling’ of mechanical dyssynchrony is perhaps the most feasible method for routine clinical applications. Two parameters are known: apical rocking and septal flash (figure 1) Both are known to have a high specificity for predicting response.^{25, 26} Apical rocking is the apical transverse motion due to an inhomogeneity of myocardial contraction and function, and requires an apical four chamber view with a visible apex. LBBB causes early septal contraction which moves the apex towards the septum, while delayed lateral wall contraction subsequently ‘rocks’ the apex towards the lateral side. Szulik et al. proved the predictive value for volumetric response, with comparable

strength for both visually assessed and automatically quantified apical rocking.²⁵ Ghani et al. confirmed these results and further showed that apical rocking predicts long-term clinical outcome in terms of hospitalisation for heart failure.⁶ Septal flash shows similar results. A septal flash is a short inward septal motion, occurring due to early septal contraction, interrupted by delayed free wall contraction. Parsai et al. found the presence of septal flash to be predictive for both clinical and volumetric response.²⁷ On top of known predictors, the value of septal flash in prediction models was significant.²²

IVMD is the delay in onset of outflow between the left and right ventricle. Delayed activation and subsequent contraction of the LV free wall due to LBBB leads to a delayed rise in LV pressure and outflow. LV dyssynchrony therefore lengthens the LV pre-ejection period, increasing IVMD, while 'normal' right ventricular (RV) activation leads to a fast rise in pressure and outflow through the RV outflow tract. IVMD can, however, be confounded by reduced RV function and a lengthened RV pre-ejection period. It can be easily measured using pulsed-wave Doppler signals obtained in any standard echocardiogram. IVMD reflects dyssynchrony of interventricular dynamics, by subtracting the difference in onset between QRSONset and flow through both the left and right ventricular outflow tract (LV and RV pre-ejection period, respectively). Although a cut-off of 40 ms is used to determine dyssynchrony, IVMD has a linear relationship with response, and a specific cut-off for response is unsuitable.²⁸ It is therefore not applicable for patient selection, although the probability of response can be determined.

DEFORMATION IMAGING

Deformation imaging or strain analysis with echocardiography uses either tissue Doppler imaging or speckle tracking echocardiography. The latter is less angle dependent and covers the whole ventricular wall, in contrast to tissue Doppler imaging, and is therefore more reliable for detection of delayed activated segments.

Septal to lateral wall delay (SL delay) is obtained by either tissue Doppler velocity imaging or speckle tracking echocardiography, calculated by the time difference between peak velocity (Doppler) or contraction (Doppler and/or speckle tracking) of the basal septal and lateral wall.⁵ SL delay thereby reflects both early septal and late lateral wall contraction caused by delayed free wall activation. Using tissue Doppler imaging, SL delay is measured by sampling in the basal septal and lateral wall, which is sensitive to sampling.²⁹ As for all time-based parameters, defining the maximum peak is of importance. The maximal peak can be early

or late, depending on the interaction with tethering myocardium and ventricular dynamics. Septal deformation can have a late maximum peak, while contraction starts early, resulting in an earlier first peak (baseline septal strain in figure 2). A dyssynchronous ventricle can therefore be deemed synchronous. Moreover, despite the promising results of single-centre studies, so far no multicentre trial has proved the diagnostic power of SL delay.³

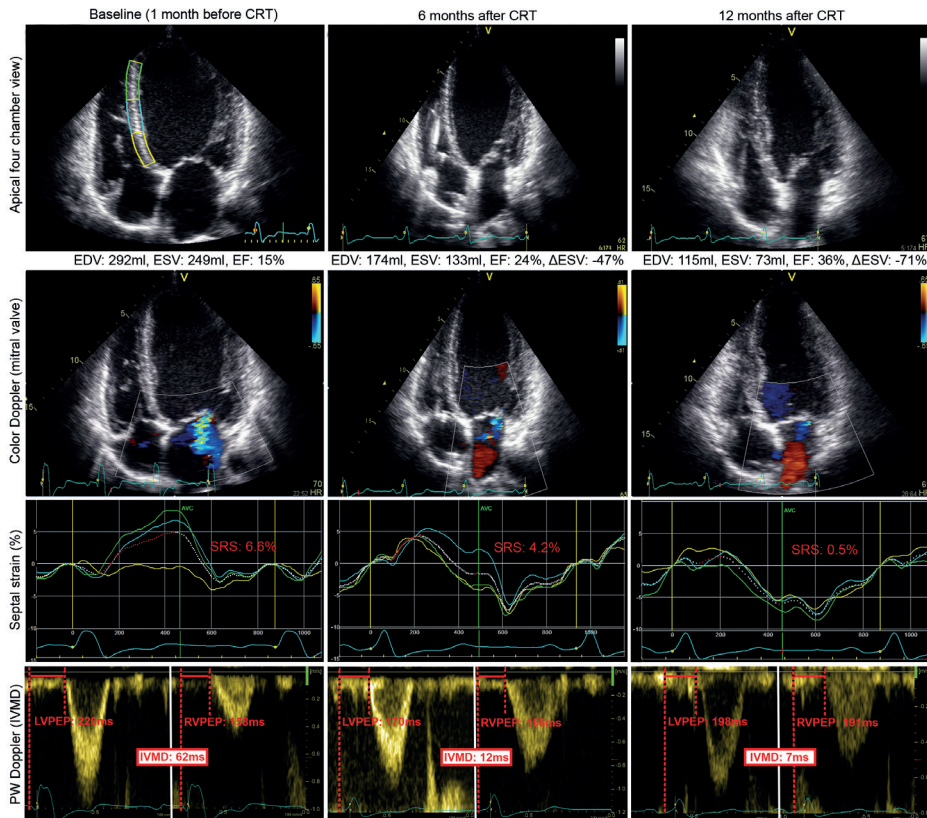


FIGURE 2. Example of echocardiographic data obtained from a responder to CRT

Apical four-chamber view, colour Doppler, septal strain and pulsed-wave Doppler acquisition of a responder to CRT, before, and 6 and 12 months after implantation. Note the continuous decrease in LV volume, decrease in mitral regurgitation, improvement in septal strain and decrease in IVMD over time. These data suggest a continuous process of reverse remodelling. Septal strain: basal, light blue and green lines represent basal, mid and apical inferoseptal segmental strain, respectively. The three curves represent the segments illustrated in baseline echocardiogram in the upper left panel. The white dashed curve represents the average septal strain. SRS_{sept} is marked red, as all rebound stretch after initial shortening, during systole. IVMD is represented by pulsed-wave Doppler signals of the left and right ventricular outflow tract. EDV: end-diastolic volume, ESV: end-systolic volume, EF: ejection fraction, Δ ESV change in ESV: compared with baseline, SRS: systolic rebound stretch, LVPEP: left ventricular pre-ejection period, RVPEP: right-ventricular pre-ejection period, IVMD: interventricular mechanical delay. Volumes are derived by biplane Simpson's method.

Most deformation parameters use time delays in peak contraction, either absolute, relative or as a standard deviation, to determine evidence of dyssynchrony.³⁰ These parameters suffer from the same definition-based limitations as SL delay. Parameters that incorporate the entire strain curve are therefore more promising. Moreover, high-quality images are required to determine segmental differences, which is not always feasible, especially in patients with dilated ventricles due to heart failure. The interventricular septum is therefore of particular interest, as echocardiographic imaging of the septum is almost always feasible and reproducible. Its central position in the ultrasound window guarantees adequate image quality. Moreover, the septum provides information on interventricular interaction as well as intraventricular properties. Derived parameters, such as SRSsept or identification of septal strain patterns, are promising as predictors of outcome (figure 2 and table 2).^{4, 31} SRSsept is the total amount of systolic rebound stretch, after initial shortening of the septum. Early septal shortening disrupted by contralateral delayed free wall contraction causes rebound stretch. SRSsept thereby assesses the amount of wasted work for the septum that can be recruited by CRT. Septal dyssynchrony can show multiple typical patterns, of which Leenders et al. discriminated three types.³² These patterns (and SRSsept) are even influenced by myocardial viability and predict both clinical and volumetric response to CRT (figure 2).³¹⁻³³ Risum et al. recently demonstrated the role of LV strain pattern recognition on top of electrocardiographic predictors for outcome.³⁴ However, results depend on the ultrasound machine and speckle tracking echocardiography software used. The majority of algorithms to determine myocardial strain are unknown and lack validation. Inter-vendor differences are known and limit translation to other ultrasound machines than the most commonly published, i.e. GE EchoPac, General Electric Healthcare, Milwaukee, USA.³⁵ Intraobserver and interobserver coefficients of variation are relatively high for SRSsept (19.5% and 16.3%, respectively).⁴ Despite the small number of clinical trials, all agree on the potential strength of septal strain parameters derived by speckle tracking echocardiography (table 1).^{33, 36-38} A multicentre trial is required to prove their benefit in clinical decision making.

TABLE 2. Studies on septal dyssynchrony parameters predicting response to CRT

First author	Design	n	Parameter and cut-off	Response prediction ($\geq 15\%$ Δ ESV)	Outcome	Strengths and/or limitations
De Boeck ⁴	Prospective single centre	62	SRSsept >4.7%	Sens/spec: 81%/81%, AUC: 0.94 \pm 0.04, B: 2.41, p=0.005		Relatively high inter- and intra-observer variability (COV: 14.2 and 15.6%)
Leenders ³¹	Prospective single centre	101	SRSsept >4.7%	Multivariate analysis, B: 3.78, p<0.001	Survival (death, LVAD or transplant) with HR: 5.8 (2.3-14.3)	No HF hospitalisation or morbidity
Chan ³⁷	Prospective single centre	43	SRSsept >4.7%	AUC: 0.86 \pm 0.06*		No multivariate analysis
van 't Sant ²¹	Retrospective single centre	227	SRSsept (continuous)	Multivariate analysis, B: 1.19		SRSsept assessed as continuous variable. No specific cut-off used
Ghani ³⁸	Retrospective single centre	138	SRSsept >4.0%	Sens/spec: 66%/66%, AUC: 0.70	Data on outcome not published (although registered)	Analysis on AP4CH instead of septal single wall
Leenders ³²	Retrospective single centre	132	Septal deformation patterns	Type 1 and 2 predict response vs. type 3, Δ ESV: 37 \pm 20 & 24 \pm 24 vs 5 \pm 20ml, p<0.001		Validated by mechanistic computer model
Marechoux ³³	Prospective single centre	101	Septal deformation patterns	Responders: pattern 1&2 vs 3: 92% vs. 59%, p<0.0001, Sens/spec: 74%/74%	18 months event-free survival (death or HF hospitalisation): Pattern 1&2 vs. 3: 95% vs 75%, p=0.01	Relative short follow-up
Risum ³⁶	Prospective single centre	67	LBBB deformation pattern	Sens/spec: 91%/95%		Complex pattern description
Risum ³⁴	Prospective multicentre	208	LBBB deformation pattern		Absence of LBBB increases 4 year risk of death, HF hospitalisation, LVAD or HTx, HR 3.1 (1.64-5.88)	Complex pattern description

Studies on septal dyssynchrony parameters, derived from speckle tracking echocardiography, predicting response to cardiac resynchronization therapy. All studies are single centre, prospective trials.*; when added to a model with clinical characteristics (gender, LBBB, QRS duration, heart failure aetiology). AUC: area under the curve in ROC analysis, B: beta-coefficient, COV: coefficient of variation, Δ ESV difference in end-systolic volume, HF: heart failure, HR: hazard ratio, HTx: heart transplantation, LBBB: left bundle branch block, LVAD: left ventricular assist device, n: number of patients, p: p-value, sens: sensitivity, spec: specificity, SRSsept: systolic rebound stretch of the septum.

Dyssynchrony can also be assessed by three-dimensional echocardiography (3DE). The predominant 3DE parameter is the systolic dyssynchrony index, using the standard deviation of difference from a reference time point in the QRS complex to minimal systolic volume of sixteen segments. Systolic dyssynchrony index (mean cut-off 9.8%) was able to predict treatment response with a sensitivity and specificity of 93% and 75% respectively.³⁹ The intra-class correlation coefficients for intraobserver and interobserver variability were high (0.95 and 0.92 respectively). Nevertheless, the echocardiographic image quality (i.e. spatial and temporal resolution) needs to be adequate for analysis, which is not always feasible. QRS triggering should also be adequate, as triggering after QRS onset will miss early septal contraction and overestimate the onset and therefore underestimate time-to-peak values. Moreover, these parameters have been tested in single-centre studies, and therefore require validation in a multicentre trial. The diagnostic power of the systolic dyssynchrony index can therefore be overrated, as has been observed for previous parameters (e.g. SL delay).^{3, 5}

OPTIMISING LEAD POSITION

Radial strain obtained with speckle tracking echocardiography from parasternal short axis images prior to implantation can indicate segments with delayed peak contraction. During implantation, LV lead placement can be guided to these segments, resulting in a remote, adjacent (i.e. neighbouring), or concordant placement, based on the 17-segment model of the American Heart Association. Observational studies have shown that a concordant or adjacent position to the latest contracting segment is superior to a remote position, in terms of reverse remodelling, death and hospitalisation during two years of follow-up.^{40, 41} Targeting the latest contracting segment with radial strain has been implemented in two randomised clinical trials, the TARGET and STARTER trial. Patients were randomised to targeted or conventional LV lead placement.^{1, 42} Targeted placement led to a higher percentage of concordant or adjacent positions and showed improvement in both volumetric response (LV change in end-systolic volume, TARGET: $-30\pm 29\%$ vs. $-20\pm 25\%$ and STARTER: -46 ± 33 ml vs. -26 ± 23 ml) and clinical outcome (percentage of patients reaching endpoint of death and hospitalisation for heart failure, TARGET: 22% vs. 42% and STARTER: 14% vs. 21%). A large number of leads in the unguided group were placed in a favourable position by chance. Per-protocol analysis of both studies showed that patients (guided or unguided) with concordant or adjacently placed leads had a better response and outcome.^{1, 42}

Another advantage of strain analysis is information on myocardial viability by peak strain values. Scarred regions are known to have lower strain amplitudes, and pacing in a region of scar tissue correlates to non-response.⁴³ Both abovementioned trials excluded segments with peak strain <10%, thereby excluding potentially scarred segments, which may have contributed significantly to the positive effects of echo-guided lead positioning. Sub-analysis showed that absence of scar near the LV lead was a strong predictor for volumetric response and reduced all-cause mortality in the TARGET trial.⁴⁴ Moreover, sub-analysis of the STARTER trial indicated that echo-guided LV lead placement improved survival especially in patients with ischaemic cardiomyopathy.⁴⁵ Notwithstanding these results, peak radial strain has shortcomings as an indicator for viability, as the sensitivity and specificity were only 33 and 72% respectively, compared with MRI with delayed enhancement.⁴⁶ Peak strain values might be underestimated in a dyssynchronous ventricle, as both pre and rebound stretch would decrease the absolute peak value.

High image quality is important for reliable strain analysis, which is relatively difficult to obtain in typical CRT patients with dilated left ventricles. Segments distal from the echo probe (i.e. basal and mid-inferoseptal, inferior and inferolateral segments) are prone to noise, and therefore result in more random strain curves. Even if quality is sufficient, time-to-peak strain values can be quite comparable between segments, as can be appreciated in figure 3. Using longitudinal strain could be a solution, it has more pronounced regional differences and is more robust than radial strain.⁴⁷ Lastly, loading conditions need to be identical between recordings, which means that changes in heart rhythm disturb the result. 3DE could be an answer to the above-mentioned difficulties, assessing the entire left ventricle in a single recording, although current techniques require multiple consecutive beats.⁴⁸

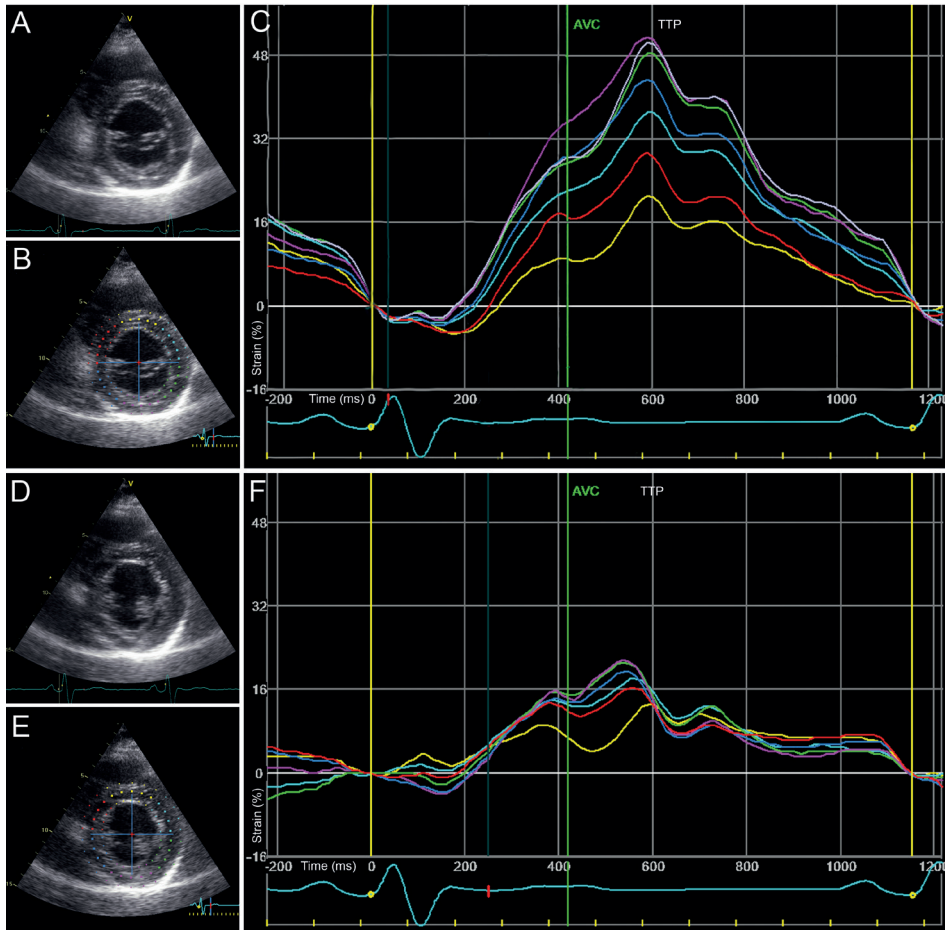


FIGURE 3. Radial strain analysis of parasternal short-axis images

Parasternal short-axis (PSAX) views and radial strain analysis of a patient with left bundle branch block, imaged prior to CRT implantation. LV lead placement resulted in a mid-posterolateral position (green curve in figure 3F). Decrease in end-systolic volume after six months of therapy was 49% (from 88 to 43ml). A & D: B-mode images with excellent echocardiographic quality of PSAX mitral valve level and papillary muscle level. B & E: Region of interest (ROI) placement for radial strain analysis of both PSAX views. C & F: Strain curves of corresponding ROIs, note the similarity in time-to-peak strain. There is no single area with latest activation. TTP: time to peak strain

OPTIMISATION OF DEVICE CONFIGURATION

Echocardiography can be used to optimise atrioventricular (AV) and/or interventricular (VV) delays. AV delay optimisation influences ventricular filling and may cause fusion with intrinsic conduction, thereby also influencing intraventricular and interventricular interaction. VV delay optimisation also influences intraventricular and interventricular dynamics, leading to more homogenous LV contraction. Optimisation methods used in previous trials are: iterative or Ritter method of mitral valve inflow characteristics, velocity time integral of Doppler echocardiography of LVOT, and dyssynchrony indices using visual assessment, speckle tracking echocardiography or tissue Doppler imaging. Optimisation influences acute haemodynamic and mechanical interaction.⁴⁹ Van Deursen et al. showed the interaction between electrocardiography, strain analysis by speckle tracking echocardiography, IVMD, velocity time integral of the LVOT, and blood pressure based on finger plethysmography, while adjusting either the AV or VV delay in CRT patients.⁴⁹

Optimisation has comparable results on long-term outcome to standard or fixed delays.⁵⁰ The SMART-AV study, for example, showed no benefit of echocardiographic optimisation with an iterative method compared with a fixed AV delay of 120 ms.² Although Mullens et al. showed that 47% of clinical non-responders (no significant New York Heart Association (NYHA) class or 6-minute walking test improvement) had a suboptimal AV delay, no trials so far have been published on the effects of optimisation on change in volumetric response.⁵¹ Except for the unpublished RESPONSE-HF study, which showed no benefit of VV delay optimisation in non-responders in a preliminary report.⁵⁰ All echocardiographic optimisation methods optimise relatively small changes (10 to 20 ms difference in AV and/or VV delay) with a parameter prone to noise. Patient repositioning, breathing, echocardiographic probe displacement, and other physiological disturbances all influence results. Even if one were to overcome the first three, reliable and reproducible measurement requires numerous iterations.^{52, 53} This implies even more time-consuming protocols, which are unlikely to be used by clinicians. Moreover, blinding observers for settings using the iterative method leads to an even larger spread in optimums compared with unblinded optimisation, suggesting a significant amount of observer bias.⁴⁷ The optimal AV delay can also differ during different physiological conditions (i.e. rest and exercise) and may change due to remodelling.^{54, 55} These limitations currently make echocardiography unsuitable for optimisation.

DEFINING RESPONSE WITH ECHOCARDIOGRAPHY

2

For response prediction, an echocardiogram is performed at least six months after CRT implantation, to compare volumetric status pre- and post-implantation (after a period of preferred reverse remodelling). Reverse remodelling is characterised by a decrease in LV volume. A $\geq 15\%$ decrease in LV end-systolic volume is commonly used to define response to CRT, or if lower, non-response. Although clinical response to CRT is multifactorial and is observed in patients without remodelling, volumetric change (i.e. decrease in end-systolic volume) predicts clinical response and prognosis of CRT patients. A larger decrease in end-systolic volume means fewer hospitalisations for heart failure and a lower mortality rate. When divided into subgroups (negative, non-responder, normal, and super-responder), there is an upscaling effect. Super-responders had almost no events during five years of follow-up, while non and negative responders have progressive heart failure and subsequent events.⁵⁶ Moreover, end-systolic volume decrease is preferred over clinical parameters (NYHA class, 6-minute walking distance, and quality of life score.⁵⁷ Quality of life and reverse remodelling do not always overlap, as patients can show improvement in one without the other.⁵⁸ Clinical parameters should not be disregarded, as an increase in quality of life or NYHA class can be as important to a patient as survival. Health status responders, defined by the Kansas City Cardiomyopathy Questionnaire (KCCQ) score, have a 76% lower risk of subsequent events.⁵⁸ A reason for the missing link could be the time of volumetric assessment.⁵⁹ Studies have shown that reverse remodelling is a continuous process, with patients still showing improvement after a year of CRT (figure 2).²⁸ Patients who are below the threshold of response at 6 months could become responders afterwards. Even patients with a proven response can have a reversal in effect, as volumetric assessment 14 months after initial response can show an increase in end-systolic volume to pre-CRT levels.⁶⁰ Assessment after 14 months of CRT proved to be a better predictor of major adverse cardiac events. These results necessitate a continuous re-evaluation of volumetric status.

FUTURE DIRECTIONS

Echocardiography could play a larger role in CRT, especially if 3D acquisition were to become more feasible for clinical practice. Increased spatial and temporal resolution could make 3DE applicable for fast acquisition of volumetric status and myocardial strain.^{14, 39} A

single acquisition could therefore incorporate information on function, volume, viability, dyssynchrony, and options for LV lead positioning.

Although validation in a large multicentre trial is required, dyssynchrony parameters based on patterns (i.e. SRSsept and strain patterns) instead of timing are promising for response prediction. These indices define a treatable substrate of dyssynchrony and have shown their predictive value in several studies.^{31, 34}

Patients with LVEF >35% (especially in patients with LBBB) are an interesting group for further research. These individuals might benefit from CRT. Whether their LV volumes should be determined by echocardiography or MRI and whether guidelines should distinguish between the technique used, also requires further study. Lastly, measurement variability should be addressed for reliable assessment. Measuring and averaging multiple beats should be common practice, although not all software tools incorporate average values for volume and ejection fraction (i.e. Xcelera, Philips).

CONCLUSION

Echocardiography is a practical clinical tool and used for assessment of volumetric status, function and outcome in CRT patients (central illustration). Clinicians should know its shortcomings when implementing results in clinical decision making. Specific cut-off values determined by a less accurate technique require a lenient approach. So far, response prediction and patient selection by mechanical dyssynchrony parameters have been disappointing. However a new set of parameters (i.e. deformation imaging) has shown promising results in single-centre studies and requires a multicentre approach to prove its benefit. While implementation of AV or VV delay optimisation is difficult with current techniques, deformation parameters may guide LV lead placement, increasing response rates and improving prognosis. We therefore conclude that echocardiography is a friend of CRT, with known limitations. Their relationship could become even stronger, with promising applications of 3DE and deformation imaging to patient selection and optimisation of lead placement.

REFERENCES

1. Khan FZ, Virdee MS, Palmer CR, Pugh PJ, O'Halloran D, Elsik M, et al. Targeted left ventricular lead placement to guide cardiac resynchronization therapy: the TARGET study: a randomized, controlled trial. *J Am Coll Cardiol*. 2012;59:1509-1518.
2. Ellenbogen KA, Gold MR, Meyer TE, Fernandez Lozano I, Mittal S, Waggoner AD, et al. Primary results from the SmartDelay determined AV optimization: a comparison to other AV delay methods used in cardiac resynchronization therapy (SMART-AV) trial: a randomized trial comparing empirical, echocardiography-guided, and algorithmic atrioventricular delay programming in cardiac resynchronization therapy. *Circulation*. 2010;122:2660-8.
3. Chung ES, Leon AR, Tavazzi L, Sun JP, Nihoyannopoulos P, Merlini J, et al. Results of the Predictors of Response to CRT (PROSPECT) trial. *Circulation*. 2008;117:2608-16.
4. De Boeck BW, Teske AJ, Meine M, Leenders GE, Cramer MJ, Prinzen FW, et al. Septal rebound stretch reflects the functional substrate to cardiac resynchronization therapy and predicts volumetric and neurohormonal response. *Eur J Heart Fail*. 2009;11:863-71.
5. Bax JJ, Bleeker GB, Marwick TH, Molhoek SG, Boersma E, Steendijk P, et al. Left ventricular dyssynchrony predicts response and prognosis after cardiac resynchronization therapy. *J Am Coll Cardiol*. 2004;44:1834-40.
6. Ghani A, Delnoy PP, Ottervanger JP, Misier AR, Smit JJ, Adiyaman A, et al. Apical rocking is predictive of response to cardiac resynchronization therapy. *Int J Cardiovasc Imaging*. 2015;31:717-25.
7. Ruschitzka F, Abraham WT, Singh JP, Bax JJ, Borer JS, Brugada J, et al. Cardiac-resynchronization therapy in heart failure with a narrow QRS complex. *N Engl J Med*. 2013;369:1395-405.
8. Wood PW, Choy JB, Nanda NC, Becher H. Left ventricular ejection fraction and volumes: it depends on the imaging method. *Echocardiography*. 2014;31:87-100.
9. Brignole M, Auricchio A, Baron-Esquivias G, Bordachar P, Boriani G, Breithardt OA, et al. 2013 ESC Guidelines on cardiac pacing and cardiac resynchronization therapy: the Task Force on cardiac pacing and resynchronization therapy of the European Society of Cardiology (ESC). Developed in collaboration with the European Heart Rhythm Association (EHRA). *Eur Heart J*. 2013;34:2281-2329.
10. Russo AM, Stainback RF, Bailey SR, Epstein AE, Heidenreich PA, Jessup M, et al. ACCF/HRS/AHA/ASE/HFSA/SCAI/SCCT/SCMR 2013 appropriate use criteria for implantable cardioverter-defibrillators and cardiac resynchronization therapy. *Heart Rhythm*. 2013;10:e11-58.

11. Cleland JG, Abraham WT, Linde C, Gold MR, Young JB, Claude Daubert J, et al. An individual patient meta-analysis of five randomized trials assessing the effects of cardiac resynchronization therapy on morbidity and mortality in patients with symptomatic heart failure. *Eur Heart J*. 2013;34:3547-56.
12. Chung ES, Katra RP, Ghio S, Bax J, Gerritse B, Hilpisch K, et al. Cardiac resynchronization therapy may benefit patients with left ventricular ejection fraction >35%: a PROSPECT trial substudy. *Eur J Heart Fail*. 2010;12:581-7.
13. Kaufmann BA, Min SY, Goetschalckx K, Bernheim AM, Buser PT, Pfisterer ME, et al. How reliable are left ventricular ejection fraction cut offs assessed by echocardiography for clinical decision making in patients with heart failure? *Int J Cardiovasc Imaging*. 2013;29:581-8.
14. Driessen MM, Kort E, Cramer MJ, Doevendans PA, Angevaere MJ, Leiner T, et al. Assessment of LV ejection fraction using real-time 3D echocardiography in daily practice: direct comparison of the volumetric and speckle tracking methodologies to CMR. *Neth Heart J*. 2014;22:383-90.
15. de Haan S, de Boer K, Commandeur J, Beek AM, van Rossum AC, Allaart CP. Assessment of left ventricular ejection fraction in patients eligible for ICD therapy: Discrepancy between cardiac magnetic resonance imaging and 2D echocardiography. *Neth Heart J*. 2014;22:449-55.
16. Hoffmann R, Barletta G, von Bardeleben S, Vanoverschelde JL, Kasprzak J, Greis C, et al. Analysis of left ventricular volumes and function: a multicenter comparison of cardiac magnetic resonance imaging, cine ventriculography, and unenhanced and contrast-enhanced two-dimensional and three-dimensional echocardiography. *J Am Soc Echocardiogr*. 2014;27:292-301.
17. Malm S, Frigstad S, Sagberg E, Larsson H, Skjaerpe T. Accurate and reproducible measurement of left ventricular volume and ejection fraction by contrast echocardiography: a comparison with magnetic resonance imaging. *J Am Coll Cardiol*. 2004;44:1030-5.
18. Saloux E, Labombarda F, Pellissier A, Anthune B, Dugue AE, Provost N, et al. Diagnostic value of three-dimensional contrast-enhanced echocardiography for left ventricular volume and ejection fraction measurement in patients with poor acoustic windows: a comparison of echocardiography and magnetic resonance imaging. *J Am Soc Echocardiogr*. 2014;27:1029-40.
19. Marwick TH. Hype and hope in the use of echocardiography for selection for cardiac resynchronization therapy: the Tower of Babel revisited. *Circulation*. 2008;117:2573-6.
20. Thibault B, Harel F, Ducharme A, White M, Ellenbogen KA, Frasure-Smith N, et al. Cardiac resynchronization therapy in patients with heart failure and a QRS complex <120 milliseconds: the Evaluation of Resynchronization Therapy for Heart Failure (LESSER-EARTH) trial. *Circulation*. 2013;127:873-81.

21. Van't Sant J, Ter Horst IA, Wijers SC, Mast TP, Leenders GE, Doevendans PA, et al. Measurements of electrical and mechanical dyssynchrony are both essential to improve prediction of CRT response. *J Electrocardiol.* 2015.
22. Brunet-Bernard A, Marechaux S, Fauchier L, Guiot A, Fournet M, Reynaud A, et al. Combined score using clinical, electrocardiographic, and echocardiographic parameters to predict left ventricular remodeling in patients having had cardiac resynchronization therapy six months earlier. *Am J Cardiol.* 2014;113:2045-51.
23. Anderson LJ, Miyazaki C, Sutherland GR, Oh JK. Patient selection and echocardiographic assessment of dyssynchrony in cardiac resynchronization therapy. *Circulation.* 2008;117:2009-23.
24. Cleland JG, Daubert JC, Erdmann E, Freemantle N, Gras D, Kappenberger L, et al. The effect of cardiac resynchronization on morbidity and mortality in heart failure. *N Engl J Med.* 2005;352:1539-49.
25. Szulik M, Tillekaerts M, Vangeel V, Ganame J, Willems R, Lenarczyk R, et al. Assessment of apical rocking: a new, integrative approach for selection of candidates for cardiac resynchronization therapy. *Eur J Echocardiogr.* 2010;11:863-9.
26. Sohal M, Amraoui S, Chen Z, Sammut E, Jackson T, Wright M, et al. Combined identification of septal flash and absence of myocardial scar by cardiac magnetic resonance imaging improves prediction of response to cardiac resynchronization therapy. *J Interv Card Electrophysiol.* 2014;40:179-90.
27. Parsai C, Baltabaeva A, Anderson L, Chaparro M, Bijmens B, Sutherland GR. Low-dose dobutamine stress echo to quantify the degree of remodelling after cardiac resynchronization therapy. *European heart journal.* 2009;30:950-8.
28. Ghio S, Freemantle N, Scelsi L, Serio A, Magrini G, Pasotti M, et al. Long-term left ventricular reverse remodelling with cardiac resynchronization therapy: results from the CARE-HF trial. *Eur J Heart Fail.* 2009;11:480-8.
29. De Boeck BW, Meine M, Leenders GE, Teske AJ, van Wessel H, Kirkels JH, et al. Practical and conceptual limitations of tissue Doppler imaging to predict reverse remodelling in cardiac resynchronisation therapy. *Eur J Heart Fail.* 2008;10:281-90.
30. Leenders GE, Cramer MJ, Bogaard MD, Meine M, Doevendans PA, De Boeck BW. Echocardiographic prediction of outcome after cardiac resynchronization therapy: conventional methods and recent developments. *Heart Fail Rev.* 2011;16:235-50.

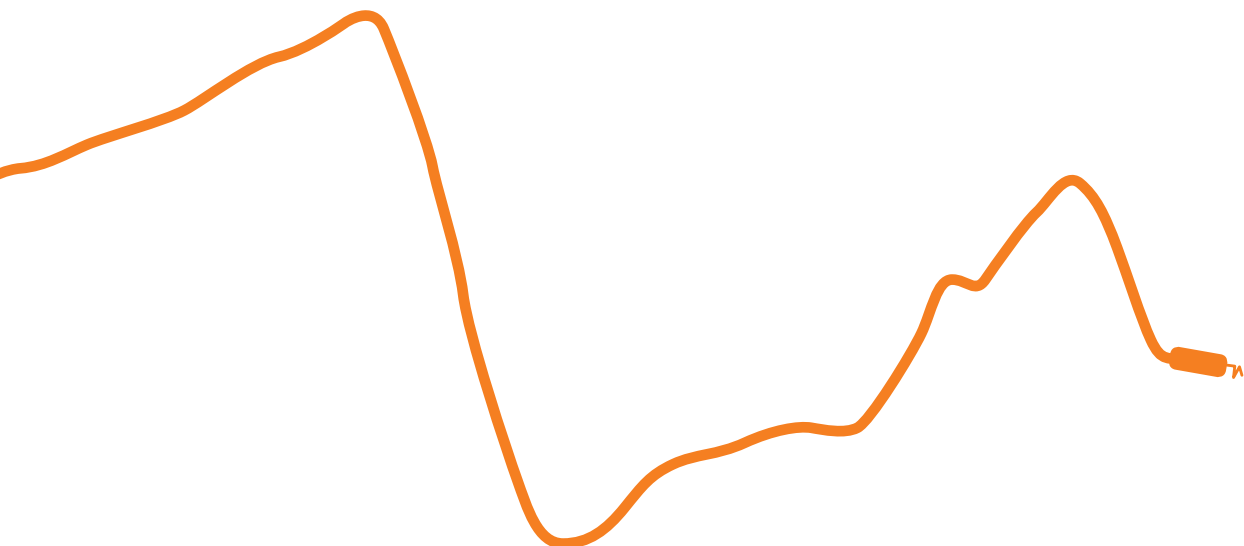
31. Leenders GE, De Boeck BW, Teske AJ, Meine M, Bogaard MD, Prinzen FW, et al. Septal rebound stretch is a strong predictor of outcome after cardiac resynchronization therapy. *J Card Fail.* 2012;18:404-12.
32. Leenders GE, Lumens J, Cramer MJ, De Boeck BW, Doevendans PA, Delhaas T, et al. Septal deformation patterns delineate mechanical dyssynchrony and regional differences in contractility: analysis of patient data using a computer model. *Circulation Heart failure.* 2012;5:87-96.
33. Marechaux S, Guiot A, Castel AL, Guyomar Y, Semichon M, Delelis F, et al. Relationship between two-dimensional speckle-tracking septal strain and response to cardiac resynchronization therapy in patients with left ventricular dysfunction and left bundle branch block: a prospective pilot study. *J Am Soc Echocardiogr.* 2014;27:501-11.
34. Risum N, Tayal B, Hansen TF, Bruun NE, Jensen MT, Lauridsen TK, et al. Identification of Typical Left Bundle Branch Block Contraction by Strain Echocardiography Is Additive to Electrocardiography in Prediction of Long-Term Outcome After Cardiac Resynchronization Therapy. *J Am Coll Cardiol.* 2015;66:631-41.
35. van Everdingen WM, Paiman ML, van Deursen CJ, Cramer MJ, Vernooy K, Delhaas T, et al. Comparison of septal strain patterns in dyssynchronous heart failure between speckle tracking echocardiography vendor systems. *J Electrocardiol.* 2014.
36. Risum N, Jons C, Olsen NT, Fritz-Hansen T, Bruun NE, Hojgaard MV, et al. Simple regional strain pattern analysis to predict response to cardiac resynchronization therapy: rationale, initial results, and advantages. *Am Heart J.* 2012;163:697-704.
37. Chan YH, Wu LS, Kuo CT, Wang CL, Yeh YH, Ho WJ, et al. Incremental value of inefficient deformation indices for predicting response to cardiac resynchronization therapy. *J Am Soc Echocardiogr.* 2013;26:307-15.
38. Ghani A, Delnoy PP, Adiyaman A, Ottervanger JPM, Misier AR, Smit JJ, et al. Septal rebound stretch as predictor of echocardiographic response to cardiac resynchronization therapy. *IJC Heart & Vasculature.* 2015;7:6.
39. Kleijn SA, Aly MF, Knol DL, Terwee CB, Jansma EP, Abd El-Hady YA, et al. A meta-analysis of left ventricular dyssynchrony assessment and prediction of response to cardiac resynchronization therapy by three-dimensional echocardiography. *Eur Heart J Cardiovasc Imaging.* 2012;13:763-75.
40. Ypenburg C, van Bommel RJ, Delgado V, Mollema SA, Bleeker GB, Boersma E, et al. Optimal left ventricular lead position predicts reverse remodeling and survival after cardiac resynchronization therapy. *J Am Coll Cardiol.* 2008;52:1402-9.

- 2
41. Kristiansen HM, Vollan G, Hovstad T, Keilegavlen H, Faerestrand S. The impact of left ventricular lead position on left ventricular reverse remodelling and improvement in mechanical dyssynchrony in cardiac resynchronization therapy. *Eur Heart J Cardiovasc Imaging*. 2012;13:991-1000.
 42. Saba S, Marek J, Schwartzman D, Jain S, Adelstein E, White P, et al. Echocardiography-guided left ventricular lead placement for cardiac resynchronization therapy: results of the Speckle Tracking Assisted Resynchronization Therapy for Electrode Region trial. *Circ Heart Fail*. 2013;6:427-34.
 43. Wong JA, Yee R, Stirrat J, Scholl D, Krahn AD, Gula LJ, et al. Influence of pacing site characteristics on response to cardiac resynchronization therapy. *Circ Cardiovasc Imaging*. 2013;6:542-550.
 44. Khan FZ, Virdee MS, Read PA, Pugh PJ, O'Halloran D, Fahey M, et al. Effect of low-amplitude two-dimensional radial strain at left ventricular pacing sites on response to cardiac resynchronization therapy. *J Am Soc Echocardiogr*. 2010;23:1168-76.
 45. Daya HA, Alam MB, Adelstein E, Schwartzman D, Jain S, Marek J, et al. Echocardiography-guided left ventricular lead placement for cardiac resynchronization therapy in ischemic vs nonischemic cardiomyopathy patients. *Heart Rhythm*. 2014;11:614-9.
 46. Bakos Z, Ostenfeld E, Markstad H, Werther-Evaldsson A, Roijer A, Arheden H, et al. A comparison between radial strain evaluation by speckle-tracking echocardiography and cardiac magnetic resonance imaging, for assessment of suitable segments for left ventricular lead placement in cardiac resynchronization therapy. *Europace*. 2014;16:1779-86.
 47. Jones S, Shun-Shin MJ, Cole GD, Sau A, March K, Williams S, et al. Applicability of the iterative technique for cardiac resynchronization therapy optimization: full-disclosure, 50-sequential-patient dataset of transmitral Doppler traces, with implications for future research design and guidelines. *Europace*. 2014;16:541-50.
 48. Aly MF, Kleijn SA, de Boer K, Abd El-Hady YA, Sorour KA, Kandil HI, et al. Comparison of three-dimensional echocardiographic software packages for assessment of left ventricular mechanical dyssynchrony and prediction of response to cardiac resynchronization therapy. *Eur Heart J Cardiovasc Imaging*. 2013;14:700-10.
 49. van Deursen CJ, Wecke L, van Everdingen WM, Stahlberg M, Janssen MH, Braunschweig F, et al. Vectorcardiography for optimization of stimulation intervals in cardiac resynchronization therapy. *J Cardiovasc Transl Res*. 2015;8:128-37.
 50. Auger D, Hoke U, Bax JJ, Boersma E, Delgado V. Effect of atrioventricular and ventriculoventricular delay optimization on clinical and echocardiographic outcomes of patients treated with cardiac resynchronization therapy: a meta-analysis. *Am Heart J*. 2013;166:20-9.

51. Mullens W, Grimm RA, Verga T, Dresing T, Starling RC, Wilkoff BL, et al. Insights from a cardiac resynchronization optimization clinic as part of a heart failure disease management program. *J Am Coll Cardiol*. 2009;53:765-73.
52. Sohaib SM, Whinnett ZI, Ellenbogen KA, Stellbrink C, Quinn TA, Bogaard MD, et al. Cardiac resynchronisation therapy optimisation strategies: systematic classification, detailed analysis, minimum standards and a roadmap for development and testing. *Int J Cardiol*. 2013;170:118-31.
53. Pabari PA, Willson K, Stegemann B, van Geldorp IE, Kyriacou A, Moraldo M, et al. When is an optimization not an optimization? Evaluation of clinical implications of information content (signal-to-noise ratio) in optimization of cardiac resynchronization therapy, and how to measure and maximize it. *Heart Fail Rev*. 2011;16:277-90.
54. Sun JP, Lee AP, Grimm RA, Hung MJ, Yang XS, Delurgio D, et al. Optimisation of atrioventricular delay during exercise improves cardiac output in patients stabilised with cardiac resynchronisation therapy. *Heart*. 2012;98:54-9.
55. Stanton T, Haluska BA, Leano R, Marwick TH. Hemodynamic benefit of rest and exercise optimization of cardiac resynchronization therapy. *Echocardiography*. 2014;31:980-8.
56. Foley PW, Chalil S, Khadjooi K, Irwin N, Smith RE, Leyva F. Left ventricular reverse remodelling, long-term clinical outcome, and mode of death after cardiac resynchronization therapy. *Eur J Heart Fail*. 2011;13:43-51.
57. Yu CM, Bleeker GB, Fung JW, Schalij MJ, Zhang Q, van der Wall EE, et al. Left ventricular reverse remodeling but not clinical improvement predicts long-term survival after cardiac resynchronization therapy. *Circulation*. 2005;112:1580-6.
58. Versteeg H, van 't Sant J, Cramer MJ, Doevendans PA, Pedersen SS, Meine M. Discrepancy between echocardiographic and patient-reported health status response to cardiac resynchronization therapy: results of the PSYHEART-CRT study. *Eur J Heart Fail*. 2014;16:227-34.
59. Ypenburg C, van Bommel RJ, Borleffs CJ, Bleeker GB, Boersma E, Schalij MJ, et al. Long-term prognosis after cardiac resynchronization therapy is related to the extent of left ventricular reverse remodeling at midterm follow-up. *J Am Coll Cardiol*. 2009;53:483-90.
60. van 't Sant J, Fiolet AT, Ter Horst IA, Cramer MJ, Mastenbroek MH, van Everdingen WM, et al. Volumetric Response beyond Six Months of Cardiac Resynchronization Therapy and Clinical Outcome. *PLoS one*. 2015;10:e0124323.
61. De Boeck BW, Teske AJ, Meine M, Leenders GE, Cramer MJ, Prinzen FW, et al. Septal rebound stretch reflects the functional substrate to cardiac resynchronization therapy and predicts volumetric and neurohormonal response. *Eur J Heart Fail*. 2009;11:863-71.



Comparison of septal strain patterns in dyssynchronous heart failure between speckle tracking echocardiography vendor systems



Wouter M. van Everdingen (MD)^{1,2}, Marie-Louise Paiman (MD)²,
Caroline J.M. van Deursen (MD, PhD)^{2,3}, Maarten J. Cramer (MD, PhD)¹,
Kevin Vernooy (MD, PhD)³, Tammo Delhaas (MD, PhD)⁴, Frits W. Prinzen (PhD)².

¹ Department of Cardiology, University Medical Center Utrecht, Utrecht, The Netherlands

² Department of Physiology, CARIM, Maastricht University Medical Center, Maastricht, The Netherlands

³ Department of Cardiology, Maastricht University Medical Center, Maastricht, The Netherlands

⁴ Department of Biomedical Engineering, Maastricht University Medical Center, Maastricht, The Netherlands

Journal of Electrocardiology 2015, 48 (4):609-616.

ABSTRACT

Aim: To analyse inter-vendor differences of speckle tracking echocardiography (STE) in imaging cardiac deformation in patients with dyssynchronous heart failure.

Methods of results: Eleven patients (all with LBBB, median age 60.7 years, nine males) with implanted cardiac resynchronization therapy devices were prospectively included. Ultrasound systems of two vendors (i.e. General Electric and Philips) were used to record images in the apical four chamber view. Regional longitudinal strain patterns were analysed with vendor specific software in the basal, mid and apical septal segments. Systolic strain (SS), time to peak strain (TTP) and septal rebound stretch (SRS) were determined during four pacing settings, resulting in 44 unique strain patterns per segment (total 132 patterns). Cross correlation was used to analyse the comparability of the shape of 132 normalized strain patterns. Correlation of strain patterns of the two systems was high (R^2 median: 0.68, interquartile range: 0.53-0.82). Accordingly, strain patterns of intrinsic rhythm were recognized equally using both systems, when divided into three types. GE based SS (18.9±4.7%) was significantly higher than SS determined by the Philips system (13.4±4.3%). TTP was slightly but non-significantly lower in GE (384±77 ms) compared to Philips (404±83 ms) derived strain signals. Correlation of SRS between the systems was poor, due to minor differences in the strain signal and timing of aortic valve closure.

Conclusions: The two systems provide similar shape of strain patterns. However, important differences are found in the amplitude, timing of systole and SRS. Until STE is standardized, clinical decision making should be restricted to pattern analysis.

INTRODUCTION

The introduction of speckle tracking echocardiography (STE) has brought new possibilities to the field of myocardial deformation analysis.¹ STE allows calculating myocardial deformation patterns from B-mode grayscale images in an ultrasound beam angle-independent manner.² The application field of STE is still growing, ranging from myocardial infarction to dyssynchrony, congenital heart disease and cardiomyopathies.³⁻⁶

Several vendors have developed software packages for STE deformation analysis, to be used in combination with their own ultrasound machines. Unfortunately, the implemented algorithms are not publicly available and investigators lack insight about the exact method of strain calculation. Moreover, some studies suggest that estimated strain values differ, not only between ultrasound equipment, but also when applying various analysis tools to the same signals.⁷⁻¹¹

An area where strain measurements are increasingly used is assessment of dyssynchrony. In this area, highly complicated strain patterns are found. To assess cardiac status in these patients, not only strain amplitude (e.g. peak systolic strain) is used, but also various indices of mechanical dyssynchrony, such as time to peak strain (TTP), septal rebound stretch (SRS) and septal strain patterns.¹²⁻¹⁴ Septal deformation patterns translate to interventricular dynamics and have shown to predict response and outcome of cardiac resynchronization therapy (CRT).^{6,15} These results were obtained by EchoPac strain analysis on General Electric (GE) acquired echocardiographic studies. Discrepancies in estimated strain parameters caused by vendor specific differences could therefore lead to conflicting data from different centres and even to misdiagnosis.

The purpose of the present study was to compare strain patterns and derived parameters obtained by ultrasound equipment and software of two widely used vendors, i.e. GE and Philips. Strain patterns were compared, with respect to their global strain pattern shape, and inter-vendor, intra- and interobserver agreement of absolute strain amplitude (SS), and commonly used indices like TTP and SRS. Our hypothesis is, based on other studies and own observations, that absolute values differ between vendors while patterns may be more alike.

METHODS

3

The study was performed according to the principles of the Declaration of Helsinki. All participants gave fully informed written consent prior to investigation. Eleven CRT patients were prospectively investigated in the Maastricht University Medical Center (MUMC). The device was implanted in the MUMC at least six months before entering the study (2006 to 2012). Prior to CRT, all patients were diagnosed with heart failure (NYHA I-IV), left bundle branch block (LBBB) and QRS duration >150ms. Patients were selected from two CRT trials, and gave consent to participate in sub-studies. They were selected based on known echocardiographic window and favourable response to CRT (LVEF >35%). Responders were thought to have a bigger difference in strain patterns between the used CRT settings. Other inclusion criteria were; sinus rhythm and age ≥ 18 . Patients with complete AV-block or permanent atrial fibrillation were excluded from participation.

Ultrasound machines of two vendors, GE Vivid 7 (General Electric Healthcare, Milwaukee, USA) and Philips iE33 (Philips Medical Systems, Best, The Netherlands), were used. To avoid interobserver variability during acquisition, the same echocardiography specialist investigated each patient on both machines. Acquisition on both machines was performed successively (i.e. only a few minutes apart) in the MUMC. The order (i.e. acquisition with GE or Philips first) was randomly assigned. To induce a wide range of strain patterns, images were recorded in four conditions: pre-programmed biventricular pacing, single site left ventricular (LV) pacing, single site right ventricular (RV) pacing and during intrinsic rhythm (pacing off). There was a pause of at least 20 seconds between pacing modalities, to reach a new hemodynamic steady state. In every setting, the following images were stored during at least three cardiac cycles: 2D-images of the interventricular septum in the apical four chamber view for STE, and continuous wave Doppler images of the left ventricular outflow tract for offline determination of the aortic valve closure timing (AVC). Images were recorded during breath hold. The framerate of 2D-images for STE was optimized between 60 to 90Hz. Systole was defined as the period between the R-wave and subsequent AVC. The R-wave was chosen, instead of the mitral valve closure time due to its higher reproducibility.

We focused on the interventricular septum, because imaging quality of the LV lateral wall is often poor in dilated hearts of heart failure patients. Imaging the septum has a higher reproducibility.¹⁶ Moreover, due to interventricular dynamics, a wide range of septal stain

patterns is inducible by altering CRT settings. Septal deformation imaging (i.e. categorization of strain patterns and SRS) can predict response and outcome of CRT.

OFFLINE ANALYSIS

Offline analysis of recorded images was performed with corresponding software packages of both vendors. Raw (i.e. non-compressed) echocardiographic data was exported with both systems. QLAB 8.0 (Philips Medical Systems, Best, The Netherlands) was used for all Philips iE33 derived images. EchoPac (PC version 112; GE Healthcare, Milwaukee, USA) was used for all GE Vivid 7 acquired images. 44 longitudinal strain patterns were analysed from eleven patients in three separate segments, resulting in a total of 132 strain patterns per vendor. Three consecutive beats were selected for both vendors, based on the ECG signal. Timing of reference length (L_0) was defined at the top of the R-wave for both vendors. Exported Philips images started at the R-wave, and therefore L_0 couldn't be placed at a prior point (e.g. QRS-onset). Manual LV border tracing of the septum was performed according to the vendors' preferences (end systolic for GE and end diastolic for Philips). The septum was divided in three segments: apical (ApIS), mid (MIS) and basal (BIS) inferoseptal. A segment was neglected if the software could not track displacement, even after repeatedly adjusting the region of interest (ROI). In QLAB, standard settings were used, although the setting of 'mesh' was turned to its highest value, to obtain the highest possible spatial resolution. Standard 'out-of-the-box' settings for filtering and smoothening were used with EchoPac. Analysis was performed blinded for the results of the other vendor.

EchoPac uses an ROI of six segments across the septum and LV free wall in the apical four chamber view, according to the sixteen-segment model. QLAB 8.0 has an additional seventh segment, situated at the apex. The latter is according to the recommendations of the American Heart Association.¹⁷ As a result, the position of the segments in QLAB was slightly shifted towards the base. We adjusted the ROI of EchoPac to match the position of the segments of QLAB. For each setting and for each segment, strain values in time were exported to Matlab R2012b for further analysis of strain data with author-written general scripts.

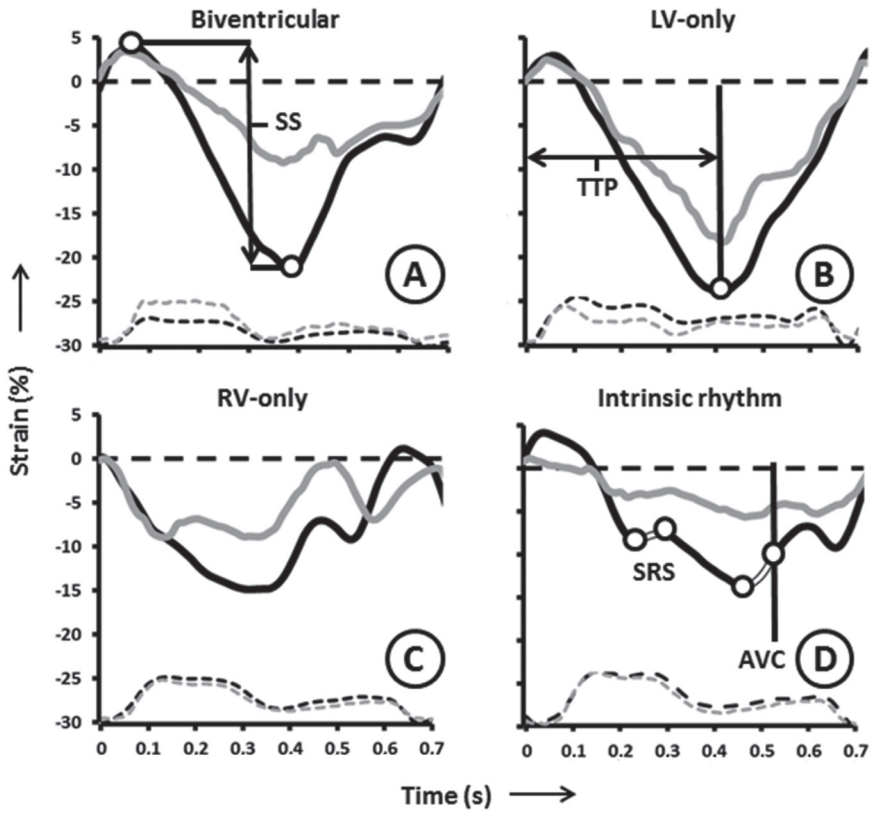


FIGURE 1. Examples of strain parameters

Strain patterns of the mid septal segment of patient 1. Each setting (A: biventricular pacing, B: LV-only pacing, C: RV-only pacing and D: intrinsic rhythm) is represented by one beat (Black: GE and grey: Philips). Patterns were time corrected in all panels. For the black signal, systolic strain calculation (SS) is shown in panel A, time to peak strain (TTP) in panel B and septal rebound stretch (SRS), all systolic upward deflections after initial shortening, in panel D. In this case SRS equalled the sum of the two strain changes indicated by the white parts of the signal.

SYSTOLIC STRAIN AND TIME TO PEAK STRAIN

SS was chosen as a parameter for spatial deformation, to incorporate the total shortening of each beat. SS was determined as the absolute maximum difference in strain deflection for each beat (figure 1A). SS was chosen instead of generally used peak systolic strain (i.e. largest negative value during systole). Positive deflections (pre-stretch) influence peak strain

by displacing the start of shortening. SS incorporates pre-stretch and therefore reflects total shortening. Furthermore, discrepancies in L_0 influence the amount of pre-stretch and negative peak strain, while SS is relatively unaffected by L_0 . Moreover, peak systolic strain is influenced by definition of systole, which could underestimate total shortening.

TTP was determined as the difference in milliseconds between the timing of the R-wave (i.e. the reference marker for strain analysis) and the maximum negative peak strain of the analysed beat (figure 1B). Values for SS and TTP were averaged over three consecutive heartbeats.

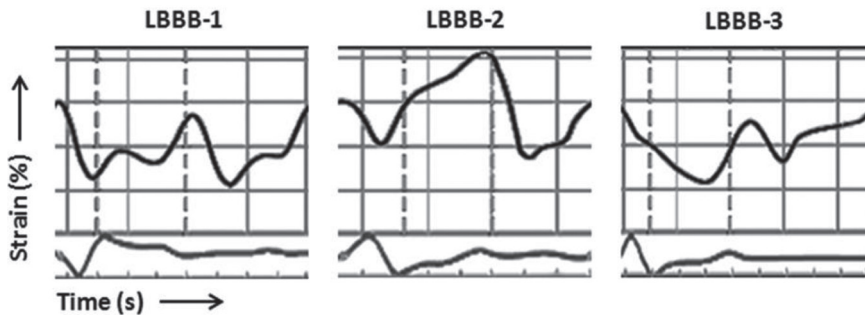


FIGURE 2. Septal strain patterns

LBBB-1: double-peaked systolic shortening, LBBB-2: early pre-ejection shortening peak followed by prominent systolic stretching, and LBBB-3: pseudonormal shortening with a late-systolic shortening peak followed by less pronounced end-systolic stretch. Adjusted from Leenders et. al.

SEPTAL REBOUND STRETCH AND LEFT BUNDLE BRANCH BLOCK PATTERNS

The amount of SRS during intrinsic rhythm was defined as the sum of all systolic stretch following prematurely terminated shortening in the systolic period (figure 1D).¹² Deformation patterns were assessed, blinded for the specific patient, and manually categorized in three different types, as described by Leenders et al.: LBBB-1, double-peaked systolic shortening; LBBB-2, early pre-ejection shortening peak followed by prominent systolic stretching; and LBBB-3, pseudonormal shortening with a late-systolic shortening peak followed by less pronounced end-systolic stretch (figure 2).¹⁵

CROSS CORRELATION

Before cross correlation, each strain signal of both vendors was normalized. The lowest value of the strain pattern was added to all data points, in order to express all values as 0.0 or higher. Next, all values were expressed as a fraction of the highest value, ranging from 0.0 to 1.0. Similarity of strain pattern shape between General Electric and Philips was analysed by cross correlation of their normalized strain signals for each specific combination of patient, setting and segment. Philips strain data was plotted on the x-axis, while GE strain data was plotted on the y-axis. The correlation coefficient of the linear least squares fitting (equation: $y=a*x$) of the data points was calculated. One of the patterns was then shifted by steps of 1ms. For each step a new correlation coefficient was calculated. After a total shift of three beats, the highest value was used as the optimal correlation coefficient of the specific patient, setting and segment. Figure 3 displays an example of the result of normalization and time correction.

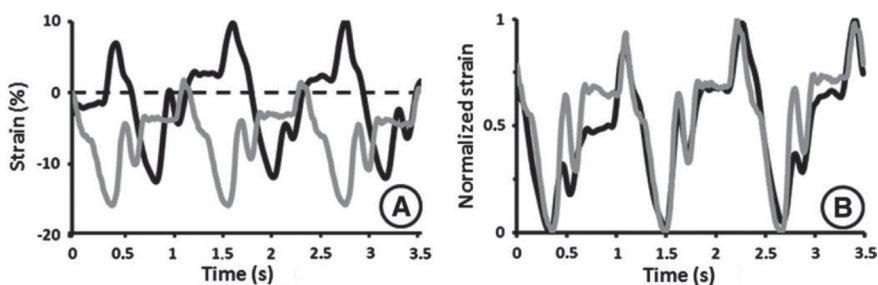


FIGURE 3. Strain normalization

Strain patterns of the mid inferoseptal (MIS) segment of patient number 8, obtained by both ultrasound systems during intrinsic rhythm (black: GE and grey: Philips). The left panel (A) shows the raw strain patterns. In the right panel (B) the signals are normalized and time corrected. The corresponding correlation coefficient was 0.92.

INTRA- AND INTEROBSERVER AGREEMENT

Intra-observer agreement of systolic strain (SS) and time to peak strain (TTP) was calculated by comparing the first and second analysis of the first (offline) observer (W.E.). There was an interval of twelve weeks between both data-analyses of the first observer. For interobserver agreement, the first dataset was compared to the dataset of a second observer (M.P.). Both investigators were blinded for their own and/or the other investigators findings.

STATISTICAL ANALYSIS

The statistical analysis was performed using SPSS 17.0 (SPSS Inc, Chicago, USA). Correlation of heart rate was also performed by two-tailed Pearson correlation. Duration of systole was compared with a paired T-test. Mixed models using repeated measurements were employed to compare the calculated values of all the parameters. Post-hoc analysis of the mixed models was performed by Bonferroni correction. Values of SRS were compared by a paired T-test and a two-tailed Pearson correlation coefficient. Bland-Altman plots were constructed for intra- and interobserver variability, of which the mean and 95% confidence interval were calculated. A p-value <0.05 was considered significant.

RESULTS

Patient characteristics are presented in table 1. For STE analysis, 119 (90%) segments were analysable for GE and 121 (92%) segments were analysable for Philips. The framerate was comparable between GE (81.5±15.1Hz) and Philips (81.3±15.4Hz). Heart rate was also comparable during the measurements with the two systems (GE: 64.0±12.2bpm, Philips: 63.9±11.6bpm) with a Pearson correlation coefficient of 0.91 (p<0.01). Pearson correlation of AVC was high (0.72, p<0.001) between vendors, although the mean AVC time of GE was significantly shorter than Philips derived AVC time (349 vs. 385ms respectively, p<0.001).

SYSTOLIC STRAIN AND TIME TO PEAK STRAIN

Results of SS and TTP are displayed in table 2. For all settings and segments, SS was on average a factor 1.4 higher for GE-acquired and –analysed signals as compared to Philips (p<0.001). Mean difference for SS between vendors was -5.49% (±4.96%, figure 4). Overall TTP was higher for Philips-derived strain signals than for GE (17±89ms), but this difference was relatively small and non-significant (p=0.053). Although the confidence interval of the difference between GE and Philips derived TTP was wide (-157 - 191ms, figure 4).

TABLE 1. Baseline characteristics

Criteria	Median (IQR) (n=11)
Gender (male)	9 (82%)
Age (years)	60.2 (57.7-68.3)
Time since CRT implantation (months)	10.8 (9.6-42.8)
BMI (kg/m ²)	26.4 (24.8-27.7)
LVEF (%)	47.0 (37.0-52.0)
LVESV (ml)	77.1 (55.7-99.6)
Percentage BIV pacing (%)	99.1 (98.2-99.8)

Median values and the interquartile range (IQR) (between parentheses) are given; except for gender, where the number of males and percentage are given. BIV: biventricular, BMI: body mass surface index, LVEF: left ventricular ejection fraction, LVESV: left ventricular end-systolic volume.

TABLE 2. Strain values

	Systolic strain (%)			Time to peak strain (ms)		
	GE	Philips	P-value	GE	Philips	P-value
Total	18.9 (4.7)	13.4 (4.3)	<0.001	384 (77)	404 (83)	0.053
Setting						
BIV	19.3 (4.3)	13.9 (3.8)	<0.001	408 (49)	414 (79)	0.772
LV	19.5 (4.8)	13.4 (5.0)	<0.001	399 (58)	420 (61)	0.103
RV	18.5 (4.6)	13.0 (4.1)	<0.001	377 (61)	394 (93)	0.582
OFF	18.3 (3.9)	13.3 (4.5)	<0.001	352 (77)	388 (95)	0.103
Segment						
BIS	17.8 (4.0)	13.2 (3.5)	<0.001	385 (74)	419 (88)	0.072
MIS	19.0 (3.3)	13.4 (4.3)	<0.001	371 (57)	382 (68)	0.367
AplS	20.4 (6.3)	13.5 (5.1)	<0.001	399 (98)	413 (91)	0.494

Mean values of absolute strain and time to peak strain. Total number of analysed patterns was 119 (90%) for General Electric (GE) and 121 (92%) for Philips. One standard deviation is given between parentheses. BIV: biventricular, LV: left ventricular pacing, RV: right ventricular pacing, OFF: intrinsic rhythm, BIS: basal inferoseptal segment, MIS: mid inferoseptal segment, AplS: apical inferoseptal segment.

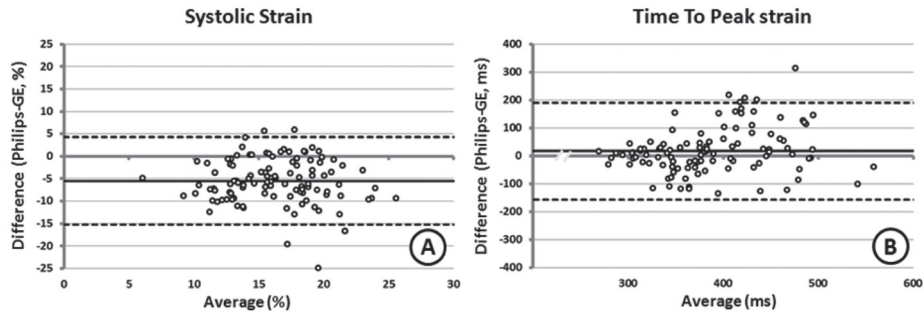


FIGURE 4. Bland Altman plots

Bland Altman plots of systolic strain (SS) and time to peak strain (TTP). Mean difference is presented as a horizontal black line, while the 95% confidence interval is given with dashed lines.

STRAIN PATTERN CORRELATION

As can be appreciated from the examples shown in figures 1 and 3, the normalized strain patterns during the entire cardiac cycle were highly similar between the two vendors. Overall comparability of the normalized strain patterns, expressed as correlation coefficient (R^2), was high (median: 0.68, interquartile range (IQR): 0.53-0.82). Correlation coefficients for the specific pacemaker settings were comparable. There were no significant differences in correlation coefficient between biventricular pacing (0.69, 0.52-0.84), single site LV pacing (0.71, 0.54-0.87), single site RV pacing (0.63, 0.46-0.71), and intrinsic rhythm (0.71, 0.62-0.80). For the specific segments, correlation was significantly higher in the MIS segment (0.78, 0.69-0.88) than in both BIS (0.60, 0.48-0.71, $p < 0.001$) and ApIS segments (0.63, 0.47-0.73, $p < 0.001$). There were no significant differences between the BIS and ApIS segment.

STRAIN PATTERN RECOGNITION

The two systems consistently (100%) recognized the same type of LBBB pattern. Pattern recognition of intrinsic rhythm led to LBBB-1 in three cases (double-peaked systolic shortening) and LBBB-3 in all other cases (pseudonormal shortening with a late-systolic shortening peak followed by less pronounced end-systolic stretch. See figure 5 for a detailed overview of strain patterns and their categorization.

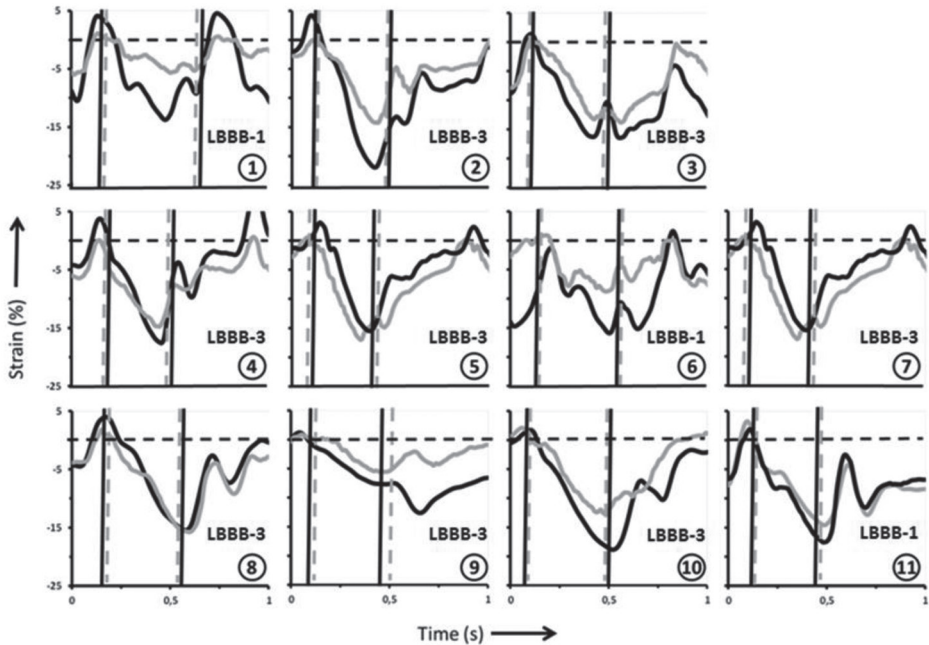


FIGURE 5. Overview of LBBB strain patterns of all patients

Overview of intrinsic rhythm (LBBB) strain patterns of the mid inferoseptal (MIS) segment, emphasizing the difference in onset and end of systole (dashed lines) in the eleven patients. Strain patterns are only time-corrected, and not normalized. The recognized LBBB strain pattern is indicated in the lower right corner. Black: GE, grey: Philips.

SRS

The correlation between the SRS values obtained by the two systems was low and non-significant (Pearson's $R=0.137$, $p=0.480$). The mean value for SRS during intrinsic rhythm differed slightly between GE ($1.47 \pm 2.32\%$) and Philips ($1.85 \pm 1.90\%$).

INTRA-OBSERVER AGREEMENT

The overall intra-observer agreement for SS was high. The average difference in SS between both measurements of the first observer was -0.02% (95% CI: -4.65 - 4.69) for GE and -0.26% (-4.28 - 4.02) for Philips based measurements. Intra-observer agreement of TTP showed an average difference between both measurements of -5 ms (-91 - 80) for GE-derived strain and -38 ms (-180 - 104) for Philips-derived strain.

INTEROBSERVER AGREEMENT

The overall interobserver agreement for SS was good. The average difference between measurements of the first and second observer was for 0.57% (-6.43-5.28) GE and -0.03% (-3.98-3.90) for Philips. Interobserver agreement of TTP showed an average difference between both observers of -6ms (-86-99) for GE-derived strain and -1ms (-137-136) for Philips-derived strain.

DISCUSSION

This study shows that the results of speckle tracking echocardiography in dyssynchronous heart failure are dependent on the echocardiographic system used. This study is the first to compare strain patterns of dyssynchronous ventricles between two commonly used ultrasound systems and corresponding software. Septal strain signals derived from GE and Philips ultrasound systems with corresponding speckle tracking analysis software have a comparable pattern, but the systolic amplitude (SS) was a factor 1.4 larger when measured with the GE system compared to the Philips system. TTP was not significantly different, but showed a trend towards a difference between systems. SRS, a parameter of dyssynchrony, did not correlate at all between systems. This was partly also due to inter-vendor differences in the timing of systole, obtained from Doppler flow measurements in the timing of aortic valve closure.

COMPARABILITY OF STRAIN PATTERNS

Categorization of LBBB septal strain patterns can be used to predict CRT response,¹⁸ the agreement between both vendors is therefore of importance. SRS is a parameter derived from those strain signals and is highly promising as predictor of CRT response (studies based on GE system).^{12, 15, 19} Because SRS is a complicated strain index, it is an excellent test case for vendor comparison. Unfortunately, the correlation of SRS values derived by the two vendors was poor. The latter may be explained by several factors. SRS values are often small in contrast to the entire pattern. Complex deformation patterns are relatively more influenced by variability in echo acquisition. Minor deflections, such as SRS, can therefore be under- or overestimated. The contraction of the myocardium is a complex three-dimensional (3D) movement, whereas conventional STE is based on 2D images. Saito et al. demonstrated the

effect of out of plane motion of speckles in two-dimensional (2D) ultrasound images.²⁰ Minor probe placement differences between investigations introduce variations, although limited by using the same echocardiography specialist for each patient. The exact same position of the ultrasound probe is unachievable. 3D STE could avoid this relative angle dependency and form an alternative for 2D acquisition.^{21, 22} However, differences between vendors in strain values are even known to occur when using 3D STE analysis.^{11, 23} Another explanation could be the observed differences in AVC between the systems. A systematic error between vendors in determining aortic valve closure timing by Doppler signals is therefore likely. Note that timing of AVC is crucial for correct SRS quantification, because systolic stretch often continues into the isovolumic relaxation phase. Over- or underestimation of the onset of the systolic period by subjective, observer-dependent timing of valve closure from Doppler signals can easily occur and bias the TTP and SRS results. Moreover, time delays between the ultrasound- and ECG-signal within the ultrasound machine are known to exist.²⁴ Time delays between the ECG signal and Doppler and between the ECG and B-mode images may well vary. These unknown amounts of time delays could have biased the timing of systole and therefore values of TTP and SRS.

Remarkably there were no patients with a LBBB-2 type strain pattern. The types of strain patterns are based on computer models and patient data of echocardiographic examinations prior to CRT implantation. As patients in this study were analysed at least 6 months after implantation, reverse remodelling has influenced the interaction of septal and lateral wall. LBBB-2 pattern is seen in patients with hypo-contraction of the septum and normal contraction of the lateral wall.¹⁵ As resynchronization recruits the septum, septal contraction is increased after remodeling.²⁵ Even when biventricular pacing is turned off, septal contraction is probably better compared to before implantation. The fact that there were no LBBB-2 patterns found, could be the result of a more comparable contractile function of septal and lateral wall, resulting in LBBB-1 and -3 patterns. Due to the small sample size, it could also be a coincidence.

SYSTOLIC STRAIN

The poor agreement of SS between both vendors hampers broad application of STE. Peak strain values have been used as criterion for the absence or presence of scar (\geq and $<4.5\%$ peak longitudinal strain, for example), so a difference between the two systems creates a considerable grey zone in the adjudication of scar.²⁶ It is not clear whether the differences

found are the result of an overestimation of deformation by the GE, an underestimation by Philips, or a combination of both. GE derived strain often displayed pre-stretch (see figure 5), which could attribute to the higher SS, although the parts of pre-stretch are too small to account for the difference between both vendors. Differences in the reference frame (L_0) are another explanation. As strain is the difference of deformation relative to a baseline value ($\sigma=(L-L_0)/L_0$). Even if the definition of the reference frame (top of the R-wave) is similar, the actual phase of the mechanical deformation can be different. As the chosen ECG lead can differ between vendors, beside possible timing differences between the ECG signal and B-mode recordings.

The systematic difference in strain amplitude between GE and Philips is not in line with results of earlier studies that found comparable or higher peak strain values for Philips.^{7-9, 18, 27} However, the assessed parameters for spatial displacement differ between this and other studies. SS is the amplitude of an entire beat (figure 1A), in contrast to peak (systolic) strain values, which are often limited to systole and neglect positive deflections above zero (i.e. pre-stretch). Moreover, methods for determining peak strain were often not mentioned or even differed between modalities. Koopman et al. defined the peak strain of GE within the systole and also used post-systolic values for Philips.⁷ This could have led to overestimation, as post-systolic strain values can be larger (more negative). Besides that, those studies used an earlier version of QLAB (7.0 red.), were not performed in dyssynchronous hearts (which have more complex strain patterns) and measured global strain, thereby including the LV free wall.^{9, 27}

The absence of comparison with a gold standard is a limitation of this and many STE studies. GE speckle tracking has been compared to MRI tagging. But one study by Amundsen et al. observed an underestimation of longitudinal strain by GE.²⁸, though they used an unvalidated software package (TagTrack) for MRI tagging. These results are in contrast to another study, which found an overestimation of longitudinal peak strain by GE, with validated MRI tagging software (HARP).²⁹ Unfortunately there are no studies comparing Philips derived strain values to MRI tagging.

INTRA- AND INTEROBSERVER AGREEMENT

Intra- and interobserver agreement was good, with acceptable limits of agreement in Bland Altman plots for both SS and TTP in the two vendors. These values are in line with earlier studies, which found relatively high intra- and interobserver agreement of peak strain for

longitudinal strain analysis with QLAB and EchoPac.^{7, 8, 27} The mean difference in TTP was higher for Philips compared to GE, for both intra- and interobserver agreement. A possible explanation could be the observed noise in Philips derived strain patterns, whereas GE derived strain appears more smoothed.

DIFFERENCES BETWEEN ALGORITHMS

Strain value depends on the chosen reference length (L_0), which, on its turn, depends on the reference moment. Differences in the timing of L_0 between vendors will result in changes in strain values. As the R-wave is influenced by the chosen ECG-vector, ECG-lead placement and definition of the software, minor changes in timing of L_0 will result in variability of strain values.

An obvious discrepancy between the algorithms is the ROI. As mentioned, QLAB 8.0 has an additional segment, situated at the apex. As a result, the position of the segments on the myocardium is shifted. The correlation coefficients found could therefore be an underestimation. The lower correlations between vendors found in the BIS and ApIS segments compared to the MIS segment may also be explained by their position on the ultrasound window, often influenced by the probe angle and thereby the view.

Both vendors cooperate in the currently ongoing European Association of Cardiovascular Imaging (EACVI) and the American Society of Echocardiography (ASE) Standardization Task Force, standardizing (longitudinal) strain derived by STE.³⁰ Results on standardization are of interest, as this study shows that absolute values differ between two commonly used ultrasound systems.

LIMITATIONS

The small patient population may be seen as a limitation, although the number of CRT settings, and attuned statistical analysis (mixed model with repeated measurements) compensate, resulting in 44 unique echocardiographic images of each vendor. Variations in patient position could have influenced echocardiographic image quality, whereas small variations in heart rhythm may have confined comparability of strain pattern analysis. These variations were reduced by consecutive acquisition with the two systems by a single echocardiographer. This study however lacks information on test–retest variability, as the

study protocol did not include repeated image acquisition within the same ultrasound systems. Earlier mentioned differences between vendors, regarding segments and size of the ROI, and definition and timing of L_0 , limit comparability; and these discrepancies endorse the need for standardization. The STE analysis software used in this study was up-to-date at the time of investigation, however recently became outdated. As mentioned, recent software of both vendors underwent standardization and should be more uniform compared to the found discrepancies.

CONCLUSIONS

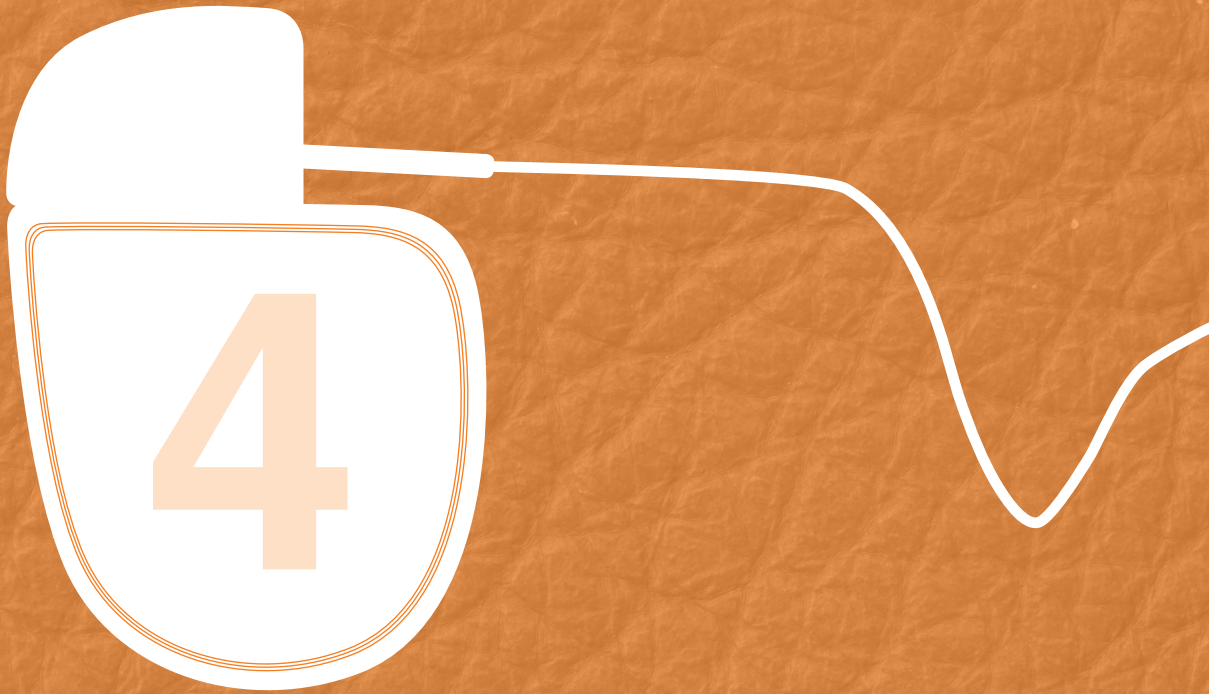
The two ultrasound systems and their corresponding analysis software provide similar shapes of strain patterns. However, there are large differences in absolute strain amplitude and septal rebound stretch. Moreover, timing of systole differs between the systems, which may influence calculated values of strain during systole. As a consequence, values obtained by different systems are difficult to compare. The present data therefore clearly emphasize the need for standardization of speckle tracking echocardiography analysis on such parameters. Future improvements of speckle tracking should focus on standardization by achieving consensus on a similar marker for L_0 , the region of interest, as well as spatial displacement interpretation. For now, clinical decision making should be restricted to pattern analysis.

REFERENCES

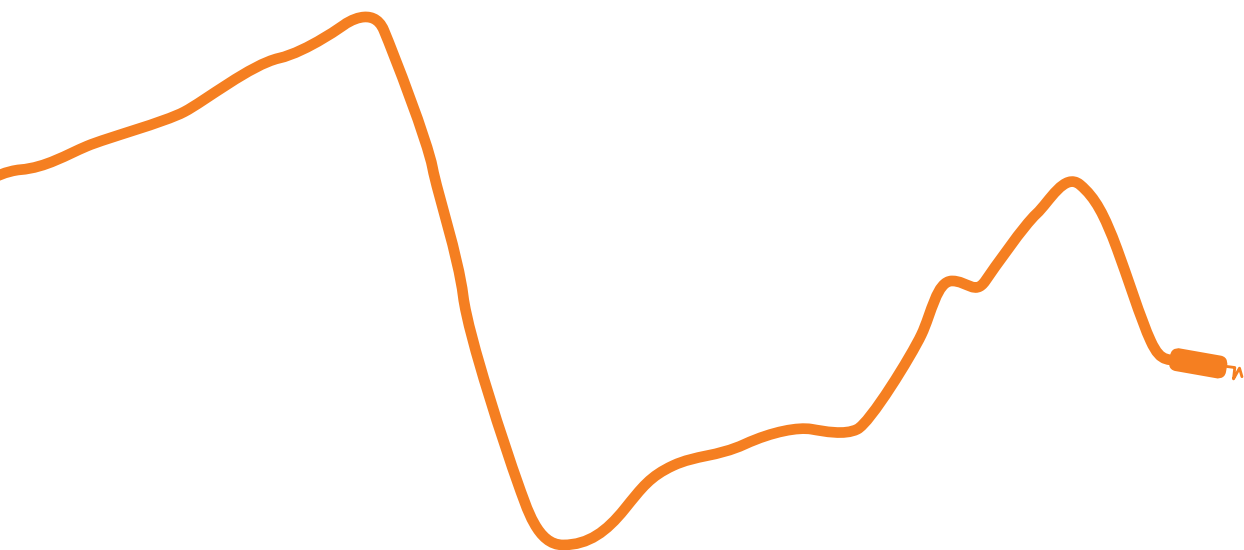
1. Teske AJ, De Boeck BW, Melman PG, Sieswerda GT, Doevendans PA, Cramer MJ. Echocardiographic quantification of myocardial function using tissue deformation imaging, a guide to image acquisition and analysis using tissue Doppler and speckle tracking. *Cardiovasc Ultrasound*. 2007;5:27-46.
2. Leitman M, Lysyansky P, Sidenko S, Shir V, Peleg E, Binenbaum M, et al. Two-dimensional strain-a novel software for real-time quantitative echocardiographic assessment of myocardial function. *J Am Soc Echocardiogr*. 2004;17:1021-9.
3. Mollema SA, Nucifora G, Bax JJ. Prognostic value of echocardiography after acute myocardial infarction. *Heart*. 2009;95:1732-45.
4. Parra DA, Vera K. New imaging modalities to assess cardiac function: not just pretty pictures. *Curr Opin Pediatr*. 2012;24:557-64.
5. Cikes M, Sutherland GR, Anderson LJ, Bijnens BH. The role of echocardiographic deformation imaging in hypertrophic myopathies. *Nat Rev Cardiol*. 2010;7:384-96.
6. Leenders GE, Cramer MJ, Bogaard MD, Meine M, Doevendans PA, De Boeck BW. Echocardiographic prediction of outcome after cardiac resynchronization therapy: conventional methods and recent developments. *Heart Fail Rev*. 2011;16:235-50.
7. Koopman LP, Slorach C, Hui W, Manlhiot C, McCrindle BW, Friedberg MK, et al. Comparison between different speckle tracking and color tissue Doppler techniques to measure global and regional myocardial deformation in children. *J Am Soc Echocardiogr*. 2010;23:919-28.
8. Koopman LP, Slorach C, Manlhiot C, McCrindle BW, Jaeggi ET, Mertens L, et al. Assessment of myocardial deformation in children using Digital Imaging and Communications in Medicine (DICOM) data and vendor independent speckle tracking software. *J Am Soc Echocardiogr*. 2011;24:37-44.
9. Sun JP, Lee AP, Wu C, Lam YY, Hung MJ, Chen L, et al. Quantification of left ventricular regional myocardial function using two-dimensional speckle tracking echocardiography in healthy volunteers - A multi-center study. *Int J Cardiol*. 2012;167(2):495-501.
10. Nelson MR, Hurst RT, Raslan SF, Cha S, Wilansky S, Lester SJ. Echocardiographic measures of myocardial deformation by speckle-tracking technologies: the need for standardization? *J Am Soc Echocardiogr*. 2012;25:1189-94.

11. Gayat E, Ahmad H, Weinert L, Lang RM, Mor-Avi V. Reproducibility and inter-vendor variability of left ventricular deformation measurements by three-dimensional speckle-tracking echocardiography. *J Am Soc Echocardiogr.* 2011;24:878-85.
12. De Boeck BW, Teske AJ, Meine M, Leenders GE, Cramer MJ, Prinzen FW, et al. Septal rebound stretch reflects the functional substrate to cardiac resynchronization therapy and predicts volumetric and neurohormonal response. *Eur J Heart Fail.* 2009;11:863-71.
13. Risum N, Jons C, Olsen NT, Fritz-Hansen T, Bruun NE, Hojgaard MV, et al. Simple regional strain pattern analysis to predict response to cardiac resynchronization therapy: rationale, initial results, and advantages. *Am Heart J.* 2012;163:697-704.
14. Marechaux S, Guiot A, Castel AL, Guyomar Y, Semichon M, Delelis F, et al. Relationship between two-dimensional speckle-tracking septal strain and response to cardiac resynchronization therapy in patients with left ventricular dysfunction and left bundle branch block: a prospective pilot study. *J Am Soc Echocardiogr.* 2014;27:501-11.
15. Leenders GE, Lumens J, Cramer MJ, De Boeck BW, Doevendans PA, Delhaas T, et al. Septal deformation patterns delineate mechanical dyssynchrony and regional differences in contractility: analysis of patient data using a computer model. *Circ Heart Fail.* 2012;5:87-96.
16. Negishi K, Lucas S, Negishi T, Hamilton J, Marwick TH. What is the primary source of discordance in strain measurement between vendors: imaging or analysis? *Ultrasound Med Biol.* 2013;39:714-20.
17. Cerqueira MD, Weissman NJ, Dilsizian V, Jacobs AK, Kaul S, Laskey WK, et al. Standardized myocardial segmentation and nomenclature for tomographic imaging of the heart: a statement for healthcare professionals from the Cardiac Imaging Committee of the Council on Clinical Cardiology of the American Heart Association. *Circulation.* 2002;105:539-42.
18. Castel AL, Szymanski C, Delelis F, Levy F, Menet A, Mailliet A, et al. Prospective comparison of speckle tracking longitudinal bidimensional strain between two vendors. *Arch Cardiovasc Dis.* 2014;107:96-104.
19. Lumens J, Leenders GE, Cramer MJ, De Boeck BW, Doevendans PA, Prinzen FW, et al. Mechanistic evaluation of echocardiographic dyssynchrony indices: patient data combined with multiscale computer simulations. *Circ Cardiovasc Imaging.* 2012;5:491-9.
20. Saito K, Okura H, Watanabe N, Hayashida A, Obase K, Imai K, et al. Comprehensive evaluation of left ventricular strain using speckle tracking echocardiography in normal adults: comparison of three-dimensional and two-dimensional approaches. *J Am Soc Echocardiogr.* 2009;22:1025-30.

21. Altman M, Bergerot C, Aussoleil A, Davidsen ES, Sibellas F, Ovize M, et al. Assessment of left ventricular systolic function by deformation imaging derived from speckle tracking: a comparison between 2D and 3D echo modalities. *Eur Heart J Cardiovasc Imaging*. 2014;15:316-23.
22. Maffessanti F, Nesser HJ, Weinert L, Steringer-Mascherbauer R, Niel J, Gorissen W, et al. Quantitative evaluation of regional left ventricular function using three-dimensional speckle tracking echocardiography in patients with and without heart disease. *Am J Cardiol*. 2009;104:1755-62.
23. Aly MF, Kleijn SA, de Boer K, Abd El-Hady YA, Sorour KA, Kandil HI, et al. Comparison of three-dimensional echocardiographic software packages for assessment of left ventricular mechanical dyssynchrony and prediction of response to cardiac resynchronization therapy. *Eur Heart J Cardiovasc Imaging*. 2013;14:700-10.
24. Walker A, Olsson E, Wranne B, Ringqvist I, Ask P. Time delays in ultrasound systems can result in fallacious measurements. *Ultrasound Med Biol*. 2002;28:259-63.
25. Klimusina J, De Boeck BW, Leenders GE, Faletra FF, Prinzen F, Averaimo M, et al. Redistribution of left ventricular strain by cardiac resynchronization therapy in heart failure patients. *Eur J Heart Fail*. 2011;13:186-94.
26. Roes SD, Mollema SA, Lamb HJ, van der Wall EE, de Roos A, Bax JJ. Validation of echocardiographic two-dimensional speckle tracking longitudinal strain imaging for viability assessment in patients with chronic ischemic left ventricular dysfunction and comparison with contrast-enhanced magnetic resonance imaging. *Am J Cardiol*. 2009;104:312-7.
27. Risum N, Ali S, Olsen NT, Jons C, Khouri MG, Lauridsen TK, et al. Variability of global left ventricular deformation analysis using vendor dependent and independent two-dimensional speckle-tracking software in adults. *J Am Soc Echocardiogr*. 2012;25:1195-203.
28. Bansal M, Cho GY, Chan J, Leano R, Haluska BA, Marwick TH. Feasibility and accuracy of different techniques of two-dimensional speckle based strain and validation with harmonic phase magnetic resonance imaging. *J Am Soc Echocardiogr*. 2008;21:1318-25.
29. Amundsen BH, Crosby J, Steen PA, Torp H, Slordahl SA, Stoylen A. Regional myocardial long-axis strain and strain rate measured by different tissue Doppler and speckle tracking echocardiography methods: a comparison with tagged magnetic resonance imaging. *Eur J Echocardiogr*. 2009;10:229-37.
30. Thomas JD, Badano LP. EACVI-ASE-industry initiative to standardize deformation imaging: a brief update from the co-chairs. *Eur Heart J Cardiovasc Imaging*. 2013;14:1039-40.



Comparison of strain parameters in dyssynchronous heart failure between speckle tracking echocardiography vendor systems



Wouter M. van Everdingen (MD)¹, Alexander H. Maass (MD, PhD)², Kevin Vernooij (MD, PhD)³, Mathias Meine (MD, PhD)¹, Cornelis P. Allaart (MD, PhD)⁴, Frederik J. de Lange (MD, PhD)⁵, Arco J. Teske (MD PhD)¹, Bastiaan Geelhoed (PhD)², Michiel Rienstra (MD, PhD)², Isabelle C. Van Gelder (MD, PhD)², Marc A. Vos (PhD)⁶, Maarten J. Cramer (MD, PhD)¹

¹ Department of Cardiology, University Medical Center Utrecht, Utrecht, The Netherlands.

² Department of Cardiology, Thoraxcenter, University of Groningen, University Medical Center Groningen, Groningen.

³ Department of Cardiology, Maastricht University Medical Center, Maastricht, The Netherlands.

⁴ Department of Cardiology, VU University Medical Center, Amsterdam, The Netherlands.

⁵ Department of Cardiology, Academic Medical Center, Amsterdam, The Netherlands.

⁶ Department of Medical Physiology, University of Utrecht, Utrecht, The Netherlands.

ABSTRACT

Background: Although mechanical dyssynchrony parameters derived by speckle tracking echocardiography (STE) may predict response to cardiac resynchronization therapy (CRT), comparability of parameters derived with different STE vendors is unknown.

Methods: In the MARC study, echocardiographic images of heart failure patients obtained before CRT implantation were prospectively analysed with vendor specific STE software (GE EchoPac and Philips QLAB) and vendor-independent software (TomTec 2DCPA). Response was defined as change in left ventricular (LV) end-systolic volume between examination before and six-months after CRT implantation. Basic longitudinal strain and mechanical dyssynchrony parameters (septal to lateral wall delay (SL-delay), septal systolic rebound stretch (SRSsept), and systolic stretch index (SSI)) were obtained from either separate septal and lateral walls, or total LV apical four chamber. Septal strain patterns were categorized in three types. The coefficient of variation and intra-class correlation coefficient (ICC) were analysed. Dyssynchrony parameters were associated with CRT response using univariate regression analysis and C-statistics.

Results: Two-hundred eleven patients were analysed. GE-cohort (n=123): age 68 years (interquartile range (IQR): 61-73), 67% male, QRS-duration 177ms (IQR: 160-192), LV ejection fraction: $26\pm 7\%$. Philips-cohort (n=88): age 67 years (IQR: 59-74), 60% male, QRS-duration: 179ms (IQR: 166-193), LV ejection fraction: 27 ± 8 . LV derived peak strain was comparable in the GE- (GE: $-7.3\pm 3.1\%$, TomTec: $-6.4\pm 2.8\%$, ICC: 0.723) and Philips-cohort (Philips: $-7.7\pm 2.7\%$, TomTec: $-7.7\pm 3.3\%$, ICC: 0.749). SL-delay showed low ICC values (GE vs. TomTec: 0.078 and Philips vs. TomTec: 0.025). ICC's of SRSsept and SSI were higher but only weak (GE vs. TomTec: SRSsept: 0.470, SSI: 0.467) (Philips vs. QLAB: SRSsept: 0.419, SSI: 0.421). Comparability of septal strain patterns was low (Cohen's kappa, GE vs. TomTec: 0.221 and Philips vs. TomTec: 0.279). Septal strain patterns, SRSsept and SSI were associated with changes in LV

end-systolic volume for all vendors. SRSsept and SSI had relative varying C-statistic values (range: 0.530-0.705) and different cut-off values between vendors.

Conclusions: Although global longitudinal strain analysis showed fair comparability, assessment of dyssynchrony parameters was vendor specific and not applicable outside the context of the implemented platform. While the standardization taskforce took an important step for global peak strain, further standardization of STE is still warranted.

BACKGROUND

4

Speckle tracking echocardiography (STE) is used to assess myocardial deformation and strain in research setting as well as in clinical practice.^{1,2} The use of STE in cardiac resynchronization therapy (CRT) has received increasing interest the past years, with respect to multiple aspects: optimization of left ventricular (LV) lead positioning, myocardial viability, optimization of CRT device configuration, determining mechanical dyssynchrony, and predicting volumetric response and outcome.³⁻⁷ Response prediction is an important aspect of clinical decision making, since 20-50% of patients are still non-responders to CRT despite meeting internationally acknowledged selection criteria.⁸ Prediction of volumetric response and outcome to CRT has been approached using several STE derived parameters for mechanical dyssynchrony.^{3, 7, 9, 10} Publications on these parameters mainly use STE software of General Electric EchoPac (Chicago, Illinois, United States).^{3, 9, 11, 12} However, several other commercially available vendor dependent and independent software platforms have been developed for ST.^{9, 10, 13} Between these platforms, differences in derived results are known, complicating the interpretation of specific study results and restricting their use in clinical practice.^{14, 15} A taskforce of the European Association of Cardiovascular Imaging and American Society of Echocardiography (EACVI/ASE) was appointed to standardize longitudinal strain results and specifically global values.¹⁶ However, inter vendor comparability of results obtained in patients with LV dyssynchrony is unknown. It was the aim of this study to compare strain parameters and more specifically dyssynchrony parameters derived from longitudinal strain analysis of different vendors of STE software, implemented specifically in CRT patients, as well as the association of derived dyssynchrony parameters with volumetric response to CRT. STE software of two commonly used vendors was used (i.e. GE EchoPac and Philips QLAB (Philips Medical Systems, Best, The Netherlands)), and the vendor-independent system of TomTec 2DCPA (TomTec Imaging Systems GmbH, Unterschleissheim, Germany). The hypothesis of this study is that vendors may have good agreement on global parameters and timing indices in patients eligible for CRT, while agreement on more detailed parameters and dyssynchrony parameters may be poor.

MATERIAL AND METHODS

STUDY DESIGN

The Markers and Response to CRT (MARC) study was designed to investigate predictors for response on CRT, including several echocardiographic parameters.¹⁷ The study was initiated and coordinated by the six centres within the framework of the Centre for Translational Molecular Medicine (CTMM), project COHFAR (grant 01C-203), and additionally supported by Medtronic (Fridley, Minnesota, USA). Study monitoring was done by Medtronic, data management and validation by the investigators (MR, BG) in collaboration with Medtronic. The study was approved by the institutional review boards of all participating centres. All patients gave written informed consent. The trial was registered at clinicaltrials.gov: NCT01519908.

STUDY PARTICIPANTS

Two hundred and forty patients eligible for CRT according to the most recent international guidelines were included in the MARC study.^{18, 19} In short, MARC study inclusion criteria were: sinus rhythm and optimal pharmacological heart failure therapy, QRS-duration ≥ 130 ms in patients with left bundle branch block (LBBB) and QRS-duration of ≥ 150 ms in non-LBBB patients with NYHA class II and QRS-duration ≥ 120 ms in LBBB patients with NYHA class III. Exclusion criteria were severe renal insufficiency, an upgrade from a bradycardia pacemaker or CRT-P to CRT-D, permanent atrial fibrillation, flutter or tachycardia, right bundle branch block, and permanent 2nd or 3rd degree atrioventricular block. Before and six months after CRT implantation, data were recorded at the outpatient department, including electrocardiographic and echocardiographic examination. Patients were excluded for this sub-analysis if frame rate of the apical four chamber (AP4CH) view was below 35Hz, in case of irregular heart rhythm, unanalysable images due to technical errors or if image quality was very poor.

ECHOCARDIOGRAPHIC EXAMINATION

Echocardiographic examinations were performed by participating centres and analysed at the echocardiographic core lab situated in the UMC Utrecht (Utrecht, the Netherlands). Echocardiographic examinations made in this study were performed on either GE Vivid7, GE Vivid9, or Philips iE33 ultrasound machines. Standard images included a AP4CH view,

zoomed and focused on the LV. Of these images both image quality and frame rate were optimized for offline analysis. Analysis of apical rocking and interventricular mechanical delay (IVMD) are described in earlier work.¹⁷ Pulsed-wave Doppler images of the LV outflow tract were obtained for definition of aortic valve closure time. QRS-onset and aortic valve closure time were used to define systole.

VOLUMETRIC RESPONSE

LV ejection fraction, LV end-systolic and end-diastolic volumes were measured by biplane Simpson's method.²⁰ Volumetric response to CRT was defined as the percentage of change in LV end-systolic volume between echocardiographic examination before and six months after CRT implantation. Patients were classified as responder in case of $\geq 15\%$ reduction in LV end-systolic volume.

SPECKLE TRACKING ECHOCARDIOGRAPHY

Echocardiographic AP4CH images were subjected to offline speckle tracking analysis (WE, MC). The optimal images for speckle tracking were selected and used for the vendor dependent and independent platform (supplemental figure 1). All images were scored for quality (poor, average, or high) by two experienced observers. Image quality was categorized as high if the total LV myocardium was visible during the entire cardiac cycle, average if one or two segments were not clearly visible and poor in all other cases. Images were exported to vendor specific software (GE EchoPac 11.3 and Philips QLAB 10.0) in standard formats and exported as DICOM-files for vendor independent software (TomTec 2D Cardiac Performance Analysis (2DCPA) version 1.2.1.2). Speckle tracking was performed with standard settings for all vendors. For each platform, a region of interest (ROI) was placed by user defined markers to incorporate the entire myocardial wall. Repeat adjustments of the ROI were done if tracking quality was insufficient. The myocardial wall was separated into six segments by all platforms (i.e. basal and mid inferoseptal, apical septal, apical lateral and basal and mid anterolateral). Philips QLAB analyses an additional true apical segment (i.e. 17 segment model of the AHA), which was excluded for the septal and lateral wall strain curves, as it was part of both walls.²¹ Segments were also excluded if adequate tracking was not achievable. The basal inferoseptal, mid inferoseptal and apical septal segment were averaged into a global septal wall strain curve. The apical lateral, basal anterolateral and mid anterolateral segment were averaged into a global lateral wall strain curve. Results from

a single wall were excluded if tracking of more than one segment was unachievable. The entire myocardial wall was used for both Philips and GE analysis. TomTec analysis resulted in separate datasets for the endocardial and epicardial border. The epicardial border at the apical and mid ventricular lateral wall was often outside the echocardiographic window, and was therefore excluded in TomTec analysis. This was done even though differences between endo- and epicardial layers are known.²² The marker for reference length (L_0) was placed at onset of QRS-complex for GE derived images, both for GE EchoPac and TomTec 2DCPA. L_0 of Philips derived images could not be altered in QLAB and was automatically placed in the QRS-complex. L_0 was manually placed at a similar position for Philips derived images analysed with TomTec 2DCPA. Therefore, both direct comparisons (GE vs. TomTec and Philips vs. TomTec) had similar L_0 positions.

OFFLINE ANALYSIS

Results of speckle tracking analysis were stored and exported for offline analysis with Matlab 2014b (Mathworks, Natick, MA, USA). Author written Matlab scripts allowed for input of valve closure times and semi-automatic calculation of strain parameters. Results of strain parameters were based on global strain curves. Global strain curves were averages of the segments representing the global LV or the separate septal or lateral wall.

PARAMETERS

BASIC STRAIN PARAMETERS

Five basic strain parameters were obtained for global LV, septal wall and lateral wall strain curves. 1) Pre-stretch was defined as maximal positive peak strain, occurring after QRS onset and before shortening (figure 1). 2) Peak strain was the maximal negative peak strain during the entire cardiac cycle. 3) Systolic strain was the maximal negative strain during systole. 4) Time to maximal peak (TTP_{max}) was the time difference from L_0 to most negative peak strain. 5) Time to first peak (TTP_{first}) was the time difference from L_0 to first negative peak.

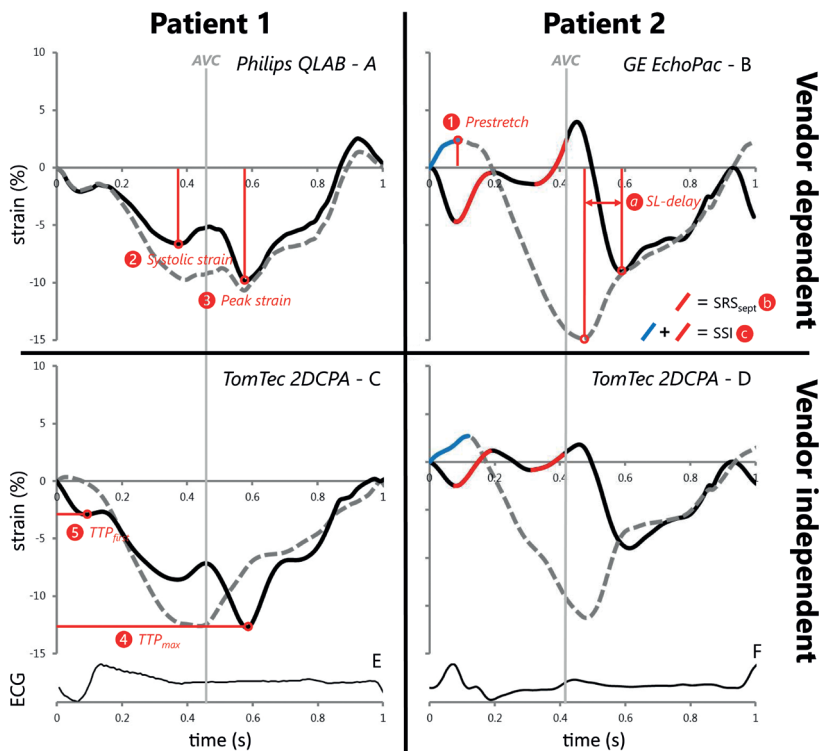


FIGURE 1. Examples strain patterns of two patients

Examples strain curves of the septal (solid black curve) and lateral wall (dashed grey curve) derived with vendor dependent and independent speckle tracking echocardiography software. Aortic valve closure (AVC) is marked with a thin solid grey line. Philips was used for echocardiographic examination in patient number 1 (A & C), and GE was used for patient 2 (B & D). Corresponding ECGs are shown below (E & F). SRS_{sept} is marked red and lateral wall pre-stretch is marked blue in patient number 2. AVC: aortic valve closure, MVC: mitral valve closure, SL-delay: septal to lateral wall delay, SRS_{sept}: septal systolic rebound stretch, SSI: systolic stretch index, TTP_{first}: time to first peak shortening, TTP_{max}: time to maximal peak shortening.

DYSSYNCHRONY PARAMETERS

Four dyssynchrony parameters were compared. a) Septal to lateral wall delay (SL-delay) was calculated as the difference in TTP_{max} of the septal and lateral walls. b) Septal systolic rebound stretch (SRS_{sept}) was defined as the cumulative amount of stretch after initial shortening of the septum, occurring during systole (figure 1).³ c) Systolic stretch index (SSI) was defined as the sum of SRS_{sept} and lateral wall pre-stretch.⁹ d) Septal strain curves were

categorized in three LBBB pattern types, determined by their shape, based on earlier work of our group.²³ LBBB-1: double-peaked systolic stretch, LBBB-2: early pre-ejection shortening peak followed by prominent systolic stretching and LBBB-3: pseudo normal shortening with a late-systolic shortening peak followed by less pronounced end-systolic stretch (figure 2).

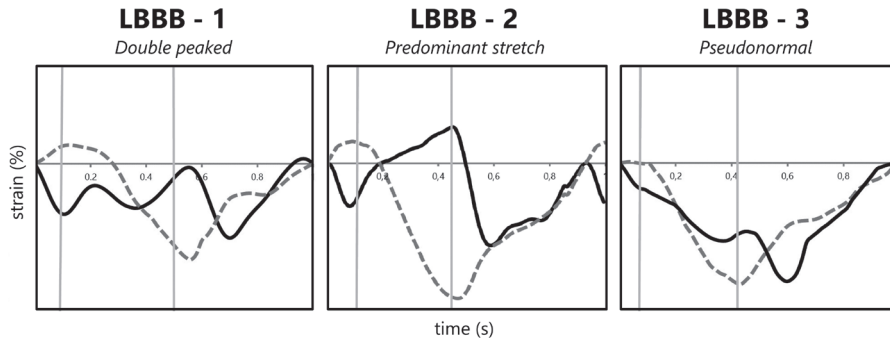


FIGURE 2. Examples of septal strain pattern types

Septal strain patterns are categorized in three types: LBBB-1: double peak rebound stretch, LBBB-2: predominant stretch and LBBB-3: pseudo normal shortening, according to Leenders et al.²³ The septal strain curve is displayed as a solid black line, while the lateral wall strain curve is displayed as a dashed grey line. LBBB: left bundle branch block.

CROSS-CORRELATION

The similarity of strain curves between vendor dependent and independent software was analysed by cross correlation of strain signals obtained from the same patient and image. Strain data of the vendor dependent analysis was interpolated and plotted on the horizontal axis, while data of the vendor independent analysis was plotted on the vertical axis. Least squares fitting ($y=a*x$) of this data was used to calculate the coefficient of determination (R^2). Strain data of the vendor dependent analysis was shifted by steps of 1ms and R^2 was calculated for each step. After a total shift of 100ms, the highest value was used as the optimal correlation coefficient.

INTRA-OBSERVER AGREEMENT

Categorization of septal strain curves of all patients were analysed a second time with vendor-specific and vendor independent software for intra-observer agreement. There was an interval of at least 20 weeks between the data-analyses.

STATISTICAL ANALYSIS

Statistical analysis was performed (BG and MR) using R version 3.2.4 (The R foundation for Statistical Computing), SAS software version 9.4 (SAS Institute, Cary, NC, USA) and the R-packages psych version 1.5.8 (for calculation of Cohen's kappa coefficients, ICCs and their associated p-values). Comparison of subgroups on baseline characteristics and strain parameters of GE and Philips was performed using a student t-test or Wilcoxon test, dependent on normality of data. Categorical data was compared using a Fisher exact test or Chi-Square tests if more than two categories were present. To compare vendor dependent to vendor independent data, strain parameters were compared by a paired t-test or Wilcoxon test, dependent on normality of data. The coefficient of variation (COV), intra-class correlation coefficient (ICC), and Bland-Altman plots were also used for comparison between vendors. For Bland-Altman plots, the mean, standard deviation and 95% confidence interval (i.e. limits of agreement) were calculated. Cross-correlation results were compared using a pairwise t-test with Bonferroni correction. Agreement of LBBB pattern categorization was assessed using Cohen's kappa coefficient. ICC and Cohen's kappa results were classified as follows; ≥ 0.75 : excellent, 0.60-0.74: good, 0.40-0.59: weak, and < 0.40 : poor. Univariate regression analysis with change in LVESV as a continuous variable was used to test dyssynchrony parameters as predictors for response to CRT. The C-statistic and cut-off value were calculated for each dyssynchrony parameter, with volumetric response (LVESV reduction $\geq 15\%$) as a dichotomous parameter. A p-value < 0.05 was considered significant for all tests.

RESULTS

STUDY POPULATION

Two-hundred-eleven of 240 MARC study patients were included in this sub-analysis, 123 in the GE-cohort and 88 in the Philips-cohort. Nineteen patients were excluded for GE analysis, of which five were excluded from the main study, two had irregular heart rhythm, four had a frame rate below 35Hz, four had overall low image quality and two had only one analysable segment for the lateral wall. Ten patients were excluded for Philips analysis, of which four were already excluded from the main study, five were stored in a datafile not analysable for STE and one had a frame rate below 35Hz. There were no significant differences in baseline characteristics between cohorts (table 1), except for frame rate. Frame rate was higher in the GE-cohort (61 ± 12 Hz) compared to the (Philips-cohort 55 ± 7 Hz, $p < 0.001$). LV end-diastolic and end-systolic volumes tended to be lower in the Philips-cohort compared to the GE-cohort. LV ejection fraction was comparable, as were conventional electrical dyssynchrony (i.e. QRS duration and morphology) and mechanical dyssynchrony parameters (i.e. IVMD, apical rocking and septal flash). IVMD was above the cut-off value of 40ms in both groups, septal flash was seen in approximately half of all patients, while apical rocking was observed in around 60% of patients. CRT response rate was non-significantly different in the two cohorts (GE-cohort: 59% vs. Philips-cohort: 65%), with non-significantly differences in end-systolic volume reduction (GE-cohort: $20 \pm 23\%$ vs. Philips-cohort: 25 ± 26 , $p = 0.208$).

GE ECHOCARDIOGRAPHIC IMAGES

GE BASIC STRAIN PARAMETERS

Comparison of strain results obtained with vendor dependent and independent STE software resulted in a good to excellent ICC for peak strain and systolic strain for global LV and septal wall (table 2). COV was relatively low, as was the mean difference in Bland-Altman plots (figure 3). Nevertheless, the standard deviations of the Bland-Altman plots were relatively large, ranging from 2.2 to 2.8%. The ICC of peak and systolic strain of the lateral wall were weak (0.595 and 0.565 respectively), with an even larger standard deviation in Bland-Altman plots (3.6 and 3.7%, respectively). The ICC of TTP_{first} and TTP_{max} of both walls and the global LV were poor to weak, with relatively large COV and large standard deviations in Bland-Altman plots.

TABLE 1. Baseline characteristics

	GE-cohort (n=123)	Philips-cohort (n=88)	p-value
Age (years)	68.3 (61.3-73.4)	67.2 (59.0-73.9)	0.450
Gender (n, % male)	82 (66.7%)	53 (60.2%)	0.384
BMI (kg/m ²)	26.5 (23.8-29.6)	26.2 (23.6-29.3)	0.813
NYHA Class (n, %)			0.869
I	1 (0.8%)	0 (0.0%)	
II	77 (62.6%)	53 (60.2%)	
III	45 (36.6%)	35 (39.8%)	
QRS duration (ms)	177 (160-192)	179 (166-193)	0.293
QRS morphology (n, %)			0.311
LBBB	68 (56.7%)	55 (64.7%)	
IVCD	52 (43.3%)	30 (35.3%)	
LVEDV (ml)	183.3 (148.8-247.7)	168.0 (132.0-211.8)	0.051
LVESV (ml)	135.3 (100.7-194.7)	130.3 (92.8-167.3)	0.087
LVEF (%)	25.6±7.3	26.5±7.9	0.406
LVEDD (cm)	6.3±0.8	6.2±0.8	0.591
IVMD (ms)	47.1±28.8	46.3±30.2	0.855
Apical rocking (n, %)	71 (58.2%)	56 (63.6%)	0.476
Septal flash (n, %)	56 (47.5%)	42 (48.8%)	0.888
Frame rate (Hz)	61±12	55±7	<.001
Image quality (n, %)			0.011
Poor	31 (25.2%)	8 (9.1%)	
Average	54 (43.9%)	50 (56.8%)	
High	38 (31.0%)	30 (34.1%)	
ESV reduction	20.4±22.9	24.9±25.7	0.208
Responders (n, %)	65 (58.6%)	54 (65.1%)	0.375

Standard deviations are given with ± symbol, for non-normal distributed data, the median is given with the interquartile range between brackets. BMI: body mass index, NYHA: New York Heart Association, LV: left ventricular, LVEDV: LV end-diastolic volume, LVESV: LV end-systolic volume, LVEF: LV ejection fraction, LVEDD: LV end-diastolic diameter, IVCD: intra-ventricular conduction delay, IVMD: interventricular mechanical delay.

TABLE 2. Strain parameters derived from GE echocardiographic images

	GE EchoPac (n=123)	TomTec 2DCPA (n=123)	COV	ICC (p-value)	Bland-Altman (mean diff±SD)
LV					
1) Pre-stretch (%)	0.4 (0.0-1.4)	0.7 (0.1-1.7)	1.218	0.631 (<0.001)	-0.3±1.0
2) Peak strain (%)	-7.3±3.1	-6.4±2.8	-0.424	0.723 (<0.001)	-0.8±2.2
3) Systolic strain (%)	-6.4±3.2	-5.6±3.2	-0.504	0.752 (<0.001)	-0.8±2.2
4) TTP _{max} (ms)	511 (426-587)	488 (429-593)	0.201	0.676 (<0.001)	-2±86
5) TTP _{first} (ms)	400 (158-458)	421 (316-471)	0.480	0.195 (0.015)	-34±205
Septum					
1) Pre-stretch (%)	0.3 (0.0-1.0)	0.7 (0.0-1.5)	1.337	0.470 (<0.001)	-0.4±1.1
2) Peak strain (%)	-8.0±3.1	-7.2±3.2	-0.392	0.707 (<0.001)	-0.8±2.4
3) Systolic strain (%)	-6.7±3.5	-6.0±3.5	-0.517	0.667 (<0.001)	-0.7±2.8
4) TTP _{max} (ms)	531 (378-626)	520 (414-606)	0.336	0.261 (0.002)	-9±189
5) TTP _{first} (ms)	208 (135-376)	311 (151-420)	0.521	0.486 (<0.001)	-39±142
Lateral wall					
1) Pre-stretch (%)	1.6 (0.5-3.1)	1.2 (0.2-2.4)	0.951	0.524 (<0.001)	0.3±1.9
2) Peak strain (%)	-8.5 (-11.4- -5.8)	-6.5 (-10.2- -4.3)	-0.462	0.595 (<0.001)	-1.4±3.6
3) Systolic strain (%)	-6.6 (-10.8- -4.2)	-5.5 (-9.0- -3.0)	-0.532	0.565 (<0.001)	-1.2±3.7
4) TTP _{max} (ms)	500 (456-541)	514 (445-556)	0.149	0.444 (<0.001)	-7±101
5) TTP _{first} (ms)	475 (419-520)	431 (300-522)	0.302	0.136 (0.066)	47±206
Dyssynchrony					
a) SL-delay (ms)	25 (-132-110)	-13 (-121-101)	-14.440	0.078 (0.194)	-2±226
b) SRSsept (%)	1.7 (0.8-3.4)	1.1 (0.1-1.9)	0.937	0.470 (<0.001)	1.0±2.0
c) SSI (%)	3.8 (2.1-5.9)	2.6 (1.3-3.8)	0.720	0.467 (<0.001)	1.3±3.0

Means and standard deviations are given with ± symbol. For non-normal distributed data, the median is given with the interquartile range between brackets. COV: coefficient of variation, ICC: intra-class correlation coefficient, diff: difference, SD: standard deviation, LV: strain derived from global LV in apical four chamber view, TTP_{max}: time to maximal peak shortening, TTP_{first}: time to first peak shortening, SL-delay: time delay between septal and lateral peak shortening, SSI: systolic stretch index, SRSsept: septal systolic rebound stretch. LBBB type: type of LBBB strain patterns, based on definition by Leenders et al.²³

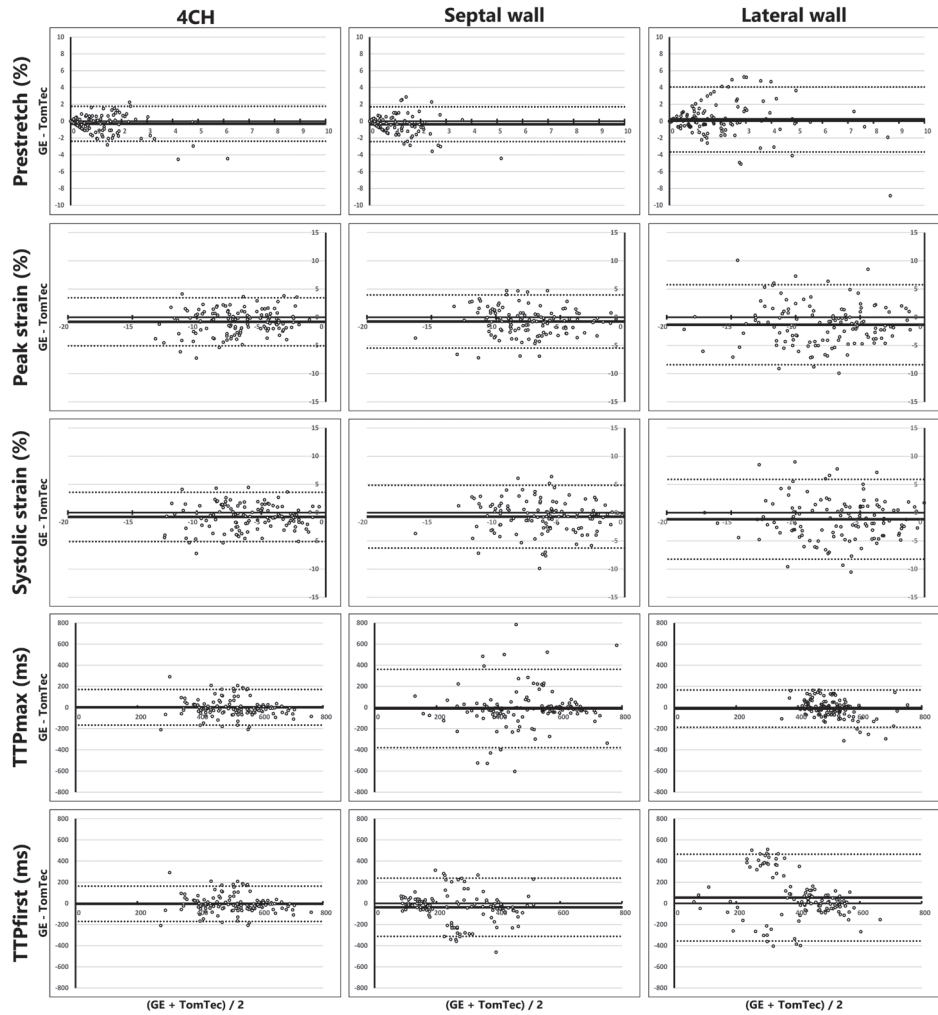


FIGURE 3. Bland-Altman plots of GE EchoPac vs. TomTec 2DCPA

Bland-Altman plots of all strain parameters, comparing GE Echopac and TomTec 2DCPA derived results. Each column represents either results obtained from the total LV or from the separate septal or lateral wall. On each x-axis the average result of the two techniques is given per patient, while on the y-axis the difference is given. The mean difference is depicted with a thick black horizontal line, while the 95% confidence interval is depicted with dashed lines. AP4CH: apical four chamber view, GE: General Electric, TTP_{first} : time to first peak, TTP_{max} : time to maximal peak.

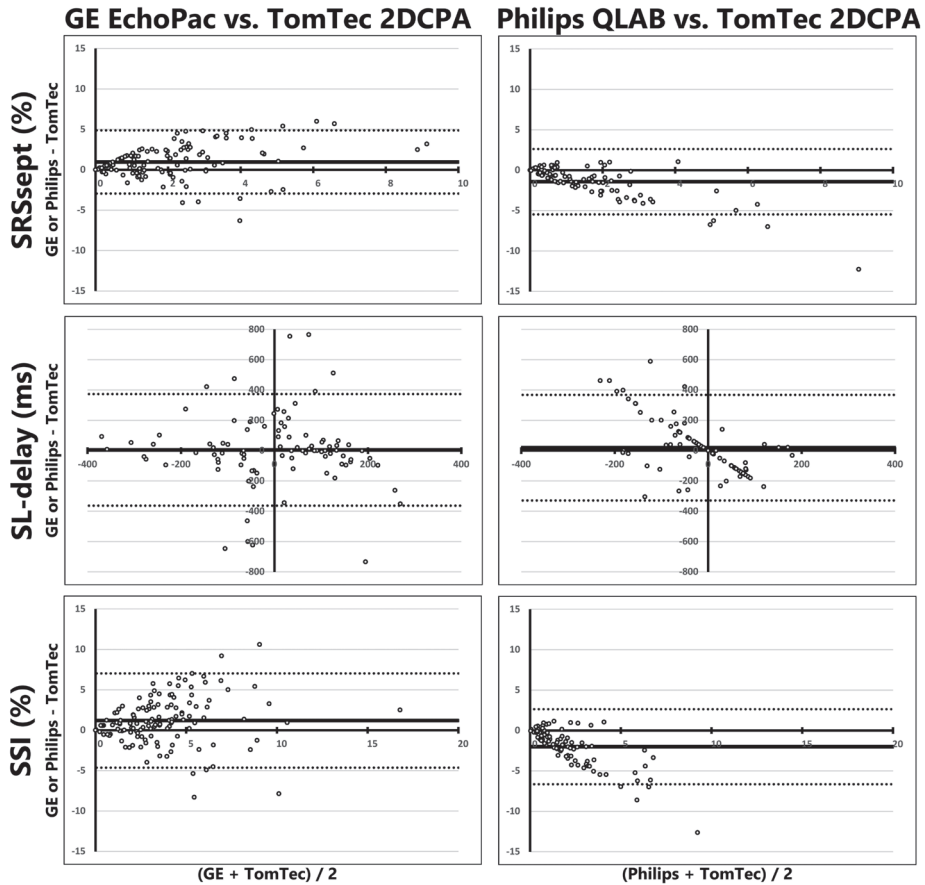


FIGURE 4. Bland-Altman plots of dyssynchrony parameters

Bland-Altman plots of dyssynchrony parameters, comparing GE Echopac and TomTec 2DCPA (left panels) and Philips QLAB and TomTec 2DCPA (right panels) derived results. On each x-axis the average result of the two techniques is given per patient, while on the y-axis the difference is given. The mean difference is depicted with a thick black horizontal line, while the 95% confidence interval is depicted with dashed lines. GE: General Electric, SRSsept: systolic rebound stretch of the septum, SL-delay: septal to lateral wall delay, SSI: systolic stretch index.

GE DYSSYNCHRONY PARAMETERS

Dyssynchrony indices derived from GE images showed varied results. SL-delay showed a poor ICC (0.078) and high COV (-14.4) and wide limits of agreement in the Bland-Altman plots (mean difference: 2 ± 226 ms). The ICC of SRSsept was weak (0.470), COV was relatively high (0.937) and the Bland-Altman plots showed relative wide limits of agreement ($1.0 \pm 2.0\%$, figure 4). SSI showed similar results, ICC was also weak (0.467), COV was relatively high (0.720) and Bland-Altman plots showed a difference between vendors with relative wide limits of agreement ($1.3 \pm 3.0\%$, figure 4). Cohen's kappa coefficient of agreement on LBBB pattern categorization was low (0.221). Cohen's kappa coefficient of intra-observer agreement was good for GE EchoPac (0.685) and weak for TomTec 2DCPA analysis (0.493) (figure 5).

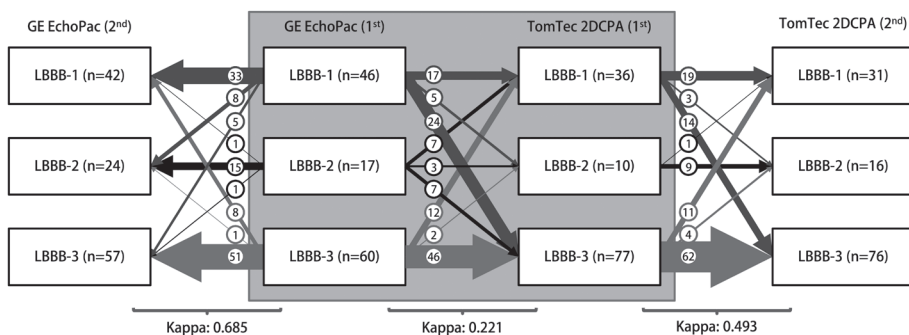


FIGURE 5. Strain pattern categorization for GE derived echocardiographic images

Schematic overview of strain pattern categorization for GE derived echocardiographic images, analysed with GE EchoPac and TomTec 2DCPA. Agreement between vendor-specific (GE EchoPac and vendor-independent (TomTec 2DCPA) software is given in the middle grey square, with corresponding Cohen's kappa given underneath. Both analyses were performed twice (1st and 2nd), to determine the intra-observer agreement. Arrows indicate the reclassification of patients between vendors or between the first (1st) and second attempt (2nd). LBBB-1: double-peaked systolic stretch, LBBB-2: predominant stretch, and LBBB-3: pseudo normal shortening.

PHILIPS ECHOCARDIOGRAPHIC IMAGES

PHILIPS BASIC STRAIN PARAMETERS

Comparison of vendor dependent and independent STE results derived from Philips echocardiographic images showed a similar pattern in results to GE (table 3). Namely, peak and systolic strain showed a smaller bias and COV than pre-stretch, timing parameters (i.e. TTP_{\max} and TTP_{first}) and dyssynchrony indices. ICCs were overall lower than GE derived results. Peak strain and systolic strain of the global LV showed an excellent ICC (0.749 and 0.802 respectively), with a relatively low COV and low mean difference in Bland-Altman plots (table 3 and figure 6). The ICC of peak and systolic strain of the septal and lateral wall were good (ranging from 0.626 to 0.680). Results on pre-stretch showed a high COV, poor ICC and wide limits of agreement in Bland-Altman results for all three comparisons (i.e. global LV, septal and lateral wall).

TABLE 3. Strain parameters derived from Philips echocardiographic images

	Philips QLAB (n=88)	TomTec 2DCPA (n=88)	COV	ICC (p-value)	Bland-Altman (mean diff±SD)
LV					
1) Pre-stretch (%)	0.0 (0.0-0.0)	0.0 (0.0-0.2)	4.125	-0.052 (0.684)	-0.1±0.6
2) Peak strain (%)	-7.7±2.7	-7.7±3.3	-0.350	0.749 (<0.001)	0.0±2.1
3) Systolic strain (%)	-6.8±3.0	-7.0±3.5	-0.435	0.802 (<0.001)	0.2±2.0
4) TTP _{max} (ms)	527 (444-592)	492 (396-559)	0.185	0.376 (<0.001)	34±113
5) TTP _{first} (ms)	361 (112-438)	361 (118-413)	0.567	0.165 (0.061)	2±213
Septum					
1) Pre-stretch (%)	0.0 (0.0-0.0)	0.0 (0.0-0.4)	3.990	-0.035 (0.627)	-0.3±0.9
2) Peak strain (%)	-7.6±2.7	-8.0±3.7	-0.363	0.626 (<0.001)	0.5±2.8
3) Systolic strain (%)	-6.5±3.0	-7.0±3.9	-0.468	0.667 (<0.001)	0.5±2.9
4) TTP _{max} (ms)	541 (442-598)	477 (346-575)	0.202	0.109 (0.155)	61±179
5) TTP _{first} (ms)	361 (118-426)	161 (114-342)	0.534	0.232 (0.014)	84±185
Lateral wall					
1) Pre-stretch (%)	0.0 (0.0-0.1)	0.3 (0.0-0.8)	2.728	0.324 (<0.001)	-0.5±1.0
2) Peak strain (%)	-8.0 (-9.4 - -6.1)	-9.0 (-11.1 - -6.3)	-0.345	0.631 (<0.001)	1.3±3.0
3) Systolic strain (%)	-6.4 (-9.0 - -5.2)	-8.0 (-11.1 - -4.9)	-0.436	0.680 (<0.001)	1.5±3.0
4) TTP _{max} (ms)	542 (454-597)	476 (434-538)	0.175	0.531 (<0.001)	36±87
5) TTP _{first} (ms)	376 (107-461)	433 (216-481)	0.550	0.060 (0.290)	-41±239
Dyssynchrony					
a) SL-delay (ms)	0 (0-0)	-20 (-121-120)	-10.694	0.025 (0.409)	24±180
b) SRSsept (%)	0.7 (0.3-1.2)	1.7 (0.6-3.3)	1.030	0.419 (<0.001)	-1.5±2.1
c) SSI (%)	0.8 (0.4-1.5)	2.3 (1.1-4.2)	1.024	0.421 (<0.001)	-2.0±2.4

Means and standard deviations are given with ± symbol, for non-normal distributed data, the median is given with the interquartile range between brackets. COV: coefficient of variation, ICC: intra-class correlation coefficient, diff: difference, SD: standard deviation, LV: strain derived from global LV in apical four chamber view, TTP_{max}: time to maximal peak shortening, TTP_{first}: time to first peak shortening, SL-delay: time delay between septal and lateral peak shortening, SSI: systolic stretch index, SRSsept: septal systolic rebound stretch. LBBB type: type of LBBB strain patterns, based on definition by Leenders et al.²³

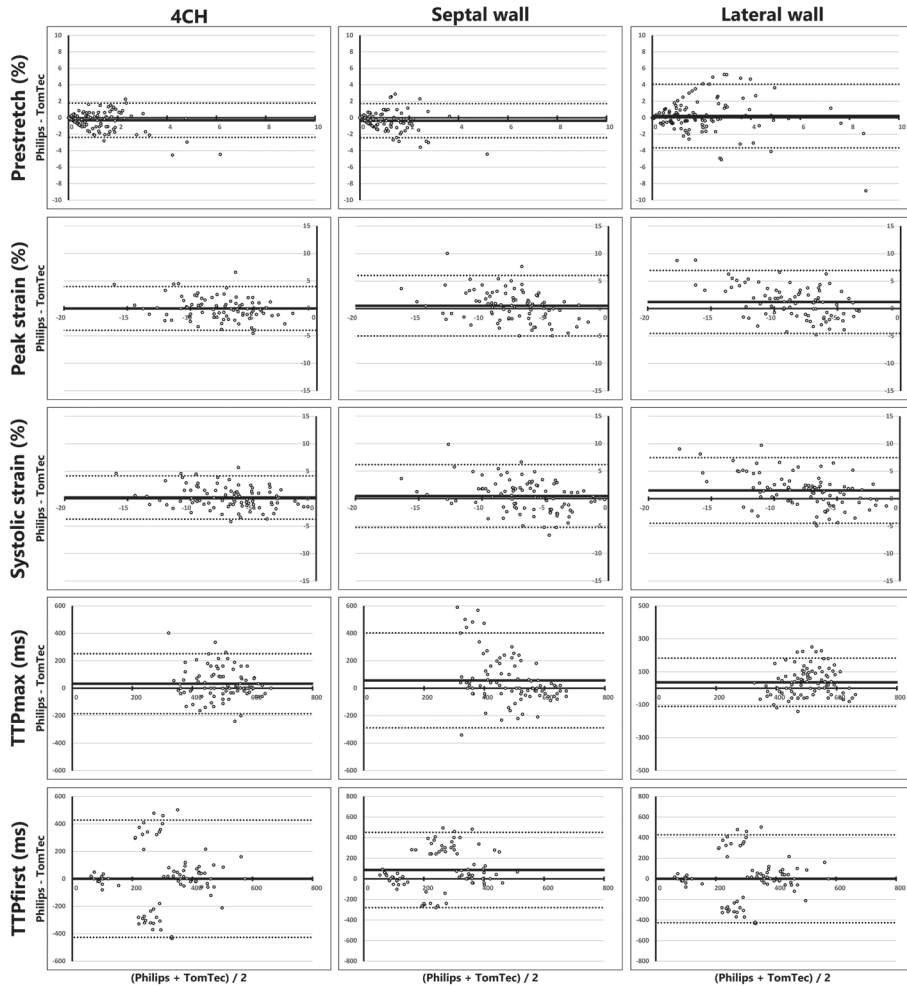


FIGURE 6. Bland Altman plots of Philips QLAB vs. TomTec 2DCPA

Bland-Altman plots of all strain parameters, comparing Philips QLAB and TomTec 2DCPA derived results. Each column represents either results obtained from the total LV or from the separate septal or lateral wall. On each x-axis the average result of the two techniques is given per patient, while on the y-axis the difference is given. The mean difference is depicted with a thick black horizontal line, while the 95% confidence interval is depicted with dashed lines. AP4CH: apical four chamber view, TTP_{first} : time to first peak, TTP_{max} : time to maximal peak.

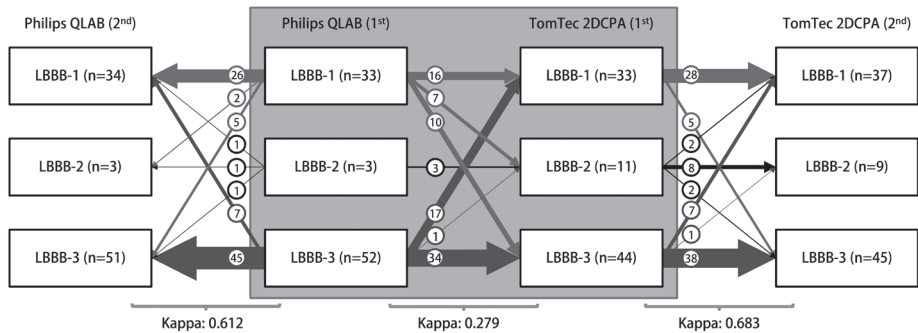


FIGURE 7. Strain pattern categorization for Philips derived echocardiographic images

Schematic overview of strain pattern categorization for Philips derived echocardiographic images, analysed with Philips QLAB and TomTec 2DCPA. Agreement between vendor-specific (Philips QLAB) and vendor-independent (TomTec 2DCPA) software is given in the middle grey square, with corresponding Cohen's kappa given underneath. Both analyses were performed twice (1st and 2nd), to determine the intra-observer agreement. Arrows indicate the reclassification of patients between vendors, or between the first (1st) and second attempt (2nd). LBBB-1: double-peaked systolic stretch, LBBB-2: predominant stretch, and LBBB-3: pseudo normal shortening.

PREDICTION OF VOLUMETRIC RESPONSE

GE ECHOCARDIOGRAPHIC IMAGES

For GE derived images, GE EchoPac derived SRSsept, SSI, and LBBB pattern categorization showed a significant association with volumetric response to CRT in univariate analysis, while TomTec 2DCPA derived parameters did not (table 4). The SL-delay showed no significant association with volumetric response. C-statistic values were comparable between GE EchoPac and TomTec 2DCPA Except for SSI, cut-off values for response prediction were higher for GE EchoPac (SL-delay: 144ms, SRSsept: 1.61% and SSI: 2.98%) compared to TomTec 2DCPA (SL-delay: -101ms, SRSsept 0.46%, SSI: 3.72%).

TABLE 4. Prediction of volumetric response to CRT with GE derived echocardiographic images

Parameter	Univariate analysis (n=123)			Receiver operating characteristics (n=123)	
	B	SD	p-value	C-statistic	Cut-off value
<i>GE</i> SL-delay	0.820	12.997	0.950	0.512	0.144
<i>TomTec</i> SL-delay	22.334	13.081	0.091#	0.573	-0.101
<i>GE</i> SRSsept	3.146	0.911	<0.001	0.599	1.614
<i>TomTec</i> SRSsept	0.503	1.362	0.713	0.544	0.455
<i>GE</i> SSI	2.296	0.653	<0.001	0.619	2.980
<i>TomTec</i> SSI	1.250	0.818	0.129	0.530	3.715
<i>GE</i> LBBB-type (type 1 or 2 vs. 3)	18.536	4.003	<0.001		
<i>TomTec</i> LBBB-type (type 1 or 2 vs. 3)	8.151	4.464	0.071		

Prediction of volumetric response to CRT, with results of univariate regression analysis (B, SD and p-value) and receiver operating characteristics (C-statistic, R^2 and cut-off). Univariate analyses are based on a change in LVESV on a continuous scale, while receiver operating characteristics are based on a cut-off of $\geq 15\%$ reduction in LVESV. GE: General Electric EchoPac, TomTec: TomTec 2DCPA, B: beta coefficient, SD: standard deviation, SL-delay: septal-to-lateral wall delay, SRSsept: septal systolic rebound stretch, SSI: systolic stretch index, LBBB-type: septal strain pattern categorization according to Leenders et al..

PHILIPS ECHOCARDIOGRAPHIC IMAGES

For Philips derived images, both Philips QLAB and TomTec 2DCPA showed a significant association with volumetric response to CRT for SRSsept, SSI and LBBB pattern categorization (table 5). Only the SL-delay showed no significant association with volumetric response. The C-statistic values were overall reasonable (i.e. ranging from 0.564 to 0.705) and comparable between vendor dependent and independent analysis. The cut-off values for response prediction were apparently different, with lower values for Philips QLAB (SL-delay: 0ms, SRSsept: 0.79% and SSI: 0.83%) compared to TomTec 2DCPA (SL-delay: -80ms, SRSsept: 1.18% and SSI: 2.35%).

TABLE 5. Prediction of volumetric response to CRT with Philips derived echocardiographic images

Parameter	Univariate analysis (n=88)			Receiver operating characteristics (n=88)	
	B	SD	p-value	C-statistic	Cut-off value
<i>Philips</i> SL-delay	58.897	38.368	0.129	0.564	0.000
<i>TomTec</i> SL-delay	-23.910	16.952	0.162	0.569	-0.080
<i>Philips</i> SRSsept	10.072	2.653	<0.001	0.697	0.790
<i>TomTec</i> SRSsept	3.842	0.997	<0.001	0.686	1.180
<i>Philips</i> SSI	7.346	2.257	0.002	0.661	0.830
<i>TomTec</i> SSI	3.860	0.863	<0.001	0.705	2.345
<i>Philips</i> LBBB-type (type 1 or 2 vs. 3)	20.091	5.418	<0.001		
<i>TomTec</i> LBBB-type (type 1 or 2 vs. 3)	22.069	5.122	<0.001		

Prediction of volumetric response to CRT, with results of univariate regression analysis (B, SD and p-value) and receiver operating characteristics (C-statistic, R^2 and cut-off). Univariate analyses are based on a change in LVESV on a continuous scale, while receiver operating characteristics are based on a cut-off of $\geq 15\%$ reduction in LVESV. Philips: Philips QLAB, TomTec: TomTec 2DCPA, B: beta coefficient, SD: standard deviation, SL-delay: septal-to-lateral wall delay, SRSsept: septal systolic rebound stretch, SSI: systolic stretch index, LBBB-type: septal pattern categorization according to Leenders et al..

DISCUSSION

Comparability of speckle tracking echocardiography platforms on apical four chamber LV peak and systolic strain is fair in patients with heart failure and dyssynchrony. We observed relevant differences in more specific strain parameters (i.e. pre-stretch, TTP_{max} and TTP_{first}) and indices representing dyssynchrony (i.e. SRSsept, SSI and SL-delay). Results on strain pattern categorization (i.e. LBBB patterns) were disappointing as agreement between vendors was low. However, the inter-observer agreement, using the same STE software twice, on strain pattern categorization was better. Although most dyssynchrony parameters showed a weak but significant association with changes in LV end-systolic volume, the cut-off values were apparently different. STE software of different vendors can therefore not be used interchangeably for more specific purposes than peak strain.

VENDOR VARIABILITY

To the best of our knowledge, this is the first study to compare results of different STE software packages, specifically for mechanical dyssynchrony in CRT-candidates. The average differences of peak strain and systolic strain were small and non-significant between vendor dependent and vendor independent STE packages. Nevertheless, TomTec had lower values compared to GE EchoPac and higher values compared to Philips QLAB. Unfortunately, we cannot define the source of discordance, as a gold-standard for deformation imaging (i.e. sonomicrometry) was not available in our study. The relative high correlation for global longitudinal strain between STE platforms is in accordance with earlier publications.¹⁶ There are currently no publications on vendor comparison studies on STE in patients with heart failure and dyssynchrony, besides a small comparative study by our own group.²⁴ Moreover, comparison to earlier publications on peak strain and timing values is difficult as previous studies implemented older versions of STE software, while we used the most recent versions. STE software is constantly under development, partly due to the STE standardization taskforce of the EACVI/ASE. This task force includes among its members representatives of several vendors. Their efforts resulted in small and acceptable differences between vendors for global longitudinal strain.^{16, 25} However, the variability among vendors in more specific longitudinal strain features is not yet elucidated, nor is the exact bias between vendors with respect to regional strain assessment. Furthermore, the cohort studied for standardization consisted of a wide range of subjects (mean LVEF 60%, global longitudinal strain -19.2%) and is therefore not representative for CRT patients with dilated hearts, reduced LV function, and complex deformation characteristics.²³ Moreover, CRT patients can have suboptimal acoustic windows which affects image quality and reliability of strain analysis. In the current study, comparable AP4CH peak longitudinal strain values were found in CRT patients, although the limits of agreement of Bland-Altman plots were relatively wide, and results for individual patients varied significantly. The discrepancies between the current study and the publications by Farsalinos et al. and Yang et al. may therefore be ascribed to the examined populations.^{16, 26} A mechanistic modelling study showed higher variability in peak strain among vendors and a higher inter-observer variability in a dilated thin-walled LV.²⁷ This modelling study suggests a lower level of agreement among vendors in heart failure patients, which might explain the findings in our current observations.

ECHOCARDIOGRAPHIC IMAGES AND SPECKLE TRACKING ALGORITHMS

4 Differences between manufacturers are largely attributed to discrepancies in STE algorithms. Albeit recently thoroughly investigated,¹⁶ the algorithms of the majority of commercially available speckle tracking software have lacked published validation.²⁷ They are furthermore not open-source. TomTec 2DCPA uses DICOM images and thereby imports images with lower frame rate and lower image quality compared to the raw image files used by the vendor dependent platforms. Lower frame rates influence temporal resolution, which hampers reliable assessment of both strain values and timing indices. The image quality directly influences spatial resolution, decreasing reliable tracking of speckles. TomTec also displays separate endo- and epicardial strain curves for each segment, and mean myocardial wall strain results are not given. The use of endocardial strain data might have caused a slight overestimation of peak strain values.²² GE EchoPac uses 'global' wall myocardial strain by default, although users can choose between endocardial, epicardial or mid myocardial layers. Lastly, the method used by Philips QLAB is unknown, although a global myocardial based approach is likely. Timing of the reference length is also of importance for standardization, as differences in the onset of strain curves directly influences absolute strain values as wells as timing indices. As mentioned, timing of reference length was uniformed for TomTec analysis compared to both vendor dependent platforms.

MECHANICAL DYSSYNCHRONY INDICES

Absolute values of mechanical dyssynchrony indices were significantly lower for Philips, compared to TomTec. Whereas the results on dyssynchrony parameters obtained from GE images displayed higher values for GE compared to TomTec. Although the source of discordance is unknown, dyssynchrony seems underestimated by Philips QLAB speckle tracking algorithms. Underestimation of dyssynchrony is exemplified by results for the SL-delay obtained by Philips QLAB (median 0ms, interquartile range 0 – 0ms). The discrepancies of Philips QLAB with both other vendors are remarkable, as both GE EchoPac and TomTec 2DCPA displayed large variation for SL-delay. Moreover, as the Bland-Altman plot of SL-delay in figure 4 shows, the discrepancy between Philips QLAB and TomTec 2DCPA, a large number of results are on a line ($y=-0.5*x$), indicating a large variation in SL-delay for TomTec, while Philips values were mainly close to zero. Philips' derived septal and lateral wall strain curves were often quite similar, as can be appreciated in the example in figure

1. It seems that segmental strain curves are more smoothed by Philips QLAB. While no gold-standard for deformation imaging was applied, the relative absence of dyssynchrony obtained with Philips STE software is striking.

Although intra-observer agreement of strain pattern categorization is relatively good, strain pattern categorization showed apparent variations among vendors. Strain patterns were earlier found to be more robust between vendors.²⁴ This discrepancy could be attributed to changes in STE algorithms, as there were almost no LBBB type 2 patterns found by Philips. LBBB type 2 is the most distinctive septal deformation pattern, with predominant stretch almost in completely opposite direction to the lateral wall. Higher percentages of LBBB type 2 were observed in the same (i.e. Philips imaged) patient with TomTec. The cohorts of GE and Philips were not significantly different, and conventional dyssynchrony parameters such as apical rocking, septal flash and IVMD were comparable. Therefore, the relative absence of LBBB type 2 patterns is likely caused by the inability to detect dyssynchrony using QLAB. Given the above-mentioned differences in both continuous and categorical dyssynchrony parameters, one might postulate that STE with Philips QLAB is less suitable for detection of dyssynchrony in a CRT population. However, despite the lower values, the predictive value of Philips QLAB derived dyssynchrony parameters is at least comparable to the vendor independent analysis of TomTec 2DCPA. Although Philips QLAB and TomTec 2DCPA were able to predict volumetric response to CRT with the implemented dyssynchrony parameter, the cut-off values were different. Even though cut-off values for GE EchoPac derived parameters were higher, the values are different from earlier published values.^{3, 9} These differences may be ascribed to the used software versions or the examined populations. Vendor specific cut-off values should therefore be used for each STE platform.

ECHOCARDIOGRAPHIC IMAGE QUALITY

Echocardiographic analysis in the current study was restricted to AP4CH images, as speckle tracking analysis of these images is relevant for dyssynchrony in patients with left bundle branch block and has higher reproducibility.¹⁵ However, echocardiographic AP4CH images with adequate image quality can be difficult in patients with dilated hearts. Patient anatomy and cardiac size both complicate echocardiographic acquisition, as can be observed from the number of echocardiograms with poor image quality. Although this is not reflected in our results, lateral wall acquisition can be difficult in heart failure patients. It was surprising that lateral wall cross-correlation values were significantly higher compared to septal wall

values for all vendors. Lower septal wall cross-correlation values can be explained by the higher complexity of septal strain patterns (i.e. LBBB type 1 and 2, figure 2). This in contrast to strain patterns of the lateral wall, which often had a similar shape between patients, also seen in the agreement on TTP_{max} for lateral wall strain. Complex septal deformation pattern can more easily be misinterpreted, resulting in lower correlations and wider limits of agreement in Bland-Altman plots. The poor agreement in septal strain analysis was also seen in the low Cohen's kappa values of septal strain pattern categorization.

LIMITATIONS

Although this study consists of relatively large subgroups, it is a sub-analysis with inherent limitations. However, images were prospectively collected for analysis with STE software. Nonetheless, patients underwent echocardiographic examination by a single vendor, which was assigned dependent of the centre of implantation and therefore non-randomized. Ideally patients would undergo echocardiographic examination by both vendors, making a direct comparison between GE and Philips possible. Moreover, there was no gold-standard used in this study, making it impossible to determine the source of variability. Test-retest variability was not part of the imaging protocol, although consecutive measurements are subject to variation.¹⁶ Nevertheless, the large and comparable subgroups permitted a reliable comparison of vendors, and large differences were seen. This is in contrast to previous studies, in which most echocardiographic dyssynchrony parameters (i.e. SRSsept, SSI, and SL-delay) were tested solely on one vendor (i.e. GE EchoPac).

CLINICAL IMPLICATIONS

Although global LV peak strain correlates reasonable between vendor systems, the results of individual patients between vendors may vary, as indicated by the wide limits of agreement in Bland-Altman plots. This variation hampers translation of deformation parameters obtained by STE to clinical practice. All three STE vendors were capable to predict response to CRT, using the implemented dyssynchrony parameters. Although the diagnostic value of GE EchoPac derived parameters is well validated in prior studies,^{10, 28} further work is needed to confirm the predictive value of these parameters in clinical practice. Differences between vendors can be large, hampering direct translation from pre-clinical work to the clinical implementation of speckle tracking derived dyssynchrony parameters and patterns in all

echo laboratories, with a myriad of echo-machines. We recommend that in patients eligible for CRT, clinicians should use reference and cut-off values specific to the STE vendor.

CONCLUSIONS

This study proves the general fair comparability of longitudinal peak strain, although results for individual cases and more complex strain parameters can differ significantly. Moreover, we have demonstrated that dyssynchrony parameters derived with different vendors are associated with volumetric response to CRT, but that cut-off values do not correlate well between vendors. While the standardization taskforce took an important first step for global peak strain, further standardization of STE in patients eligible for CRT is still warranted.

REFERENCES

1. Teske AJ, De Boeck BW, Melman PG, Sieswerda GT, Doevendans PA, Cramer MJ. Echocardiographic quantification of myocardial function using tissue deformation imaging, a guide to image acquisition and analysis using tissue Doppler and speckle tracking. *Cardiovasc Ultrasound*. 2007;5:27.
2. Schroeder J, Hamada S, Grundlinger N, Rubeau T, Altiok E, Ulbrich K, et al. Myocardial deformation by strain echocardiography identifies patients with acute coronary syndrome and non-diagnostic ECG presenting in a chest pain unit: a prospective study of diagnostic accuracy. *Clin Res Cardiol*. 2016;105:248-56.
3. De Boeck BWL, Teske AJ, Meine M, Leenders GE, Cramer MJ, Prinzen FW, et al. Septal rebound stretch reflects the functional substrate to cardiac resynchronization therapy and predicts volumetric and neurohormonal response. *Eur J Heart Fail*. 2009;11:863-871.
4. Khan FZ, Virdee MS, Palmer CR, Pugh PJ, O'Halloran D, Elsik M, et al. Targeted left ventricular lead placement to guide cardiac resynchronization therapy: the TARGET study: a randomized, controlled trial. *J Am Coll Cardiol*. 2012;59:1509-1518.
5. van Deursen CJ, Wecke L, van Everdingen WM, Stahlberg M, Janssen MH, Braunschweig F, et al. Vectorcardiography for optimization of stimulation intervals in cardiac resynchronization therapy. *J Cardiovasc Transl Res*. 2015;8:128-37.
6. Leenders GE, Cramer MJ, Bogaard MD, Meine M, Doevendans PA, De Boeck BW. Echocardiographic prediction of outcome after cardiac resynchronization therapy: conventional methods and recent developments. *Heart Fail Rev*. 2011;16:235-50.
7. van Everdingen WM, Schipper JC, van 't Sant J, Ramdat Misier K, Meine M, Cramer MJ. Echocardiography and cardiac resynchronisation therapy, friends or foes? *Netherlands heart journal*. 2016;24:25-38.
8. Daubert JC, Saxon L, Adamson PB, Auricchio A, Berger RD, Beshai JF, et al. 2012 EHRA/HRS expert consensus statement on cardiac resynchronization therapy in heart failure: implant and follow-up recommendations and management. *Europace*. 2012;14:1236-86.
9. Lumens J, Tayal B, Walmsley J, Delgado-Montero A, Huntjens PR, Schwartzman D, et al. Differentiating Electromechanical From Non-Electrical Substrates of Mechanical Discoordination to Identify Responders to Cardiac Resynchronization Therapy. *Circ Cardiovasc Imaging*. 2015;8:e003744.

10. Leenders GE, De Boeck BW, Teske AJ, Meine M, Bogaard MD, Prinzen FW, et al. Septal rebound stretch is a strong predictor of outcome after cardiac resynchronization therapy. *J Card Fail.* 2012;18:404-12.
11. Marechaux S, Guiot A, Castel AL, Guyomar Y, Semichon M, Delelis F, et al. Relationship between two-dimensional speckle-tracking septal strain and response to cardiac resynchronization therapy in patients with left ventricular dysfunction and left bundle branch block: a prospective pilot study. *J Am Soc Echocardiogr.* 2014;27:501-11.
12. Risum N, Tayal B, Hansen TF, Bruun NE, Jensen MT, Lauridsen TK, et al. Identification of Typical Left Bundle Branch Block Contraction by Strain Echocardiography Is Additive to Electrocardiography in Prediction of Long-Term Outcome After Cardiac Resynchronization Therapy. *J Am Coll Cardiol.* 2015;66:631-41.
13. Riffel JH, Keller MG, Aurich M, Sander Y, Andre F, Giusca S, et al. Assessment of global longitudinal strain using standardized myocardial deformation imaging: a modality independent software approach. *Clin Res Cardiol.* 2015;104:591-602.
14. Koopman LP, Slorach C, Hui W, Manlhiot C, McCrindle BW, Friedberg MK, et al. Comparison between different speckle tracking and color tissue Doppler techniques to measure global and regional myocardial deformation in children. *J Am Soc Echocardiogr.* 2010;23:919-28.
15. Negishi K, Lucas S, Negishi T, Hamilton J, Marwick TH. What is the primary source of discordance in strain measurement between vendors: imaging or analysis? *Ultrasound Med Biol.* 2013;39:714-20.
16. Farsalinos KE, Daraban AM, Unlu S, Thomas JD, Badano LP, Voigt JU. Head-to-Head Comparison of Global Longitudinal Strain Measurements among Nine Different Vendors: The EACVI/ASE Inter-Vendor Comparison Study. *J Am Soc Echocardiogr.* 2015;28:1171-1181, e2.
17. Maass AH, Vernooij K, Wijers SC, van 't Sant J, Cramer MJ, Meine M, et al. Refining success of cardiac resynchronization therapy using a simple score predicting the amount of reverse ventricular remodelling: results from the Markers and Response to CRT (MARC) study. *Europace.* 2017.
18. Brignole M, Auricchio A, Baron-Esquivias G, Bordachar P, Boriani G, Breithardt OA, et al. 2013 ESC Guidelines on cardiac pacing and cardiac resynchronization therapy. *Eur Heart J.* 2013;34:2281-2329.

19. Russo AM, Stainback RF, Bailey SR, Epstein AE, Heidenreich PA, Jessup M, et al. ACCF/HRS/AHA/ASE/HFSA/SCAI/SCCT/SCMR 2013 appropriate use criteria for implantable cardioverter-defibrillators and cardiac resynchronization therapy. *J Am Coll Cardiol*. 2013;61:1318-68.
20. Lang RM, Badano LP, Mor-Avi V, Afilalo J, Armstrong A, Ernande L, et al. Recommendations for cardiac chamber quantification by echocardiography in adults: an update from the American Society of Echocardiography and the European Association of Cardiovascular Imaging. *Eur Heart J Cardiovasc Imaging*. 2015;16:233-70.
21. Cerqueira MD, Weissman NJ, Dilsizian V, Jacobs AK, Kaul S, Laskey WK, et al. Standardized myocardial segmentation and nomenclature for tomographic imaging of the heart: a statement for healthcare professionals from the Cardiac Imaging Committee of the Council on Clinical Cardiology of the American Heart Association. *Circulation*. 2002;105:539-42.
22. Leitman M, Lysiansky M, Lysyansky P, Friedman Z, Tyomkin V, Fuchs T, et al. Circumferential and longitudinal strain in 3 myocardial layers in normal subjects and in patients with regional left ventricular dysfunction. *J Am Soc Echocardiogr*. 2010;23:64-70.
23. Leenders GE, Lumens J, Cramer MJ, De Boeck BW, Doevendans PA, Delhaas T, et al. Septal deformation patterns delineate mechanical dyssynchrony and regional differences in contractility: analysis of patient data using a computer model. *Circ Heart Fail*. 2012;5:87-96.
24. van Everdingen WM, Paiman ML, van Deursen CJ, Cramer MJ, Vernoooy K, Delhaas T, et al. Comparison of septal strain patterns in dyssynchronous heart failure between speckle tracking echocardiography vendor systems. *J Electrocardiol*. 2015;48:609-16.
25. Voigt JU, Pedrizzetti G, Lysyansky P, Marwick TH, Houle H, Baumann R, et al. Definitions for a common standard for 2D speckle tracking echocardiography: consensus document of the EACVI/ASE/Industry Task Force to standardize deformation imaging. *J Am Soc Echocardiogr*. 2015;28:183-93.
26. Yang H, Marwick TH, Fukuda N, Oe H, Saito M, Thomas JD, et al. Improvement in Strain Concordance between Two Major Vendors after the Strain Standardization Initiative. *J Am Soc Echocardiogr*. 2015;28:642-8.
27. D'Hooge J, Barbosa D, Gao H, Claus P, Prater D, Hamilton J, et al. Two-dimensional speckle tracking echocardiography: standardization efforts based on synthetic ultrasound data. *Eur Heart J Cardiovasc Imaging*. 2016;17:693-701.
28. Van't Sant J, Ter Horst IA, Wijers SC, Mast TP, Leenders GE, Doevendans PA, et al. Measurements of electrical and mechanical dyssynchrony are both essential to improve prediction of CRT response. *J Electrocardiol*. 2015;48:601-8.

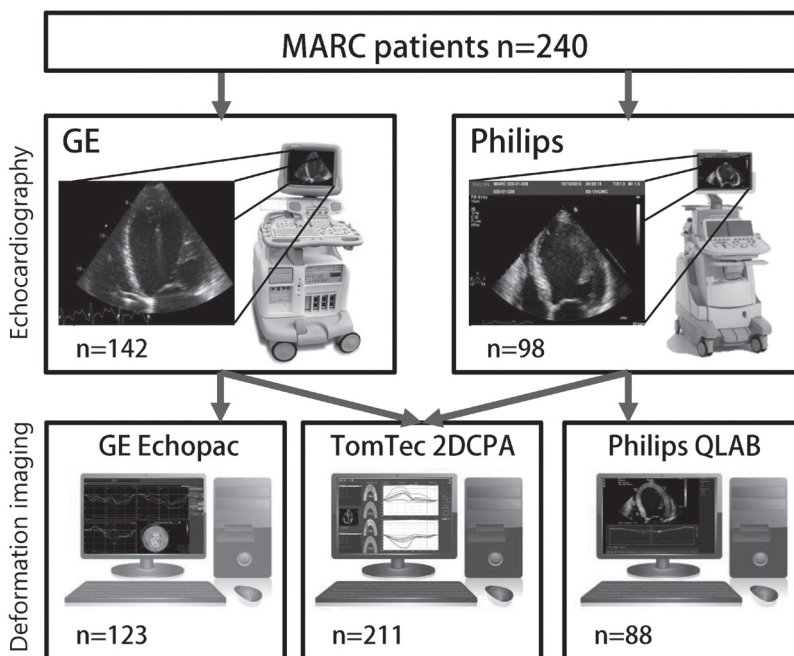
SUPPLEMENTARY MATERIAL

SUPPLEMENTARY TABLE 1. Cross-correlation of strain curves

	GE EchoPac vs. TomTec 2DCPA			
	Overall (n=123)	High (n=34)	Average (n=58)	Poor (n=31)
Global LV	0.835±0.213 [†]	0.903±0.113	0.802±0.242	0.821±0.226
Septal wall	0.682±0.290 ^{††}	0.729±0.254	0.630±0.319	0.728±0.257
Lateral wall	0.800±0.244 [†]	0.892±0.123 [*]	0.792±0.242	0.713±0.312 [*]

	Philips QLAB vs. TomTec 2DCPA			
	Overall (n=88)	High (n=30)	Average (n=50)	Poor (n=8)
Global LV	0.898±0.156 ^{††}	0.924±0.108	0.890±0.154	0.850±0.283
Septal wall	0.712±0.293 ^{††}	0.723±0.269	0.672±0.319	0.905±0.084
Lateral wall	0.827±0.226 ^{††}	0.859±0.201	0.829±0.221	0.701±0.314

Results of cross-correlation of strain curves, categorized by image quality. Mean coefficient of determination (R^2) and standard deviations are given with \pm symbol. Global LV: global 4CH LV results. [†]: $p < 0.05$ between groups for overall analysis, ^{*}: $p < 0.05$ between image qualities.

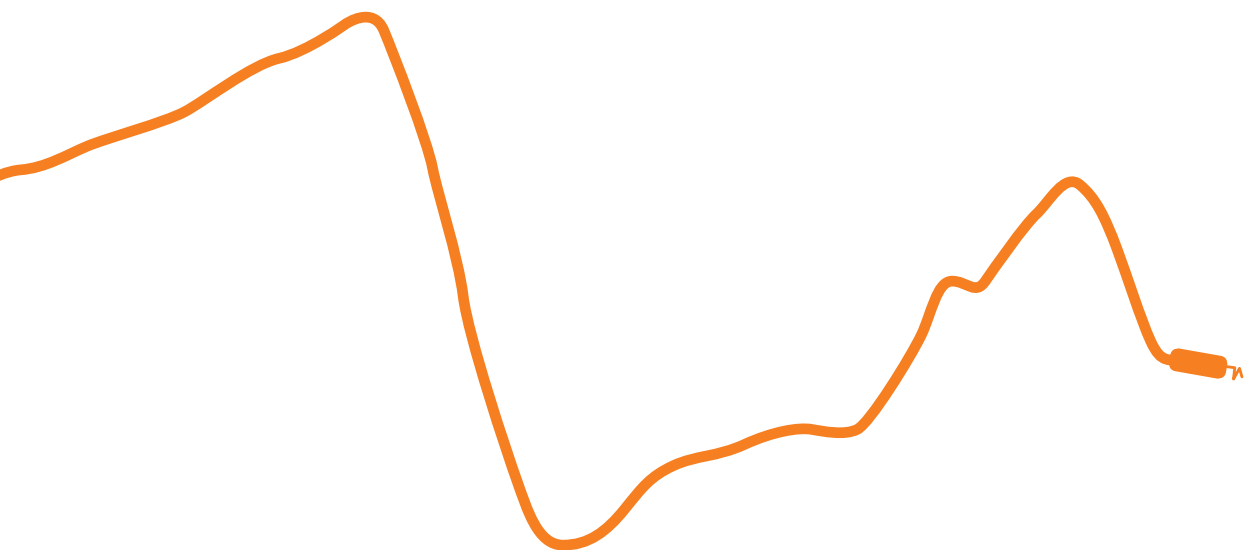


SUPPLEMENTARY FIGURE 1. Study flow diagram

Study flow diagram of the vendor comparison study. A total of 240 patients were included in 6 medical centres in the Netherlands. For GE EchoPac, 142 patients were included of which 123 echocardiograms were eligible for STE analysis. For Philips QLAB 88 of 98 echocardiograms were eligible for STE analysis. All echocardiograms were also analyzed with TomTec 2DCPA. Potential reasons for exclusions were: technical errors in the data format, low frame rate (<35Hz), very poor image quality and irregular heart rhythm. MARC: markers of response to cardiac resynchronization therapy.



Comparison of strain imaging techniques in CRT candidates: CMR tagging, CMR feature tracking and speckle tracking echocardiography



Wouter M. van Everdingen (MD)^{1*}, Alwin Zweerink (MD)^{2*}, Robin Nijveldt (MD, PhD)², Odette A.E. Salden (MD)¹, Mathias Meine (MD, PhD)¹, Alexander H. Maass (MD, PhD)³, Kevin Vernooij (MD, PhD)⁴, Frederik J. de Lange (MD, PhD)⁵, Albert C. van Rossum (MD, PhD)², Pierre Croisille (MD, PhD)⁶, Patrick Clarysse (PhD)⁶, Bastiaan Geelhoed (PhD)³, Michiel Rienstra (MD, PhD)³, Isabelle C. Van Gelder (MD, PhD)³, Marc A. Vos (PhD)⁷, Cornelis P. Allaart (MD, PhD)^{2*}, Maarten J. Cramer (MD, PhD)^{1*}

* the first two and last two authors contributed equally to the manuscript.

¹ Department of Cardiology, University Medical Centre Utrecht, Utrecht, The Netherlands.

² Department of Cardiology, and Institute for Cardiovascular Research (ICaR-VU), VU University Medical Centre, Amsterdam, The Netherlands.

³ Department of Cardiology, Thoraxcenter, University of Groningen, University Medical Centre Groningen, Groningen.

⁴ Department of Cardiology, Maastricht University Medical Centre, Maastricht, The Netherlands.

⁵ Department of Cardiology, Academic Medical Centre, Amsterdam, The Netherlands.

⁶ Université de Lyon, UJM-Saint-Etienne, INSA, CNRS UMR 5520, INSERM U1206, CREATIS, F-42023, Saint-Etienne, France.

⁷ Department of Medical Physiology, University of Utrecht, Utrecht, The Netherlands.

International Journal of Cardiovascular Imaging (2017, Oct 17)

ABSTRACT

Purpose: Parameters using myocardial strain analysis may predict response to cardiac resynchronization therapy (CRT). As the agreement between currently available strain imaging modalities is unknown, three different modalities were compared.

Materials and methods: Twenty-seven CRT-candidates, prospectively included in the MARC study, underwent cardiac magnetic resonance (CMR) imaging and echocardiographic examination. Left ventricular (LV) circumferential strain was analysed with CMR tagging (CMR-TAG), CMR feature tracking (CMR-FT), and speckle tracking echocardiography (STE). Basic strain values and parameters of dyssynchrony and discoordination obtained with CMR-FT and STE were compared to CMR-TAG.

Results: Agreement of CMR-FT and CMR-TAG was overall fair, while agreement between STE and CMR-TAG was often poor. For both comparisons, agreement on discoordination parameters was highest, followed by dyssynchrony and basic strain parameters. For discoordination parameters, agreement on systolic stretch index (SSI) was highest, with fair intra-class correlation coefficients (ICC) (CMR-FT: 0.58, STE: 0.55). ICC of septal systolic rebound stretch (SRS_{sept}) was poor (CMR-FT: 0.41, STE: 0.30). Internal stretch factor of septal and lateral wall ($ISF_{sep-lat}$) showed fair ICC values (CMR-FT: 0.53, STE: 0.46), while the ICC of the total LV (ISF_{LV}) was fair for CMR-FT (0.55) and poor for STE (0.32). The CURE index had a fair ICC for both comparisons (CMR-FT: 0.49, STE: 0.41).

Conclusion: Although comparison of STE to CMR-TAG was limited by methodological differences, agreement between CMR-FT and CMR-TAG was overall higher compared to STE and CMR-TAG. CMR-FT is a potential clinical alternative for CMR-TAG and STE, especially in the detection of discoordination in CRT-candidates.

INTRODUCTION

Cardiac resynchronization therapy (CRT) is an established treatment for patients with heart failure, reduced left ventricular (LV) ejection fraction, and a prolonged QRS caused by a left bundle branch block (LBBB) or nonspecific intraventricular conduction delay.¹ CRT aims to restore LV mechanics and improve hemodynamic by resynchronization of LV electrical activation.² Unfortunately, the effect of CRT is limited in 30-40% of the patients, partly due to a lack of optimal criteria for patient selection.^{3, 4} In current international guidelines the selection criteria for CRT are limited to clinical parameters, ECG parameters and LV ejection fraction $\leq 35\%$.¹ Patient selection for CRT may be improved with additional parameters reflecting mechanical dyssynchrony or discoordination obtained with strain analysis on imaging.⁴⁻⁷ These parameters reflect the LV mechanical consequences caused by an inhomogeneous electrical activation. Mechanical dyssynchrony parameters are based on timing differences between particular LV segments.^{8, 9} However, these mechanical dyssynchrony parameters showed disappointing results in large multi-centre trials.⁹ More promising parameters focus on discoordination, reflecting a percentage or fraction of opposing (i.e. inefficient) deformation.^{6, 10-12} These parameters are determined using myocardial strain analysis, which can be obtained with several cardiac imaging techniques, including cardiac magnetic resonance imaging (CMR) with tagging (CMR-TAG), CMR cine images and a post-processing technique named feature tracking (CMR-FT), and speckle tracking echocardiography (STE).^{13, 14} Although CMR-TAG is regarded as the non-invasive 'gold-standard', it is generally limited to scientific applications, requiring specific imaging protocols, sequences, and dedicated post-processing software. Clinical application of CMR-FT and STE is more feasible compared to CMR-TAG, as both techniques are applicable to images obtained during standard clinical imaging protocols.¹⁴⁻¹⁶ Nevertheless, both techniques (i.e. CMR-FT and STE) lack validation on strain parameters reflecting mechanical dyssynchrony and discoordination. Thus, no study has yet compared results obtained with all three techniques (i.e. CMR-TAG, CMR-FT and STE) in patients eligible for CRT. This study aims to compare circumferential strain parameters obtained with CMR-FT and STE versus gold-standard CMR-TAG in patients eligible for CRT. The comparison of indices reflecting mechanical dyssynchrony and discoordination are of specific interest.

MATERIALS AND METHODS

5 This sub study is part of the Markers of Acute Response to CRT (MARC) study (Cohfar, CTMM, The Netherlands, clinicaltrials.gov: NCT01519908), which was designed to investigate predictors for response on CRT. The MARC study included two-hundred-forty patients planned for CRT implantation in six medical centres in the Netherlands, using previously published in- and exclusion criteria.¹⁷ Twenty-seven of the 240 patients were included in this sub-study, as these patients gave consent for an additional CMR examination including myocardial tagging in the VU university medical centre (Amsterdam, The Netherlands). All subjects gave written informed consent and the local medical ethics committees approved data collection and management. The investigation conforms to the principles outlined in the Declaration of Helsinki.

ECHOCARDIOGRAPHIC EXAMINATION

Echocardiographic examinations were performed on either GE Vivid7, GE Vivid9 (General Electric Healthcare, Chicago, Illinois, USA), or Philips iE33 (Philips Medical Systems, Best, The Netherlands) ultrasound machines prior to CRT implantation by all participating centres and analysed by the echocardiographic core lab (WE and MC, UMC Utrecht, Utrecht, The Netherlands).

ACQUISITION - STANDARD ECHOCARDIOGRAPHIC IMAGES

Standard echocardiographic images were obtained, including a parasternal short axis view at the papillary muscle and at the mitral valve level.¹⁸ Image quality and frame rate (50-100Hz) were optimized for offline speckle tracking analysis. Pulsed-wave Doppler images of the mitral valve inlet and LV outflow tract were obtained of mitral valve and aortic valve closure (AVC) to define systole.

OFFLINE ANALYSIS - SPECKLE TRACKING ECHOCARDIOGRAPHY

Echocardiographic images were exported as DICOM-files for vendor-independent strain analysis (TomTec 2D Cardiac Performance Analysis (2DCPA) version 1.2.1.2, TomTec Imaging Systems, Unterschleissheim, Germany). A region of interest was placed by user defined markers at the endocardial border. The epicardial border was excluded, as it often lacked a clear border zone. The region of interest was automatically separated into

six segments. Segments were excluded if, even after repeated adjustment of the region of interest, adequate tracking was not achievable. The marker for reference length was placed at QRS onset.

STE results were exported for analysis with author written scripts for Matlab 2014b (Mathworks, Natick, MA, USA). Segmental strain curves were discarded in case of low signal-to-noise ratio as judged by two independent investigators (WE and AZ). At least two segments needed to be analysable per wall. Results of strain parameters of the septum were based on averages of maximal four septal segments (i.e. basal- and mid-level of inferoseptal and anteroseptal segments) while the lateral wall parameters were based on averages of maximal four lateral wall segments (i.e. basal- and mid-level of inferolateral and anterolateral segments). The post-processing and selection of analysable segments and averaging into one septal and one lateral wall strain curve, was similar for STE, CMR-TAG and CMR-FT.

CARDIAC MAGNETIC RESONANCE IMAGING

CMR examinations were performed on a 1.5T system (Magnetom Avanto, Siemens, Erlangen, Germany) with the use of a phased array cardiac receiver coil. Although performed on a different moment compared to STE, both standard CMR cine images for the CMR-FT analysis and CMR tagging images were obtained in the same examination.

ACQUISITION - STANDARD CMR IMAGES

Standard CMR cine images were acquired using a retrospectively ECG-gated balanced steady-state free-precession (SSFP) sequence during end-expiratory breath holding. A stack of 8-12 consecutive short axis cine images was acquired covering the entire LV. Typical image acquisition parameters were: slice thickness 5mm, slice gap 5mm, echo time (TE) 1.6ms, repetition time (TR) 3.2ms, temporal resolution <50ms, in-plane spatial resolution 1.5 by 2.1mm, flip angle 60 degrees. The number of reconstructed temporal phases within the cardiac cycle was set at 20. Subsequently, high temporal resolution (TE 1.7ms, TR 3.4ms, temporal resolution ~15ms) cine imaging of the LV in the three-chamber view was performed to assess the opening and closure times of the mitral and aortic valve.

ACQUISITION - CMR TAGGING IMAGES

Before contrast injection, tagged images were acquired at three short-axis slices (basal, mid, apical) using a complementary spatial modulation of magnetization (CSPAMM) line tagging

sequence with segmented ECG-gated acquisitions and serial breath holds.¹⁶ Typical image acquisition parameters were: slice thickness 6mm, TE 1.7ms, TR 3.6ms, temporal resolution <15ms, in-plane spatial resolution 1.3 by 4.3mm, flip angle 20 degrees, tag spacing 7mm. The number of reconstructed temporal phases within the cardiac cycle was set at 55.

OFFLINE ANALYSIS – CMR TAGGING

Tagged CMR images were exported and analysed (AZ, RN) with the SinMod technique (inTag, v2.0, CREATIS lab, Lyon, France, run as a plug-in for OsiriX Imaging Software v6.5, Pixmeo, Switzerland).¹⁹ Apical slices were discarded, while basal and mid short-axis slices were used for analysis in order to match the STE slice positions. After selecting the area of interest, endocardial and epicardial contours were manually drawn in the end-systolic phase and automatically propagated. A template was placed dividing the LV in six equally sized regions, similar to STE. The myocardium was divided in three layers (i.e. endo-, mid-, epi-wall layer). Results of the mid-wall layer were used, as these results are independent of contour placement.

OFFLINE ANALYSIS – CMR FEATURE TRACKING

Semi-automated FT analysis software (QStrain Research Edition evaluation version 1.3.0.10, Medis, Leiden, The Netherlands) was used to analyse short-axis cine images corresponding with the mid and basal slice-location of the CMR-TAG images (AZ and RN). Apical slices were discarded to match STE. First, endo- and epicardial contours were manually drawn in both end-diastolic and end-systolic frames and propagated automatically. Both endocardial and epicardial features were included for strain analysis, resulting in myocardial strain. The LV was divided in six regions, similar to the other techniques.

PARAMETERS

BASIC STRAIN PARAMETERS

The following parameters were obtained for the septal and lateral wall (figure 1). 1) Peak strain was the maximal negative peak strain during the cardiac cycle. 2) AVC strain was defined as the strain value at aortic valve closure. 3) Time to maximal peak (TTP_{max}) was the time difference between the start of the strain curve to most negative peak strain. Furthermore, 4) average systolic strain rate (i.e. average strain rate between mitral valve closure and AVC) and 5) average diastolic strain rate (i.e. average strain rate after AVC) were obtained.

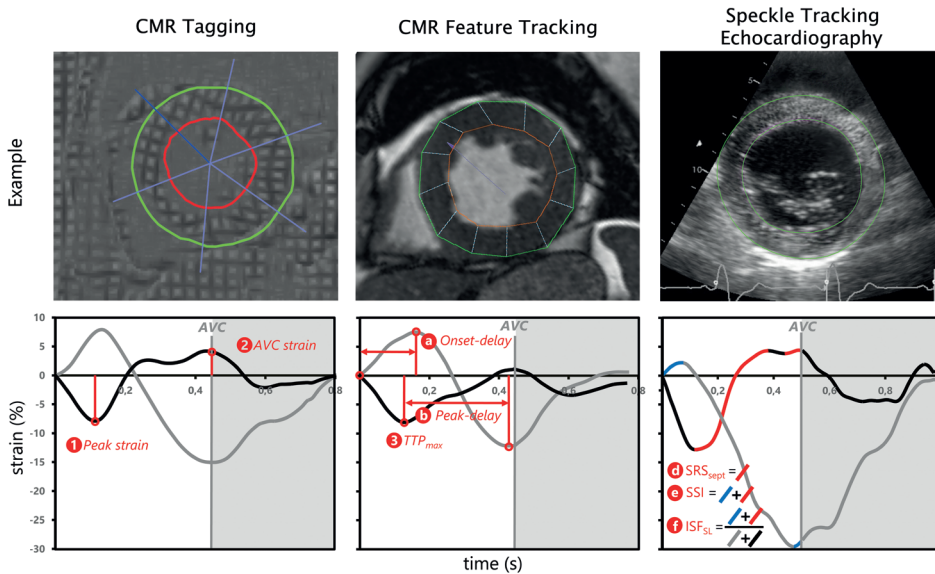


FIGURE 1. Overview of imaging techniques and corresponding myocardial strain analysis

Examples of imaging techniques (top row) and resulting strain signals (bottom row) of one specific patient. Each column represents a single technique with the corresponding strain results. Examples of derived parameters are shown per graph. Basic strain parameters are indicated with a number, dyssynchrony and discoordination parameters are indicated with a character. Strain signals of the septum (black line) and lateral wall (grey line) are given, with the aortic valve closure (grey vertical line) as end of systole. CMR: cardiac magnetic resonance imaging, AVC: aortic valve closure, AVC strain: strain value at aortic valve closure, TTP_{max} : time to maximal peak shortening, onset-delay: time delay between onset of shortening of septal and lateral wall, peak-delay: septal to lateral wall delay of TTP_{max} , SRS_{sept} : systolic rebound stretch of the septum, SSI: systolic stretch index, $ISF_{sep-lat}$: internal stretch fraction of septal and lateral wall.

DYSSYNCHRONY PARAMETERS

Three parameters of dyssynchrony were analysed. a) Onset-delay was determined as the absolute time delay between onset of shortening of the septal and lateral wall. b) Peak delay was calculated as the absolute difference between lateral and septal wall TTP_{max} . c) The TTP_{SD} was calculated as the standard deviation of TTP_{max} of all analysable segments of the total LV.

REGIONAL DISCOORDINATION PARAMETERS

Three regional discoordination parameters were analysed. d) Systolic rebound stretch of the septum (SRS_{sept}) was defined as the total amount of systolic stretch after initial shortening

of the septum (figure 1). e) Systolic stretch index (SSI) was calculated by adding SRS_{sept} to all systolic stretch of the lateral wall.¹¹ f) Internal stretch factor (ISF) was calculated as the fraction of all systolic stretch compared to cumulative systolic shortening for the septal and lateral wall ($ISF_{sep-lat}$). g) Septal strain curves were categorized in three types, determined by their shape, LBBB-1: double-peaked systolic stretch, LBBB-2: early pre-ejection shortening peak followed by prominent systolic stretching and LBBB-3: pseudo normal shortening with a late-systolic shortening peak, followed by less pronounced end-systolic stretch (figure 2).¹²

5

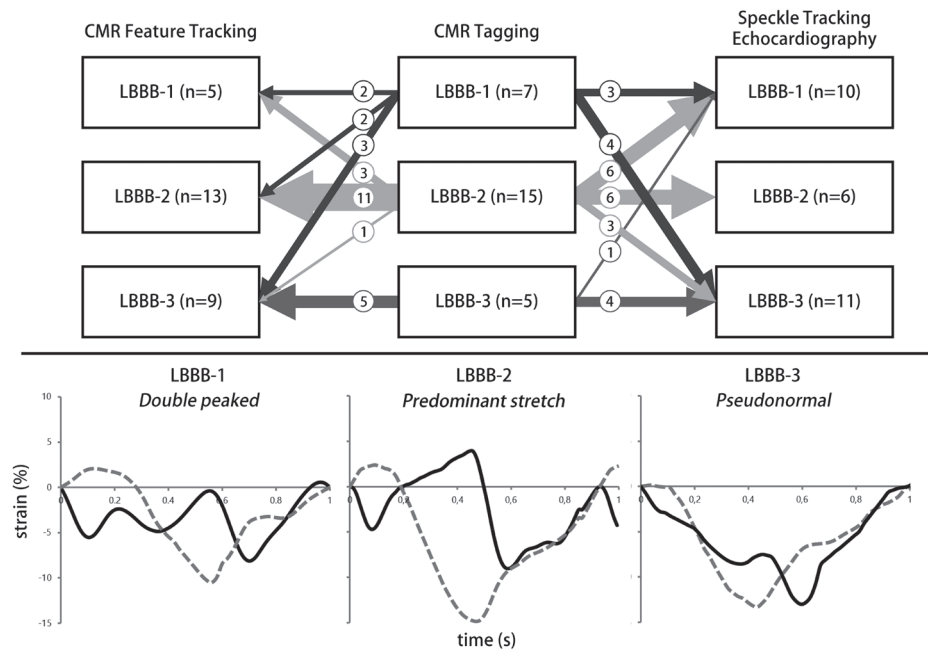


FIGURE 2. LBBB pattern categorization

Septal strain pattern categorization and distribution of strain patterns found by the three imaging techniques. The distribution per imaging technique is given vertical in the upper panel. The cross-over of patients from CMR tagging to speckle tracking echocardiography and CMR feature tracking is displayed by arrows. The thickness of the arrows matches the number of patients crossing over. The number of patients crossing over is also given by a number in each arrow. Specific examples of the three patterns are given in the lower panel. Black curve: septal strain, grey dashed curved: lateral wall strain. CMR: cardiac magnetic resonance imaging, LBBB-1: double peak shortening, LBBB-2: predominant stretch, LBBB-3: pseudo-normal shortening, n: number of patients.

DISCOORDINATION PARAMETERS OF THE TOTAL LV

Finally, two discoordination parameters reflecting the total LV were analysed. h) The internal stretch factor of the total LV (ISF_{LV}) was determined using all analysable segments. ISF_{LV} was determined as the total amount of stretch divided by the total amount of shortening during systole (supplemental figure 1).²⁰ i) Lastly, the circumferential uniformity ratio estimates (CURE) was calculated, ranging from 0 (total dyssynchrony) to 1 (perfectly synchronous).²¹

STATISTICAL ANALYSIS

Statistical analysis was performed (BG and MR) using R version 3.3.2 (The R foundation for Statistical Computing), and the R-packages psych version 1.5.8 (for calculation of Cohen's kappa coefficients, ICCs and their associated p-values). Results obtained with the three techniques were compared using the intra-class correlation coefficient (ICC) for absolute agreement between techniques (ICC2 according to Shrout and Fleiss)²² and Spearman rank or Pearson correlation coefficient (R) depending on normality of data. An $ICC \geq 0.75$ was classified as excellent, 0.60-0.74 as good, 0.40-0.59 as fair, and <0.40 as poor.²³ Bland-Altman plots were made to observe the agreement between modalities. The mean difference and limits of agreement (± 1.96 standard deviation) of the Bland-Altman plot were used a reference of agreement. Lastly, Cohen's kappa coefficient was calculated as the level of agreement between modalities on septal strain pattern categorization. A statistical result with a p-value <0.05 was deemed significant.

RESULTS

STUDY POPULATION

Twenty-seven patients with CMR tagging images were included, of which a detailed description is given in table 1. In these patients 94% of all segments were analysable with CMR-TAG, 87% with CMR-FT and 89% with STE. Frame rate of echocardiographic images was on average 65 ± 11 Hz, which corresponds to a temporal resolution of ~ 15 ms. Temporal resolution of CMR-TAG was ~ 14 ms, while it was ~ 40 ms for CMR-FT.

TABLE 1. Baseline characteristics

Variable	Total cohort (n=27)
Age (years)	65.1 ±9.7
Gender (n, male)	15 (56%)
BMI (kg/m ²)	26.3 ±3.9
Aetiology (n, ischemic cardiomyopathy)	7 (26%)
QRS width (ms)	183 (167-194)
Sinus rhythm (%)	100%
QRS morphology (n)	
LBBB	21 (81%)
IVCD	6 (19%)
NYHA class (n)	
II	17 (63%)
III	10 (37%)
Medication (n)	
Beta-blockers	23 (85%)
Diuretics	22 (81%)
ACE / ATII inhibitors	17 (63%)
Aldosterone antagonists	10 (37%)
CMR - LVEDV (ml)	317 ±100
CMR - LVESV (ml)	239 ±99
CMR - LVEF (%)	26.7 ±8.8
CMR - LV mass	131 (118-157)

Mean and standard deviation are given with ± symbol, median and interquartile range between brackets. BMI: body surface mass index, CMR: cardiac magnetic resonance imaging, LBBB: left bundle branch block, IVCD: intraventricular conduction delay, NYHA: New York Heart Association, ATII: angiotensin receptor II, LVEDV: left ventricular end-diastolic volume, LVESV: left ventricular end-systolic volume, LVEF: left ventricular ejection fraction, LV: left ventricular.

TABLE 2. Strain parameters of each myocardial strain analysis modality

	CMR tagging	CMR feature tracking	STE
Basic strain septum			
1 - AVC strain septum (%)	2.4±5.8	-1.1±5.0	-6.8±7.1
2 - Peak strain septum (%)	-4.0±2.8	-5.1±3.6	-10.4±5.4
3 - TTP _{max} septum (ms)	195±179	379±211	459±173
4 - Systolic strain rate septum (%/s)	5.4±16.4	-3.0±12.9	-15.9±16.1
5 - Diastolic strain rate septum (%/s)	-1.1±10.8	2.1±10.9	-1.9±29.0
Basic strain lateral wall			
1 - AVC strain lateral (%)	-12.6±3.2	-12.0±3.5	-14.5±5.3
2 - Peak strain lateral (%)	-13.4±2.7	-12.4±3.6	-15.8±5.5
3 - TTP _{max} lateral (ms)	424±33	404±31	474±52
4 - Systolic strain rate lateral (%/s)	-32.2±7.9	-30.8±9.3	-32.8±11.9
5 - Diastolic strain rate lateral (%/s)	29.7±13.2	27.8±13.7	12.5±25.0
Dyssynchrony			
a - Onset-delay (ms)	55±25	58±46	57±61
b - Peak-delay (ms)	268±127	189±104	144±104
c - TTP _{SD} (ms)	149±48	159±44	149±52
Discoordination septal and lateral wall			
d - SRS _{sept} (%)	7.2±4.5	3.8±2.6	3.6±3.9
e - SSI (%)	8.7±5.5	5.1±3.8	5.0±4.4
f - ISF _{sep-lat}	0.43±0.25	0.29±0.21	0.25±0.16
g -Septal strain patterns (n, %)			
LBBB-1	7 (26)	5 (19)	10 (37)
LBBB-2	15 (56)	13 (48)	6 (22)
LBBB-3	5 (19)	9 (33)	11 (41)
Discoordination total LV			
h - ISF _{LV}	0.46±0.22	0.35±0.17	0.37±0.13
i - CURE	0.81±0.09	0.77±0.09	0.78±0.06

CMR: cardiac magnetic resonance imaging, TAG: tagging, FT: feature tracking, STE: speckle tracking echocardiography, AVC strain: strain value at aortic valve closure, TTP_{max}: time to maximal peak shortening, Onset-delay: time delay between onset of shortening of septal and lateral wall, Peak-delay: septal to lateral wall delay of TTP_{max}, TTP_{SD}: standard deviation of time to peak max of all segments, SRS_{sept}: septal systolic rebound stretch, SSI: systolic stretch index, ISF_{sep-lat}: internal stretch factor of septum and lateral wall, ISF_{LV}: internal stretch factor of all left ventricular segments, CURE: circumferential uniformity ratio estimates.

BASIC STRAIN PARAMETERS

Overall, agreement of CMR-TAG and CMR-FT was higher compared to agreement of CMR-TAG and STE for basic strain parameters. This applied for ICC values, Bland-Altman characteristics and the correlation coefficient (R) (table 3). 1) For CMR-FT AVC strain of the septum was fair (ICC 0.55, R 0.67), while it was poor for STE (ICC 0.23, R 0.47). The ICC of AVC strain of the lateral wall was fair for CMR-FT (ICC 0.50, R 0.50) and poor for STE (ICC 0.08, R 0.10). 2) Peak strain of the septum had a fair ICC for CMR-FT (ICC 0.58, R 0.55) and a poor ICC for STE (ICC 0.155, 0.42). Lateral wall peak strain also had a fair ICC for CMR-FT (ICC 0.54, R 0.59) and a poor ICC for STE (ICC 0.01, R 0.02). 3) TTP_{max} of the septal and lateral wall showed an apparent wide distribution in the Bland-Altman plots for both comparisons (figure 3). Septal TTP_{max} caused a large spread in results, while the lateral wall TTP_{max} were more similar for both comparisons. Although ICC for TTP_{max} was poor for all comparisons, CMR-FT showed better agreement with CMR-TAG compared to STE for the septum (CMR-FT: ICC 0.17, R 0.11 and STE: ICC 0.00, R -0.16) and the lateral wall (CMR-FT: ICC 0.34, R 0.40 and STE: ICC 0.13, R 0.23). 4) Systolic strain rate showed comparable results to AVC strain. For CMR-FT systolic strain rate of the septum was fair (ICC 0.56, R 0.66), while it was poor for STE (ICC 0.25, R 0.45). ICC of the systolic strain rate of the lateral wall was fair for CMR-FT (ICC 0.575, R 0.58) and poor for STE (ICC 0.05, R 0.05). 5) Diastolic strain rate showed good ICC for the septal (ICC 0.64, R 0.66) and excellent ICC for the lateral wall (ICC 0.82, 0.82) for CMR-TAG vs. CMR-FT. ICC of diastolic strain rate was poor for both walls comparing CMR-TAG and STE (septum: ICC 0.34, R 0.50, lateral wall: ICC 0.23, R 0.38).

TABLE 3. Intra-class correlation and correlation of CMR tagging vs. CMR feature tracking and CMR tagging vs. speckle tracking echocardiography.

	CMR-TAG vs. CMR-FT (n=27)		CMR-TAG vs. STE (n=27)	
	ICC (95% CI)	R	ICC (95% CI)	R
Basic strain septum				
1 - AVC strain septum (%)	0.55 (0.09 - 0.79)	0.67‡	0.23 (-0.10 - 0.56)	0.47*
2 - Peak strain septum (%)	0.58 (0.26 - 0.78)	0.55†	0.155 (-0.10 - 0.45)	0.42*
3 - TTP _{max} septum (ms)	0.17 (-0.11 - 0.47)	0.11	0.00 (-0.15 - 0.22)	-0.16
4 - Systolic strain rate septum (%/s)	0.56 (0.16 - 0.79)	0.66‡	0.25 (-0.10 - 0.57)	0.45*
5 - Diastolic strain rate septum (%/s)	0.64 (0.35 - 0.82)	0.66‡	0.34 (-0.05 - 0.635)	0.50†
Basic strain lateral wall				
1 - AVC strain lateral (%)	0.50 (0.16 - 0.74)	0.50†	0.08 (-0.27 - 0.43)	0.10
2 - Peak strain lateral (%)	0.54 (0.22 - 0.76)	0.59†	0.01 (-0.31 - 0.36)	0.02
3 - TTP _{max} lateral (ms)	0.34 (0.00 - 0.63)	0.40*	0.13 (-0.12 - 0.41)	0.23
4 - Systolic strain rate lateral (%/s)	0.575 (0.26 - 0.78)	0.58†	0.05 (-0.35 - 0.42)	0.05
5 - Diastolic strain rate lateral (%/s)	0.82 (0.65 - 0.91)	0.82‡	0.23 (-0.08 - 0.53)	0.38
Dyssynchrony				
a - Onset-delay (ms)	0.42 (0.05 - 0.69)	0.23	0.024 (-0.37 - 0.40)	-0.08
b - Peak-delay (ms)	0.45 (0.045 - 0.715)	0.46*	0.23 (-0.09 - 0.53)	0.27
c - TTP _{SD} (ms)	0.46 (0.11 - 0.71)	0.49†	0.20 (-0.20 - 0.54)	0.19
Regional discoordination				
d - SRS _{sept} (%)	0.41 (-0.06 - 0.72)	0.65‡	0.30 (-0.05 - 0.60)	0.41*
e - SSI (%)	0.58 (0.00 - 0.83)	0.68‡	0.55 (0.02 - 0.81)	0.70‡
f - ISF _{sep-lat}	0.53 (0.10 - 0.77)	0.45*	0.46 (-0.06 - 0.76)	0.69‡
Disoordination total LV				
h - ISF _{LV}	0.55 (0.15 - 0.78)	0.66‡	0.32 (-0.02 - 0.61)	0.42*
i - CURE	0.485 (0.145 - 0.725)	0.37	0.41 (0.06 - 0.67)	0.36

CI: confidence interval, ICC: intra-class correlation coefficient, R: correlation coefficient, for other abbreviations see table 2. P-values for statistical significance of R-values are given with: *: p-value <0.05, †: p-value <0.01, ‡: p-value <0.001.

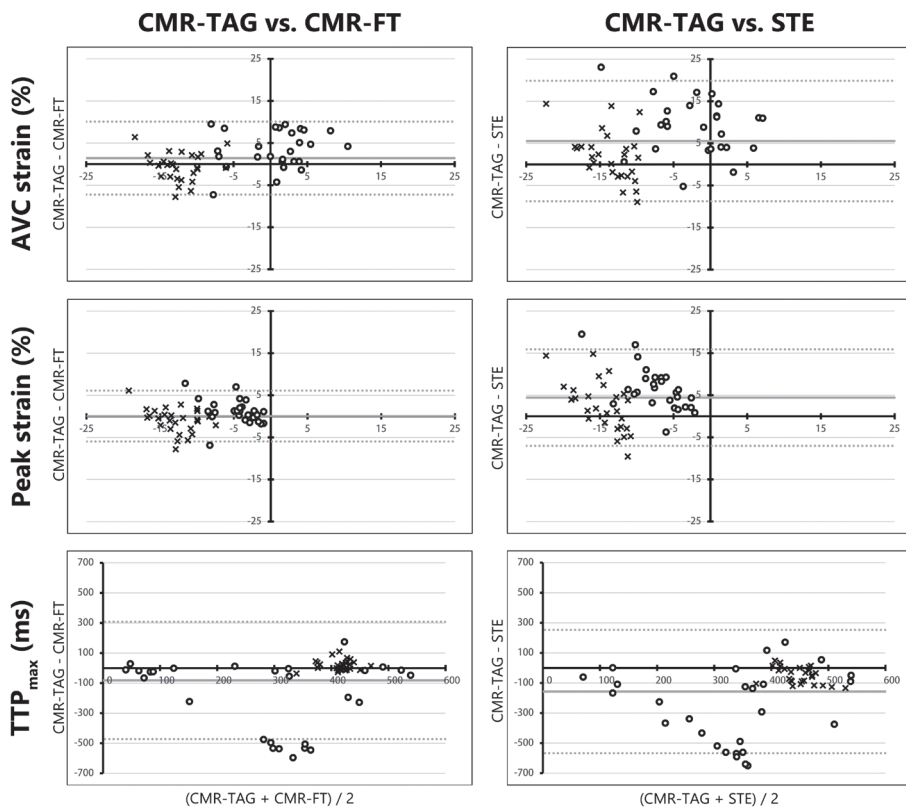


FIGURE 3. Bland-Altman plots of basic strain parameters

Bland-Altman plots for CMR-TAG vs. CMR-FT and CMR-TAG vs. STE of three basic strain parameters. The mean of two techniques is plotted on the x-axis and the difference on the y-axis. The mean difference is displayed as a solid red line, while the limits of agreement are displayed as dotted red lines. Septal values are given as dots, while lateral wall values are given as crosses. AVC strain: strain at aortic valve closure time, Peak strain: highest negative peak strain value, TTP_{max} : time to maximal peak strain, CMR: cardiac magnetic resonance imaging, TAG: tagging, FT: feature tracking, STE: speckle tracking echocardiography.

DYSSYNCHRONY PARAMETERS

a) Onset delay was quite similar for CMR-TAG and CMR-FT, with a mean difference in the Bland-Altman plot of -2.5ms (supplemental figure 2). The corresponding ICC was fair (ICC 0.42, R 0.23). CMR-TAG vs. STE also had a low mean difference of -1.9ms, although the limits of agreement were larger, combined with a poor ICC (ICC 0.024, R -0.08). b) Peak

delay of CMR-TAG was overall larger compared to CMR-FT and STE (supplemental figure 2). ICC was fair for CMR-FT (ICC 0.45, R 0.46), and poor for STE (ICC 0.23, R 0.27). TTP_{SD} (c) showed a fair ICC for CMR-FT (ICC 0.46, R 0.49), and poor ICC for STE (ICC 0.20, R 0.19).

REGIONAL DISCOORDINATION PARAMETERS

d) SRS_{sept} showed a fair ICC for CMR-FT (ICC 0.41, R 0.65), while agreement was poor for STE (ICC 0.30, R 0.41). CMR-TAG showed overall higher values for SRS_{sept} compared to both other imaging techniques. The difference of CMR-TAG to CMR-FT and STE were mostly positive, indicating an underestimation by CMR-FT and STE (figure 4). e) SSI also showed an overall underestimation by CMR-FT and STE compared to CMR-TAG. Agreement on SSI was fair for CMR-FT (ICC 0.58, R 0.68) and STE (ICC 0.55, R 0.70). f) $ISF_{sep-lat}$ was comparable between techniques, ICC's of both CMR-FT (ICC 0.53, R 0.45) and STE (ICC 0.46, R 0.69) were fair. Overall values were still lower by CMR-FT and STE compared to CMR-TAG (figure 4). For septal strain patterns (g) the kappa value of CMR-TAG vs. CMR-FT (0.465 $p < 0.001$) was higher compared to the kappa of CMR-TAG vs. STE (0.265, $p < 0.001$). The number of patients crossing over from LBBB-1 or LBBB-2 on the one hand, and LBBB-3 on the other, using CMR-TAG and CMR-FT is rather low ($n=4$, 15%), especially compared to CMR-TAG and STE ($n=8$, 30%) (figure 2).

DISCOORDINATION PARAMETERS OF THE TOTAL LV

ICC of ISF_{LV} (h) of CMR-FT (ICC 0.55, R 0.66) was the highest off all dyssynchrony and discoordination parameters. Both ICC and R values were lower for STE (ICC 0.32, R 0.42). The CURE index (i) showed rather comparable values between techniques (figure 5) with relative narrow limits of agreement in the Bland-Altman plot. Both CMR-FT (ICC 0.485, R 0.37) and STE (ICC 0.41, R 0.36) resulted in a fair ICC value for CURE compared to CMR-TAG (table 3).

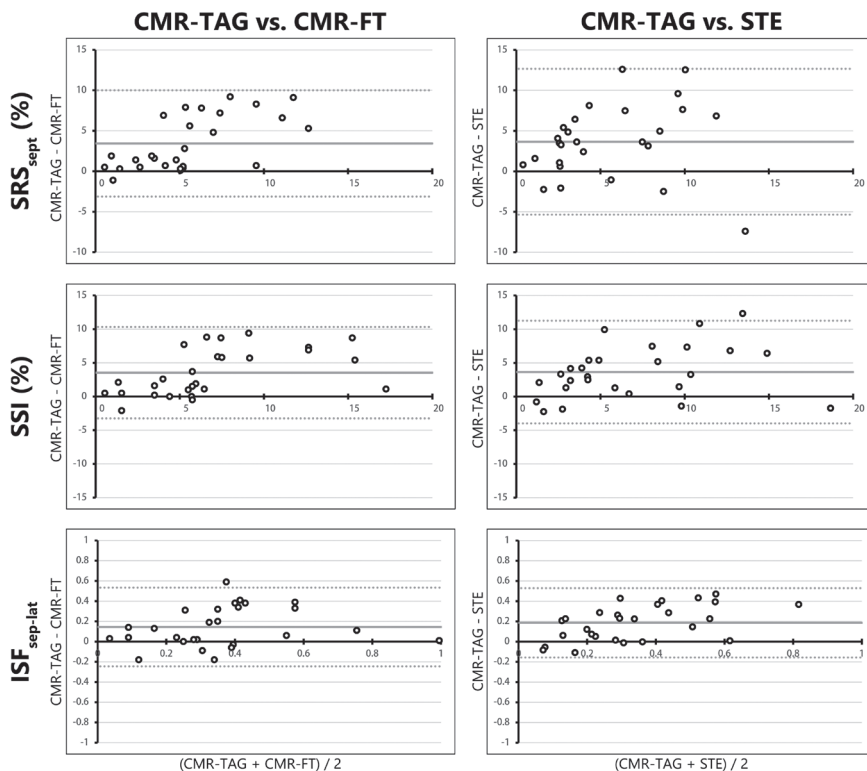


FIGURE 4. Bland-Altman plots of regional discoordination parameters

Bland-Altman plots for CMR-TAG vs. CMR-FT and CMR-TAG vs. STE of regional discoordination parameters (i.e. SRS_{sept} , SSI and $ISF_{sep-lat}$). The mean value of one patient analysed with the two techniques is plotted on the x-axis and the difference on the y-axis. The mean difference is displayed as a solid red line, while the limits of agreement are displayed as dotted red lines. SRS_{sept} : septal systolic rebound stretch, SSI: systolic stretch index, $ISF_{sep-lat}$: internal stretch factor of septum and lateral wall, CMR: cardiac magnetic resonance imaging, TAG: tagging, FT: feature tracking, STE: speckle tracking echocardiography.

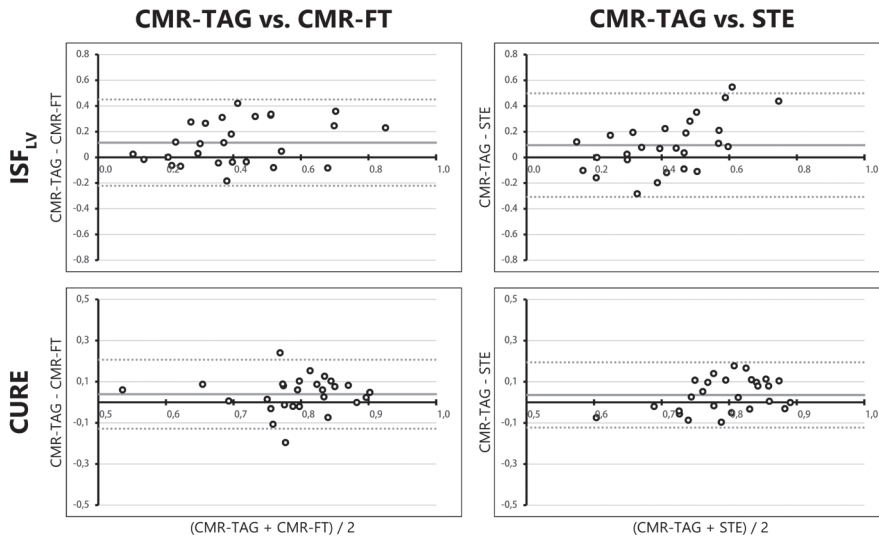


FIGURE 5. Bland-Altman plots of discoordination parameters of the total LV

Bland-Altman plots for CMR-TAG vs. CMR-FT and CMR-TAG vs. STE of two discoordination parameters, obtained from the total LV. The mean value of one patient analysed with the two techniques is plotted on the x-axis and the difference on the y-axis. The mean difference is displayed as a solid red line, while the limits of agreement are displayed as dotted red lines. ISF_{LV} : internal stretch factor of the total LV, CURE: circumferential uniformity ratio estimates, LV: left ventricle, CMR: cardiac magnetic resonance imaging, TAG: tagging, FT: feature tracking, STE: speckle tracking echocardiography.

DISCUSSION

This study explores the comparison of strain parameters in CRT candidates of two widely available strain analysis techniques, speckle tracking echocardiography and CMR feature tracking, with gold-standard CMR tagging. While most basic strain and dyssynchrony parameters differed substantially between techniques, there were apparent similarities found for discoordination parameters. This finding is promising, as discoordination parameters are potential predictors for CRT response.^{10, 11, 20} The CMR-based techniques (i.e. CMR-TAG and CMR-FT) showed the highest agreement, shown in fair ICC values, higher R values, and relative narrow limits of agreement of the Bland-Altman plots. STE mostly had a poor agreement with CMR-TAG. CMR-FT may therefore be a valuable alternative to CMR-TAG for analysis of discoordination parameters in patients eligible for CRT.

COMPARISON OF IMAGING TECHNIQUES

To the best of our knowledge, this is the first study to compare strain parameters between different strain analysis techniques in a CRT patient population. The overall agreement between CMR-FT and CMR-TAG was higher compared to the agreement between STE and CMR-TAG. We would like to discuss three considerations to ascribe this difference. Firstly, STE uses a different imaging source, while both CMR-FT and CMR-TAG are obtained with the same imaging modality. Second, as part of the protocol, echocardiographic examinations and CMR scans were not performed on the same day. Therefore, physiological differences, such as loading conditions and heart rate, may have interfered with agreement of STE and CMR-TAG. Third, the imaging plane used for CMR and echocardiography is possibly different. Echocardiographic parasternal short-axis views were obtained from a single intercostal position, angulating the echo probe to the mitral valve annulus plane and the papillary muscle plane. These imaging planes may thereby be partly oblique, while CMR imaging planes were 'true' short-axis views. Furthermore, CMR-FT and CMR-TAG images were acquired on the almost exact same slice position, while the anatomical plane of STE images may be different. Another factor causing discrepancies between techniques is the specific manufacturer used for strain analysis with either CMR-TAG, CMR-FT, or STE.²⁴ Results of CMR-TAG, CMR-FT, and STE are contemporary, as they are dependent on specific analysis algorithms which are constantly under development. Although earlier studies show less favourable agreement of CMR-TAG and CMR-FT,^{25, 26} recent developments are more promising.^{27, 28} This trend is in accordance with our results, as we found that CMR-FT had fair agreement with CMR-TAG. However, further improvements are necessary, as results obtained with different imaging techniques can still differ largely for the individual patient. These differences may have underestimated the agreement between STE and CMR-TAG, compared to CMR-TAG vs. CMR-FT. Nevertheless, echocardiography has its known limitations. High quality images are required for reliable strain analysis with STE,^{29, 30} but can be difficult in this selection of patients. Frame rate is directly related to the temporal resolution, which is often high in echocardiographic images, especially compared to the relative low frame rate of standard cine images used for CMR-FT. A low frame rate causes under sampling and may lead to misinterpretation of peak and time-to-peak values in strain signals.²⁹ The frame rate of CMR-TAG was relatively high and comparable to STE in our study. Therefore, CMR-TAG may be considered a true gold-standard technique in this study, as imaging quality and frame rate of the implemented tagging protocol were optimized.

ASSESSMENT OF STRAIN PARAMETERS

Peak strain parameters showed fair correlation, especially between CMR techniques, except for timing indices of the septum. The maximal peak of septal strain can shift easily in case of dyssynchrony, as there are often multiple peaks (e.g. LBBB-1 and -2 patterns). Changes in absolute strain values of these peaks can drastically change TTP_{max} . In previous studies, most dyssynchrony and discoordination parameters have been primarily analysed with a single imaging technique. While some (i.e. CURE and ISF_{LV}) are predominantly used in CMR-based studies,²⁰ others (i.e. SRS_{sept} , peak-delay and septal strain patterns) are primarily derived with STE.¹² In our study, basic strain parameters, and more complex parameters of mechanical dyssynchrony showed apparent variations among the three techniques. However, the three techniques did show fair agreement on discoordination parameters. This indicates that these parameters adequately reflect mechanical discoordination and that they are detectable by multiple modalities. Discoordination parameters are promising as predictors for CRT response.^{10, 11, 20} The predictive value of discoordination parameters is even known in combination with electrocardiographic parameters.^{6, 11} ISF_{LV} and CURE are predictors of CRT response and use information of all available LV segments,³¹ therefore reflecting total LV discoordination.^{20, 21} These parameters are also less susceptible to outliers compared to basic strain parameters, as they contain information on all segments.^{20, 21} Parameters being calculated using averages of multiple segments (i.e. SRS_{sept} and SSI) also showed fair agreement between modalities. Obtaining deformation characteristics using averages of multiple segments may therefore reduce noise and measurement variability. Specific pre-specified septal strain patterns are known to predict CRT response, as LBBB-1 and LBBB-2 patterns are associated with volumetric response after CRT, while LBBB-3 is not.^{12, 32} The relative high agreement between CMR-TAG and CMR-FT on LBBB-1 and LBBB-2 on the one hand, and LBBB-3 on the other is therefore promising for further implementation of septal strain pattern categorization using CMR.¹²

MYOCARDIAL STRAIN ORIENTATION

STE parameters are mainly validated with longitudinal strain,^{33, 34} while CMR is predominantly based on circumferential strain.^{20, 21} Circumferential strain is more intuitive, as mid-myocardial fibres are orientated in the circumferential direction and short-axis images represent all segments distributed around the LV at each level (i.e. basal, mid or apical).³⁵ The method of determining circumferential strain calculation differs between the three methods.

Both the CMR-FT and STE software track specific myocardial details, respectively 'features' and 'speckles', of the endo- and epicardial border.¹⁴ The specific wall layer used for strain analysis differed between techniques. The results of the endocardial layer were used for STE, as the epicardial layer often lacked an appropriate border zone. Strain values of CMR-FT were a product of endocardial and epicardial strain. This is in contrast to CMR-TAG, of which strain of the mid-wall layer was used.¹⁹ The difference between the approaches may have biased the overall level of agreement. Endocardial strain is known to give higher peak values compared to epicardial strain,³⁶ and might also be higher than midmyocardial values, which can be appreciated in the positive mean difference between CMR-TAG and STE on peak strain and AVC-strain in the Bland-Altman results. This difference may have also affected the agreement of dyssynchrony and discoordination parameters.

LIMITATIONS

CMR imaging with myocardial tagging was performed in a small subset of patients from the MARC study, which may have given outliers a relatively large effect on results. The patient population was moreover limited to patients eligible for CRT, reducing variability in measurements. These results should therefore be validated in a larger cohort. However, strain measurements are of particular interest in this specific population to improve patient selection for CRT. As mentioned, the study protocol has also influenced results, as echocardiographic and CMR examination were not performed on the same day. Moreover, differences in imaging plane between CMR and STE are possible and strain analysis was not performed on the same wall layers. ECG triggering differs between imaging techniques, as ECG electrodes were repositioned between examinations and a different lead may have been used. Moreover, ECG triggering of STE was placed at QRS onset, while the top of the R wave is used for CMR. ECG triggering affects the reference value and may have affected subsequent values of timing and absolute changes. While STE relied on end-diastolic region of interest placement, CMR-FT used both end-systolic and end-diastolic region of interests to determine myocardial strain. The reliability of CMR-FT may therefore be higher. Echocardiography was moreover obtained with ultrasound machines from two vendors, possibly introducing differences in source data. The overall lower agreement of CMR-TAG and STE should therefore be appreciated carefully. STE was performed with circumferential strain obtained from short axis images, for a more direct comparison between techniques. While circumferential strain is widely used in scientific publications, standardization of

algorithms of STE has also mainly been done for longitudinal strain.^{5, 34} Longitudinal strain assessed with STE may therefore have a higher reliability and reproducibility compared to circumferential strain. The effect of using longitudinal or circumferential strain derived with STE for prediction of CRT response deserves attention in future work.

CLINICAL APPLICATION

The overall reasonable agreement between CMR-TAG and CMR-FT is promising for clinical application. CMR-FT might be a reasonable alternative for CMR-TAG and STE, as suitable CMR cine images are more easily available in clinical practice, compared to the highly specialized CMR-TAG protocols. Detection of mechanical discoordination with CMR-FT is a valuable addition to CMR, which already constitutes an important imaging tool in CRT-candidates for accurate determination of the LV ejection fraction and scar tissue localization.³¹ On the other hand, a portable and bed-side tool like STE might have the highest clinical applicability, of which most discoordination parameters also showed fair agreement compared to the CMR-TAG. The reasonable agreement of the three techniques on mechanical discoordination parameters is moreover promising for the prediction of response to CRT. The implemented discoordination parameters were previously associated with CRT response in single centre studies.^{10, 11, 20} However, previous markers of CRT response failed to take the final step to clinical application, partly because validation to gold-standard techniques was missing.⁹ As the specific methods and modality may slightly differ from previous publications, further studies are needed for implementation into clinical practice. Future studies will focus on the predictive value of these parameters using follow-up data in this specific population.

CONCLUSIONS

In conclusion, comparison of strain analysis techniques showed that CMR-FT had an overall fair agreement with gold-standard CMR-TAG. Although agreement between STE and CMR-TAG was overall lower, direct comparison was limited by technical and methodological differences. The agreement was highest in parameters of mechanical discoordination, compared to basic strain or dyssynchrony parameters. CMR-FT is therefore a potentially valuable clinical alternative for CMR-TAG and STE, especially in the evaluation of mechanical discoordination in CRT-candidates.

REFERENCES

1. Brignole M, Auricchio A, Baron-Esquivias G, Bordachar P, Boriani G, Breithardt OA, et al. 2013 ESC Guidelines on cardiac pacing and cardiac resynchronization therapy. *Eur Heart J*. 2013;34:2281-2329.
2. Sweeney MO, Prinzen FW. Ventricular pump function and pacing: physiological and clinical integration. *Circ Arrhythm Electrophysiol*. 2008;1:127-39.
3. Daubert JC, Saxon L, Adamson PB, Auricchio A, Berger RD, Beshai JF, et al. 2012 EHRA/HRS expert consensus statement on cardiac resynchronization therapy in heart failure: implant and follow-up recommendations and management. *Europace*. 2012;14:1236-86.
4. Auricchio A, Prinzen FW. Non-responders to cardiac resynchronization therapy: the magnitude of the problem and the issues. *Circ J*. 2011;75:521-7.
5. van Everdingen WM, Schipper JC, van 't Sant J, Ramdat Misier K, Meine M, Cramer MJ. Echocardiography and cardiac resynchronisation therapy, friends or foes? *Neth Heart J*. 2016;24:25-38.
6. Risum N, Tayal B, Hansen TF, Bruun NE, Jensen MT, Lauridsen TK, et al. Identification of Typical Left Bundle Branch Block Contraction by Strain Echocardiography Is Additive to Electrocardiography in Prediction of Long-Term Outcome After Cardiac Resynchronization Therapy. *J Am Coll Cardiol*. 2015;66:631-41.
7. Wang CL, Wu CT, Yeh YH, Wu LS, Chan YH, Kuo CT, et al. Left bundle-branch block contraction patterns identified from radial-strain analysis predicts outcomes following cardiac resynchronization therapy. *Int J Cardiovasc Imaging*. 2017;33:869-877.
8. Leenders GE, Cramer MJ, Bogaard MD, Meine M, Doevendans PA, De Boeck BW. Echocardiographic prediction of outcome after cardiac resynchronization therapy: conventional methods and recent developments. *Heart Fail Rev*. 2011;16:235-50.
9. Chung ES, Leon AR, Tavazzi L, Sun JP, Nihoyannopoulos P, Merlino J, et al. Results of the Predictors of Response to CRT (PROSPECT) trial. *Circulation*. 2008;117:2608-16.
10. Leenders GE, De Boeck BW, Teske AJ, Meine M, Bogaard MD, Prinzen FW, et al. Septal rebound stretch is a strong predictor of outcome after cardiac resynchronization therapy. *J Card Fail*. 2012;18:404-12.

11. Lumens J, Tayal B, Walmsley J, Delgado-Montero A, Huntjens PR, Schwartzman D, et al. Differentiating Electromechanical From Non-Electrical Substrates of Mechanical Discoordination to Identify Responders to Cardiac Resynchronization Therapy. *Circ Cardiovasc Imaging*. 2015;8:e003744.
12. Leenders GE, Lumens J, Cramer MJ, De Boeck BW, Doevendans PA, Delhaas T, et al. Septal deformation patterns delineate mechanical dyssynchrony and regional differences in contractility: analysis of patient data using a computer model. *Circ Heart Fail*. 2012;5:87-96.
13. Revah G, Wu V, Huntjens PR, Piekarski E, Chyou JY, Axel L. Cardiovascular magnetic resonance features of mechanical dyssynchrony in patients with left bundle branch block. *Int J Cardiovasc Imaging*. 2016;32:1427-1438.
14. Pedrizzetti G, Claus P, Kilner PJ, Nagel E. Principles of cardiovascular magnetic resonance feature tracking and echocardiographic speckle tracking for informed clinical use. *J Cardiovasc Magn Reson*. 2016;18:51.
15. Harrild DM, Han Y, Geva T, Zhou J, Marcus E, Powell AJ. Comparison of cardiac MRI tissue tracking and myocardial tagging for assessment of regional ventricular strain. *Int J Cardiovasc Imaging*. 2012;28:2009-18.
16. Zwanenburg JJ, Gotte MJ, Kuijter JP, Heethaar RM, van Rossum AC, Marcus JT. Timing of cardiac contraction in humans mapped by high-temporal-resolution MRI tagging: early onset and late peak of shortening in lateral wall. *Am J Physiol Heart Circ Physiol*. 2004;286:H1872-80.
17. Maass AH, Vernooy K, Wijers SC, van 't Sant J, Cramer MJ, Meine M, et al. Refining success of cardiac resynchronization therapy using a simple score predicting the amount of reverse ventricular remodelling: results from the Markers and Response to CRT (MARC) study. *Europace*. 2017;euw445.
18. Lang RM, Badano LP, Mor-Avi V, Afilalo J, Armstrong A, Ernande L, et al. Recommendations for cardiac chamber quantification by echocardiography in adults: an update from the American Society of Echocardiography and the European Association of Cardiovascular Imaging. *Eur Heart J Cardiovasc Imaging*. 2015;16:233-70.
19. Miller CA, Borg A, Clark D, Steadman CD, McCann GP, Clarysse P, et al. Comparison of local sine wave modeling with harmonic phase analysis for the assessment of myocardial strain. *J Magn Reson Imaging*. 2013;38:320-8.

20. Kirn B, Jansen A, Bracke F, van Gelder B, Arts T, Prinzen FW. Mechanical discoordination rather than dyssynchrony predicts reverse remodeling upon cardiac resynchronization. *Am J Physiol Heart Circ Physiol*. 2008;295:H640-6.
21. Helm RH, Leclercq C, Faris OP, Ozturk C, McVeigh E, Lardo AC, et al. Cardiac dyssynchrony analysis using circumferential versus longitudinal strain: implications for assessing cardiac resynchronization. *Circulation*. 2005;111:2760-7.
22. Shrout PE, Fleiss JL. Intraclass correlations: uses in assessing rater reliability. *Psychol Bull*. 1979;86:420-8.
23. Castillo E, Osman NF, Rosen BD, El-Shehaby I, Pan L, Jerosch-Herold M, et al. Quantitative assessment of regional myocardial function with MR-tagging in a multi-center study: interobserver and intraobserver agreement of fast strain analysis with Harmonic Phase (HARP) MRI. *J Cardiovasc Magn Reson*. 2005;7:783-91.
24. van Everdingen WM, Paiman ML, van Deursen CJ, Cramer MJ, Vernoooy K, Delhaas T, et al. Comparison of septal strain patterns in dyssynchronous heart failure between speckle tracking echocardiography vendor systems. *J Electrocardiol*. 2015;48:609-16.
25. Wu L, Germans T, Guclu A, Heymans MW, Allaart CP, van Rossum AC. Feature tracking compared with tissue tagging measurements of segmental strain by cardiovascular magnetic resonance. *J Cardiovasc Magn Reson*. 2014;16:10.
26. Onishi T, Saha SK, Ludwig DR, Marek JJ, Cavalcante JL, Schelbert EB, et al. Feature tracking measurement of dyssynchrony from cardiovascular magnetic resonance cine acquisitions: comparison with echocardiographic speckle tracking. *J Cardiovasc Magn Reson*. 2013;15:95.
27. Moody WE, Taylor RJ, Edwards NC, Chue CD, Umar F, Taylor TJ, et al. Comparison of magnetic resonance feature tracking for systolic and diastolic strain and strain rate calculation with spatial modulation of magnetization imaging analysis. *J Magn Reson Imaging*. 2015;41:1000-12.
28. Singh A, Steadman CD, Khan JN, Horsfield MA, Bekele S, Nazir SA, et al. Inter-technique agreement and interstudy reproducibility of strain and diastolic strain rate at 1.5 and 3 Tesla: a comparison of feature-tracking and tagging in patients with aortic stenosis. *J Magn Reson Imaging*. 2015;41:1129-37.
29. Rosner A, Barbosa D, Aarsaether E, Kjonas D, Schirmer H, D'Hooge J. The influence of frame rate on two-dimensional speckle-tracking strain measurements: a study on silico-simulated models and images recorded in patients. *Eur Heart J Cardiovasc Imaging*. 2015;16:1137-47.

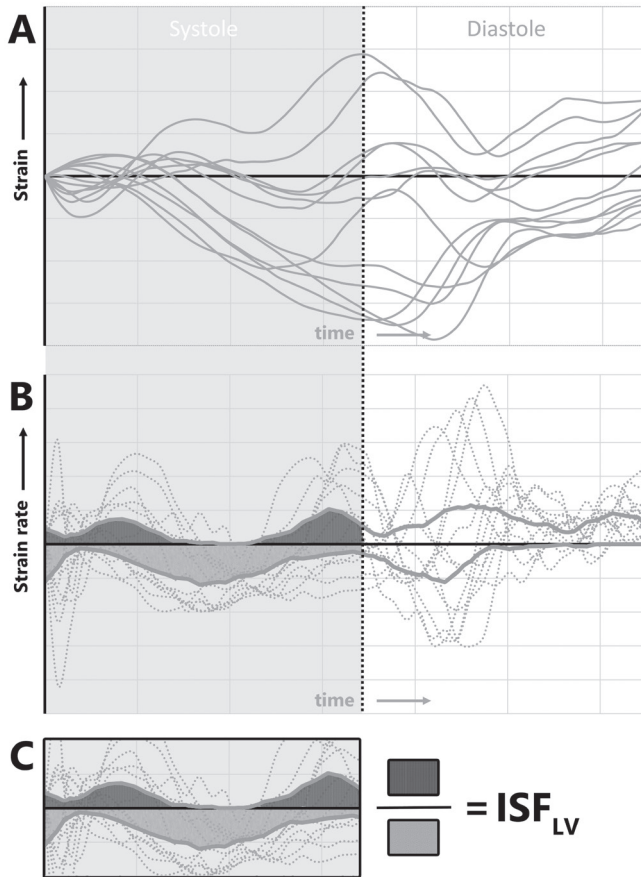
30. D'Hooge J, Barbosa D, Gao H, Claus P, Prater D, Hamilton J, et al. Two-dimensional speckle tracking echocardiography: standardization efforts based on synthetic ultrasound data. *Eur Heart J Cardiovasc Imaging*. 2016;17:693-701.
31. Bilchick KC, Dimaano V, Wu KC, Helm RH, Weiss RG, Lima JA, et al. Cardiac magnetic resonance assessment of dyssynchrony and myocardial scar predicts function class improvement following cardiac resynchronization therapy. *J Am Coll Cardiol Img*. 2008;1:561-8.
32. Marechaux S, Guiot A, Castel AL, Guyomar Y, Semichon M, Delelis F, et al. Relationship between two-dimensional speckle-tracking septal strain and response to cardiac resynchronization therapy in patients with left ventricular dysfunction and left bundle branch block: a prospective pilot study. *J Am Soc Echocardiogr*. 2014;27:501-11.
33. De Boeck BW, Teske AJ, Meine M, Leenders GE, Cramer MJ, Prinzen FW, et al. Septal rebound stretch reflects the functional substrate to cardiac resynchronization therapy and predicts volumetric and neurohormonal response. *Eur J Heart Fail*. 2009;11:863-71.
34. Farsalinos KE, Daraban AM, Unlu S, Thomas JD, Badano LP, Voigt JU. Head-to-Head Comparison of Global Longitudinal Strain Measurements among Nine Different Vendors: The EACVI/ASE Inter-Vendor Comparison Study. *J Am Soc Echocardiogr*. 2015;28:1171-1181, e2.
35. de Simone G, Ganau A, Roman MJ, Devereux RB. Relation of left ventricular longitudinal and circumferential shortening to ejection fraction in the presence or in the absence of mild hypertension. *J Hypertens*. 1997;15:1011-7.
36. Leitman M, Lysiansky M, Lysyansky P, Friedman Z, Tyomkin V, Fuchs T, et al. Circumferential and longitudinal strain in 3 myocardial layers in normal subjects and in patients with regional left ventricular dysfunction. *J Am Soc Echocardiogr*. 2010;23:64-70.

SUPPLEMENTARY MATERIAL

SUPPLEMENTARY TABLE 1. Bland-Altman characteristics of CMR tagging vs. feature tracking and CMR tagging vs. STE.

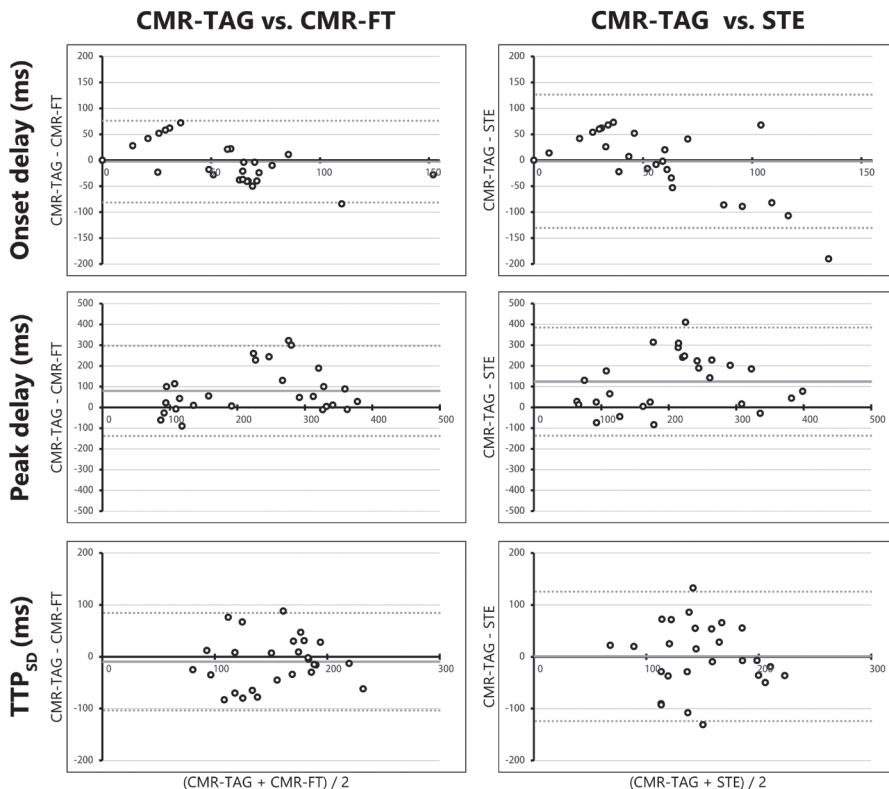
	CMR-TAG vs. CMR-FT (n=27)	CMR-TAG vs. STE (n=27)
Basic strain septum		
1 - AVC strain septum (%)	3.5 (-5.2 - 12.2)	9.2 (-4.0 - 22.5)
2 - Peak strain septum (%)	1.1 (-4.5 - 6.7)	6.4 (-3.4 - 16.2)
3 - TTP _{max} septum (ms)	-183 (-656 - 289)	-264 (-754 - 226)
4 - Systolic strain rate septum (%/s)	8.4 (-16.0 - 32.8)	21.3 (-11.9 - 54.6)
5 - Diastolic strain rate septum (%/s)	-3.1 (-20.7 - 14.4)	0.8 (-48.8 - 50.5)
Basic strain lateral wall		
1 - AVC strain lateral (%)	-0.6 (-7.2 - 5.9)	1.9 (-9.7 - 13.4)
2 - Peak strain lateral (%)	-1.0 (-6.8 - 4.9)	2.4 (-9.4 - 14.2)
3 - TTP _{max} lateral (ms)	19 (-49 - 88)	-50 (-158 - 58)
4 - Systolic strain rate lateral (%/s)	-1.4 (-17.0 - 14.3)	0.5 (-26.9 - 27.9)
5 - Diastolic strain rate lateral (%/s)	1.9 (-13.7 - 17.6)	17.2 (-28.9 - 63.2)
Dyssynchrony		
a - Onset-delay (ms)	-3 (-81 - 76)	-2 (-130 - 126)
b - Peak-delay (ms)	80 (-138 - 297)	124 (-136 - 385)
c - TTP _{SD} (ms)	-9 (-103 - 85)	1 (-124 - 126)
Discoordination septal and lateral wall		
d - SRS _{sept} (%)	3.4 (-3.1 - 10.0)	3.7 (-5.3 - 12.7)
e - SSI (%)	3.5 (-3.2 - 10.3)	3.6 (-4.0 - 11.3)
f - ISF _{sep-lat}	0.14 (-0.245 - 0.53)	0.19 (-0.16 - 0.53)
Discoordination total LV		
h - ISF _{LV}	0.11 (-0.22 - 0.45)	0.10 (-0.31 - 0.50)
i - CURE	0.04 (-0.13 - 0.21)	0.04 (-0.12 - 0.195)

Mean difference of the two techniques is given for each comparison (CMR-TAG minus CMR-FT and CMR-TAG minus STE), with the 95% confidence interval within brackets. For abbreviations see table 2.



SUPPLEMENTAL FIGURE 1. Method for calculation of ISF_{LV}

After calculation of the first derivative of strain (panel A), positive and negative strain rate are averaged (red lines, panel B). The areas of positive (dark grey) and negative (light grey) average strain rate during systole are divided to obtain ISF_{LV} (panel C). The end of systole is marked by the black dotted line.

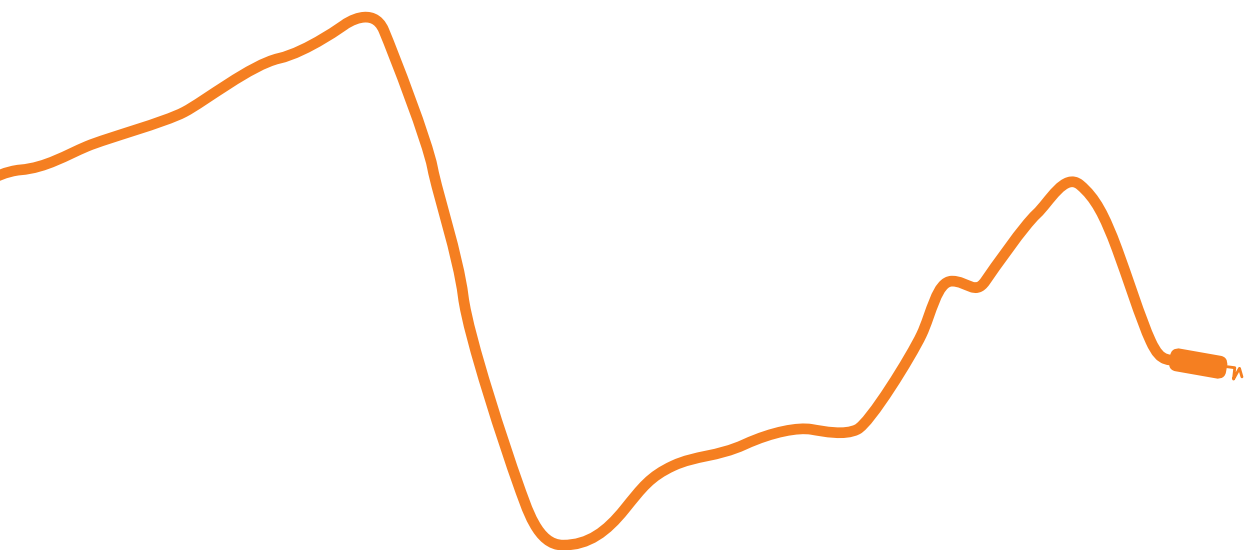


SUPPLEMENTAL FIGURE 2. Bland-Altman plots of dyssynchrony parameters

Bland-Altman plots for CMR-TAG vs. CMR-FT and CMR-TAG vs. STE of remaining parameters, not displayed in the main manuscript. On the x-axis the mean of two techniques and on the y-axis the difference. The mean difference is displayed as a solid red line, while the limits of agreement are displayed as dotted red lines. Onset delay: delay between onset of shortening of septal and lateral wall. SSI: systolic stretch index. TTP_{SD}: standard deviation of time to maximal peak of all segments, CMR: cardiac magnetic resonance imaging, TAG: tagging, FT: feature tracking, STE: speckle tracking echocardiography.



Strain imaging to predict response to cardiac resynchronization therapy: a systematic comparison of strain parameters using multiple assessment modalities



Alwin Zweerink (MD)^{1*}, Wouter M. van Everdingen (MD)^{2*}, Robin Nijveldt (MD, PhD)¹, Odette A.E. Salden (MD)², Mathias Meine (MD, PhD)², Alexander H. Maass (MD, PhD)³, Kevin Vernooij (MD, PhD)⁴, Frederik J. de Lange (MD, PhD)⁵, Marc A. Vos (PhD)⁶, Pierre Croisille (MD, PhD)⁷, Patrick Clarysse (PhD)⁷, Bastiaan Geelhoed (PhD)³, Michiel Rienstra (MD, PhD)³, Isabelle C. van Gelder (MD, PhD)³, Albert C. van Rossum (MD, PhD)¹, Maarten J. Cramer (MD, PhD)^{2*}, Cornelis P. Allaart (MD, PhD)^{2*}

* First two and last two authors contributed equally to the manuscript

¹ Department of Cardiology, and Institute for Cardiovascular Research (ICaR-VU), VU University Medical Center, Amsterdam, The Netherlands

² Department of Cardiology, University Medical Center Utrecht, Utrecht, The Netherlands

³ Department of Cardiology, Thoraxcenter, University of Groningen, University Medical Center Groningen, Groningen

⁴ Department of Cardiology, Maastricht University Medical Center, Maastricht, The Netherlands

⁵ Department of Cardiology, Academic Medical Center, Amsterdam, The Netherlands

⁶ Department of Medical Physiology, University of Utrecht, Utrecht, The Netherlands

⁷ Université de Lyon, UJM-Saint-Etienne, INSA, CNRS UMR 5520, INSERM U1206, CREATIS, F-42023, Saint-Etienne, France

Submitted

ABSTRACT

Objectives: This study aims to compare predictive performance of different strain parameters and evaluate results per imaging technique to predict cardiac resynchronization therapy (CRT) response.

Background: Myocardial strain imaging is a potential tool to improve patient selection for CRT. Various strain parameters have been proposed as predictors of CRT response measuring regional timing differences (dyssynchrony) or inefficient contraction patterns (discoordination). Also, multiple imaging techniques are presently available including CMR tagging (CMR-TAG), CMR feature tracking (CMR-FT) and speckle tracking echocardiography (STE). Despite promising results in single-modality studies, a systematic comparison of strain parameters on a multi-modality level is lacking.

Methods: Twenty-seven patients were prospectively enrolled as part of the markers and response to CRT (MARC) study and underwent both CMR- and echocardiographic examination before CRT implantation. Strain analysis was performed in the circumferential (CMR-TAG, CMR-FT and STE-circ) and longitudinal (STE-long) orientation. Regional strain values, parameters of mechanical dyssynchrony and discoordination were calculated. After twelve months, CRT response was measured by echocardiography as the change in left ventricular end-systolic volume (LVESV).

Results: Twenty-six patients (age 65 ± 9 year, 58% men) completed follow-up. Mean LVESV change was $-29 \pm 27\%$ with 17 (65%) patients showing $\geq 15\%$ reduction in LVESV. Both measures of dyssynchrony ($SD-TTP_{LV}$) and discoordination (ISF_{LV}) were strongly related to CRT response when using CMR-TAG (R^2 0.61 and R^2 0.57, respectively). However, these parameters showed poor correlations for CMR-FT and STE techniques (all $R^2 \leq 0.32$). In contrast, the end-systolic septal strain (ESS_{sep}) parameter showed a consistent high correlation with LVESV change for all techniques (CMR-TAG R^2 0.60; CMR-FT R^2 0.50; STE-circ R^2 0.43; and STE-long R^2 0.43).

Conclusions: End-systolic septal strain was the only parameter with a consistent good relation to reverse remodeling after CRT, irrespective of assessment technique. For the other strain parameters, CMR-TAG was found to be superior to CMR-FT and STE techniques.

BACKGROUND

6

Selection of heart failure patients for cardiac resynchronization therapy (CRT) is primarily guided by the presence of electrical dyssynchrony on the electrocardiogram, as guideline recommendations primarily depend on QRS duration and left bundle branch block (LBBB) morphology.^{1,2} Using guideline criteria, approximately one-third of patients show no clinical improvement after CRT implantation underlining the need for improved selection criteria.³ Myocardial strain imaging is a promising tool that quantifies the mechanical consequences of LBBB. Inhomogeneity of contraction during LBBB reduces left ventricular (LV) pump function efficiency,⁴ and CRT subsequently improves LV pump function by restoring mechanical efficiency of the heart.^{5, 6} Therefore, the detection of inefficient contraction patterns might be helpful to predict CRT response.⁷⁻⁹ Over the past years a variety of strain parameters has been proposed to serve as markers for CRT response. Two types of parameters that can be assessed are measures of dyssynchrony (i.e. regional timing differences) and discoordination (i.e. simultaneously opposing shortening and stretching segments).⁷⁻¹² Both types can be calculated on a regional (i.e. septal to lateral) and segmental (i.e. 17 segments model) scale. In addition, the visual classification of septal strain patterns to a pre-defined category has been proposed to predict CRT benefit.¹³ Most of these parameters were introduced using a single-imaging modality, but at present multiple imaging modalities are available. Cardiovascular magnetic resonance (CMR) imaging was the first modality to offer non-invasive assessment of myocardial strains by the implementation of myocardial taglines (CMR-TAG) and showed promising results in the prediction of CRT response.^{8, 10, 14} Although CMR-TAG is often used as reference technique in scientific research, availability is limited in clinical practice. Speckle tracking echocardiography (STE), on the other hand, is widely available as a bedside tool and offers strain analysis as well. Although STE analysis is highly dependent on the quality of the available acoustic windows, this technique showed promising results in the prediction of CRT outcome as well.^{7, 9, 15} The latest development in the field of myocardial strain analysis is CMR feature tracking (CMR-FT). This emerging post-processing technique shows similarities with STE but uses CMR cine images instead that offer high image quality.¹⁶⁻¹⁸

Despite promising results of multiple strain parameters used in single-modality studies, a direct comparison of the parameters in available modalities is lacking. This study aims to

compare the predictive performance of different strain parameters using multiple imaging techniques, in relation to CRT response.

METHODS

STUDY POPULATION

This pre-defined sub-study with focus on myocardial strain imaging techniques is part of the Markers And Response to CRT (MARC) study which was designed to investigate predictors of CRT response. The MARC study included two-hundred-forty patients planned for CRT implantation in six medical centers in the Netherlands. Details on the original MARC study were published previously.¹⁹ In this sub-study, twenty-seven patients were included for a comprehensive imaging protocol with additional CMR examination including myocardial tagging in the VU university medical center (Amsterdam, The Netherlands). All patients gave written informed consent and all local medical ethics committees approved data collection and management. The investigation conforms to the principles outlined in the Declaration of Helsinki.

IMAGE ACQUISITION: CMR IMAGING

All patients underwent CMR examination at the VU university medical center (Amsterdam, the Netherlands) on a 1.5T whole body system (Magnetom Avanto, Siemens, Erlangen, Germany) with the use of a phased array cardiac receiver coil. Both CMR cine images for CMR-FT analysis and CMR-TAG images were obtained in the same examination. Standard CMR cine images were acquired using a retrospectively ECG-gated balanced steady-state free-precession (SSFP) sequence during end-expiratory breath holding. A stack of 8-12 consecutive short axis cine images was acquired covering the full LV. Temporal resolution was <50ms and the number of reconstructed temporal phases within the cardiac cycle was set at 20. Subsequently, high temporal resolution (~15ms) cine imaging of the LV in the three-chamber view was performed to assess the opening and closure times of the mitral and aortic valve. Tagged images were acquired at the basal and mid-LV short-axis slices using a complementary spatial modulation of magnetization (CSPAMM) line tagging sequence with segmented ECG-gated acquisitions and serial breath holds.²⁰ Temporal resolution was <15ms and the number of reconstructed temporal phases within the cardiac cycle was set at 55.

IMAGE ACQUISITION: ECHOCARDIOGRAPHY

Echocardiographic examinations were performed by participating centers and sent to the echocardiographic core lab (University Medical Center Utrecht, Utrecht, The Netherlands) for detailed analysis. Examinations were performed on GE Vivid7, GE Vivid9, or Philips iE33 ultrasound machines. Standard echocardiographic images were obtained, including a parasternal short axis (PSAX) view at the papillary muscle level and at the mitral valve level and an apical four chamber view (AP4CH) view, zoomed and focused on the LV. An additional zoomed and trimmed image of the interventricular septum in the AP4CH was recorded for septal single wall analysis with higher frame rates. Images were obtained of three consecutive beats. Image quality and frame rate of all images were optimized for offline speckle tracking analysis (frame rates are reported in the results section). Pulsed-wave Doppler images of the LV outflow tract and mitral valve inlet were obtained for definition of aortic valve and mitral valve closure, respectively.

IMAGE POST-PROCESSING

Strain analysis was performed in the circumferential (CMR-TAG, CMR-FT and STE-circ) and longitudinal (STE-long) orientation. Post-processing of CMR-TAG images was performed by dedicated software using the SinMod technique (inTag v2.0, CREATIS, Lyon, France),²¹ as a plug-in for OsiriX (v6.5, Pixmeo, Switzerland). Semi-automated CMR-FT analysis software (QStrain Research Edition v1.3.0.10 evaluation version, Medis, Leiden, The Netherlands) was used to analyze short-axis cine images corresponding with the mid-LV and basal slice-location of the CMR-TAG images. Both endocardial and epicardial features were included for strain analysis. Echocardiographic images of the two PSAX views (STE-circ), AP4CH view and septal single wall (STE-long) were used for offline speckle tracking analysis. Images were exported as DICOM-files for vendor independent strain analysis with TomTec 2D Cardiac Performance Analysis (2DCPA, version 1.2.1.2, TomTec Imaging Systems GmbH, Munich, Germany). Endocardial features were included for strain analysis. A detailed description of the post-processing steps for the CMR-TAG, CMR-FT and STE analysis has been published previously and is given in the supplemental material.²²

STRAIN PARAMETERS

Five subsets of strain parameters were evaluated. First, basic strain values were quantified by the septal and lateral maximal negative peak strain (peak strain); and septal and lateral

end-systolic strain (ESS) at aortic valve closure. Secondly, mechanical dyssynchrony was measured by the septal to lateral wall delay of onset of shortening (onset-delay); the time difference in peak contraction (peak-delay)¹²; and the standard deviation in time to peak of the total LV (SD-TTP_{LV})¹¹. Thirdly, discoordination of the septal and lateral wall was measured by: systolic rebound stretch of the septum (SRS_{sep})⁷; the systolic stretch index (SSI_{sep-lat})⁹; and the internal stretch index (ISF_{sep-lat}). Fourthly, discoordination parameters that include all LV segments were calculated by the: circumferential uniformity ratio estimate (CURE_{LV}) index¹⁰; and the internal stretch index of the total LV (ISF_{LV})⁸. Lastly, septal strain patterns were visually categorized to the following pre-specified septal strain patterns: double peaked systolic shortening (LBBB-1); early pre-ejection shortening followed by prominent systolic stretch (LBBB-2); and pseudonormal shortening with a late-systolic shortening peak and less pronounced end-systolic stretch (LBBB-3).¹³ Strain parameters are illustrated in figure 1 and further explained in the supplemental material.

ASSESSMENT OF CRT RESPONSE

Echocardiographic assessment of LV volumes was performed before and twelve months after CRT implantation. LV end-systolic volume (LVESV) was measured using the biplane Simpson's method by two experienced observers. Volumetric response was calculated as the percent change in LVESV between baseline and twelve-month follow-up. Patients with $\geq 15\%$ reduction in LVESV were classified CRT responders.

STATISTICAL ANALYSIS

Statistical analysis was performed in the study core lab (University Medical Center Groningen, Groningen, The Netherlands) by statisticians (BG, MR) using the commercially available R software (R Foundation for Statistical Computing, Vienna, Austria). Continuous variables are expressed as mean \pm standard deviation or in absence of a normal distribution as median and interquartile range. Categorical variables are presented as absolute numbers and percentages. Strain parameters were compared between CRT responder groups by an independent student t-test, or a non-parametric test when appropriate. Correlations between strain parameters and volumetric CRT response were assessed using the Pearson's correlation coefficient or when normal distribution was absent, the Spearman's Rho correlation coefficient. Receiver operating characteristics (ROC) curve analysis was used to determine the predictive value of all parameters. Statistical differences between the three pre-specified

septal strain pattern groups towards volumetric CRT response were tested with pairwise t-tests with Bonferroni adjusted p -values. A p -value of <0.05 was considered statistically significant.

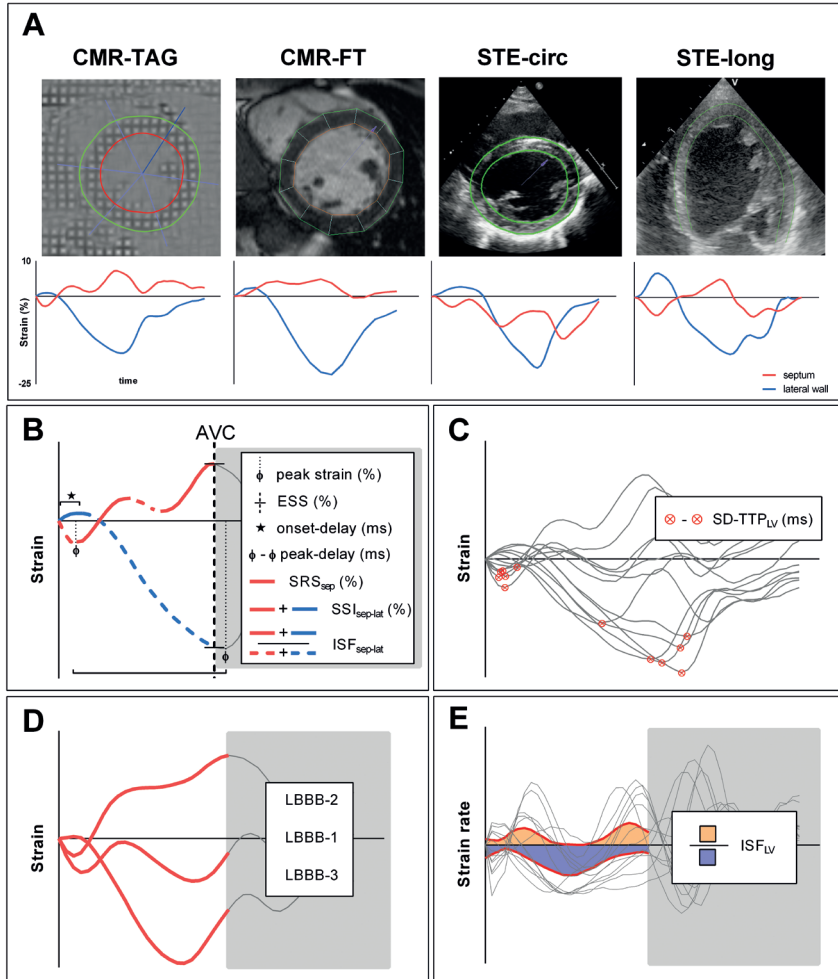


FIGURE 1. Imaging techniques and strain parameters

(A) Typical example of a LBBB patient with strain analysis in the circumferential (CMR-TAG, CMR-FT and STE-circ) and longitudinal (STE-long) orientation; (B) Strain parameters calculated from the septum (red) and/or lateral wall (blue) including peak negative peak strain (peak strain), end-systolic strain (ESS), septal to lateral time delay onset contraction (onset-delay) and peak contraction (peak-delay), systolic rebound stretch of the septum (SRS_{sep}), systolic stretch index (SS_{1 sep-lat}) and internal stretch index (ISF_{sep-lat}); (C) the standard deviation of time to peak strain of all segments (SD-TTP_{LV}); (D) septal strain patterns defined as double peaked shortening (LBBB-1), predominant stretching (LBBB-2) or pseudonormal shortening (LBBB-3); (E) The internal stretch factor including all LV segments (ISF_{LV}).

TABLE 1. Patient characteristics at baseline and at twelve months follow-up

Variable	Total group (n=26)	Responders (n=17)	Non-responders (n=9)
Age (years)	65 ± 9	63 ± 10	68 ± 8
Gender (n, % male)	15 (58%)	9 (53%)	6 (67%)
BMI (kg/m ²)	26 ± 4	27 ± 4*	24 ± 2*
QRS width (ms)	182 (166 – 193)	187 (180 – 202) [†]	165 (143 – 176) [†]
QRS morphology (n, % LBBB)	21 (81%)	16 (94%)*	5 (56%)*
Etiology (n, % ICM)	7 (27%)	1 (6%) [†]	6 (67%) [†]
NYHA class (n, %)			
Class II	17 (65%)	12 (71%)	5 (56%)
Class III	9 (35%)	5 (29%)	4 (44%)
Medication (n, %)			
Beta-blockers	22 (85%)	15 (88%)	7 (78%)
Diuretics	21 (81%)	14 (83%)	7 (78%)
ACE / ATII inhibitors	17 (65%)	11 (65%)	6 (67%)
Aldosterone antagonist	10 (39%)	8 (47%)	2 (22%)
Lab – creatinine value (unit)	77 (68 – 85)	76 (67 – 79)	80 (69 – 95)
Lab – BNP value (unit)	637 (230 – 1603)	686 (276 – 1591)	554 (214 – 1607)
Echo – LVEDV (ml)	181 ± 68	203 ± 73 [†]	141 ± 32 [†]
Echo – LVESV (ml)	138 ± 62	159 ± 65 [†]	98 ± 31 [†]
Echo – LVEF (%)	26 ± 8	23 ± 7*	31 ± 8*
CMR – LVEDV (ml)	313 ± 100	348 ± 105 [†]	248 ± 46 [†]
CMR – LVESV (ml)	234 ± 98	266 ± 105 [†]	174 ± 44 [†]
CMR – LVEF (%)	27 ± 9	25 ± 10	30 ± 6
CMR – LV mass (gr)	130 (117 – 156)	145 (124 – 173)*	115 (97 – 132)*
CMR – Scar (% LV mass)	1.8 (0.0 – 8.6)	0.0 (0.0 – 1.9) [†]	9.5 (5.0 – 19.5) [†]
CMR – Scar pattern (n, % ICM)	8 (31%)	2 (12%) [†]	6 (67%) [†]
CMR – RVEF (%)	51 ± 12	49 ± 13	54 ± 10
Follow-up (12 months)			
Echo – LVEDV (ml)	141 ± 48	140 ± 53	142 ± 42
Echo – LVESV (ml)	78 (69 – 116)	74 (52 – 96)	79 (76 – 123)
Echo – LVEF (%)	37 ± 11	40 ± 12*	32 ± 6*
Echo – Change in LVESV (%)	-29 ± 27	-44 ± 17 [†]	0 ± 14 [†]

BMI: body mass index, LBBB: left bundle branch block, BNP: brain natriuretic peptide, ICM: ischemic cardiomyopathy, LVEDV: left ventricular end-diastolic volume, LVESV: left ventricular end-systolic volume, LVEF, left ventricular ejection fraction, RVEF: right ventricular ejection fraction. Statistical difference between responders and non-responders marked with *: $p < 0.05$ and with [†]: $p < 0.01$.

RESULTS

Twenty-six patients completed the study protocol including clinical follow-up of twelve months. One patient was lost to follow-up because of non-cardiac death (i.e. lung carcinoma). A detailed description of the patient characteristics is given in table 1. From all segments, 94% were considered analyzable with CMR-TAG, 87% with CMR-FT, 87% with STE-circ and 95% with STE-long. Frame rate of echocardiographic images was on average 65 ± 11 Hz, which corresponds to a temporal resolution of ~ 15 ms. Temporal resolution of CMR-TAG was ~ 14 ms, while it was ~ 40 ms for CMR-FT. Mean LVESV change after twelve months was $-29 \pm 27\%$ with 17 (65%) patients becoming CRT responders.

6 STRAIN PARAMETERS AND THEIR RELATION TO CRT RESPONSE

Basic strain values measured as peak strain of the septum and lateral wall showed weak correlations with LVESV change as demonstrated in table 2 and figure 2. On the other hand, ESS_{sep} showed one of the highest coefficients of determination of all parameters using CMR-TAG (R^2 0.60, $p < 0.001$). Other imaging techniques showed good results for ESS_{sep} as well (CMR-FT R^2 0.50; STE-circ R^2 0.43; and STE-long R^2 0.43) as illustrated in figure 3. Dyssynchrony of all LV segments measured by $SD-TTP_{\text{LV}}$ showed the highest correlations using CMR-TAG (R^2 0.61, $p < 0.001$). However, the other imaging techniques demonstrated disappointing results for $SD-TTP_{\text{LV}}$ (CMR-FT R^2 0.10; STE-circ R^2 0.08; and STE-long R^2 0.14, all non-significant). The other dyssynchrony measures onset-delay and peak-delay showed weaker coefficients of determination with LVESV change and results were subject to large variation between imaging techniques. Discoordination markers measured from the septal and lateral wall were all moderately associated with LVESV change and predictive performance was similar for different imaging techniques. Of these parameters, $ISF_{\text{sep-lat}}$ showed best results (CMR-TAG R^2 0.47; CMR-FT R^2 0.39; STE-circ R^2 0.48; and STE-long R^2 0.39, all $p < 0.001$). Discoordination of all LV segments measured by ISF_{LV} yielded one of the highest coefficient of determination using CMR-TAG (R^2 0.57, $p < 0.001$). However, the other imaging techniques demonstrated disappointing results for ISF_{LV} (CMR-FT R^2 0.26, $p = 0.008$; STE-circ R^2 0.29, $p = 0.004$; and STE-long R^2 0.32, $p = 0.003$). The $CURE_{\text{LV}}$ parameter showed weak coefficients of determination with LVESV change, irrespective of imaging technique. As demonstrated in table S1, CMR-TAG and CMR-FT classified half of the patients as LBBB-

2 pattern, whereas LBBB-2 pattern was found in only a quarter of the patients by means of STE techniques. In general, the LBBB-2 pattern was associated to the largest reduction in LVESV, irrespective of its technique (see figure 4). Patients with pattern LBBB-1 showed relatively less reverse remodeling and results differed more between techniques with more remodeling for STE compared to CMR. The LBBB-3 pattern is in particular of interest to exclude non-responders to CRT but only CMR-TAG was accurate in doing this.

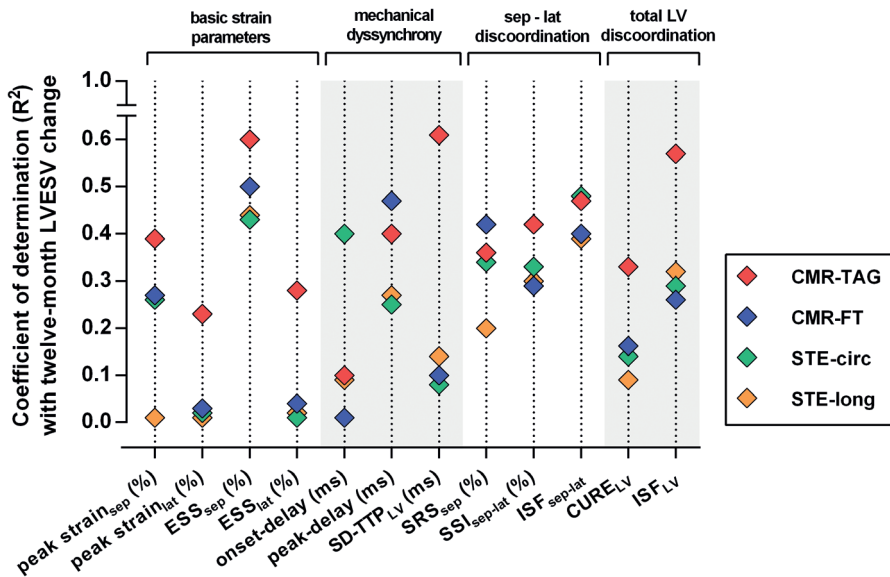


FIGURE 2. Coefficient of determination of all strain parameters towards volumetric CRT response

Coefficient of determination of all strain parameters towards changes in LVESV after twelve months CRT are displayed for CMR-TAG (red); CMR-FT (blue); STE-circ (green) and STE-long (orange). For abbreviations see figure 1.

TABLE 2. Coefficient of determination (R^2) and area under the curve (AUC) of strain parameters and CRT response (echocardiographic LVESV change after twelve months)

	CMR tagging		CMR feature tracking		STE circumferential		STE longitudinal		
	R^2	AUC	R^2	AUC	R^2	AUC	R^2	AUC	
basic strain parameters	N = 26								
	peak strain septum (%)	0.39 ; $p < 0.001$	0.85 ; $p = 0.002$	0.27 ; $p = 0.007$	0.73 ; $p = 0.064$	0.26 ; $p = 0.009$	0.70 ; $p = 0.106$	0.01 ; $p = 0.701$	0.50 ; $p = 0.921$
	peak strain lateral (%)	0.23 ; $p = 0.013$	0.77 ; $p = 0.026$	0.03 ; $p = 0.392$	0.61 ; $p = 0.344$	0.02 ; $p = 0.466$	0.62 ; $p = 0.341$	0.02 ; $p = 0.467$	0.73 ; $p = 0.060$
	ESS _{sep} (%)	0.60 ; $p < 0.001$	0.89 ; $p < 0.001$	0.50 ; $p < 0.001$	0.87 ; $p < 0.001$	0.43 ; $p < 0.001$	0.79 ; $p = 0.014$	0.43 ; $p < 0.001$	0.80 ; $p = 0.012$
basic strain parameters	ESS _{lat} (%)	0.28 ; $p = 0.005$	0.72 ; $p = 0.066$	0.04 ; $p = 0.348$	0.58 ; $p = 0.554$	0.01 ; $p = 0.611$	0.61 ; $p = 0.404$	0.02 ; $p = 0.494$	0.72 ; $p = 0.067$
	onset-delay (ms)	0.10 ; $p = 0.122$	0.73 ; $p = 0.064$	0.01 ; $p = 0.612$	0.61 ; $p = 0.376$	0.40 ; $p < 0.001$	0.80 ; $p = 0.010$	0.09 ; $p = 0.137$	0.69 ; $p = 0.116$
	peak-delay (ms)	0.40 ; $p = 0.001$	0.90 ; $p < 0.001$	0.47 ; $p < 0.001$	0.85 ; $p = 0.002$	0.25 ; $p = 0.010$	0.70 ; $p = 0.106$	0.27 ; $p = 0.007$	0.75 ; $p = 0.044$
	SD-TTP _{LV} (ms)	0.61 ; $p < 0.001$	0.94 ; $p < 0.001$	0.10 ; $p = 0.113$	0.67 ; $p = 0.188$	0.08 ; $p = 0.151$	0.60 ; $p = 0.460$	0.14 ; $p = 0.061$	0.52 ; $p = 0.825$
mechanical dyssynchrony	SRS _{sep} (%)	0.36 ; $p < 0.001$	0.88 ; $p < 0.001$	0.42 ; $p < 0.001$	0.82 ; $p = 0.006$	0.34 ; $p = 0.002$	0.79 ; $p = 0.018$	0.20 ; $p = 0.020$	0.73 ; $p = 0.062$
	SSI _{sep-lat} (%)	0.42 ; $p < 0.001$	0.91 ; $p < 0.001$	0.29 ; $p = 0.004$	0.77 ; $p = 0.031$	0.33 ; $p = 0.002$	0.84 ; $p = 0.006$	0.30 ; $p = 0.004$	0.80 ; $p = 0.010$
	ISF _{sep-lat}	0.47 ; $p < 0.001$	0.92 ; $p < 0.001$	0.39 ; $p < 0.001$	0.83 ; $p = 0.007$	0.48 ; $p < 0.001$	0.90 ; $p < 0.001$	0.39 ; $p < 0.001$	0.94 ; $p < 0.001$
sep-lat discordance	CURE _{LV}	0.33 ; $p = 0.002$	0.86 ; $p = 0.004$	0.15 ; $p = 0.047$	0.61 ; $p = 0.373$	0.14 ; $p = 0.063$	0.66 ; $p = 0.197$	0.09 ; $p = 0.139$	0.66 ; $p = 0.201$
	ISF _{LV}	0.57 ; $p < 0.001$	0.96 ; $p < 0.001$	0.26 ; $p = 0.008$	0.75 ; $p = 0.039$	0.29 ; $p = 0.004$	0.92 ; $p < 0.001$	0.32 ; $p = 0.003$	0.77 ; $p = 0.024$

AUC: area under the curve; R^2 : coefficient of determination; ESS: end-systolic strain, onset-delay: septal to lateral wall delay onset contraction, peak-delay: septal to lateral wall peak delay shortening, SD-TTP_{LV}: standard deviation in time to peak contraction of the total LV, SRS_{sep}: systolic rebound stretch of the septum, SSI_{sep-lat}: systolic stretch index, ISF_{sep-lat}: internal stretch factor of the septal and lateral wall, CURE_{LV}: circumferential uniformity ratio estimate of the total LV, ISF_{LV}: internal stretch factor of the total LV.

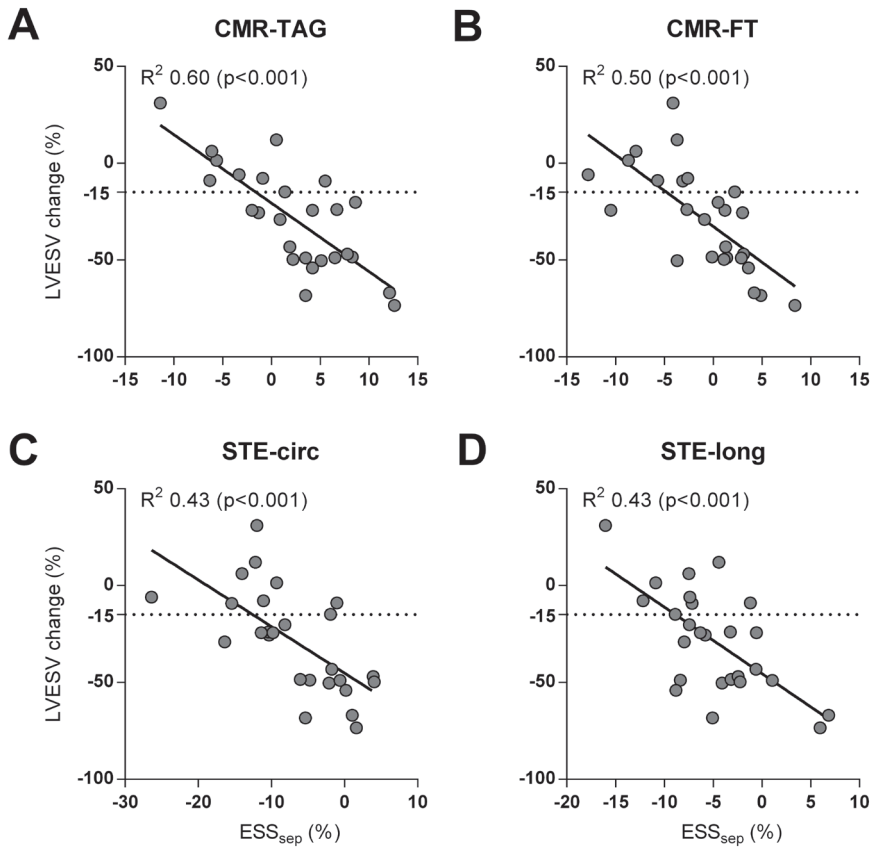


FIGURE 3. Correlation between end-systolic septal strain (ESS_{sep}) and LVESV change per imaging technique

The basic strain parameter end-systolic septum strain (ESS_{sep}) consistently shows a high coefficient of determination with LVESV change independent of imaging modality (A) CMR-TAG; (B) CMR-FT; (C) STE-circ and (D) STE-long.

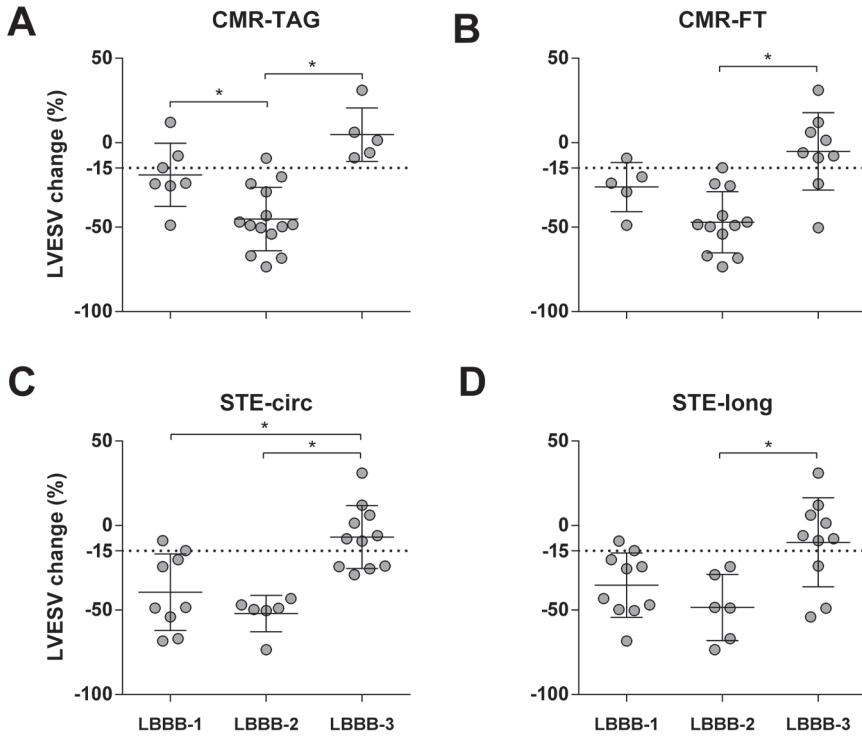


FIGURE 4. Classification of septal strain patterns to estimate CRT response

Septum strain patterns are classified to pre-specified categories: double peaked shortening (LBBB-1), predominant stretching (LBBB-2) or pseudonormal shortening (LBBB-3) using (A) CMR-TAG; (B) CMR-FT; (C) STE-circ and (D) STE-long. Statistical differences ($p < 0.05$) between LBBB categories are marked with an asterisk.

DISCUSSION

This study offered the unique opportunity to compare a variety of strain parameters using multiple imaging techniques in a population that is eligible for CRT. We found both measures of dyssynchrony (regional timing differences, in time units) and discoordination (inefficient contraction patterns, in % strain units) to be strongly related to CRT response when using CMR-TAG. However, these parameters showed weaker correlations for CMR-FT and STE techniques. In contrast, the end-systolic septal strain parameter showed a consistent good

relation to reverse remodeling after CRT, irrespective of assessment technique. In addition, the classification of a septal strain pattern with early pre-ejection shortening followed by predominant stretch (i.e. LBBB-2 pattern) was associated with large reduction in LVESV. Overall, predictive performance of CMR-TAG was found to be superior to CMR-FT and STE techniques.

COMPARISON OF STRAIN PARAMETERS

In patients with LBBB, mechanical dyssynchrony is a direct consequence of the conduction disorder with early activation of the septum and late activation of the lateral wall. Contraction of the septum takes place under low LV pressure (i.e. low wall tension) whereas the lateral wall contracts during rising LV pressures, thus increasing the regional work load.⁴ Consequently, compensatory mechanisms increase contractility of the lateral wall whereas contractility of the septum is reduced. This results in the lateral wall pushing the septum back during systole (i.e. discoordination), reducing LV pump function efficiency. Therefore, both the assessment of LV dyssynchrony and discoordination can be used to estimate CRT benefit. Our results indicate that measures of dyssynchrony and discoordination on a segmental scale (i.e. $SD-TTP_{LV}$ and ISF_{LV}) yield the strongest association with CRT response. These measures use twelve individual segments distributed over the basal and mid-LV slice to quantify the total amount of mechanical substrate for resynchronization. From a physiological point of view, the ISF_{LV} parameter proposed by Kirn et al. is closest related to the amount of inefficient pump function that can be attributed to the LBBB conduction disorder by indexing the amount of systolic stretching (i.e. wasting myocardial work) to the amount of systolic shortening (i.e. useful myocardial work).⁸ We found a similar cut-off value (0.34) to predict volumetric CRT response compared to their findings. (0.40) In contrast, assessing the circumferential uniformity of segmental strain values by complex Fourier analysis (i.e. CURE index) showed rather disappointing association with CRT response.¹⁰ Possibly, the presence of stretching segments instead of non-uniformity in contraction between segments is of more importance to determine benefit from CRT. Overall, strain parameters on a regional (i.e. septal to lateral) scale showed weaker associations with CRT response compared to parameters incorporating all LV segments, possibly because of the exclusion of anterior and posterior segments. Comparing dyssynchrony parameters (i.e. onset-delay and peak-delay) with discoordination parameters (i.e. SRS_{sep} , $SSI_{sep-lat}$ and $ISF_{sep-lat}$) on a regional scale, the latter showed consistent reasonable correlations with CRT response for all techniques,

whereas dyssynchrony parameters were more subject to variation between methods. Best results were found for the $ISF_{\text{sep-lat}}$ parameter indexing the amount of stretching to the amount of shortening in the septal and lateral wall region.

SEPTAL STRAIN ANALYSIS

Typical septal contraction patterns have been introduced to identify 'true' LBBB activation.¹⁵ These septal strain patterns were identified using patient data combined with computer modeling, resulting in distinct LBBB septal deformation patterns characterized by double peaked shortening (LBBB-1) or predominant stretching (LBBB-2).¹³ Patients lacking true LBBB activation were characterized by pseudo-normal shortening of the septum (LBBB-3) and showed less reverse remodeling compared to patients with LBBB-1 and LBBB-2. We found the LBBB-2 pattern always to be associated with CRT response, irrespective of the imaging modality that was used for visualization. The value of the other septal patterns varied per imaging modality.

Quantification of the septal behavior by end-systolic septal strain (ESS_{sep}) showed a consistent high correlation with LVESV change, irrespective of imaging technique (figure 3). Assessment of this parameter is relatively simple as illustrated in figure 1 and requires strain analysis of the septum only. We found higher (positive) strain values (i.e. net septal stretch throughout the systolic phase) to be associated with more extensive reverse remodeling after CRT. Previous studies showed that electrical resynchronization improves systolic function by recruiting myocardial work from the septum.^{6,7} Therefore, systolic rebound stretch of the septum (SRS_{sep}) is used to predict CRT outcome.^{7,9,23} In our study, ESS_{sep} was even closer related with LVESV changes than SRS_{sep} , possibly because ESS_{sep} is the result of both systolic shortening and stretching whereas SRS_{sep} merely measures the cumulative amount of systolic stretching. In case of preserved septal function characterized by an initial pseudo-normal shortening followed by late-systolic rebound stretching (LBBB-3 pattern), net systolic strain changes (ESS_{sep}) will be negative whereas SRS_{sep} may overestimate the amount of CRT-response that can be expected.

COMPARISON OF STRAIN IMAGING TECHNIQUES

Previously, we compared strain values between imaging techniques and found that most parameters were not interchangeable for different modalities.²² The current study demonstrates that there is only one parameter that performs equally well for all techniques,

when related to CRT response. For the other strain parameters, CMR-TAG demonstrated higher correlation coefficients with LVESV change compared to other imaging techniques. Strain parameters including all LV segments (i.e. ISF_{LV} and $SD-TTP_{LV}$) performed best for CMR-TAG, but results were rather disappointing for CMR-FT and STE techniques. Differences were most pronounced for $SD-TTP_{LV}$ measuring the standard deviation in segmental time to peak contraction throughout the LV. A possible explanation for this finding might be that measuring $SD-TTP_{LV}$ requires not only high image quality to visualize all individual segments, but also sufficient temporal resolution to measure segmental timing differences. CMR-TAG combines excellent image quality with high frame rates whereas CMR-FT might be hampered by the lower temporal resolution that was used for cine imaging, and STE by the lower image quality and higher inter-study variation compared to CMR-TAG.²⁴ In this study, temporal resolution of the cine images for CMR-FT analysis was lower compared to the high temporal resolution of the CMR-TAG sequence (~40ms vs. ~14ms). Using higher temporal resolutions for CMR-FT might improve predictive performance of this technique, although a temporal resolution of ~40ms is typically used in standard clinical cine-imaging protocols. CMR-FT enables myocardial strain analysis using specialized post-processing software on standard CMR cine images.^{18, 25} Although this relatively new technique has not been extensively validated yet, we recently showed reasonable agreement with CMR-TAG.²² Predictive performance of CMR-FT was highest for strain parameters derived from the septal and lateral wall (ESS_{sep} ; peak-delay; SRS_{sep} ; $ISF_{sep-lat}$) whereas parameters including all LV segments ($SD-TTP_{LV}$; ISF_{LV}) were poorly related to CRT outcome. Possibly, the measurement variability of CMR-FT is too high to sample strain on a segmental scale.²⁶ Despite promising results in the present study, data on CMR-FT in this specific patient population are scarce and further validation of this technique is needed.

In general, performance of STE was comparable to CMR-FT. STE analysis was performed in both the circumferential and longitudinal direction, each with associated strengths and weaknesses. Circumferential strain markers are considered to be more sensitive to deformation abnormalities because of the predominant circumferential fiber orientation.²⁷ Echocardiographic image quality, however, is often more favorable in the AP4CH view (STE-long) compared to the PSAX view (STE-circ). Taken together, overall performance of STE-circ and STE-long was very similar. Comparing dyssynchrony and discoordination parameters for STE, best results were found for the $ISF_{sep-lat}$ parameter. Although STE benefits from relatively high temporal resolutions allowing precise time measurements between regional peak strain

values, parameters of mechanical dyssynchrony showed weaker associations with CRT response than measures of discoordination. Possibly, the lower signal-to-noise ratio of STE hampers accurate assessment of regional strain peaks.

LIMITATIONS

The main limitation of this study is that the number of patients is relatively small. Due to the limited availability of CMR-TAG sequences and post-processing software in clinical practice, only a small proportion of the original MARC population was included in the present sub-study. Despite the limited sample size, this is the first study to perform a systematic comparison between strain parameters and strain imaging techniques. Secondly, only a small proportion of the patients had ischemic CMP which limits the confounding effects of scar tissue on strain parameters. For example, a myocardial infarction located at the septum might influence septal strain assessment with less negative or even positive strain values due to akinetic tissue or passive stretching, thus resembling strain patterns seen in patients with explicit discoordination. Unfortunately, the number of patients with myocardial infarction was too low to evaluate the effects of septal scar on strain parameters. The influence of scarred segments, however, has previously been investigated for other discoordination parameters. These studies showed a limited effect of myocardial scarring on the predictive value of these parameters.^{7, 9, 13}

CONCLUSIONS

In conclusion, end-systolic septal strain (ESS_{sep}) showed a consistent good relation to reverse remodeling after CRT, irrespective of the technique used for assessment. In addition, classification of a septal strain pattern with early pre-ejection shortening followed by predominant stretch was associated with large LVESV reductions. For the remaining strain parameters, predictive performance of CMR-TAG was found to be superior to CMR-FT and STE techniques.

PERSPECTIVE

CLINICAL COMPETENCIES

Myocardial strain imaging provides new diagnostic tools that could potentially improve patient selection for CRT. At present, various strain parameters and multiple imaging techniques have been proposed to serve as clinical markers of CRT response. In a first step to evaluate the clinical implications of these markers, we performed a systematic comparison of strain parameters on a multi-modality level. We found the end-systolic septal strain (ESS_{sep}) parameter to be strongly related to CRT response, irrespective of modality. Although CMR-TAG demonstrates overall superior results compared to other imaging techniques, it is limited available in clinical practice. On the other hand, standard CMR imaging is increasingly used to screen CRT candidates by measuring LV ejection fraction combined with scar visualization to target LV lead placement. Additional CMR-FT strain analysis of the septum could potentially expand diagnostic yield of this comprehensive imaging technique. When CMR imaging is not accessible, STE can also be used to estimate CRT benefit. This might be most useful in patients with a 'grey-zone' recommendation for CRT to guide clinical decision making.

REFERENCES

1. Ponikowski P, Voors AA, Anker SD, Bueno H, Cleland JG, Coats AJ, et al. 2016 ESC Guidelines for the diagnosis and treatment of acute and chronic heart failure. *Eur Heart J*. 2016;37:2129-2200.
2. Yancy CW, Jessup M, Bozkurt B, Butler J, Casey DE, Jr., Drazner MH, et al. 2013 ACCF/AHA guideline for the management of heart failure. *J Am Coll Cardiol*. 2013;62:e147-239.
3. Daubert C, Behar N, Martins RP, Mabo P, Leclercq C. Avoiding non-responders to cardiac resynchronization therapy: a practical guide. *Eur Heart J*. 2016.
4. Zweerink A, de Roest GJ, Wu L, Nijveldt R, de Cock CC, van Rossum AC, et al. Prediction of Acute Response to Cardiac Resynchronization Therapy by Means of the Misbalance in Regional Left Ventricular Myocardial Work. *J Card Fail*. 2015.
5. Prinzen FW, Vernooij K, De Boeck BW, Delhaas T. Mechano-energetics of the asynchronous and resynchronized heart. *Heart Fail Rev*. 2011;16:215-224.
6. Russell K, Eriksen M, Aaberge L, Wilhelmsen N, Skulstad H, Gjesdal O, et al. Assessment of wasted myocardial work: a novel method to quantify energy loss due to uncoordinated left ventricular contractions. *Am J Physiol Heart Circ Physiol*. 2013;305:H996-1003.
7. De Boeck BWL, Teske AJ, Meine M, Leenders GE, Cramer MJ, Prinzen FW, et al. Septal rebound stretch reflects the functional substrate to cardiac resynchronization therapy and predicts volumetric and neurohormonal response. *Eur J Heart Fail*. 2009;11:863-871.
8. Kirn B, Jansen A, Bracke F, van Gelder B, Arts T, Prinzen FW. Mechanical discoordination rather than dyssynchrony predicts reverse remodeling upon cardiac resynchronization. *American Journal of Physiology-Heart and Circulatory Physiology*. 2008;295:H640-H646.
9. Lumens J, Tayal B, Walmsley J, Delgado-Montero A, Huntjens PR, Schwartzman D, et al. Differentiating Electromechanical From Non-Electrical Substrates of Mechanical Discoordination to Identify Responders to Cardiac Resynchronization Therapy. *Circ Cardiovasc Imaging*. 2015;8:e003744.
10. Bilchick KC, Dimaano V, Wu KC, Helm RH, Weiss RG, Lima JA, et al. Cardiac Magnetic Resonance Assessment of Dyssynchrony and Myocardial Scar Predicts Function Class Improvement Following Cardiac Resynchronization Therapy. *JACC: Cardiovascular Imaging*. 2008;1:561-568.
11. Pouleur AC, Knappe D, Shah AM, Uno H, Bourgoun M, Foster E, et al. Relationship between improvement in left ventricular dyssynchrony and contractile function and clinical outcome with cardiac resynchronization therapy: the MADIT-CRT trial. *Eur Heart J*. 2011;32:1720-9.

12. Tanaka H, Nesser HJ, Buck T, Oyenuga O, Janosi RA, Winter S, et al. Dyssynchrony by speckle-tracking echocardiography and response to cardiac resynchronization therapy: results of the Speckle Tracking and Resynchronization (STAR) study. *Eur Heart J*. 2010;31:1690-700.
13. Leenders GE, Lumens J, Cramer MJ, De Boeck BW, Doevendans PA, Delhaas T, et al. Septal deformation patterns delineate mechanical dyssynchrony and regional differences in contractility: analysis of patient data using a computer model. *Circ Heart Fail*. 2012;5:87-96.
14. Russel IK, Zwanenburg JJ, Germans T, Marcus JT, Allaart CP, de Cock CC, et al. Mechanical dyssynchrony or myocardial shortening as MRI predictor of response to biventricular pacing? *J Magn Reson Imaging*. 2007;26:1452-1460.
15. Risum N, Tayal B, Hansen TF, Bruun NE, Jensen MT, Lauridsen TK, et al. Identification of Typical Left Bundle Branch Block Contraction by Strain Echocardiography Is Additive to Electrocardiography in Prediction of Long-Term Outcome After Cardiac Resynchronization Therapy. *J Am Coll Cardiol*. 2015;66:631-641.
16. Jackson T, Sohal M, Chen Z, Child N, Sammut E, Behar J, et al. A U-shaped type II contraction pattern in patients with strict left bundle branch block predicts super-response to cardiac resynchronization therapy. *Heart Rhythm*. 2014;11:1790-1797.
17. Revah G, Wu V, Huntjens PR, Piekarski E, Chyou JY, Axel L. Cardiovascular magnetic resonance features of mechanical dyssynchrony in patients with left bundle branch block. *Int J Cardiovasc Imaging*. 2016.
18. Pedrizzetti G, Claus P, Kilner PJ, Nagel E. Principles of cardiovascular magnetic resonance feature tracking and echocardiographic speckle tracking for informed clinical use. *J Cardiovasc Magn Reson*. 2016;18:51.
19. Maass AH, Vernooy K, Wijers SC, van 't Sant J, Cramer MJ, Meine M, et al. Refining success of cardiac resynchronization therapy using a simple score predicting the amount of reverse ventricular remodelling: results from the Markers and Response to CRT (MARC) study. *Europace*. 2017.
20. Zwanenburg JJ, Gotte MJ, Kuijper JP, Heethaar RM, van Rossum AC, Marcus JT. Timing of cardiac contraction in humans mapped by high-temporal-resolution MRI tagging: early onset and late peak of shortening in lateral wall. *Am J Physiol Heart Circ Physiol*. 2004;286:H1872-H1880.
21. Miller CA, Borg A, Clark D, Steadman CD, McCann GP, Clarysse P, et al. Comparison of local sine wave modeling with harmonic phase analysis for the assessment of myocardial strain. *J Magn Reson Imaging*. 2013;38:320-328.

22. van Everdingen WM, Zweerink A, Nijveldt R, Salden OAE, Meine M, Maass AH, et al. Comparison of strain imaging techniques in CRT candidates: CMR tagging, CMR feature tracking and speckle tracking echocardiography. *Int J Cardiovasc Imaging*. 2017.
23. Leenders GE, De Boeck BW, Teske AJ, Meine M, Bogaard MD, Prinzen FW, et al. Septal rebound stretch is a strong predictor of outcome after cardiac resynchronization therapy. *J Card Fail*. 2012;18:404-12.
24. Grothues F, Moon JC, Bellenger NG, Smith GS, Klein HU, Pennell DJ. Interstudy reproducibility of right ventricular volumes, function, and mass with cardiovascular magnetic resonance. *Am Heart J*. 2004;147:218-23.
25. Schuster A, Hor KN, Kowallick JT, Beerbaum P, Kutty S. Cardiovascular Magnetic Resonance Myocardial Feature Tracking: Concepts and Clinical Applications. *Circ Cardiovasc Imaging*. 2016;9:e004077.
26. Wu L, Germans T, Guclu A, Heymans MW, Allaart CP, van Rossum AC. Feature tracking compared with tissue tagging measurements of segmental strain by cardiovascular magnetic resonance. *J Cardiovasc Magn Reson*. 2014;16:10.
27. Helm RH, Leclercq C, Faris OP, Ozturk C, McVeigh E, Lardo AC, et al. Cardiac dyssynchrony analysis using circumferential versus longitudinal strain: implications for assessing cardiac resynchronization. *Circulation*. 2005;111:2760-2767.

SUPPLEMENTAL MATERIAL

Strain imaging to predict response to cardiac resynchronization therapy:

a systematic comparison of strain parameters using multiple assessment modalities

6

SUPPLEMENTAL METHODS

IMAGE ACQUISITION: CARDIAC MAGNETIC RESONANCE

Typical image acquisition parameters for cardiac magnetic resonance (CMR) imaging were: (1) cine imaging: slice thickness 5mm, slice gap 5mm, echo time (TE) 1.6ms, repetition time (TR) 3.2ms, in-plane spatial resolution 1.5 by 2.1mm, flip angle 60 degrees. (2) High temporal cine imaging: TE 1.7ms, TR 3.4ms. (3) Myocardial tagging: slice thickness 6mm, TE 1.7ms, TR 3.6ms, in-plane spatial resolution 1.3 by 4.3mm, flip angle 20 degrees, tag spacing 7mm.

POST-PROCESSING: CMR-TAG

Post-processing of CMR myocardial tagging (CMR-TAG) images was performed by a semi-automated procedure. After selecting the area of interest, endo- and epi-cardial contours were manually drawn in the end-systolic phase and automatically propagated. A template was placed dividing the left ventricle (LV) in six equally sized regions (anterior, anterolateral, inferolateral, inferior, inferoseptal, anteroseptal). The myocardium was divided in three layers (endo-, mid-, epi-wall layer). Septum strain was averaged from the anteroseptal and inferoseptal segments of the mid-wall layer in both the mid-LV and basal slice. This was repeated for the lateral wall strain averaging the anterolateral and inferolateral segments. Individual strain curves were discarded in case of low signal-to-noise ratio as judged by two independent investigators. The presence of at least two analyzable strain curve (out of four), for both the septum and the lateral wall, resulted in inclusion of the patient.

POST-PROCESSING: CMR-FT

For post-processing of CMR feature tracking (CMR-FT) images, first the endo- and epi-cardial contours were manually drawn in both end-diastolic and end-systolic frames and propagated automatically. A template was placed dividing the LV in six regions, similar to the CMR-TAG post-processing technique. The processing steps for quality screening and averaging segments are also similar to the CMR-TAG analysis.

POST-PROCESSING: STE

For speckle tracking echocardiography (STE) analysis, a region of interest was placed by user defined markers at the endocardial border on the apical four chamber (AP4CH) view

6

for longitudinal strain and on the parasternal short axis (PSAX) view of the mitral valve level and papillary muscle level for circumferential strain. The myocardial wall was automatically separated into six segments for all views, based on the American Heart Association 17 segment model.¹ Segments were excluded, even after repeated adjustment of the ROI, if adequate tracking was not achievable. For septal single wall analysis, an ROI was placed endocardial on AP4CH view images along the interventricular septum, from base to apex, thereby excluding the apical cap. The marker for reference length (L_0) was placed at onset of QRS-complex. Results were stored and exported for offline analysis with Matlab 2014b (Mathworks, Natick, MA, USA). Author written Matlab scripts were implemented, with input of valve closure times and semi-automatic calculation of strain parameters. The processing steps of the PSAX images (STE-circ) for quality screening and averaging segments are similar to the CMR-TAG analysis. For AP4CH images (STE-long), a minimum of two out of three segments representing the septal wall (i.e. basal, mid and apical inferoseptum) were averaged, this was repeated for the lateral wall (basal, mid, and apical lateral). Septal single wall analysis resulted in an averaged strain curve for specific septum strain measurements.

STRAIN PARAMETERS

Basic strain parameters were obtained for the septal and lateral wall and include the maximal negative peak strain during the entire cardiac cycle (peak strain); and the end-systolic strain value at aortic valve closure (ESS). Mechanical dyssynchrony was quantified by measuring the septum to lateral delay in onset shortening (onset-delay); the difference in time to peak contraction (peak-delay);² and the standard deviation of time to peak contraction on a segmental scale throughout the LV (SD-TTP_{LV}).³ Discoordination of the septal and lateral wall was measured by systolic rebound stretch of the septum (SRS_{sep}) as the cumulative amount of systolic stretch after initial shortening; the systolic stretch index (SSI_{sep-lat}) measuring systolic stretch of both the septum and the lateral wall; and the internal stretch factor (ISF_{sep-lat}) calculated as the fraction of the total amount of stretch in both regions divided by the total amount of shortening in both regions.⁴⁻⁶ Discoordination markers derived from segmental strains of the total LV include the circumferential uniformity ratio estimate (CURE_{LV}) index that measures the variation in segmental strains per time point using Fourier analysis, ranging from 0 (dyssynchronous) to 1 (synchronous); and the internal stretch factor of the total LV (ISF_{LV}) by dividing the total amount of stretch by the total amount of shortening. Integrating the average positive strain rate during systole resulted in the total amount of stretch, while integrating average negative strain rate resulted in the total amount of shortening.^{5,7} Septal strain patterns were classified as: double peaked systolic shortening (LBBB-1); early pre-ejection shortening followed by prominent systolic stretch (LBBB-2); and pseudonormal shortening with a late-systolic shortening peak and less pronounced end-systolic stretch (LBBB-3).^{8,9}

ECHOCARDIOGRAPHIC ASSESSMENT OF CRT OUTCOME

LV end-diastolic volume (LVEDV), end-systolic volume (LVESV), and ejection fraction (LVEF) were measured by two experienced observers and in accordance with the guidelines of the American Society of Echocardiography and European Association of Echocardiography.¹⁰ Echocardiographic volumes were obtained using the biplane Simpson's method. If image quality of the apical two chamber view was deemed unsuitable for reliable biplane volume assessment, solely the AP4CH view was used instead. All echocardiographic parameters were measured on three separate beats and averaged.

TABLE S1. Septal strain patterns and volumetric CRT response (echocardiographic LVESV change after twelve months)

N = 26	CMR tagging	CMR feature tracking	STE circumferential	STE longitudinal
LBBB-1	-19 ± 19* n=7 (27%)	-26 ± 15 n=5 (19%)	-39 ± 23 [†] n=9 (35%)	-35 ± 19 n=10 (38%)
LBBB-2	-45 ± 19* [‡] n=14 (54%)	-47 ± 18 [‡] n=12 (46%)	-52 ± 11 [†] n=6 (23%)	-49 ± 20 [†] n=6 (23%)
LBBB-3	+5 ± 16 [‡] n=5 (19%)	-5 ± 23 [‡] n=9 (35%)	-7 ± 19 ^{†‡} n=11 (42%)	-10 ± 26 [†] n=10 (38%)

LBBB-1: double peaked shortening and LBBB-2: predominant stretching represent abnormal septal strain patterns. The LBBB-3 pattern represents pseudonormal shortening of the septum. Statistical differences between LBBB categories per imaging modality are marked with: *, pattern 1 vs. 2, †: pattern 1 vs. 3, and ‡: pattern 2 vs. 3.

TABLE S2. Predictive value of septal strain patterns for volumetric CRT response (reduction in LVESV at twelve months ≥15%)

N = 26	CMR tagging		CMR feature tracking		STE circumferential		STE longitudinal	
	R	NR	R	NR	R	NR	R	NR
LBBB-1 or LBBB-2	n=17 (65%)	n=4 (15%)	n=15 (58%)	n=2 (8%)	n=13 (50%)	n=2 (8%)	n=14 (54%)	n=2 (8%)
LBBB-3	n=0 (0%)	n=5 (19%)	n=2 (8%)	n=7 (27%)	n=4 (15%)	n=7 (27%)	n=3 (12%)	n=7 (27%)
sens/spec	100% / 56%		88% / 78%		76% / 78%		82% / 78%	

R: responders, NR: non-responders, sens: sensitivity, spec: specificity, for other abbreviations see table S1.

Strain imaging to predict response to cardiac resynchronization therapy:
a systematic comparison of strain parameters using multiple assessment modalities

TABLE S3. Predictive value of strain parameters for CRT volumetric response (reduction in LVESV at twelve months $\geq 15\%$)

	CMR tagging		CMR feature tracking		STE circumferential		STE longitudinal					
	AUC	sens/spec	cut-off value	sens/spec	cut-off value	AUC	sens/spec	cut-off value				
N = 26												
peak strain septum (%)	0.85	71% / 89%	-3.0	0.73	65% / 89%	-4.6	0.70	82% / 56%	-12.9	0.50	18% / 10%	-2.0
peak strain lateral (%)	0.77	82% / 67%	-12.4	0.61	71% / 56%	-10.9	0.62	71% / 67%	-16.9	0.73	59% / 89%	-8.0
ESS _{sep} (%)	0.89	82% / 89%	+1.6	0.87	82% / 89%	-1.4	0.79	88% / 67%	-10.6	0.80	71% / 78%	-6.2
ESS _{lat} (%)	0.72	82% / 67%	-11.8	0.58	82% / 44%	-9.6	0.61	59% / 67%	-15.1	0.72	65% / 78%	-8.2
onset-delay (ms)	0.73	82% / 56%	44	0.61	76% / 56%	38	0.80	53% / 100%	60	0.69	71% / 67%	54
peak-delay (ms)	0.90	82% / 89%	221	0.75	59% / 100%	200	0.70	47% / 100%	165	0.75	82% / 56%	96
SD-TTP _{LV} (ms)	0.94	88% / 89%	138	0.67	41% / 100%	180	0.60	82% / 44%	112	0.52	35% / 89%	0.15
SRS _{sep} (%)	0.88	88% / 78%	5.0	0.82	76% / 78%	2.8	0.79	59% / 100%	3.7	0.73	76% / 67%	1.7
SSI _{sep-lat} (%)	0.91	88% / 89%	6.0	0.77	65% / 78%	4.5	0.84	71% / 100%	4.3	0.80	77% / 78%	2.8
ISF _{sep-lat}	0.92	82% / 89%	0.30	0.83	76% / 78%	0.22	0.90	94% / 78%	0.15	0.94	88% / 89%	0.22
CURE _{LV}	0.86	59% / 100%	0.80	0.61	24% / 100%	0.70	0.66	65% / 67%	0.79	0.66	100% / 33%	0.88
ISF _{LV}	0.96	94% / 89%	0.34	0.75	71% / 78%	0.29	0.92	100% / 78%	0.29	0.77	53% / 100%	0.37

AUC: area under the curve, ESS: end-systolic strain, onset-delay: septal to lateral wall delay onset contraction, peak-delay: septal to lateral wall peak delay shortening, SD-TTP_{LV}: standard deviation in time to peak contraction of the total LV, SRS_{sep}: systolic rebound stretch of the septum, SSI_{sep-lat}: systolic stretch index, ISF_{sep-lat}: internal stretch factor of the septal and lateral wall, CURE_{LV}: circumferential uniformity ratio estimate of the total LV, ISF_{LV}: internal stretch factor of the total LV.

TABLE S4. Comparison of strain parameters between responders (R) and non-responders (NR)

	CMR tagging			CMR feature tracking			STE circumferential			STE longitudinal			
	N = 26	R	NR	p-value	R	NR	p-value	R	NR	p-value	R	NR	p-value
basic strain parameters	peak strain septum (%)	-3 ± 2	-6 ± 3	0.013	-4 ± 3	-7 ± 4	0.061	-9 ± 4	-13 ± 7	0.150	-8 ± 5	-8 ± 3	0.981
	peak strain lateral (%)	-14 ± 2	-12 ± 3	0.031	-13 ± 4	-12 ± 4	0.327	-15 ± 6	-17 ± 4	0.355	-8 ± 5	-11 ± 4	0.060
	ESS _{sept} (%)	+5 ± 4	-3 ± 5	0.001	+1 ± 4	-5 ± 4	0.003	-4 ± 6	-11 ± 7	0.030	-3 ± 5	-8 ± 4	0.009
	ESS _{lat} (%)	-14 ± 2	-11 ± 4	0.057	-13 ± 3	-11 ± 4	0.486	-14 ± 6	-16 ± 4	0.410	-7 ± 6	-10 ± 4	0.072
mechanical dyssynchrony	onset-delay (ms)	58 (46 – 68)	44 (28 – 54)	0.059	67 (47 – 87)	44 (0 – 82)	0.381	70 (20 – 130)	44 (0 – 50)	0.012	76 (36 – 126)	44 (15 – 85)	0.118
	peak-delay (ms)	330 ± 92	140 ± 88	<0.001	226 ± 104	109 ± 47	<0.001	172 ± 119	92 ± 47	0.024	176 ± 102	90 ± 65	0.017
	SD-TTP _{LV} (ms)	175 ± 31	97 ± 30	<0.001	165 ± 48	143 ± 35	0.196	155 ± 52	133 ± 54	0.329	140 ± 48	124 ± 44	0.429
sep – lat discoordination	SRS _{sept} (%)	9 ± 4	3 ± 3	<0.001	5 ± 3	2 ± 2	0.004	5 ± 4	1 ± 1	0.004	4 ± 3	2 ± 2	0.031
	SSI _{sept-lat} (%)	11 ± 5	4 ± 3	<0.001	6 ± 4	3 ± 2	0.013	7 ± 5	2 ± 1	<0.001	5 ± 4	2 ± 2	0.009
	ISF _{sept-lat}	0.54 ± 0.21	0.21 ± 0.15	<0.001	0.36 ± 0.22	0.16 ± 0.11	0.006	0.32 ± 0.15	0.12 ± 0.08	<0.001	0.47 ± 0.23	0.16 ± 0.08	<0.001
total LV discoordination	CURE _{LV}	0.78 ± 0.09	0.88 ± 0.04	<0.001	0.75 ± 0.10	0.80 ± 0.06	0.134	0.77 ± 0.05	0.81 ± 0.07	0.164	0.81 ± 0.04	0.84 ± 0.06	0.197
	ISF _{LV}	0.57 ± 0.19	0.24 ± 0.10	<0.001	0.40 ± 0.18	0.25 ± 0.12	0.020	0.42 ± 0.09	0.25 ± 0.11	<0.001	0.39 ± 0.17	0.23 ± 0.11	0.009

R: responders, NR: non-responders; for other abbreviations see table S2 and S3.

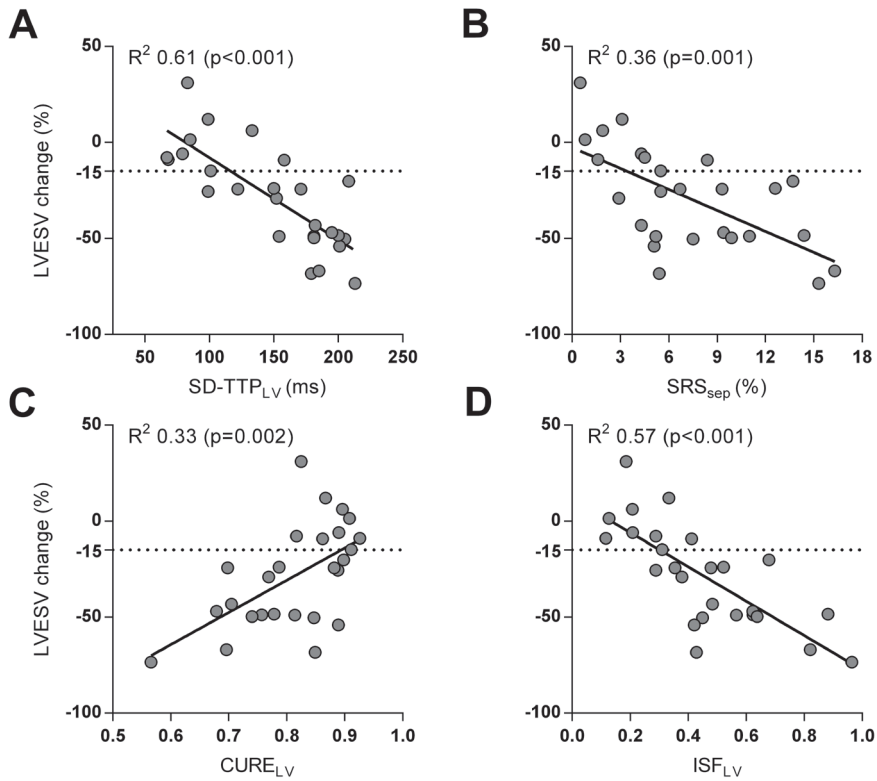


FIGURE S1. Correlation between conventional strain markers quantified by the CMR-TAG technique and LVESV change

Conventional strain parameters quantified by CMR-TAG technique are depicted for (A) SD-TTP_{LV}; (B) SRS_{sep}; (C) the CURE index and (D) ISF_{LV}. SD-TTP_{LV}, standard deviation in time to peak contraction of the total LV; SRS_{sep}, systolic rebound stretch of the septum; CURE_{LV}, circumferential uniformity ratio estimate of the total LV; ISF_{LV}, internal stretch factor of the total LV

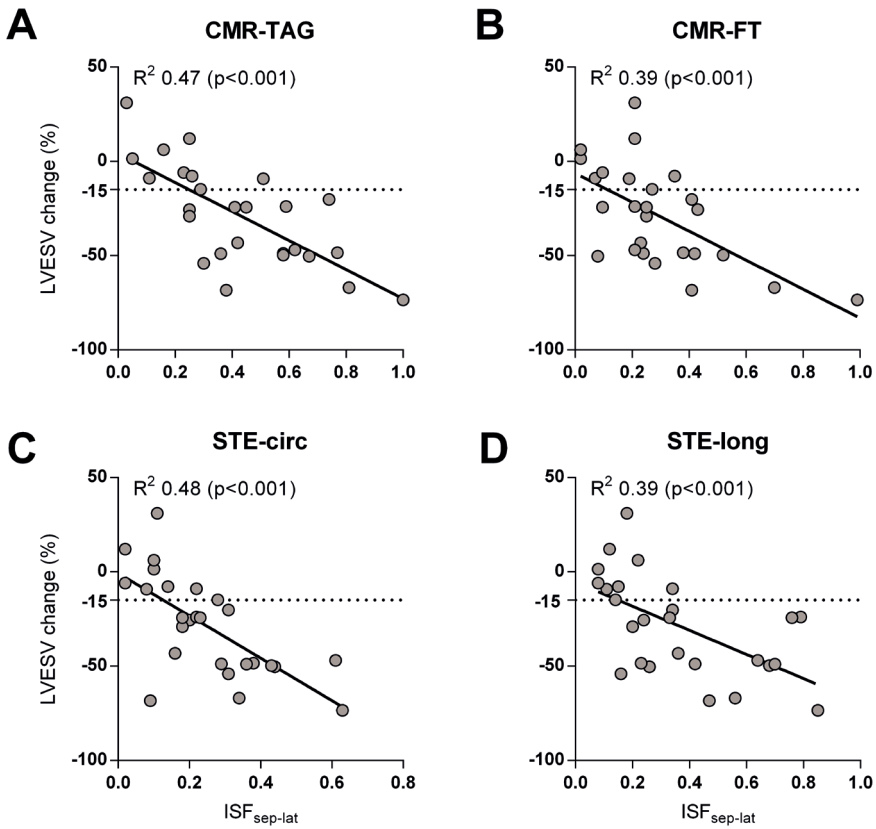


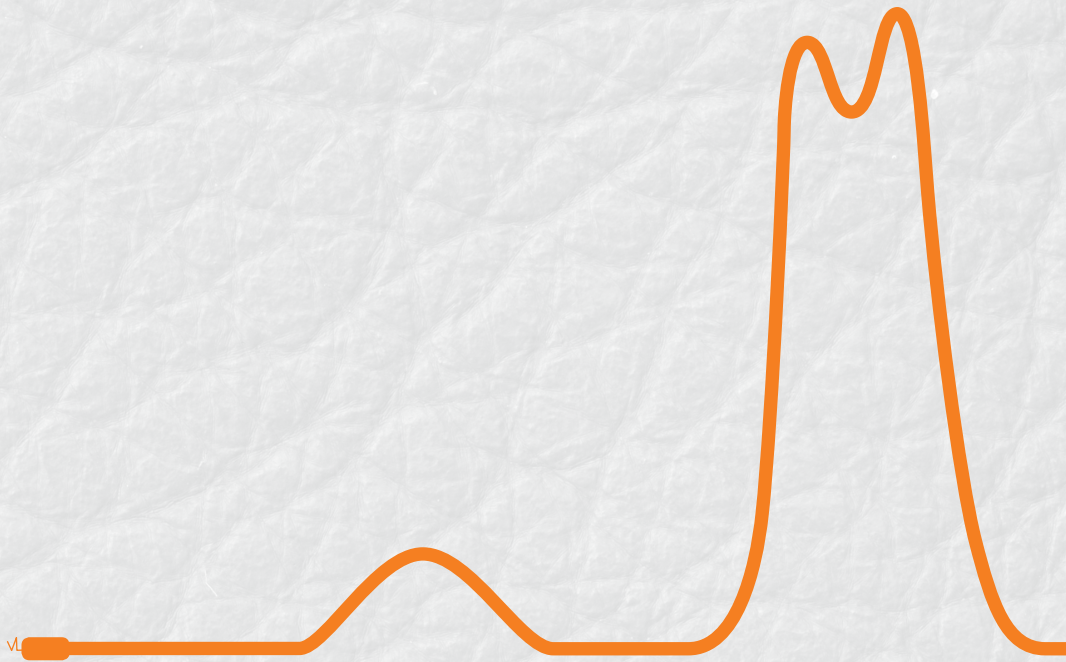
FIGURE S2. Correlation between the internal stretch factor of the septal and lateral wall (ISF_{sep-lat}) and LVESV change per imaging technique

The internal stretch factor calculated from the septal and lateral wall strain (ISF_{sep-lat}) shows a close association with CRT response for each imaging modality and is depicted for: (A) CMR-TAG; (B) CMR-FT; (C) STE-circ and (D) STE-long.

SUPPLEMENTAL REFERENCES

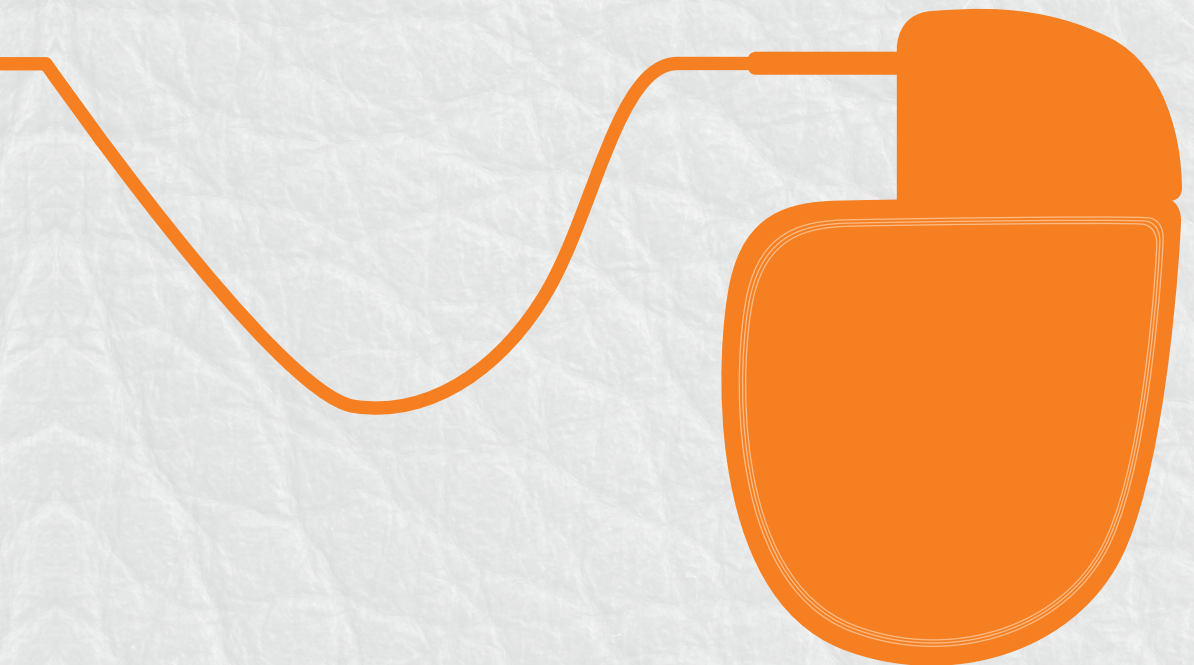
1. Cerqueira MD, Weissman NJ, Dilsizian V, Jacobs AK, Kaul S, Laskey WK, et al. Standardized myocardial segmentation and nomenclature for tomographic imaging of the heart. A statement for healthcare professionals from the Cardiac Imaging Committee of the Council on Clinical Cardiology of the American Heart Association. *Circulation*. 2002;105:539-542.

2. Tanaka H, Nesser HJ, Buck T, Oyenuga O, Janosi RA, Winter S, et al. Dyssynchrony by speckle-tracking echocardiography and response to cardiac resynchronization therapy: results of the Speckle Tracking and Resynchronization (STAR) study. *Eur Heart J*. 2010;31:1690-700.
3. Pouleur AC, Knappe D, Shah AM, Uno H, Bourgoun M, Foster E, et al. Relationship between improvement in left ventricular dyssynchrony and contractile function and clinical outcome with cardiac resynchronization therapy: the MADIT-CRT trial. *Eur Heart J*. 2011;32:1720-9.
4. De Boeck BWL, Teske AJ, Meine M, Leenders GE, Cramer MJ, Prinzen FW, et al. Septal rebound stretch reflects the functional substrate to cardiac resynchronization therapy and predicts volumetric and neurohormonal response. *Eur J Heart Fail*. 2009;11:863-871.
5. Kirn B, Jansen A, Bracke F, van Gelder B, Arts T, Prinzen FW. Mechanical discoordination rather than dyssynchrony predicts reverse remodeling upon cardiac resynchronization. *American Journal of Physiology-Heart and Circulatory Physiology*. 2008;295:H640-H646.
6. Lumens J, Tayal B, Walmsley J, Delgado-Montero A, Huntjens PR, Schwartzman D, et al. Differentiating Electromechanical From Non-Electrical Substrates of Mechanical Discoordination to Identify Responders to Cardiac Resynchronization Therapy. *Circ Cardiovasc Imaging*. 2015;8:e003744.
7. Bilchick KC, Dimaano V, Wu KC, Helm RH, Weiss RG, Lima JA, et al. Cardiac Magnetic Resonance Assessment of Dyssynchrony and Myocardial Scar Predicts Function Class Improvement Following Cardiac Resynchronization Therapy. *JACC: Cardiovascular Imaging*. 2008;1:561-568.
8. Leenders GE, Lumens J, Cramer MJ, De Boeck BW, Doevendans PA, Delhaas T, et al. Septal deformation patterns delineate mechanical dyssynchrony and regional differences in contractility: analysis of patient data using a computer model. *Circ Heart Fail*. 2012;5:87-96.
9. Marechaux S, Guiot A, Castel AL, Guyomar Y, Semichon M, Delelis F, et al. Relationship between two-dimensional speckle-tracking septal strain and response to cardiac resynchronization therapy in patients with left ventricular dysfunction and left bundle branch block: a prospective pilot study. *J Am Soc Echocardiogr*. 2014;27:501-511.
10. Lang RM, Badano LP, Mor-Avi V, Afilalo J, Armstrong A, Ernande L, et al. Recommendations for cardiac chamber quantification by echocardiography in adults: an update from the American Society of Echocardiography and the European Association of Cardiovascular Imaging. *Eur Heart J Cardiovasc Imaging*. 2015;16:233-270.



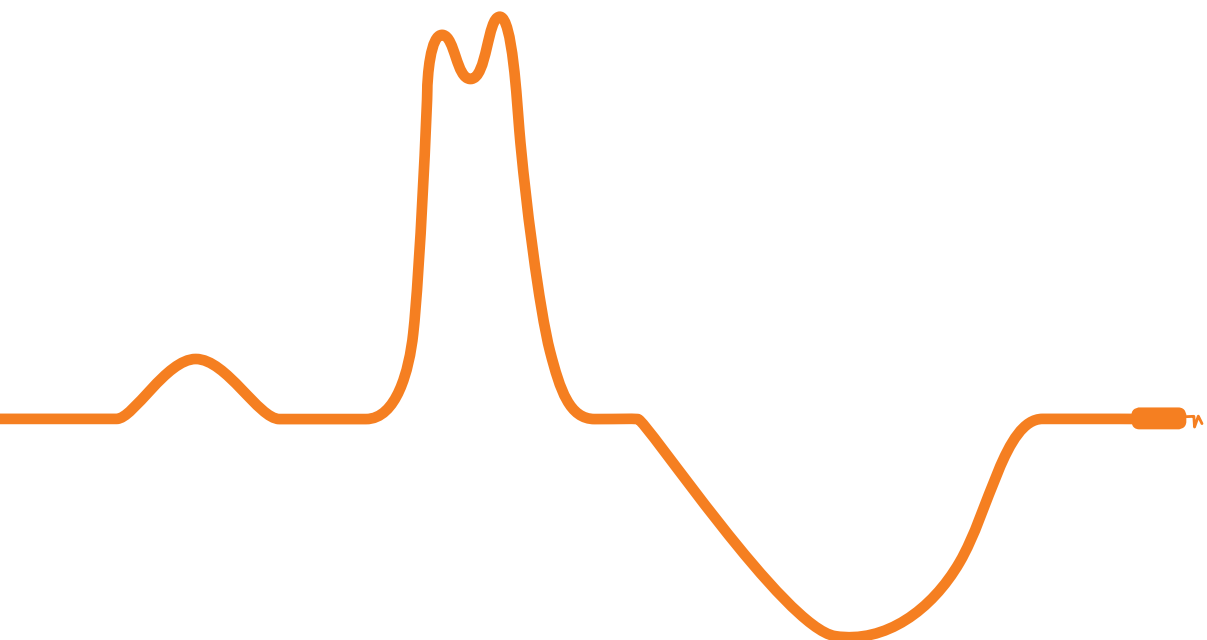
PART II

RIGHT VENTRICULAR FUNCTION





Combining computer modelling and cardiac imaging to understand right ventricular pump function



John Walmsley (PhD)¹, Wouter M. van Everdingen (MD)²,
Maarten J. Cramer (MD, PhD)³, Frits W. Prinzen (PhD)¹,
Tammo Delhaas (MD, PhD)¹ and Joost Lumens (PhD)^{1,3}

¹ CARIM School for Cardiovascular Diseases, Maastricht University Medical Center, Maastricht, The Netherlands

² University Medical Center Utrecht, Utrecht, The Netherlands

³ L'Institut de Rythmologie et Modélisation Cardiaque (IHU-LIRYC), Université de Bordeaux, Pessac, France

Cardiovascular Research 2017 Oct 1;113(12):1486-1498.

ABSTRACT

Right ventricular (RV) dysfunction is a strong predictor of outcome in heart failure and is a key determinant of exercise capacity. Despite these crucial findings, the RV remains understudied in the clinical, experimental, and computer modelling literature. This review outlines how recent advances in using computer modelling and cardiac imaging synergistically help to understand RV function in health and disease. We begin by highlighting the complexity of interactions that make modelling the RV both challenging and necessary, and then summarize the multiscale modelling approaches used to date to simulate RV pump function in the context of these interactions. We go on to demonstrate how these modelling approaches in combination with cardiac imaging have improved understanding of RV pump function in dyssynchronous heart failure and cardiac resynchronization therapy. We conclude with a perspective on key issues to be addressed by computational models of the RV in the near future.

INTRODUCTION

Whilst the overwhelming majority of clinical and experimental studies on heart failure focus on the left ventricle (LV), right ventricular (RV) failure has a particularly bleak prognosis.¹ In recent years, interest in RV function in both patients and apparently healthy individuals with a wide range of conditions has increased. These conditions range from increased mortality in patients with RV infarction,² to arrhythmogenic right ventricular cardiomyopathy (ARVC),³ to the RV's crucial role in determining exercise capacity,⁴ and to maladaptive and arrhythmogenic RV remodelling in high performance athletes.⁵ The RV can also be the systemic ventricle in some individuals with congenital heart defects (CHDs), which is a subject of growing interest as the prognosis of CHD patients continues to improve.⁶

Why is RV function so challenging to study with imaging? The RV is a thin-walled, crescent shaped structure wrapped around the right side of the LV, and lies closely against the ribcage (Figure 1). The RV has a high degree of apical trabeculation, has the moderator band that crosses the RV cavity, and has three papillary muscles.⁷ These anatomical features and its intra-thoracic position make the RV hard to image satisfactorily, especially with echocardiography. Standard 2D imaging planes oversimplify RV contraction, which is a combination of longitudinal and circumferential shortening. Due to the limited echocardiographic views in which the RV wall is clearly visible, only longitudinal function parameters are commonly used (e.g. tricuspid annular plane systolic excursion - TAPSE, s' of tissue Doppler of the tricuspid angle, longitudinal strain). 3D speckle tracking has shown that RV segments show a heterogeneous distribution of directions of contraction in normal hearts.⁸ RV function is therefore multidimensional, possibly explaining why changes measured by 3D RV ejection fraction are currently considered the most reliable global echocardiographic indicators of RV function⁹. However, volumetric measurements can be distorted by the high degree of trabecularization in the RV.¹⁰ Some of these limitations can be overcome using cardiac magnetic resonance (CMR) imaging. However, because most clinical CMR protocols and imaging planes are designed to assess LV morphology, RV endocardial contour tracing is challenging and specific axial RV slices are required for accurate RV volume measurements.¹¹

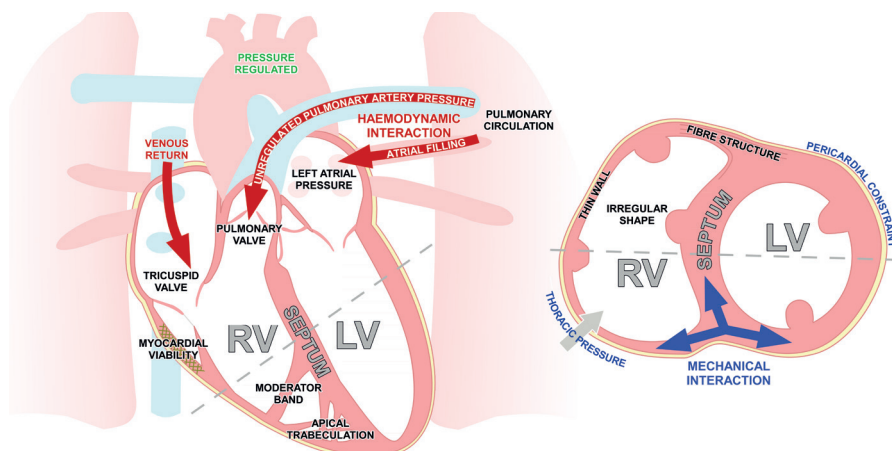


FIGURE 1. A conceptual summary of major challenges for imaging and modelling RV systolic function at rest.

Two views of the heart are shown, loosely corresponding to an apical four chamber long axis view and a parasternal ventricular short axis view. Hemodynamic interactions between the two ventricles are highlighted in red. Mechanical interactions between the two ventricles through their structural connections and the interventricular septum are highlighted in blue.

These limitations of RV imaging make computer modelling an appealing tool for studying RV function. Many cardiac models do now include the RV but, so far, few models have been used to study RV pathophysiology. Moreover, most studies that investigate the RV, including our own, use a relatively simple representation of RV structure and function. This review aims to encourage computational modellers to increase their focus on RV function, and it aims to demonstrate the power of modelling for interpreting RV imaging in pathophysiological situations to physiologists and clinicians. We begin by summarising approaches to modelling RV function considering the interactions in figure 1. We then review how models have helped to understand clinical measurements of RV function in dyssynchronous heart failure. We also address progress towards using models constructed from CMR to extract additional diagnostic information.

MODELLING RV SYSTOLIC FUNCTION

All models of the RV are necessarily simplifications of reality. Both the question under investigation and the availability of imaging and hemodynamic data determine the level of detail used when modelling different aspects of the RV and its environment.

RIGHT VENTRICULAR MORPHOLOGY

Three-dimensional biventricular models provide the opportunity to explore the effect of cardiac anatomy on pump function in detail.¹² While generic models of the ventricles are still used to understand ventricular pump function, recent years have seen rapid developments in integrating computer models and *in vivo* cardiac imaging to produce personalised or 'patient-specific' biventricular models. Models can be created by either segmenting and fitting the endocardial and epicardial surfaces and then meshing the resultant geometry, or by morphing an existing generic model to fit the imaging data.¹³ The shape of the resulting models can be used in statistical analysis for phenotyping without the need to perform simulations, as demonstrated recently for the RV in repaired Tetralogy of Fallot patients.¹⁴ Alternatively, these models can be combined with descriptions of myocardial properties and used to simulate LV and RV pump function. The tissue model can then be personalized by adjusting model parameters to reproduce measured pressures and/or deformation with a certain error range.¹⁵ The irregularity of RV structure and its thin wall mean that tracking and constructing its geometry can be significantly more challenging than for the LV, which may limit the personalization approach when modelling the RV. RV function in most geometrically detailed models is used to provide appropriate mechanical and hemodynamic boundary conditions for studying LV function, but increasing clinical interest in the RV is now leading to studies that use patient-specific models to study the RV itself.^{16, 17}

FIBRE ARCHITECTURE

Fibre structure determines the anisotropy incorporated within active and passive constitutive laws for RV myocardium. In humans, histology and dissection studies generally agree that RV epicardial myofibers are circumferentially oriented and are contiguous with the LV epicardial myofibers, whereas RV subendocardial myofibers are longitudinally oriented; that the endocardial myofibers of the RV are contiguous with those in the interventricular septum; and that the RV lacks the mid-myocardial layer of circumferentially oriented

fibres found in the LV.^{7, 18} Despite these differences from the LV, RV myocardial structure is frequently modelled using rule-based models derived from histological studies of LV fibre orientation with variation of the fibre angle within the RV.^{19, 20} Diffusion tensor CMR has also been used to estimate personalised ventricular fibre orientation *in vivo*, although these measurements may be less reliable in the thin RV free wall.

MYOCARDIAL FUNCTION

There is an accumulating body of evidence for functional differences between LV and RV myocardium, including electrophysiological and contractile function.^{21, 22} These differences can be represented using biophysically detailed sarcomere contraction models coupled to electrophysiological models to realistically simulate myocardial function.¹⁶ Detailed modelling of RV myocardium may help to address unresolved issues in RV pathophysiology, such as why the sub-tricuspid region seems to be most vulnerable to functional changes in early-stage ARVC.²³ Anisotropic passive constitutive laws for the RV myocardium have been developed based on biaxial testing using experimental animal studies,^{24, 25} and some whole-heart electrophysiology simulation studies have included left-right differences in ion channel expression.²⁶ However, most computer models use either generic or LV models to represent active and passive RV myocardial function.¹² Hill-type phenomenological models have been used in both geometrically detailed and reduced-dimensional models to simulate contraction.^{27, 28} Differences in wall thickness and pressure between the LV and RV can already generate substantial differences in wall mechanics without requiring specialised RV tissue models.²⁹ When the mechanism of RV contraction is less critical, a time-varying elastance function that gives a pressure-volume relationship that varies throughout the cardiac cycle can be used.³⁰

Regional variations in RV myocardial function can be simulated in a straightforward manner using geometrically detailed models by altering myocardial properties in, for example, a scarred region.³¹ Within cardiac models derived from imaging, regions of delayed gadolinium enhancement on CMR can be registered to the model geometry and used to define regions of fibrosis.³² However, delayed enhancement in the RV can be challenging to interpret in the RV because of the thin wall and fatty deposits on the epicardium³³.

SIMPLIFIED MODELS OF MECHANICAL VENTRICULAR INTERACTION

Ventricular mechanical interaction can occur through shared myofibers between the LV and the RV at the LV-RV attachment and through pressure differences across the interventricular septum. The main use of simplified models to study the RV has been the investigation of how mechanical interaction contributes to both LV and RV function and to the abnormal septal position observed in many cardiac pathologies.³⁴ Early models allowed for a leftwards shift in the pressure-volume relationship of one ventricle with increases in pressure on the opposite ventricle, representing increases in diastolic pressure.³⁵ This approach neglects how septal position affects ventricular pressure-volume dynamics, which can be addressed by assigning a volume of blood to the septum, giving a septal elastance dependent on the RV-LV pressure difference.^{36, 37} Subsequently, Beyar et al. proposed a 'force balance' theory, which requires that tensile forces balance at the LV-RV attachment and adjusts septal position until this balance is achieved.³⁸ The same study proposes a model incorporating bending moments of myocardial fibre layers, which reduced but did not abolish the leftwards shift of the septum with acute increases of RV pressure.

The static approaches above do not take into account the dynamic nature of ventricular pressure due to active tension generation by the myocardium. Sun et al. allowed for dynamic variation in septal position in response to cardiovascular system dynamics by using time-varying elastance models for LV and RV pressure together with an interventricular cross talk determined by septal elastance.^{30, 36} The CircAdapt model combines the 'force balance' theory in the simplified 'TriSeg' ventricular geometry with phenomenological models of active and passive myofibre stress generation and descriptions of atrial function and the systemic and pulmonary circulations.^{27, 38} CircAdapt therefore allows a dynamic interaction between RV and LV myocardial contractile function, septal position, and ventricular pressures and volumes.

PERICARDIAL CONSTRAINT

Mechanical interaction also occurs through the pericardium, which surrounds both ventricles and most of the atria.³⁹ With pericardial constraint, an increase in the volume of a chamber alters the pressure in the other chambers and, hence, diastolic filling and septal position. A common model for the pericardium is an elastic sac surrounding the four cardiac chambers, with a non-linear pressure-volume relationship determining the contribution

to chamber pressures.^{30, 35, 40} Recently, Fritz et al. proposed a more anatomically realistic representation of the pericardium and surrounding tissue compatible with imaging-derived whole-heart models.⁴¹ Pericardial constraint had a much greater influence on atrial and RV function than on LV function. Incorporating pericardial interactions allows investigation of conditions that alter pericardial behaviour such as pericarditis and cardiac tamponade, which can exacerbate ventricular interaction and alter septal position.^{30, 34}

THORACIC PRESSURES

Intrathoracic pressures are especially relevant for modelling the RV due to the pronounced effect of respiration on RV function.⁴² In multi-compartment models, the effects of variations in intrathoracic pressure that can influence both venous return and pulmonary vascular resistance can be included. Typically, this takes the form of an oscillating pressure applied equally to all compartments within the thorax (i.e. the vena cavae, heart, and pulmonary circulation).³⁰

VALVULAR FUNCTION AND BLOOD FLOW

Pulmonary and tricuspid valve function strongly influence RV systolic function by altering both preload (tricuspid regurgitation/stenosis, pulmonary regurgitation) and afterload (pulmonary stenosis, tricuspid regurgitation). The tricuspid and pulmonary valves have been modelled in much less detail than the mitral and aortic valves to date. Simple valve models open in the presence of a pressure gradient with a given resistance, which allows simulation of filling and ejection and, to an extent, stenosis.⁴³ More advanced formulations include inertial effects of flow and incorporate Bernoulli energy losses across the valve. Incorporating valvular flow within 3D models of the RV allows the study of intraventricular systolic and diastolic flow patterns as measured *in vivo* using flow reconstruction from 3D ultrasound or phase contrast CMR.^{44, 45} The role of fluid-structure interactions and kinetic effects in RV myocardial mechanics may be more pronounced than in the LV given the RV's thinner walls, but applications of intraventricular computational fluid dynamics modelling to the RV remain scarce.^{31, 46}

HEMODYNAMIC INTERACTIONS

The RV lies between the low-pressure systemic venous system and the pulmonary circulation, whose arterial pressure is not controlled through any known homeostatic mechanism.⁴⁷

There is a high degree of hemodynamic interaction between the LV and RV, both ‘forwards’ through venous return determining RV preload and left atrial filling determining LV preload, and ‘backwards’ through left atrial pressure and pulmonary pressures that determine RV afterload.⁴⁸ These interactions can be incorporated either as boundary conditions to the RV or by using a closed-loop model of the circulation. An extensive review of reduced-dimensional computational models of the circulatory system has been provided by Shi et al.⁴³ These models directly couple LV output and RV filling and *vice versa*, and contain simple models of ventricular and sometimes atrial function. They can also provide hemodynamic boundary conditions for more detailed models of the RV and LV.^{40, 49, 50.}

The pulmonary circulation normally operates with an inlet pressure (mean pulmonary artery pressure, around 14mmHg) far below the inlet pressure for the systemic circulation (mean aortic pressure, around 92mmHg), although this difference decreases during exercise.⁵¹ The most straightforward method for modelling RV afterload is a Windkessel model, which has the advantage of having a low number of parameters that are physiologically meaningful and consequently are parameterizable from clinical measurements.^{52, 53} Models with nonlinear pressure-flow relations based on experimental measurements or incorporating vascular distensibility and constriction have also been proposed.⁵⁴⁻⁵⁶ Branching tree formulations model both large arteries and veins, where inertial effects dominate, and smaller arterioles and capillaries where viscous effects dominate. These models therefore allow simulation of dynamic differences in RV afterload due to different aetiologies of pulmonary hypertension.⁵⁷ Computational fluid dynamics simulations of blood flow in the pulmonary arteries can also be used for pulmonary arterial hemodynamics.⁵⁸ Most computational fluid dynamics studies use a simple time varying elastance model for the RV as a boundary condition for the pulmonary artery model. It has been used for simulating pulmonary arterial hemodynamics in complex anatomies in CHD and in pulmonary artery hypertension.^{59, 60}

DYSSYNCHRONOUS HEART FAILURE AND CARDIAC RESYNCHRONIZATION THERAPY

THE RV IN THE DYSSYNCHRONOUS HEART

The interaction between dyssynchronous contraction, RV function, and CRT response has received relatively little attention in the literature, and the relation between RV function and

CRT response is controversial.^{61, 62} Personalized models derived from imaging that include the RV have been extensively used to study dyssynchronous heart failure and CRT, but have primarily focused on LV function to date.^{28, 63, 64}

Previous experimental work has shown that dyssynchronous electrical activation redistributes the myofibre work performed within the LV, with earlier activated regions performing relatively less external work, and late-activated regions performing relatively more external work.⁶⁵ Computer simulations of left bundle-branch block (LBBB) showed that this principle applies across both ventricles and so alterations in electrical activation sequence can expose ventricular mechanical interaction.⁶⁶ Simulation of an LBBB activation pattern reduced the external myofibre work performed by the RV free wall as well as the septum. Pre-stretch of the LV free wall by the early-activated septum and RV free wall increased LV free wall work through the Frank-Starling mechanism (figure 2). The LV myocardium then contracts against the early-activated and weak RV, forcing the LV free wall to increase its contribution to RV pump work while also stretching the early-activated septum.

Patients with broad QRS complexes frequently show an early-systolic leftwards septal motion known as ‘septal beaking’ or ‘septal flash’ that is associated with favourable response to CRT.⁶⁷ Multiple explanations for this phenomenon exist in the literature. Experimental studies in paced canine hearts suggested that this motion arose from a transient increase in RV pressure over LV pressure consistent with passive models of septal position.^{68, 69} Later, experiments in a canine model with LBBB revealed that the pressure difference between LV and RV could decline during leftwards septal motion, and that the septum itself was shortening during this motion suggesting that active contraction of the septum caused septal beaking.⁷⁰ A simulation study varied LV free wall, RV free wall, and septal timing of activation independently of one another and confirmed that septal motion could occur against a falling trans-septal pressure gradient.⁷¹ However, the major driver of septal motion was the activation time of the RV free wall relative to the LV free wall because early contraction of the septum did not lead to septal motion when RV free wall activation time was also delayed. Consequently, lack of septal beaking may imply RV dysfunction or presence of RV activation delays coexisting with LV activation delays.

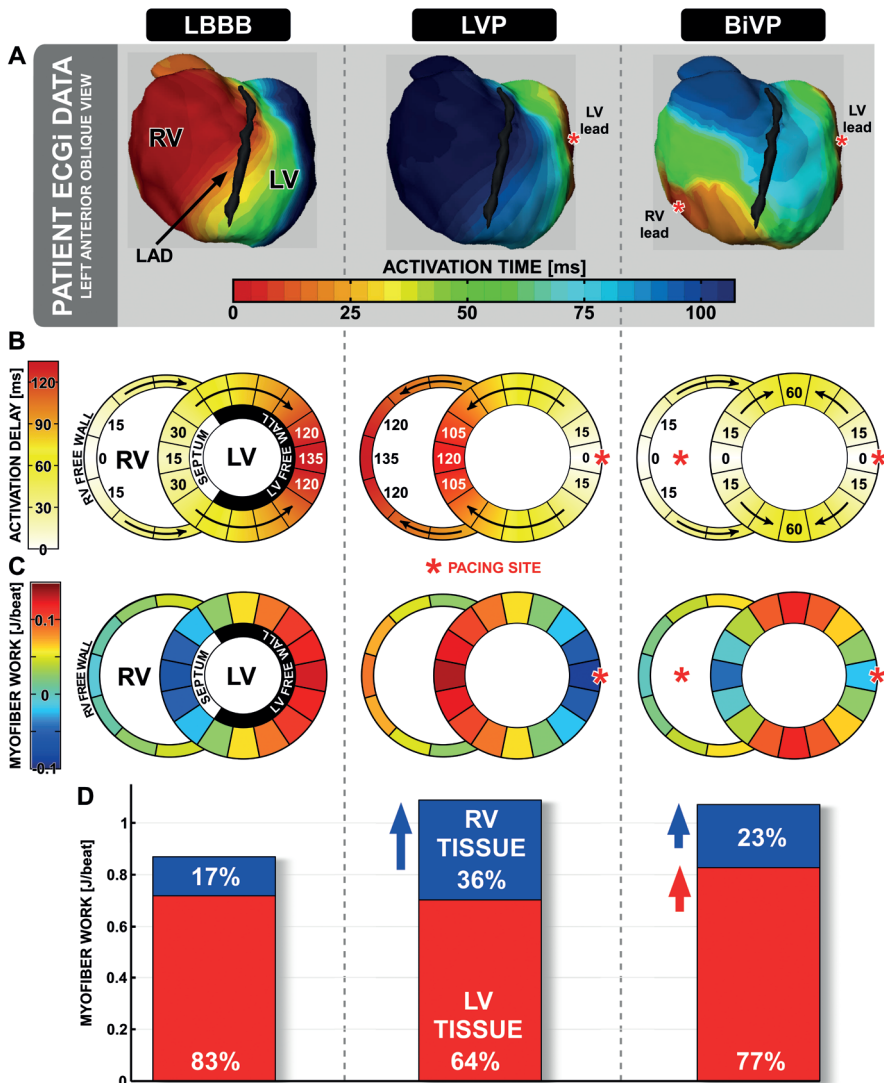


FIGURE 2. Pacing redistributes work from the LV lateral wall to the RV and septum.

A) ECG imaging in a patient with left bundle branch block (LBBB) at baseline, during LV pacing (LVP), and during biventricular pacing (BiVP). Note the late RV activation during LVP. B) shows simulated activation sequences corresponding to LBBB, LVP, and BiVP. Red asterisks indicate pacing sites. C) Color maps indicate myofiber work per ventricular wall segment. D) Bar charts indicate the proportion of ventricular pump work that is performed by the LV (red) and RV (blue) myocardium. Both LVP and BiVP increase ventricular pump work, but in LVP this effect arises through increased myofiber work in the RV myocardium (blue arrow), whereas in BiVP this effect occurs through increases in LV and RV myofiber work (red arrow). Figure is modified from Lumens J et al., *Journal of the American College of Cardiology* 2013;62:2395-2403, with permission.

THE RV IN LV-ONLY AND BIVENTRICULAR PACING

One of the major effects of successfully applied CRT is electrical resynchronization of the LV. Consequently, CRT redistributes work away from the LV free wall and towards both the septum and the RV free wall, as demonstrated by computer modelling.⁶⁶ Paradoxically, LV only pacing has been shown to provide similar benefit to biventricular pacing in many patients.⁷² Fusion of natural activation from the right bundle branch with the LV lead wave front was originally proposed as the mechanism underlying this benefit. However, patient measurements and canine experiments demonstrated that LV free wall pacing could produce similar acute benefit to biventricular pacing, despite a lack of fusion that was confirmed by electrocardiographic imaging (figure 2A).⁶⁶ In the same study, computer modelling revealed that the mechanism was again work redistribution, this time from the early-activated LV lateral wall to the RV (figure 2C). Through direct mechanical interaction, the RV could compensate for lost external work within the LV, boosting overall cardiac pump function. These computer modelling results suggest that LV-only pacing should be avoided in patients with RV dysfunction, which merits experimental and clinical investigation. How LV only pacing interacts with RV dysfunction remains unclear, and is of clinical interest as device manufacturers start to implement fusion pacing.

CONCLUSION

Computer modelling is a powerful tool for understanding cardiovascular function that has been under-utilized for studying the RV. We have demonstrated that computer modelling of the RV and cardiac imaging can work synergistically to uncover important mechanisms in a range of RV pathophysiologies and their treatment. We hope that this review will stimulate computer modelers, physiologists, and clinicians to increase their collaborative efforts to understand the ‘forgotten ventricle’.

REFERENCES

1. de Groote P, Millaire A, Foucher-Hossein C, Nugue O, Marchandise X, Ducloux G, et al. Right ventricular ejection fraction is an independent predictor of survival in patients with moderate heart failure. *J Am Coll Cardiol*. 1998;32:948-54.
2. Mehta SR, Eikelboom JW, Natarajan MK, Diaz R, Yi C, Gibbons RJ, et al. Impact of right ventricular involvement on mortality and morbidity in patients with inferior myocardial infarction. *J Am Coll Cardiol*. 2001;37:37-43.
3. Basso C, Corrado D, Marcus FI, Nava A, Thiene G. Arrhythmogenic right ventricular cardiomyopathy. *Lancet*. 2009;373:1289-300.
4. Di Salvo TG, Mathier M, Semigran MJ, Dec GW. Preserved right ventricular ejection fraction predicts exercise capacity and survival in advanced heart failure. *J Am Coll Cardiol*. 1995;25:1143-53.
5. La Gerche A, Claessen G, Dymarkowski S, Voigt JU, De Buck F, Vanhees L, et al. Exercise-induced right ventricular dysfunction is associated with ventricular arrhythmias in endurance athletes. *Eur Heart J*. 2015;36:1998-2010.
6. Davlouros PA, Niwa K, Webb G, Gatzoulis MA. The right ventricle in congenital heart disease. *Heart*. 2006;92 Suppl 1:i27-38.
7. Ho SY, Nihoyannopoulos P. Anatomy, echocardiography, and normal right ventricular dimensions. *Heart*. 2006;92 Suppl 1:i2-13.
8. Atsumi A, Ishizu T, Kameda Y, Yamamoto M, Harimura Y, Machino-Ohtsuka T, et al. Application of 3-dimensional speckle tracking imaging to the assessment of right ventricular regional deformation. *Circ J*. 2013;77:1760-8.
9. Lang RM, Badano LP, Mor-Avi V, Afilalo J, Armstrong A, Ernande L, et al. Recommendations for cardiac chamber quantification by echocardiography in adults: an update from the American Society of Echocardiography and the European Association of Cardiovascular Imaging. *Eur Heart J Cardiovasc Imaging*. 2015;16:233-70.
10. van de Veerdonk MC, Dusoswa SA, Marcus JT, Bogaard HJ, Spruijt O, Kind T, et al. The importance of trabecular hypertrophy in right ventricular adaptation to chronic pressure overload. *Int J Cardiovasc Imaging*. 2014;30:357-65.
11. Alfakih K, Plein S, Bloomer T, Jones T, Ridgway J, Sivananthan M. Comparison of right ventricular volume measurements between axial and short axis orientation using steady-state free precession magnetic resonance imaging. *J Magn Reson Imaging*. 2003;18:25-32.

12. Wang VY, Nielsen PM, Nash MP. Image-Based Predictive Modeling of Heart Mechanics. *Annual review of biomedical engineering*. 2015;17:351-83.
13. Lamata P, Niederer S, Nordsletten D, Barber DC, Roy I, Hose DR, et al. An accurate, fast and robust method to generate patient-specific cubic Hermite meshes. *Medical image analysis*. 2011;15:801-13.
14. Leonardi B, Taylor AM, Mansi T, Voigt I, Sermesant M, Pennec X, et al. Computational modelling of the right ventricle in repaired tetralogy of Fallot: can it provide insight into patient treatment? *Eur Heart J Cardiovasc Imaging*. 2013;14:381-6.
15. Chabiniok R, Wang VY, Hadjicharalambous M, Asner L, Lee J, Sermesant M, et al. Multiphysics and multiscale modelling, data-model fusion and integration of organ physiology in the clinic: ventricular cardiac mechanics. *Interface focus*. 2016;6:20150083.
16. Xi C, Latnie C, Zhao X, Tan JL, Wall ST, Genet M, et al. Patient-Specific Computational Analysis of Ventricular Mechanics in Pulmonary Arterial Hypertension. *Journal of biomechanical engineering*. 2016;138.
17. Tang D, Del Nido PJ, Yang C, Zuo H, Huang X, Rathod RH, et al. Patient-Specific MRI-Based Right Ventricle Models Using Different Zero-Load Diastole and Systole Geometries for Better Cardiac Stress and Strain Calculations and Pulmonary Valve Replacement Surgical Outcome Predictions. *PloS one*. 2016;11:e0162986.
18. Greenbaum RA, Ho SY, Gibson DG, Becker AE, Anderson RH. Left ventricular fibre architecture in man. *British heart journal*. 1981;45:248-63.
19. Potse M, Dube B, Richer J, Vinet A, Gulrajani RM. A comparison of monodomain and bidomain reaction-diffusion models for action potential propagation in the human heart. *IEEE transactions on bio-medical engineering*. 2006;53:2425-35.
20. Bayer JD, Blake RC, Plank G, Trayanova NA. A novel rule-based algorithm for assigning myocardial fiber orientation to computational heart models. *Annals of biomedical engineering*. 2012;40:2243-54.
21. Molina CE, Heijman J, Dobrev D. Differences in Left Versus Right Ventricular Electrophysiological Properties in Cardiac Dysfunction and Arrhythmogenesis. *Arrhythm Electrophysiol Rev*. 2016;5:14-9.
22. Rouleau JL, Paradis P, Shenasa H, Juneau C. Faster time to peak tension and velocity of shortening in right versus left ventricular trabeculae and papillary muscles of dogs. *Circulation research*. 1986;59:556-61.

23. Mast TP, Teske AJ, Walmsley J, van der Heijden JF, van Es R, Prinzen FW, et al. Right Ventricular Imaging and Computer Simulation for Electromechanical Substrate Characterization in Arrhythmogenic Right Ventricular Cardiomyopathy. *J Am Coll Cardiol*. 2016;68:2185-2197.
24. Sacks MS, Chuong CJ. A constitutive relation for passive right-ventricular free wall myocardium. *Journal of biomechanics*. 1993;26:1341-5.
25. Avazmohammadi R, Hill MR, Simon MA, Zhang W, Sacks MS. A novel constitutive model for passive right ventricular myocardium: evidence for myofiber-collagen fiber mechanical coupling. *Biomechanics and modeling in mechanobiology*. 2016.
26. Keller DU, Weiss DL, Dossel O, Seemann G. Influence of I(Ks) heterogeneities on the genesis of the T-wave: a computational evaluation. *IEEE transactions on bio-medical engineering*. 2012;59:311-22.
27. Lumens J, Delhaas T, Kirn B, Arts T. Three-wall segment (TriSeg) model describing mechanics and hemodynamics of ventricular interaction. *Annals of biomedical engineering*. 2009;37:2234-55.
28. Crozier A, Blazevic B, Lamata P, Plank G, Ginks M, Duckett S, et al. The relative role of patient physiology and device optimisation in cardiac resynchronisation therapy: A computational modelling study. *Journal of molecular and cellular cardiology*. 2015.
29. Lumens J, Arts T, Broers B, Boomars KA, van Paassen P, Prinzen FW, et al. Right ventricular free wall pacing improves cardiac pump function in severe pulmonary arterial hypertension: a computer simulation analysis. *Am J Physiol Heart Circ Physiol*. 2009;297:H2196-205.
30. Sun Y, Beshara M, Lucariello RJ, Chiamaramida SA. A comprehensive model for right-left heart interaction under the influence of pericardium and baroreflex. *The American journal of physiology*. 1997;272:H1499-515.
31. Yang C, Tang D, Haber I, Geva T, Del Nido PJ. In vivo MRI-Based 3D FSI RV/LV Models for Human Right Ventricle and Patch Design for Potential Computer-Aided Surgery Optimization. *Computers & structures*. 2007;85:988-997.
32. Ukwatta E, Arevalo H, Li K, Yuan J, Qiu W, Malamas P, et al. Myocardial Infarct Segmentation From Magnetic Resonance Images for Personalized Modeling of Cardiac Electrophysiology. *IEEE Trans Med Imaging*. 2016;35:1408-19.
33. Grosse-Wortmann L, Macgowan CK, Vidarsson L, Yoo SJ. Late gadolinium enhancement of the right ventricular myocardium: is it really different from the left ? *J Cardiovasc Magn Reson*. 2008;10:20.

34. Mendez C, Soler R, Rodriguez E, Lopez M, Alvarez L, Fernandez N, et al. Magnetic resonance imaging of abnormal ventricular septal motion in heart diseases: a pictorial review. *Insights into imaging*. 2011;2:483-492.
35. Beyar R, Hausknecht MJ, Halperin HR, Yin FC, Weisfeldt ML. Interaction between cardiac chambers and thoracic pressure in intact circulation. *The American journal of physiology*. 1987;253:H1240-52.
36. Maughan WL, Sunagawa K, Sagawa K. Ventricular systolic interdependence: volume elastance model in isolated canine hearts. *The American journal of physiology*. 1987;253:H1381-90.
37. Santamore WP, Shaffer T, Hughes D. A theoretical and experimental model of ventricular interdependence. *Basic research in cardiology*. 1986;81:529-38.
38. Beyar R, Dong SJ, Smith ER, Belenkie I, Tyberg JV. Ventricular interaction and septal deformation: a model compared with experimental data. *The American journal of physiology*. 1993;265:H2044-56.
39. Baker AE, Dani R, Smith ER, Tyberg JV, Belenkie I. Quantitative assessment of independent contributions of pericardium and septum to direct ventricular interaction. *The American journal of physiology*. 1998;275:H476-83.
40. Kerckhoffs RC, Neal ML, Gu Q, Bassingthwaight JB, Omens JH, McCulloch AD. Coupling of a 3D finite element model of cardiac ventricular mechanics to lumped systems models of the systemic and pulmonic circulation. *Annals of biomedical engineering*. 2007;35:1-18.
41. Fritz T, Wieners C, Seemann G, Steen H, Dossel O. Simulation of the contraction of the ventricles in a human heart model including atria and pericardium. *Biomechanics and modeling in mechanobiology*. 2014;13:627-41.
42. Claessen G, Claus P, Delcroix M, Bogaert J, La Gerche A, Heidbuchel H. Interaction between respiration and right versus left ventricular volumes at rest and during exercise: a real-time cardiac magnetic resonance study. *Am J Physiol Heart Circ Physiol*. 2014;306:H816-24.
43. Shi Y, Lawford P, Hose R. Review of zero-D and 1-D models of blood flow in the cardiovascular system. *Biomedical engineering online*. 2011;10:33.
44. Markl M, Kilner PJ, Ebbers T. Comprehensive 4D velocity mapping of the heart and great vessels by cardiovascular magnetic resonance. *J Cardiovasc Magn Reson*. 2011;13:7.
45. Gomez A, Pushparajah K, Simpson JM, Giese D, Schaeffter T, Penney G. A sensitivity analysis on 3D velocity reconstruction from multiple registered echo Doppler views. *Medical image analysis*. 2013;17:616-31.

46. de Vecchi A, Nordsletten DA, Remme EW, Bellsham-Revell H, Greil G, Simpson JM, et al. Inflow typology and ventricular geometry determine efficiency of filling in the hypoplastic left heart. *The Annals of thoracic surgery*. 2012;94:1562-9.
47. Naeije R, Chesler N. Pulmonary circulation at exercise. *Comprehensive Physiology*. 2012;2:711-41.
48. Guazzi M, Naeije R. Pulmonary Hypertension in Heart Failure: Pathophysiology, Pathobiology, and Emerging Clinical Perspectives. *J Am Coll Cardiol*. 2017;69:1718-1734.
49. Wenk JF, Ge L, Zhang Z, Soleimani M, Potter DD, Wallace AW, et al. A coupled biventricular finite element and lumped-parameter circulatory system model of heart failure. *Computer methods in biomechanics and biomedical engineering*. 2013;16:807-18.
50. Sugiura S, Washio T, Hatano A, Okada J, Watanabe H, Hisada T. Multi-scale simulations of cardiac electrophysiology and mechanics using the University of Tokyo heart simulator. *Progress in biophysics and molecular biology*. 2012;110:380-9.
51. La Gerche A, MacIsaac AI, Burns AT, Mooney DJ, Inder WJ, Voigt JU, et al. Pulmonary transit of agitated contrast is associated with enhanced pulmonary vascular reserve and right ventricular function during exercise. *J Appl Physiol (1985)*. 2010;109:1307-17.
52. Westerhof N, Lankhaar JW, Westerhof BE. The arterial Windkessel. *Medical & biological engineering & computing*. 2009;47:131-41.
53. Kheifets VO, Dunning J, Truong U, Ivy D, Hunter K, Shandas R. A Zero-Dimensional Model and Protocol for Simulating Patient-Specific Pulmonary Hemodynamics From Limited Clinical Data. *Journal of biomechanical engineering*. 2016;138.
54. Linehan JH, Haworth ST, Nelin LD, Krenz GS, Dawson CA. A simple distensible vessel model for interpreting pulmonary vascular pressure-flow curves. *J Appl Physiol (1985)*. 1992;73:987-94.
55. Linehan JH, Dawson CA. A three-compartment model of the pulmonary vasculature: effects of vasoconstriction. *J Appl Physiol Respir Environ Exerc Physiol*. 1983;55:923-8.
56. Palau-Caballero G, Walmsley J, van Empel VP, Lumens J, Delhaas T. Why Septal Motion is a Marker of Right Ventricular Failure in Pulmonary Arterial Hypertension: Mechanistic Analysis Using a Computer Model. *Am J Physiol Heart Circ Physiol*. 2016:ajpheart 00596 2016.
57. Qureshi MU, Vaughan GD, Sainsbury C, Johnson M, Peskin CS, Olufsen MS, et al. Numerical simulation of blood flow and pressure drop in the pulmonary arterial and venous circulation. *Biomechanics and modeling in mechanobiology*. 2014;13:1137-54.
58. Morris PD, Narracott A, von Tengg-Kobligk H, Silva Soto DA, Hsiao S, Lungu A, et al. Computational fluid dynamics modelling in cardiovascular medicine. *Heart*. 2016;102:18-28.

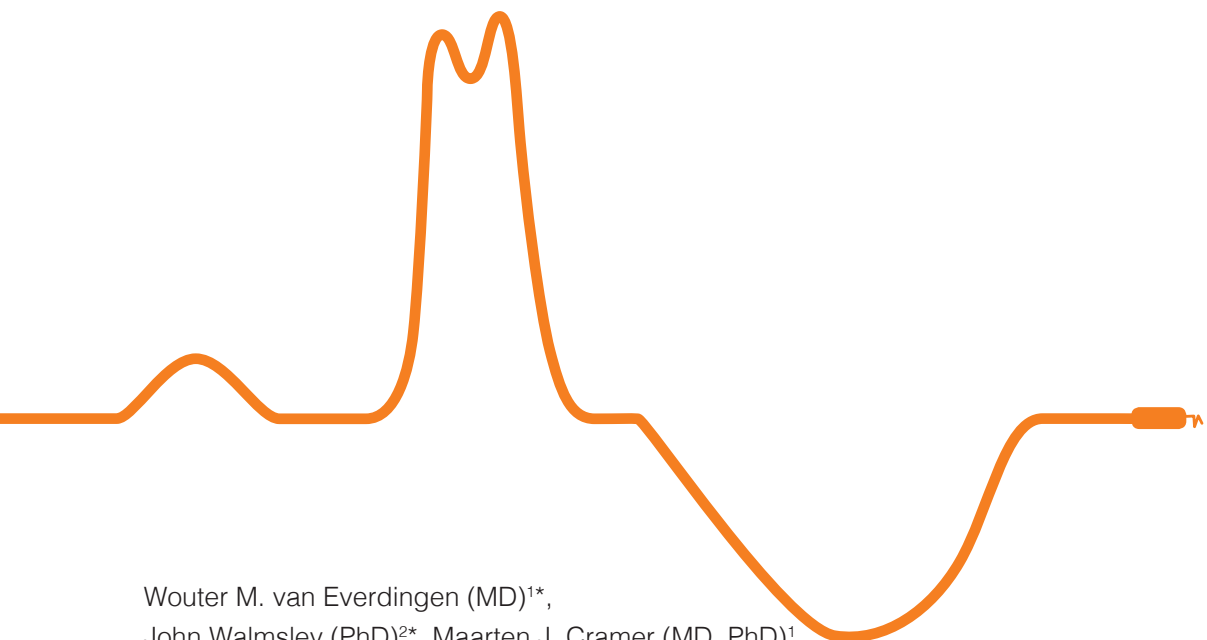
59. Bove EL, Migliavacca F, de Leval MR, Balossino R, Pennati G, Lloyd TR, et al. Use of mathematic modeling to compare and predict hemodynamic effects of the modified Blalock-Taussig and right ventricle-pulmonary artery shunts for hypoplastic left heart syndrome. *The Journal of thoracic and cardiovascular surgery*. 2008;136:312-320 e2.
60. Tang BT, Pickard SS, Chan FP, Tsao PS, Taylor CA, Feinstein JA. Wall shear stress is decreased in the pulmonary arteries of patients with pulmonary arterial hypertension: An image-based, computational fluid dynamics study. *Pulmonary circulation*. 2012;2:470-6.
61. Tabereaux PB, Doppalapudi H, Kay GN, McElderry HT, Plumb VJ, Epstein AE. Limited response to cardiac resynchronization therapy in patients with concomitant right ventricular dysfunction. *J Cardiovasc Electrophysiol*. 2010;21:431-5.
62. Sharma A, Bax JJ, Vallakati A, Goel S, Lavie CJ, Kassotis J, et al. Meta-Analysis of the Relation of Baseline Right Ventricular Function to Response to Cardiac Resynchronization Therapy. *Am J Cardiol*. 2016;117:1315-21.
63. Aguado-Sierra J, Krishnamurthy A, Villongco C, Chuang J, Howard E, Gonzales MJ, et al. Patient-specific modeling of dyssynchronous heart failure: a case study. *Progress in biophysics and molecular biology*. 2011;107:147-55.
64. Sermesant M, Chabiniok R, Chinchapatnam P, Mansi T, Billet F, Moireau P, et al. Patient-specific electromechanical models of the heart for the prediction of pacing acute effects in CRT: a preliminary clinical validation. *Medical image analysis*. 2012;16:201-15.
65. Prinzen FW, Hunter WC, Wyman BT, McVeigh ER. Mapping of regional myocardial strain and work during ventricular pacing: experimental study using magnetic resonance imaging tagging. *J Am Coll Cardiol*. 1999;33:1735-42.
66. Lumens J, Ploux S, Strik M, Gorcsan J, 3rd, Cochet H, Derval N, et al. Comparative electromechanical and hemodynamic effects of left ventricular and biventricular pacing in dyssynchronous heart failure: electrical resynchronization versus left-right ventricular interaction. *J Am Coll Cardiol*. 2013;62:2395-403.
67. Stankovic I, Prinz C, Ciarka A, Daraban AM, Kotrc M, Aarones M, et al. Relationship of visually assessed apical rocking and septal flash to response and long-term survival following cardiac resynchronization therapy (PREDICT-CRT). *Eur Heart J Cardiovasc Imaging*. 2016;17:262-9.
68. Little WC, Reeves RC, Arciniegas J, Katholi RE, Rogers EW. Mechanism of abnormal interventricular septal motion during delayed left ventricular activation. *Circulation*. 1982;65:1486-91.

69. Kingma I, Tyberg JV, Smith ER. Effects of diastolic transeptal pressure gradient on ventricular septal position and motion. *Circulation*. 1983;68:1304-14.
70. Gjesdal O, Remme EW, Opdahl A, Skulstad H, Russell K, Kongsgaard E, et al. Mechanisms of abnormal systolic motion of the interventricular septum during left bundle-branch block. *Circ Cardiovasc Imaging*. 2011;4:264-73.
71. Walmsley J, Huntjens PR, Prinzen FW, Delhaas T, Lumens J. Septal flash and septal rebound stretch have different underlying mechanisms. *Am J Physiol Heart Circ Physiol*. 2016;310:H394-403.
72. Thibault B, Ducharme A, Harel F, White M, O'Meara E, Guertin MC, et al. Left ventricular versus simultaneous biventricular pacing in patients with heart failure and a QRS complex ≥ 120 milliseconds. *Circulation*. 2011;124:2874-81.



Echocardiographic prediction of Cardiac Resynchronization Therapy response requires analysis of both mechanical dyssynchrony and right ventricular function

A combined analysis of patient data and computer simulations



Wouter M. van Everdingen (MD)^{1*},
John Walmsley (PhD)^{2*}, Maarten J. Cramer (MD, PhD)¹,
Iris van Hagen (MD)¹ Bart W.L. De Boeck (MD, PhD)³, Mathias Meine (MD, PhD)¹
Tammo Delhaas (MD, PhD)⁴ Pieter A. Doevendans (MD, PhD)¹,
Frits W. Prinzen (PhD)², Joost Lumens (PhD)^{2,4} and Geert E. Leenders (MD, PhD)¹

* van Everdingen and Walmsley contributed equally to the manuscript.

¹ University Medical Center Utrecht, Utrecht, The Netherlands.

² Maastricht University Medical Center, CARIM School for Cardiovascular Diseases, Maastricht, The Netherlands.

³ Kantonsspital Luzern, Luzern, Switzerland.

⁴ L'Institut de Rythmologie et Modélisation Cardiaque (IHU-LIRYC), Université de Bordeaux, Pessac, France.

ABSTRACT

Background: Pronounced echocardiographically measured mechanical dyssynchrony is a positive predictor of response to cardiac resynchronization therapy (CRT), while right ventricular (RV) dysfunction is a negative predictor. We investigated how RV dysfunction influences the association between mechanical dyssynchrony and left ventricular (LV) volumetric remodelling following CRT.

Methods: 122 CRT candidates (LV ejection fraction $19\pm 6\%$; QRS-width $168\pm 21\text{ms}$) were prospectively enrolled and underwent echocardiography before and six months after CRT. Volumetric remodelling was defined as percentage reduction in LV end-systolic volume. RV dysfunction was defined as RV fractional area change (RVFAC) $< 35\%$. Mechanical dyssynchrony was assessed as the time-to-peak strain between septum and LV lateral wall (Strain-SL), inter-ventricular mechanical delay (IVMD) and septal systolic rebound stretch (SRSsept). Simulations of heart failure with an LV conduction delay in the CircAdapt computer model were used to investigate how LV and RV myocardial contractility influence LV dyssynchrony and acute CRT response.

Results: In the entire patient cohort, higher baseline SRSsept, Strain-SL, and IVMD were all associated with LV volumetric remodelling in univariate analysis ($R=0.599$, 0.421 , and 0.410 , respectively, all $p<0.01$). Association between SRSsept and LV volumetric remodelling was even stronger in patients without RV dysfunction ($R=0.648$, $p<0.01$). However, none of the mechanical dyssynchrony parameters were associated with LV remodelling in the RV dysfunction subgroup. The computer simulations showed that low RV contractility reduced CRT response but hardly affected mechanical dyssynchrony. In contrast, LV contractility changes had congruent effects on mechanical dyssynchrony and CRT response.

Conclusion: Mechanical dyssynchrony parameters do not reflect the negative impact of reduced RV contractility on CRT response. Echocardiographic prediction of CRT response should therefore include parameters of mechanical dyssynchrony and RV function.

INTRODUCTION

Cardiac resynchronization therapy (CRT) is an established treatment for patients with heart failure and evidence of electrical conduction delay.^{1,2} Despite the success of CRT in large clinical trials, predicting CRT response in the individual remains challenging. Response prediction is difficult because the mechanisms through which CRT response occurs are still not completely understood. An important mode of action of CRT is the correction of mechanical dyssynchrony caused by an electrical conduction delay, resulting in improvement in myocardial efficiency.³ Attempts to predict outcome after CRT by identifying such electrical or mechanical substrates have however yielded variable results.⁴

Right ventricular (RV) function is an important predictor of echocardiographic and clinical outcome following CRT.⁵ The impact of RV function on prognosis has been demonstrated in both observational studies and in landmark CRT-trials.⁵⁻⁷ RV dysfunction is strongly associated with more advanced heart failure.^{8,9} Moreover, changes in RV function and loading can lead to mechanical dyssynchrony through ventricular interaction even without underlying electrical dyssynchrony.¹⁰ Whether RV function directly affects mechanical dyssynchrony and CRT response, and how this relates to the association with more advanced heart failure, remains unclear.^{5-7, 10, 11} We therefore used echocardiographic deformation imaging to investigate whether RV dysfunction affects baseline mechanical dyssynchrony indices in a CRT population. We also investigated how these indices related to CRT response (i.e. volumetric remodelling). CRT response was defined as the reduction in LV end-systolic volume six months after CRT. We further hypothesized that RV dysfunction could directly influence both mechanical dyssynchrony and CRT response, independent of LV condition. Because determining causation in the interaction between RV and LV myocardial dysfunction and mechanical dyssynchrony using patient data is challenging, we also performed computer simulations. Simulations were performed with the multiscale CircAdapt model of the human heart and circulation to isolate and explain the effects of RV and LV myocardial dysfunction on both mechanical dyssynchrony and CRT response.¹²

METHODS

STUDY POPULATION AND PROTOCOL

The study population consisted of a cohort of prospectively enrolled patients undergoing CRT because of medication-refractory heart failure (New York Heart Association class (NYHA) II-IV, LV ejection fraction (LVEF) <35%) and evidence of conduction disturbances (QRS \geq 120ms) with a left bundle branch block-like (LBBB) morphology on the surface electrocardiogram. Patients were excluded from the analysis if they had poor echocardiographic image quality (n=20). Echocardiographic and clinical characteristics were prospectively assessed in all patients before and six months after CRT. Care was taken to optimize heart failure medication before implantation of a CRT device. The execution of the study complied with the principles outlined in the Declaration of Helsinki on research in human subjects and with the procedures of the local Medical Ethics Committee. In compliance with Dutch law, written informed consent was waived by the local Medical Ethics Committee as all echocardiograms and CRT implantations were part of standard clinical care.

ECHOCARDIOGRAPHIC PROTOCOL

All echocardiographic data were obtained on a Vivid 7 ultrasound machine (General Electric, Chicago, USA). A minimum of three loops were acquired at breath hold and analysed offline (Echopac version 6.0.1, General Electric). In patients with atrial fibrillation, all parameters are the average over five representative beats.

TWO-DIMENSIONAL ECHOCARDIOGRAPHY AND DOPPLER IMAGING

LVEF, LV end-systolic (LVESV) and end-diastolic (LVEDV) volumes were measured by biplane Simpson's method.¹³ Reverse remodelling after CRT was defined as the percentage of reduction in LVESV between echocardiographic examination before and six months after CRT implantation. Response was defined as a reduction in LVESV of 15% or more.

Mitral regurgitation effective regurgitant orifice was quantified by the proximal is velocity surface area method. RV measurements were performed in the apical four-chamber view. RV end-diastolic and end-systolic areas were traced and were used to calculate RV fractional area change (RVFAC). RV dysfunction was defined as RVFAC <35%.¹³ Tricuspid annular plane systolic excursion (TAPSE) and trans-tricuspid pressure gradient were also measured. RVFAC was chosen to define RV dysfunction, as we expected that RVFAC provided the most adequate estimation of RV function in the presence of mechanical dyssynchrony.¹⁴

For offline deformation imaging, additional narrow sector single wall images of the septum, lateral wall of the LV and free wall of the RV were prospectively acquired from the standard apical views at 51-109Hz. The onset of the QRS complex was taken as zero reference for timing and strain measurements. Systole was defined using mitral valve closure and aortic valve closure, derived from Doppler flow patterns. Interventricular mechanical delay (IVMD) was assessed by the delay between pulmonary and aortic valve opening.

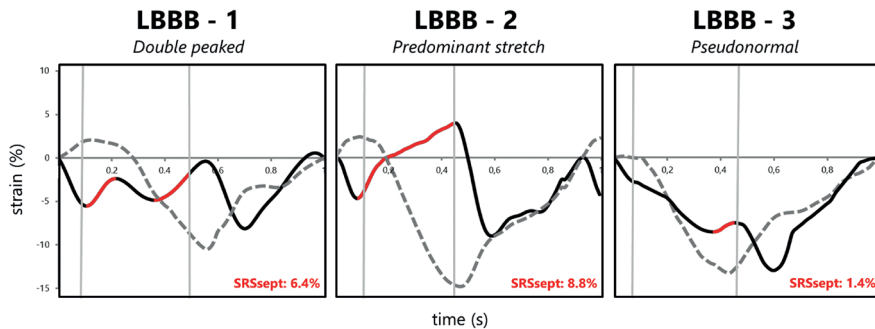


FIGURE 1. Examples of septal strain patterns and SRSsept

Three septal strain patterns (solid black curves) are displayed, LBBB-1: double-peaked shortening, LBBB-2: predominant stretch during ejection phase, and LBBB-3 pseudo-normal shortening. SRSsept (red) is indicated in the lower right corner of each panel and is determined as all systolic stretch following prematurely terminated shortening in the septum. Lateral wall strain is displayed as a dashed grey line. Horizontal solid grey lines represent the ejection phase (mitral valve closure to aortic valve closure).

DEFORMATION ANALYSIS

Dedicated speckle tracking software (GE Echopac 2DS, version 6.1) was used to derive longitudinal strain curves. The region of interest (ROI) was placed from base to apex and adapted to match wall thickness. Tracking was visually checked and the ROI adjusted if necessary. Global longitudinal deformation was calculated over the entire length of the wall. To assess LV dyssynchrony, time to peak strain difference between the LV free wall and the septum was calculated (Strain-SL). Septal systolic rebound stretch (SRSsept) was determined by summing all systolic stretch following prematurely terminated shortening in the septum, as previously described (figure 1).^{15, 16} Septal strain patterns were also categorized into Type I (double-peaked), Type II (predominant stretch during ejection), and Type III (pseudo-normal) as previously described (figure 1).¹⁷

DEVICE IMPLANTATION

Implantation was performed under local anaesthesia. RV and atrial lead were placed transvenously at conventional positions. The LV lead was aimed at a tributary of the coronary sinus overlying the LV free wall. Leads were connected to a CRT-defibrillator in all patients.

COMPUTER SIMULATIONS

The CircAdapt computational model of the human heart and circulation (www.circadapt.org) was used to simulate local ventricular myofibre mechanics and global pump function in hearts of virtual patients with different degrees of LV and RV contractile weakness, and LV conduction delay.^{12, 17, 18} More detailed descriptions of both the CircAdapt model and simulations we performed are provided in the supplementary methods.

SIMULATION OF LV AND RV FAILURE AT BASELINE

The starting point for all simulations of heart failure and CRT was a computer model representing normal healthy adult physiology obtained as described previously.¹⁷ We produced a virtual patient with heart failure and LBBB by imposing a cardiac output of 3.1L/min based on the mean value in the patient data (table 1), with a heart rate of 70bpm and mean arterial pressure of 92mmHg. We reduced the RV and LV myocardial contractility, being the intrinsic ability of myocardial tissue to generate active stress following cross bridge formation, to 60% of the contractility value in healthy myocardium. LV and RV unloaded wall areas were expanded by 10% to represent eccentric remodelling. An activation delay was imposed within the LV to represent LBBB-like activation (supplemental figure 1). The resulting LVEF and RVEF were 22% and 41%, respectively.

Beginning with the initial virtual patient with heart failure and LBBB, further worsening of RV or LV myocardial contractile weakness was simulated through further reductions in either the contractility of the RV or LV free wall from 60% down to 20% of the original healthy contractility in nine steps. This protocol resulted in nine virtual patients with varying degrees of LV myocardial dysfunction causing a decrease in LVEF to a minimum of 10%, and nine virtual patients with varying degrees of RV myocardial dysfunction causing a gradual decrease in RVEF to a minimum of 24%. Cardiac output, heart rate, and mean arterial pressure were sustained through homeostatic control mechanisms in each virtual patient. The average myofibre strain from the septal wall segments was used to calculate SRSsept for each simulation.

SIMULATION OF CARDIAC RESYNCHRONIZATION THERAPY

CRT was simulated in each virtual patient using an activation pattern representing pre-excitation of the RV apex and the LV lateral wall, as shown in supplemental figure 1. When simulating the acute effects of CRT, homeostatic control was turned off to allow for changes in stroke volume to occur. We defined the acute response to CRT in the simulations as the %-change in stroke volume after initiation of CRT once a new hemodynamic steady state was reached.

STATISTICAL ANALYSIS

Statistical analysis was performed using SPSS statistical software package (SPSS Inc., Chicago, USA). Values are presented as mean and standard deviation for continuous variables and as numbers and percentages for categorical variables. Continuous data were compared using the paired or unpaired t-test as appropriate. Categorical data were compared using the Chi-square or Fischer's Exact test. Correlation between parameters was expressed by Pearson's or Spearman's correlation coefficients as appropriate. Univariate analysis of parameters of LV function, RV function and dyssynchrony was performed to determine their relation to CRT response. The single best performing parameters for each aspect (i.e. LV function, RV function, and dyssynchrony) were used in a stepwise, forward selection, multivariable model. Three models were used to test whether baseline RV function affected prediction of reverse remodelling independent from the baseline LV function (i.e. LVEDV, LVESV or LVEF) and mechanical dyssynchrony. One model incorporated the best performing dyssynchrony and LV function parameter, one incorporated the best performing dyssynchrony and RV function parameter and one incorporated all three. A p-value <0.05 was considered statistically significant for all analyses.

MEASUREMENT VARIABILITY

Lastly, measurement variability of key echocardiographic parameters and dyssynchrony parameters was analysed by a second observer in 20 randomly selected patients and compared using the intra-class correlation coefficient. Intra-class correlation coefficient values were as follows, LVEDV: 0.98, LVESV: 0.97, LVEF: 0.77, RVEDA: 0.83, RVESA: 0.90, RVFAC: 0.93, IVMD: 0.91, SL-delay: 0.75, and SRSsept: 0.92.

TABLE 1. Baseline characteristics

Parameter	RVFAC \geq 35% (n=83)	RVFAC <35% (n=39)	p-value
Age (years)	65 \pm 11	64 \pm 12	0.716
Male (nr, %)	52 (63)	33 (85)	0.019
Rhythm (nr, %)			
Sinus rhythm	76 (92)	30 (77)	0.041
Atrial fibrillation	7 (8)	9 (23)	
NYHA-class (nr, %)			
II	8 (10)	0 (0)	0.005
III	70 (84)	30 (77)	
IV	5 (6)	9 (23)	
Medication (nr, %)			
Beta-blocker	71 (86)	25 (64)	0.010
ACE-i or ATII-antagonist	76 (92)	37 (95)	0.717
Diuretics	75 (90)	38 (97)	0.269
Aldosterone antagonist	42 (51)	23 (59)	0.440
Lead position (nr, %)			0.606
(postero)lateral	68 (82)	32 (82)	
anterolateral	7 (8)	5 (13)	
posterior	8 (10)	2 (5)	
QRS width (ms)	170 \pm 25	167 \pm 20	0.517
LBBB (nr, %)	57 (69)	23 (59)	0.313
Ischemic etiology (nr, %)	44 (53)	11 (28)	0.012
LVEDV (ml)	237 \pm 65	290 \pm 107	0.006
LVESV (ml)	188 \pm 59	247 \pm 101	0.001
LVEF (%)	21 \pm 6	16 \pm 5	<0.001
Cardiac output (L/min)	3.1 \pm 1.0	3.1 \pm 1.2	0.902
Left atrial size (mm)	48 \pm 8	54 \pm 7	<0.001
MRERO (mm ²)	8 \pm 7	14 \pm 8	0.001
SRSsept (%)	5.2 \pm 3.5	3.3 \pm 2.9	0.003
Septal strain pattern (nr, %)			0.017
1 (double peaked)	27 (33)	5 (13)	
2 (predominant stretch)	28 (34)	11 (28)	
3 (pseudo normal)	28 (34)	23 (59)	
Strain-SL (ms)	276 \pm 143	230 \pm 145	0.099
IVMD (ms)	47 \pm 26	47 \pm 26	0.983
RVEDA (cm ²)	14 \pm 5	20 \pm 5	<0.001
RVESA (cm ²)	7 \pm 4	15 \pm 4	<0.001
RVFAC (%)	49 \pm 10	25 \pm 6	<0.001
TAPSE (mm)	19 \pm 5	14 \pm 4	<0.001
2DS-RV (%)	-20.4 \pm 5.6	-14.3 \pm 4.4	<0.001
TRPG (mmHg)	30 \pm 8	35 \pm 9	0.009

2DS-RV: right ventricular free wall peak strain, ACE-i: ACE inhibitor, ATII antagonist: angiotensin receptor II antagonist, IVMD: interventricular mechanical dyssynchrony, LBBB: left bundle branch block, MRERO: mitral regurgitation effective regurgitant orifice, NYHA: New York Heart Association, LVEDV: left ventricular end-diastolic volume, LVEF: left ventricular ejection fraction, LVESV: left ventricular end-systolic volume, RVEDA: right ventricular end-diastolic area, RVESA: right ventricular end-systolic area, RVFAC: right ventricular fractional area change, SRSsept: septal systolic rebound stretch, Strain-SL: septal to lateral wall peak shortening delay, TAPSE: tricuspid annular plane systolic excursion, TRPG: tricuspid regurgitation peak gradient.

RESULTS

PATIENT STUDY

STUDY POPULATION

Table 1 shows baseline characteristics of patients with and without RV dysfunction. Patients with RV dysfunction had more advanced heart failure with more pronounced RV and LV dilatation, lower LVEF, larger left atria, more severe mitral regurgitation and higher NYHA functional class. These patients were also more often male, more often had atrial fibrillation, had higher trans-tricuspid pressure gradients and less often had an ischemic aetiology of heart failure. Of all dyssynchrony parameters, only SRSsept was significantly lower in patients with RV dysfunction.

CRT RESPONSE

In total, nine patients died (four patients without RV dysfunction and five with RV dysfunction) and three received an LV assist device implantation or heart transplantation (two patients without RV dysfunction and one with RV dysfunction) before the six-month follow-up visit. NYHA class decreased with two points in nine patients (7%), decreased one point in 65 patients (53%), remained stable in 33 patients (27%), and had missing data in fifteen (12%). NYHA class decreased significantly compared to baseline values in the subgroup without RV dysfunction. However, there was no statistically significant difference in change of NYHA class between the two subgroups (table 2). LV volumes could not be quantified at six-month follow-up in three patients. In the remaining population, CRT reduced LVEDV (256 ± 84 to 227 ± 96 ml) and LVESV (208 ± 80 to 174 ± 92 ml) and improved LVEF ($20\pm 7\%$ to $26\pm 11\%$) at six months (all $p<0.001$). RV free wall peak strain (-18.2% to -21.1% , $p<0.001$), RV end-systolic area (10 ± 6 to 9 ± 4 cm², $p<0.05$) and trans-tricuspid pressure gradient (33 ± 9 to 29 ± 9 mmHg, $p<0.05$) showed a significant improvement after CRT whereas RVFAC and TAPSE did not. Table 2 shows response in patients with and without RV dysfunction. Patients with RV dysfunction showed less LV reverse remodelling and less improvement of LVEF, but improvements in RV parameters were greater in these patients. There were 9 (28%) volumetric responders in the subgroup with RV dysfunction compared to 45 (60%) in the subgroup without RV dysfunction ($p<0.01$).

TABLE 2. CRT response in patients with and without RV dysfunction

Parameter	RVFAC $\geq 35\%$ (n=83)	RVFAC $<35\%$ (n=39)	P-value
Δ LVEDV (%)	-17 \pm 19*	-3 \pm 16	<0.001
Δ LVESV (%)	-24 \pm 23*	-7 \pm 18*	<0.001
Δ LVEF (%-point)	8 \pm 8*	4 \pm 7*	0.006
Δ 2DS-RV (%-point)	-2.3 \pm 6.0*	-4.4 \pm 4.7*	0.082
Δ RVEDA (%)	8 \pm 31	-15 \pm 34*	0.001
Δ RVESA (%)	18 \pm 44	-25 \pm 30*	<0.001
Δ RVFAC (%-point)	-4 \pm 11*	9 \pm 11*	<0.001
Δ TRPG (mmHg)	-2 \pm 9	-5 \pm 7*	0.343
Δ TAPSE (mm)	-1 \pm 4*	2 \pm 4*	<0.001
Δ NYHA-class (n, %)			
0	24 (32)*	9 (28)	0.913
-1	45 (60)*	20 (63)	
-2	6 (8)*	3 (9)	

For abbreviations see table 1. *: significant change compared to baseline.

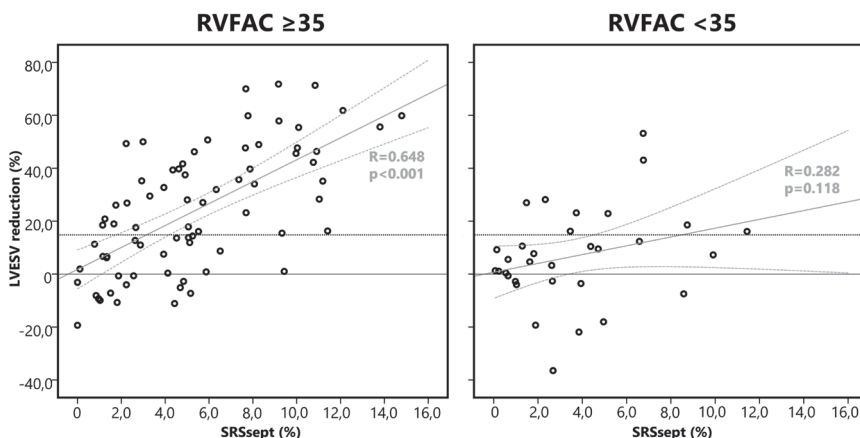


FIGURE 2. Relation of SRSsept with LV reverse remodelling in patients with and without RV dysfunction.

Patients with low RVFAC ($<35\%$) had a weaker and statistically non-significant relation between LVESV reduction and SRSsept (right panel). Those with preserved RVFAC ($\geq 35\%$) had a strong and statistically significant relation between LVESV reduction and SRSsept. The dotted horizontal line indicates the response cut-off of 15% reduction in LVESV. LVESV: Left ventricular end-systolic volume, R: correlation coefficient, RVFAC: right ventricular fractional area change, SRSsept: septal systolic rebound stretch, p: p-value.

ASSOCIATION OF BASELINE PARAMETERS WITH CRT RESPONSE

In the entire patient cohort, SRSsept showed the strongest association with volumetric response ($R=0.599$, $p<0.001$). while traditional dyssynchrony parameters also showed a correlation ($R=0.410$ for IVMD and $R=0.421$ for Strain-SL, both $p<0.001$). SRSsept had an even stronger association with volumetric response in the subgroup of patients with preserved RV function ($R=0.648$, $p<0.001$, figure 2). However, neither SRSsept nor any of the other dyssynchrony parameters correlated with volumetric response in patients with RV dysfunction.

All RV function parameters showed a significant association with LV reverse remodelling (table 3). The association between baseline RVFAC and LV reverse remodelling was strongest out of all of the RV function parameters. Of the baseline parameters reflecting LV condition, both LVEDV and LVESV were associated with reverse remodelling. There was no significant association between baseline LVEF and reverse remodelling. LVEDV showed the best correlation with LV reverse remodelling. Although changes in the R-square value were small, addition of LVEDV or RVFAC to SRSsept improved the prediction of LV reverse remodelling in multivariable regression (table 4). However, when both were included in the model, LVEDV no longer had significant independent predictive value on top of SRSsept and RVFAC. This indicates that LV reverse remodelling after CRT was more strongly associated with baseline RVFAC than with baseline LVEDV, and that RVFAC is additive to mechanical dyssynchrony parameters in their ability to predict response to CRT.

TABLE 3. Univariate relation of baseline LV and RV parameters with LV remodelling

Parameter	Δ LVESV (%)	
	R	p-value
LVEDV	-0.291	0.002
LVESV	-0.274	0.004
LVEF	0.120	0.220
TAPSE	0.342	<0.001
RVEDA	-0.242	0.012
RVESA	-0.354	<0.001
RVFAC	0.430	<0.001
2DS-RV	-0.218	0.024

R: regression coefficient, for other abbreviations see table 1.

TABLE 4. Predictive value of LV and/or RV function on top of dyssynchrony

Parameter	Δ LVESV (%)				
	Model R ²	B	SE	Beta	p-value
Model 1					
SRSsept*	0.36	3.67	0.50	0.57	<0.001
LVEDV*	0.39	-0.06	0.02	-0.20	0.010
Model 2					
SRSsept*	0.36	3.32	0.53	0.51	<0.001
RVFAC*	0.41	38.75	12.87	0.24	0.003
Model 3					
SRSsept*	0.36	3.32	0.53	0.51	<0.001
RVFAC*	0.41	38.75	12.87	0.24	0.003
LVEDV†				-0.15	0.062

B: unstandardized or regression coefficients, SE: standard error, Beta: standardized coefficients. For other abbreviations, see table 1. *: Parameter in the model, †: parameter not in the model.

SIMULATIONS

EFFECT OF LV AND RV CONTRACTILE PARAMETERS ON SRSSEPT

The baseline virtual patient with heart failure and LBBB produced a characteristic Type II LBBB myocardial deformation pattern that was similar to LV strain patterns observed in the patients (figure 3B and 3C, left panel) with an SRSsept of 9.3%. Virtual patients with decreased LV contractility had qualitative changes in their septal strain patterns (figure 3B, middle and right panels). These changes in septal strain were accompanied by a decline in SRSsept to 2.7% (figure 4A). In contrast, virtual patients with decreased RV contractility did not have qualitative changes in their septal strain patterns (figure 3C, middle and right panels). They also had only a small change in SRSsept (figure 4A), which reduced from 9.3% in the baseline heart failure with LBBB simulation to 8.6% at an RV contractility of 20% of healthy tissue.

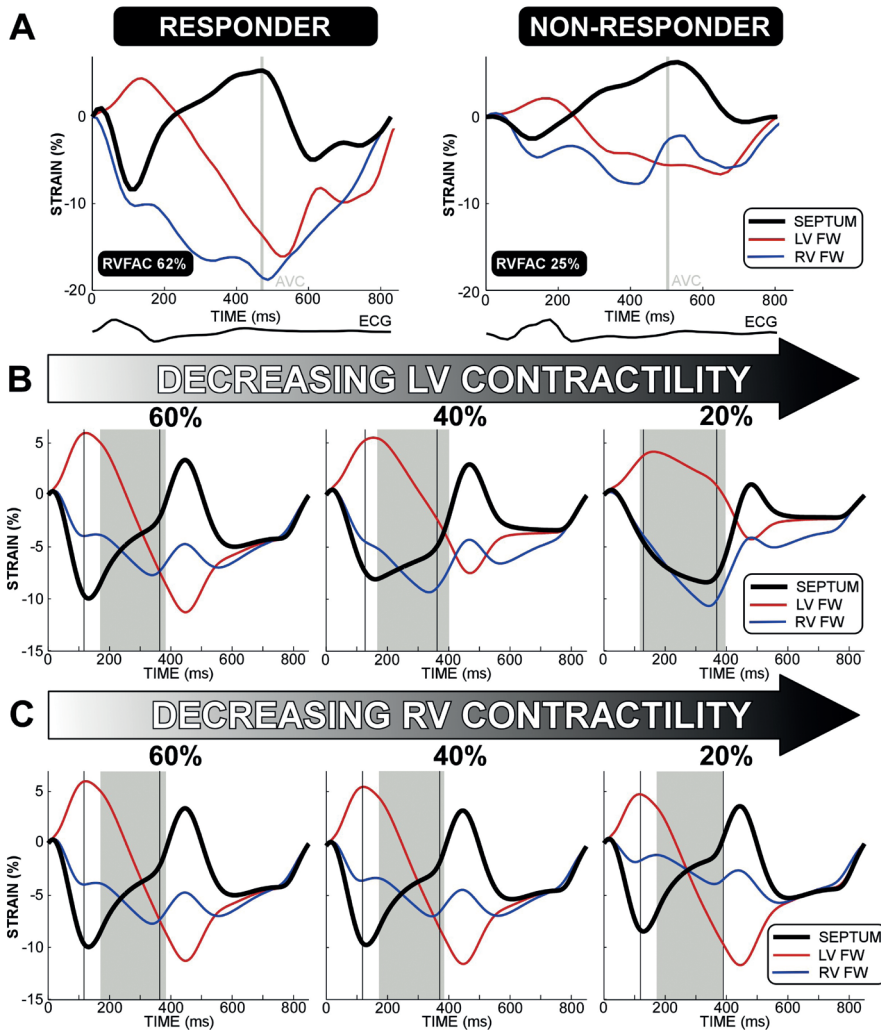


FIGURE 3. Effect of LV and RV contractility on strain patterns.

A) Septal (black line), LV free wall (red line), and RV free wall (blue line) strain patterns from a CRT responder (left) and non-responder (right) with RV dysfunction. Responder: RVFAC 72.4%, SRS_{sept} 13.8%, LVEF 14%, Δ LVESV -55.6%. Non-responder: RVFAC 24.6%, SRS_{sept} 8.6%, LVEF 12%, Δ LVESV +7.5%. B) and C) show septal (black lines), LV (dashed lines), and RV (dotted lines) strain patterns from virtual patients with reduced LV (B) or RV (C) contractility. The corresponding LV or RV contractility for each virtual patient is shown above the strain pattern. Septal strain patterns were sensitive to decreases in LV but not RV contractility. Arrows denote direction of decreasing contractility. CRT: cardiac resynchronization therapy, LV: left ventricular, RV: right ventricular, FW: free wall, SRS_{sept}: septal systolic rebound stretch, Δ LVESV: change in LV end-systolic volume after CRT.

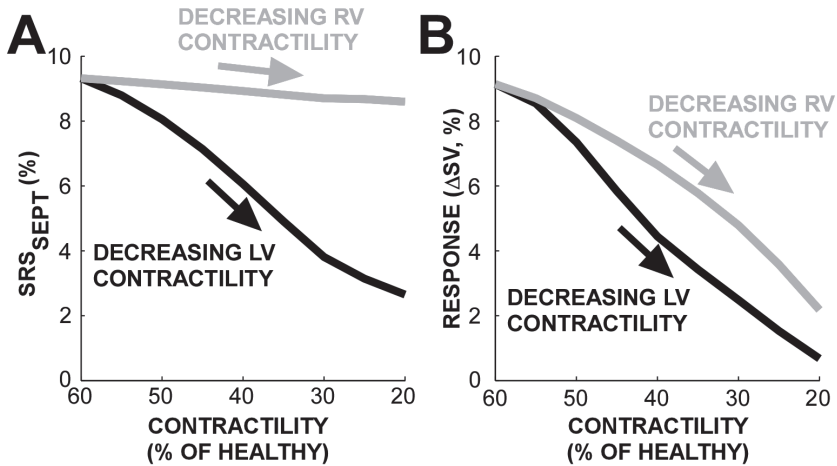


FIGURE 4. Effect of LV and RV contractility on mechanical dyssynchrony parameters in all virtual patients.

A) SRS_{sept} decreased in the virtual patients with decreased LV contractility (black line) but not in the virtual patients with decreased RV contractility (red line). B) Both the virtual patients with decreased LV (black line) and RV (red line) contractility had a decreased response to CRT. A mismatch can be observed between SRS_{sept} and CRT response in virtual patients whose RV contractility is low (red lines). CRT: cardiac resynchronization therapy, LV: left ventricular, RV: right ventricular, SRS_{sept}: septal systolic rebound stretch, SV: stroke volume.

EFFECT OF LV AND RV CONTRACTILITY ON CRT RESPONSE

In the virtual patients, reductions in both LV and RV contractility affected CRT response when an LBBB-like activation pattern was present at baseline (figure 4B). Deteriorating LV contractile function led to a decrease in the acute response to CRT from a 9.1%ΔSV with 60% LV contractility down to 0.7% when LV contractility was 20%. Comparable decreases in acute response were also seen in the simulations as RV contractility deteriorated, from a 9.1%ΔSV with RV contractility at 60% of normal down to 2.2% with an RV contractility of 20%. Comparing figure 4A and figure 4B, a mismatch between SRS_{sept} and acute response occurs when RV contractility is low, despite the presence of an appropriate LV substrate for CRT.

DISCUSSION

This study demonstrates that commonly used mechanical dyssynchrony parameters are not associated with CRT response when RV dysfunction is present. Incorporating RV function (i.e. RVFAC) with mechanical dyssynchrony in multivariate analysis improved the association with CRT response. Computer simulations demonstrated that both LV and RV myocardial dysfunction could reduce acute response to CRT. However, whereas LV contractility changes had congruent effects on dyssynchrony and CRT response, RV contractility changes hardly affected mechanical dyssynchrony. This discrepancy potentially creates a mismatch between mechanical dyssynchrony and CRT response. Therefore, response prediction using mechanical dyssynchrony parameters should be approached cautiously in patients with a dysfunctional RV. These findings emphasize the complexity of predicting CRT response and may have important implications for improvements in patient selection for CRT.

INTERACTION OF LV AND RV FUNCTION AND THEIR EFFECT ON CRT OUTCOME

In the current study population, worse baseline LV and RV function were associated with less reverse remodelling following CRT. The effects of LV and RV function on outcome are likely to be both independent effects and effects interacting with CRT. LV function was more severely reduced in patients with RV dysfunction as compared to patients with preserved RV function. RV dysfunction is known to be an important predictor of adverse prognosis in patients with both moderate and advanced heart failure.^{8,9} The same adverse prognostic effect has also been demonstrated for CRT patients with advanced (i.e. NYHA III-IV) heart failure,⁵ although a recent meta-analysis showed no effect of RV function parameters on changes in LVEF.¹⁴ In the meta-analysis of Sharma et al., RVFAC remained the strongest RV function metric for predicting volumetric response after CRT as measured by change in LVEF, and was only borderline statistically non-significant.¹⁴ The use of LVEF as outcome parameter might be a cause for discrepancy with our results. Although both LVEF and LVESV reflect changes in volumes, LVESV might have a different relation with RVFAC. The evidence is also inconclusive for CRT patients with mild heart failure.^{6,19}

The computer simulations support the hypothesis that a very weak LV is intrinsically less able to benefit from resynchronization despite the presence of an appropriate LV conduction delay.^{17,20} In the clinical situation severe adverse remodelling of the LV, which

may be irreversible, may compound this effect. The computer simulations also highlight a potential role for reduced RV contractility in limiting CRT response. In LBBB, LV myofibre work makes a large contribution to RV pump work through ventricular interaction, and CRT redistributes myofibre work from the LV free wall to the septum and RV.¹¹ As shown by our simulations, reduced RV contractility leads to reduced mechanical support from the RV after CRT and reduces LV filling, giving less improvement in LV stroke volume. It is probable that a combination of the LV and RV effects described above is responsible for the reduction in response observed in the RV dysfunction patient subgroup. The adverse effect of pacing on RV function may also be more significant in an already enlarged RV due to increased RV desynchronization following CRT.²¹

After six months of CRT, mean RV size increased and RV function slightly decreased in patients with relatively preserved baseline RV function. The increase in RV volume may represent a mild RV dysfunction induced by RV pacing. Conversely, RV function parameters tended to improve in patients with RV dysfunction, which may indicate a chronic reduction in RV afterload following resynchronization that is not represented by our acute simulations.²² Consequently, RV function following CRT in the long term is likely to be a balance between induced myocardial dysfunction and reduced afterload.

WHY DOES RV DYSFUNCTION COMPLICATE RESPONSE PREDICTION?

The dyssynchrony parameters we studied were not associated with reverse remodelling within the RV dysfunction subgroup. RV dysfunction can affect the association between CRT response and mechanical dyssynchrony parameters through two potential mechanisms, as found by the computer simulations. Firstly, RV failure can be aggravated by severely reduced LV function through pulmonary congestion and increases in RV afterload. In this situation both CRT response and mechanical dyssynchrony parameters will be reduced despite an LV conduction delay, giving a correct prediction of reduced response. The declining response to CRT with reduced LV contractility despite a constant conduction delay emphasizes the importance of LV mechanics for determining CRT response.^{17, 23, 24} However, in cases where RV myocardial function is compromised, CRT response may be reduced in a manner that is not reflected by the mechanical dyssynchrony parameters we tested. Secondly, severely reduced RVFAC in CRT candidates is a marker of both severe RV and LV dysfunction. Accordingly, we observed lower values of SRS_{sept} in the patients with RV dysfunction, reflecting the associated reduction in LV function in these patients. The higher prevalence

of Type III deformation patterns in this subgroup supports this relationship as this pattern indicates reduced LV contractility due to weakness of the lateral wall preventing septal stretch from occurring during systole (figure 3B).^{17,25} We did not observe a reduction in the other dyssynchrony parameters, emphasizing the ability of SRSsept to reflect LV contractility. The association of SRSsept with CRT response was comparable to earlier studies,^{15,17} and strongest in patients without RV dysfunction. However, as CRT response is multifactorial and influenced by for example implantation technique, therapy delivery, aetiology of heart failure and comorbidities, a considerable amount of scatter is still visible in the association between SRSsept and LVESV reduction (figure 2). Simulations suggest that the fact that all dyssynchrony parameters lost their association with CRT response in patients with RV dysfunction, reflects the inadequate representation of reduced RV contractility by these parameters. Therefore, the association with response was improved by adding a parameter influenced by RV contractility (i.e. RVFAC). Because the effects of RV function on CRT-outcome are likely to be more prominent in cases with relatively preserved LV function, adding information on LV function also improved the association with response, but to a lesser extent.

CLINICAL IMPLICATIONS

Our results indicate that RV function should be routinely quantified in all patients before CRT. If baseline RV function is reduced (RVFAC <35%), less LV remodelling should be expected after CRT. If RV function is significantly reduced, prediction of CRT response by the mechanical dyssynchrony parameters evaluated in this study should be interpreted cautiously. Although patients with RV dysfunction can benefit from CRT,⁵ our simulations suggest that the idea of refraining from CRT in some patients with severely impaired RV contractility merits further investigation. The study was underpowered to define a specific threshold for RV dysfunction to predict CRT response and further clinical studies are needed to address this issue prospectively. As RV dysfunction is present in a considerable number of CRT candidates our findings also clarify some of the difficulties of incorporation of mechanical dyssynchrony measurements into daily clinical practice. Our findings should lead to more effective implementation of dyssynchrony parameters. Further research on the underlying mechanisms should improve understanding and implementation of existing parameters.

LIMITATIONS

We only used longitudinal strain, as of three myocardial strain directions (i.e. circumferential, radial and longitudinal) it is the only suitable direction for assessment of RV function. Moreover, longitudinal strain has been standardized recently and is therefore best reproducible.²⁶ Although a segment-based approach might incorporate additional information, the current approach of global wall strain was chosen because it provides a more robust measurement and introduces less noise in the analyses.²⁷ The choice for RVFAC as the clinical parameter to reflect RV function was beneficial, since it had the strongest association with LV remodelling (table 3). However, echocardiographic measurement of RV function is complicated and it is unclear which parameter best reflects RV function in the presence of dyssynchrony. Dyssynchrony might influence functional parameters such as TAPSE and to a lesser extent RVFAC and RV strain, as apical rocking due to dyssynchronous LV contraction may also influence RV displacement. Our patient and simulated strain data (figure 3) are consistent with this hypothesis as both demonstrate abnormal RV free wall strain patterns in dyssynchronous hearts. current study is also an explorative study, and numbers were too small to perform sub analyses to identify factors that determine response in patients with RV dysfunction. Multivariate analysis was limited to a subset of best-performing parameters due to the population size. The study was underpowered to investigate the effect of smaller subgroups, such as the presence of atrial fibrillation. The findings should therefore be confirmed in larger prospective studies.

Computer simulations were performed with global contractility reduction in either the RV or LV. Regional variations in myocardial properties that may arise due to scarring or regional ischemia were not considered.¹⁸ Mitral regurgitation, which can exacerbate backwards failure, was not included in the simulations. CRT response in the simulations was assessed by acute hemodynamic changes, as opposed to long-term structural remodelling as was used in the patient population. Acute hemodynamic response does not capture all of the potential mechanisms through which CRT exerts its longer term benefits on cardiac structure, metabolism and function.²³ Furthermore, patients with RV dysfunction had worse heart failure and more severe comorbidities than the patients without RV dysfunction. Consequently, we do not exclude the possibility that other factors than RV and/or LV myocardial function are limiting response in these patients. As measuring intrinsic RV function remains challenging, our simulation results must be considered as hypothesis-generating only.

CONCLUSION

Commonly-used mechanical dyssynchrony parameters are not associated with volumetric response in CRT patients with RV dysfunction, because these parameters do not adequately reflect the impact of RV dysfunction on CRT response. RV function parameters should therefore be incorporated when predicting CRT response based on mechanical dyssynchrony.

REFERENCES

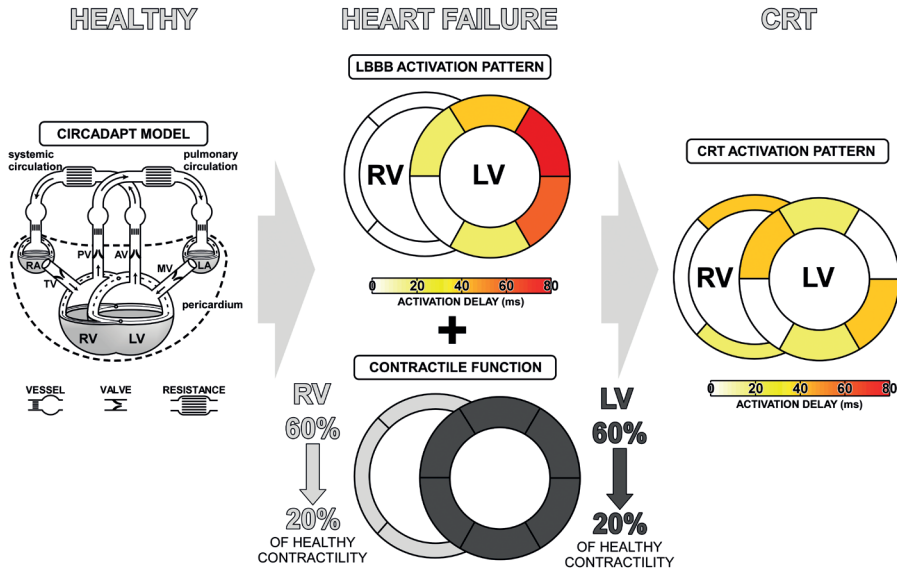
1. Abraham WT, Fisher WG, Smith AL, DeLurgio DB, Leon AR, Loh E, et al. Cardiac resynchronization in chronic heart failure. *N Engl J Med*. 2002;346:1845-1853.
2. Cleland JG, Daubert JC, Erdmann E, Freemantle N, Gras D, Kappenberger L, et al. The effect of cardiac resynchronization on morbidity and mortality in heart failure. *N Engl J Med*. 2005;352:1539-49.
3. Prinzen FW, Vernooy K, De Boeck BW, Delhaas T. Mechano-energetics of the asynchronous and resynchronized heart. *Heart Fail Rev*. 2011;16:215-24.
4. Chung ES, Leon AR, Tavazzi L, Sun JP, Nihoyannopoulos P, Merlino J, et al. Results of the Predictors of Response to CRT (PROSPECT) trial. *Circulation*. 2008;117:2608-16.
5. Damy T, Ghio S, Rigby AS, Hittinger L, Jacobs S, Leyva F, et al. Interplay between right ventricular function and cardiac resynchronization therapy: an analysis of the CARE-HF trial (Cardiac Resynchronization-Heart Failure). *J Am Coll Cardiol*. 2013;61:2153-60.
6. Kjaergaard J, Ghio S, St John Sutton M, Hassager C. Tricuspid annular plane systolic excursion and response to cardiac resynchronization therapy: results from the REVERSE trial. *J Card Fail*. 2011;17:100-7.
7. Tabereaux PB, Doppalapudi H, Kay GN, McElderry HT, Plumb VJ, Epstein AE. Limited response to cardiac resynchronization therapy in patients with concomitant right ventricular dysfunction. *J Cardiovasc Electrophysiol*. 2010;21:431-5.
8. Di Salvo TG, Mathier M, Semigran MJ, Dec GW. Preserved right ventricular ejection fraction predicts exercise capacity and survival in advanced heart failure. *J Am Coll Cardiol*. 1995;25:1143-53.
9. de Groote P, Millaire A, Foucher-Hossein C, Nogue O, Marchandise X, Ducloux G, et al. Right ventricular ejection fraction is an independent predictor of survival in patients with moderate heart failure. *J Am Coll Cardiol*. 1998;32:948-54.
10. Lumens J, Arts T, Broers B, Boomars KA, van Paassen P, Prinzen FW, et al. Right ventricular free wall pacing improves cardiac pump function in severe pulmonary arterial hypertension: a computer simulation analysis. *Am J Physiol Heart Circ Physiol*. 2009;297:H2196-205.
11. Lumens J, Ploux S, Strik M, Gorcsan J, 3rd, Cochet H, Derval N, et al. Comparative electromechanical and hemodynamic effects of left ventricular and biventricular pacing in dyssynchronous heart failure: electrical resynchronization versus left-right ventricular interaction. *J Am Coll Cardiol*. 2013;62:2395-403.

12. Walmsley J, Arts T, Derval N, Bordachar P, Cochet H, Ploux S, et al. Fast Simulation of Mechanical Heterogeneity in the Electrically Asynchronous Heart Using the MultiPatch Module. *PLoS Comput Biol*. 2015;11:e1004284.
13. Lang RM, Badano LP, Mor-Avi V, Afilalo J, Armstrong A, Ernande L, et al. Recommendations for cardiac chamber quantification by echocardiography in adults: an update from the American Society of Echocardiography and the European Association of Cardiovascular Imaging. *J Am Soc Echocardiogr*. 2015;28:1-39 e14.
14. Sharma A, Bax JJ, Vallakati A, Goel S, Lavie CJ, Kassotis J, et al. Meta-Analysis of the Relation of Baseline Right Ventricular Function to Response to Cardiac Resynchronization Therapy. *Am J Cardiol*. 2016;117:1315-21.
15. De Boeck BW, Teske AJ, Meine M, Leenders GE, Cramer MJ, Prinzen FW, et al. Septal rebound stretch reflects the functional substrate to cardiac resynchronization therapy and predicts volumetric and neurohormonal response. *Eur J Heart Fail*. 2009;11:863-71.
16. Leenders GE, De Boeck BW, Teske AJ, Meine M, Bogaard MD, Prinzen FW, et al. Septal rebound stretch is a strong predictor of outcome after cardiac resynchronization therapy. *J Card Fail*. 2012;18:404-12.
17. Leenders GE, Lumens J, Cramer MJ, De Boeck BW, Doevendans PA, Delhaas T, et al. Septal deformation patterns delineate mechanical dyssynchrony and regional differences in contractility: analysis of patient data using a computer model. *Circ Heart Fail*. 2012;5:87-96.
18. Lumens J, Tayal B, Walmsley J, Delgado-Montero A, Huntjens PR, Schwartzman D, et al. Differentiating Electromechanical From Non-Electrical Substrates of Mechanical Discoordination to Identify Responders to Cardiac Resynchronization Therapy. *Circ Cardiovasc Imaging*. 2015;8:e003744.
19. Campbell P, Takeuchi M, Bourgoun M, Shah A, Foster E, Brown MW, et al. Right ventricular function, pulmonary pressure estimation, and clinical outcomes in cardiac resynchronization therapy. *Circ Heart Fail*. 2013;6:435-42.
20. Vidal B, Delgado V, Mont L, Poyatos S, Silva E, Angeles Castel M, et al. Decreased likelihood of response to cardiac resynchronization in patients with severe heart failure. *Eur J Heart Fail*. 2010;12:283-7.
21. Varma N, Jia P, Ramanathan C, Rudy Y. RV electrical activation in heart failure during right, left, and biventricular pacing. *J Am Coll Cardiol Img*. 2010;3:567-75.

22. Stolfo D, Tonet E, Merlo M, Barbati G, Gigli M, Pinamonti B, et al. Early right ventricular response to cardiac resynchronization therapy: impact on clinical outcomes. *Eur J Heart Fail.* 2016;18:205-13.
23. Lumens J, Leenders GE, Cramer MJ, De Boeck BW, Doevendans PA, Prinzen FW, et al. Mechanistic evaluation of echocardiographic dyssynchrony indices: patient data combined with multiscale computer simulations. *Circ Cardiovasc Imaging.* 2012;5:491-9.
24. Tayal B, Sogaard P, Delgado-Montero A, Goda A, Saba S, Risum N, et al. Interaction of Left Ventricular Remodeling and Regional Dyssynchrony on Long-Term Prognosis after Cardiac Resynchronization Therapy. *J Am Soc Echocardiogr.* 2017;30:244-250.
25. Marechaux S, Guiot A, Castel AL, Guyomar Y, Semichon M, Delelis F, et al. Relationship between two-dimensional speckle-tracking septal strain and response to cardiac resynchronization therapy in patients with left ventricular dysfunction and left bundle branch block: a prospective pilot study. *J Am Soc Echocardiogr.* 2014;27:501-11.
26. Farsalinos KE, Daraban AM, Unlu S, Thomas JD, Badano LP, Voigt JU. Head-to-Head Comparison of Global Longitudinal Strain Measurements among Nine Different Vendors: The EACVI/ASE Inter-Vendor Comparison Study. *J Am Soc Echocardiogr.* 2015;28:1171-1181, e2.
27. Lumens J, Prinzen FW, Delhaas T. Longitudinal Strain: "Think Globally, Track Locally". *J Am Coll Cardiol Img.* 2015;8:1360-3.

Echocardiographic prediction of cardiac resynchronization therapy response requires analysis of both mechanical dyssynchrony and right ventricular function

SUPPLEMENTAL MATERIAL



SUPPLEMENTAL FIGURE 1. Background information on the CircAdapt simulations

Overview of the CircAdapt model (HEALTHY), consisting of the systemic and pulmonary circulations, mechanically interacting ventricles, atria, and the cardiac valves. The activation pattern and global contractility patterns used for the HEART FAILURE simulations are shown in the middle. The LV and RV cavities were also dilated by 10% to represent eccentric remodelling. The ventricular activation pattern used when simulating CRT is shown on the right. AV: aortic valve, MV: mitral valve, LA: left atrium, LV: left ventricle, PV: pulmonary valve, RA: right atrium, RV: right ventricle, TV: tricuspid valve. CRT: cardiac resynchronization therapy. The left-hand panel is modified from Lumens J, Delhaas T, Kirn B, Arts T. *Ann Biomed Eng.* 2009 Nov;37(11):2234-55.

SUPPLEMENTAL METHODS

HEALTHY CONTROL SIMULATION

In this study, we used the contraction model from Leenders et al¹ with the addition of the ability to sub-divide the ventricular walls into patches as described by Walmsley et al.² All of our simulations began from a baseline healthy simulation with no reduction in contractility or conduction delay. This baseline healthy situation simulation was arrived at through the adaptation of size, mass, and passive tissue stiffness of the vascular and cardiac walls. The adaptation process normalizes the local mechanical load on cardiac and vascular tissue to tissue-specific physiological levels.^{3,4} In normal, healthy physiology, the cardiovascular system is not operating at its maximum capacity during rest, but instead remodels in response to load under challenges such as exercise. Adaptation is therefore performed in a state of moderate exercise. We assumed a resting heart rate of 71bpm. At rest, a cardiac output of 5.1L/min and mean arterial pressure were maintained at 92mmHg through alterations in systemic vascular resistance and circulating blood volume. During the adaptation process, moderate exercise was simulated by tripling the cardiac output and doubling the heart rate, with mean arterial pressure maintained at 92mmHg. The methodology used for adaptation of tissue is described in detail by Arts et al.⁴ No further tissue adaptation was performed during the heart failure simulations. Only hemodynamic changes due to homeostatic control at rest to maintain cardiac output and mean arterial pressure are shown in those simulations.

SIMULATION CODE

The version of the CircAdapt model presented by Walmsley et al. is freely available to download from www.circadapt.org. To reproduce the results in this paper using the downloadable version, you will need to change the following lines in the file SarcEf2Sf.m prior to adaptation:

```
Line 36      tA = (0.74+0.3*L)*TimeAct;  
Line 37      tR = 0.45*TR*TimeAct;  
Line 38      tD = 0.3*TD*TimeAct;
```

The parameter tA represents the duration of myocardial contraction in the CircAdapt model. This line determines the dependence of this duration on the extension of the sarcomeres. tR is a time constant that scales the time taken for a ventricular segment to reach maximum

activation. tD is a time constant that scales the time taken for a ventricular segment to relax from maximum activation.

In PRef.mat, the parameter SfAct should be changed from 100kPa to 120kPa in the ventricular wall segments only (see the field P.Patch.SfAct). The parameter SfAct represents the contractility referred to in the main article and supplemental figure 1. Further description of the sarcomere model in CircAdapt can be found in supplemental reference 2 and the accompanying supplemental material.

SUPPLEMENTAL REFERENCES

1. Leenders GE, Lumens J, Cramer MJ et al. Septal deformation patterns delineate mechanical dyssynchrony and regional differences in contractility: Analysis of patient data using a computer model. *Circ Heart Fail.* 2012;5:87-96.
2. Walmsley J, Arts T, Derval N et al. Fast simulation of mechanical heterogeneity in the electrically asynchronous heart using the MultiPatch module. *PLoS Comput Biol* 2015;11:e1004284.
3. Arts T, Delhaas T, Bovendeerd P et al. Adaptation to mechanical load determines shape and properties of heart and circulation: the CircAdapt model. *Am J Physiol Heart Circ Physiol* 2005;288:H1943-54.
4. Arts T, Lumens J, Kroon W, Delhaas T. Control of whole heart geometry by intramyocardial mechano-feedback: a model study. *PLoS Comput Biol.* 2012 Feb;8(2):e1002369.

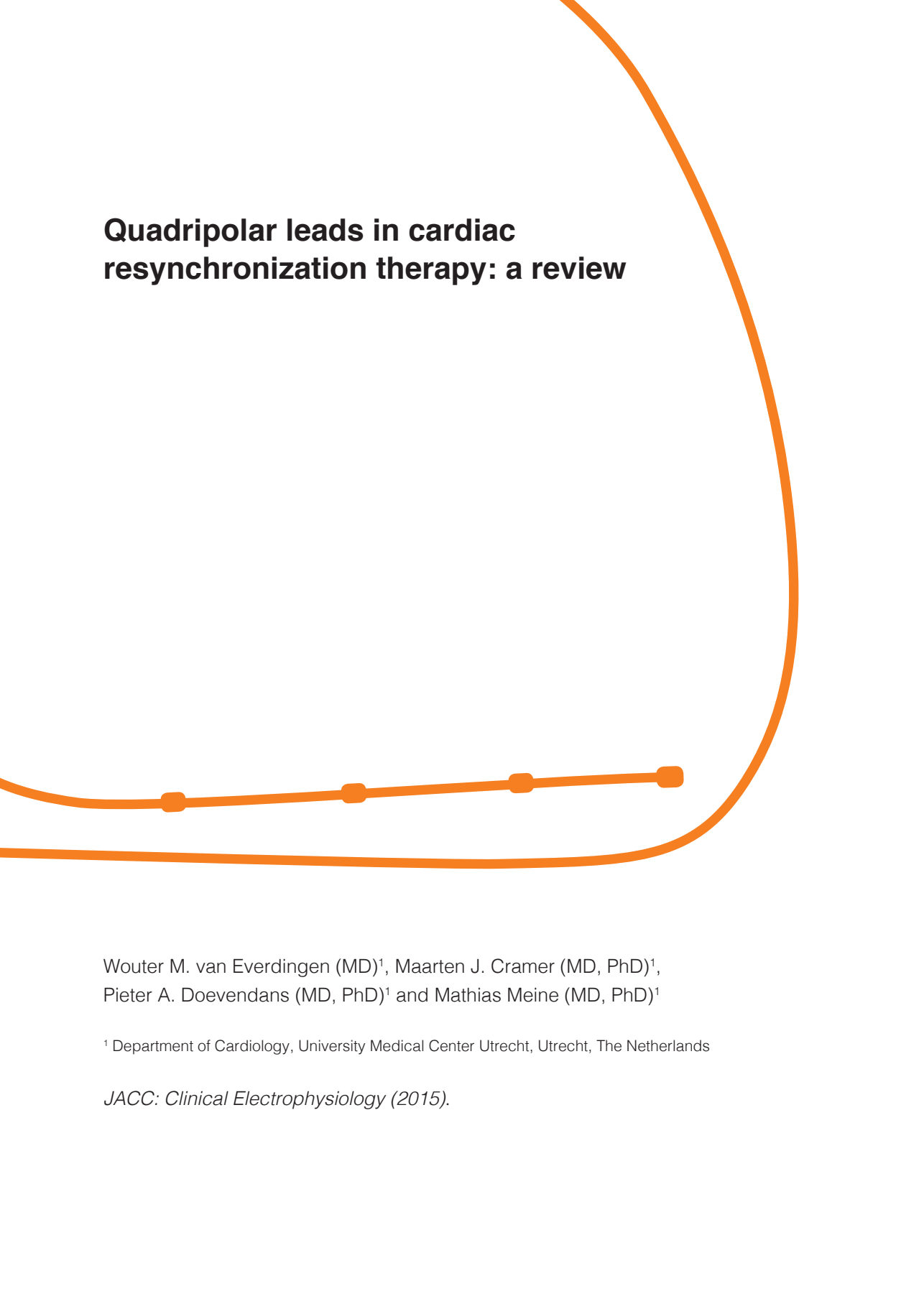


PART III

QUADRIPOlar LEFT VENTRICULAR LEADS





A thick orange line starts from the top right, curves down and left, then curves back up and right, forming a large, open shape that frames the title. A horizontal orange line with four square markers is positioned below the title.

Quadripolar leads in cardiac resynchronization therapy: a review

Wouter M. van Everdingen (MD)¹, Maarten J. Cramer (MD, PhD)¹,
Pieter A. Doevendans (MD, PhD)¹ and Mathias Meine (MD, PhD)¹

¹ Department of Cardiology, University Medical Center Utrecht, Utrecht, The Netherlands

JACC: Clinical Electrophysiology (2015).

ABSTRACT

Despite the benefit of cardiac resynchronization therapy (CRT) to patients with heart failure and conduction delay, a substantial part of patients do not respond substantially. Left ventricular lead position is an important factor in response, restricted by patient specific anatomy and local pathophysiology. Quadripolar leads could enhance response to CRT, offering four pacing locations along the distal end of the lead. Several quadripolar leads are available, all with different shapes and electrode spacing. Electrodes can be positioned in an ideal pacing location, determined by delayed mechanical or electrical activation, and away from phrenic nerve stimulation, high pacing thresholds, and fibrosis. Implantation is safe, with comparable or even lower complication rates compared to standard bipolar leads. Studies on biventricular pacing with quadripolar leads show apparent variations in acute hemodynamic response between pacing configurations, implying a patient specific response. Pacing with an optimal pacing vector of a quadripolar lead benefits acute hemodynamic response. Multipoint pacing (MPP), pacing the LV with two out of four electrodes, could further enhance response. However, larger trials are needed to confirm these results. Results on long-term outcome of CRT with quadripolar leads and the benefit of MPP are warranted. We conclude that quadripolar leads are an important improvement in the treatment of heart failure patients with CRT.

INTRODUCTION

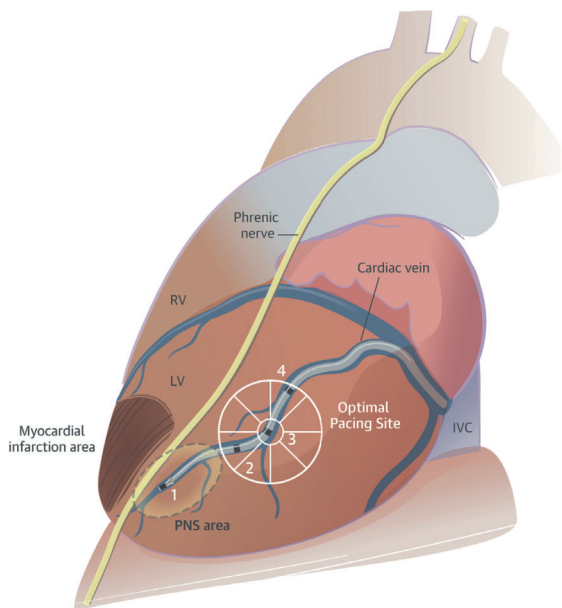
Cardiac resynchronization therapy (CRT) has proven its benefit for a selection of heart failure patients, reducing mortality and morbidity, according to renewed guidelines.^{1,2} CRT improves prognosis in patients with dilated cardiomyopathy, by inducing reverse remodeling through electromechanical resynchronization. Unfortunately a considerable proportion of patients (approximately 30-40%) show no significant response on CRT.¹ Suboptimal LV lead position is an important factor for diminished CRT response.³ Besides targeting of the posterolateral wall and avoiding apical segments, the optimal position depends on several patient specific factors.^{4,5} Even if the ideal pacing location is known, lead placement in or near this location is difficult.

Formerly, only unipolar and bipolar leads were available for transvenous epicardial LV pacing, with two electrodes are placed at the tip of the lead. These leads need to be wedged in a distal vessel, or actively fixed by dedicated systems. The anatomy of the coronary sinus (CS) and its side branches, lead instability, local pacing parameters, and phrenic nerve stimulation (PNS) could restrict lead placement. Options to overcome suboptimal positioning are available (thoroscopic placement) or emerging, such as endocardial pacing, implantation of multiple LV leads and quadripolar leads.

Quadripolar left ventricular leads have four electrodes along the distal end. These leads can pace the LV wall, via transvenous access, at several locations and multiple vectors along the lead. Optimal pacing sites (i.e. the latest mechanical or electrical activated region) could more easily be reached, during and even after implantation. Suboptimal sites can be avoided, such as areas with fibrosis due to myocardial infarction or areas with PNS (central illustration). These properties come without compromising lead stability, as the tip can be wedged in a distal part of the vein while other electrodes are placed near the optimal pacing site. Moreover, quadripolar LV leads have the ability of multipoint pacing (MPP), pacing the LV with two out of four available electrodes. Quadripolar leads therefore reinforce the discussion about optimal pacing sites, multisite pacing, and timing optimization, because a single quadripolar lead can offer multiple pacing options. This article reviews background information, recent developments, and future implications about optimizing CRT with a quadripolar lead.

Based on a systematically search in BioMedCentral, Cochrane Library, and PubMed all relevant articles in English about CRT and quadripolar leads published between December

2000 and May 2015 were selected. Further studies were sought by means of a manual search of secondary sources, including references from primary articles. All studies and trials on multipolar and quadripolar leads, regarding acute, short- and long-term results were regarded relevant. Furthermore, technical specifications of current quadripolar leads and delivery systems were sought on manufacturers' websites or by communication with their representatives.



CENTRAL ILLUSTRATION

Central illustration. Graphical representation of a heart, viewed from the lateral side. A quadripolar lead is wedged in a distal cardiac vein. Electrode 1 is close to an area of phrenic nerve stimulation and an area of myocardial infarction, while 2, 3 and 4 are positioned near the optimal pacing site. The latter possibly defined by electro-anatomical mapping or speckle tracking echocardiography. LV: left ventricle, PNS: phrenic nerve stimulation, RV: right ventricle, VCI: vena cava inferior.

DESIGN OF QUADRIPOLE LEADS

Several quadripolar leads have been developed with various shapes (figure 1) and electrode spacing (figure 2). Boston Scientific (St. Paul, MA, USA) offers three different leads with different curvature and different electrode spacing. Biotronik (Berlin, Germany) and Medtronic Inc. (Minneapolis, MN, USA) offer leads with different curvatures but similar

electrode spacing. St. Jude Medical (St. Paul, MN, USA) has one option available. Straight leads are designed for smaller distal veins, while curved leads are meant to be fixated in larger veins. Positioned in a target vessel, practical electrode spacing of these leads may be smaller. Total and effective inter-electrode distance can be of importance. However never documented, the total electrode spacing may overextend the target vessel, resulting in proximal electrodes positioned in the coronary sinus or great cardiac vein, instead of one of the tributary veins. Moreover, a pre-shaped lead design may improve positioning of proximal electrodes, which is offered by all manufacturers (figure 1). Pre-shaped leads therefore improve functionality, as unstable position in the larger cardiac veins could increase the distance to the myocardium, resulting in high pacing thresholds. A short (inter-electrode) distance diminishes the benefit of extra electrodes, as electrodes could still cause PNS or be placed on scar tissue. Although the position of the second and third electrode of the Attain Performa leads of Medtronic (1.3mm apart) were chosen because of lower PNS thresholds at small inter-electrode distances.⁶ Although there are four pacing sites, electromechanically only three separate spots can be stimulated with this lead. Moreover, in case of high pacing thresholds of the proximal electrode (e.g. due to vessel diameter), only two functionally different bipolar vectors can be used. Two leads of Boston Scientific have the same limitation, as three proximal electrodes are positioned close together. Due to the spiral shape, at least one electrode should be placed close to the myocardium, while others may become unusable.

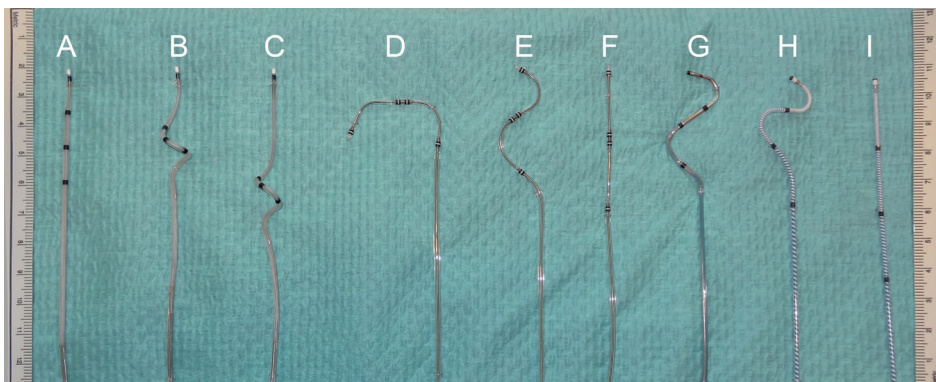


FIGURE 1. Overview of currently available quadripolar leads

Photographic overview of current quadripolar leads, with respect to curvature. Boston Scientific; Acuity X4 (A: Straight, B: Spiral S and C: Spiral L). Medtronic; Attain Performa (D: 4298, E: S 4598, F: S 4398), St. Jude Medical; G: Quartet 1458Q. Biotronik; H: Sentus, I: Sentus straight.

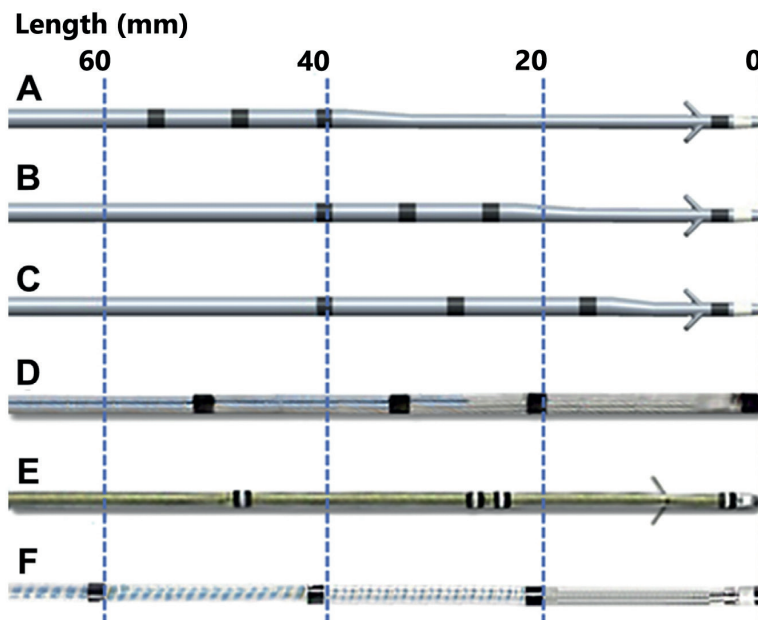


FIGURE 2. Electrode spacing of quadripolar leads

Graphical presentation of electrode spacing of current options of quadripolar leads. Boston Scientific; A: Acuity X4 Spiral L, B: Acuity X4 Spiral S and C: Acuity X4 Straight. St. Jude Medical; D: Quartet. Medtronic; E: Attain Performa (4298, 4398, S 4598) and Biotronik; F: Sentus.

The manufacturers also differ in the location of corticosteroid on quadripolar leads. The leads of Medtronic have steroid reservoirs near all four electrodes. Both Biotronik leads have a corticosteroid coating on the entire lead with a steroid reservoir at the tip. Boston Scientific and St. Jude Medical supply leads with steroid reservoirs at the tip of the lead. Beside small and clinically irrelevant differences found in a small animal study,⁷ the effect of steroid on the long-term performance of transvenous LV leads is unknown. Steroid is especially beneficial for the long-term impedance of screw-in leads.

All leads should fit through a 7 French (F) introducer, however not all leads are compatible with a 5F inner guide as most are wider (maximal width of: Botrionik: 4.8F, St. Jude Medical; 5.1F, Medtronic; 5.3F and Boston Scientific; 5.2F). Although leads are coated and therefore compatible with the inner guide for smooth introduction, the electrodes aren't coated and may cause friction.

As all manufacturers have IS-4 compatible devices, all combinations of quadripolar leads and dedicated devices can be used. However two cases have shown that problems may arise when using quadripolar leads and CRT-D devices of different manufacturers, resulting in unacceptable high impedance levels at the three proximal quadripolar electrodes.⁸ The high impedance is probably a result of misalignment of these electrodes within the spring contacts in the connector block of the device.⁸ This issue needs to be resolved, so that operators can select the preferred (quadripolar) lead for the target vessel and optimal pacing location, independent of the chosen device.

IMPLANTATION AND LONG-TERM USE

Implantation and long-term use of quadripolar leads seems safe.⁹ Quadripolar leads have a lower complication rate compared to conventional bipolar leads (table 1).^{9, 10} Even in cases of minor dislocation, alternative pacing vectors may be selected, circumventing the need for a secondary invasive procedure and thereby reducing complications.¹¹ Although Behar et al. even found a lower all-cause mortality rate in patients with quadripolar leads compared to bipolar leads, their results are based on a registry: a comparison of non-randomized cohorts.⁹ Selection bias could have driven results, as baseline characteristics show that the percentage of patients with ischemic cardiomyopathy and patients not in sinus rhythm were higher in the group with bipolar leads. Both are associated with reduced response to CRT.^{12, 13} Moreover, simple baseline characteristics as baseline and follow-up ejection fraction and end-systolic volumes, NYHA class, QRS-width and –morphology are unknown. Comparison of both groups is therefore difficult. Nevertheless, results are interesting (table 1), as a reduced mortality is compelling for full implementation in clinical practice. Unfortunately, most studies focus solely on the quadripolar leads, without comparison to bipolar leads. Moreover, most used either the quadripolar lead of St. Jude Medical or Medtronic, while performance of other leads has received little attention.^{9-11, 14-16} Results of the MORE-CRT trial, a randomized comparison of quadripolar vs. bipolar leads on performance and outcome, are therefore warranted.

TABLE 1. Studies on performance and complications of CRT with a quadripolar LV lead.

First author	Design	N	Subjects (n)	Type of quadripolar lead	Follow-up (mean in months)	Successful implantation	Complications	Repositioning lead	Lead displacement	PNS requiring lead revision
Behar ⁹	Registry/cohort. Multicenter	721	Quadripolar (n=357) vs. bipolar leads (n=364)	Quartet SJM (n=706), Attain Medtronic (n=15)	28.8	96.1 vs. 95.1% p=0.51	* 2.0 vs. 5.2% p=0.03	1.7 vs. 4.6% p=0.03	0 vs. 4.4% p<0.001	
Arias ¹⁰	Prospective single center	42	Quadripolar (n=21) vs. bipolar leads (n=21)	Quartet SJM	9	100 vs. 100%	LV lead problems: 42.9 vs. 23.8%, p<0.05	4.8 vs. 9.5% p=1.0	0 vs. 0%	
Crossley ¹¹	Prospective multicenter	1124	Quadripolar only	Attain Medtronic	6.6	97.6%	3%	0.4%	0.3%	
Forleo ¹⁵	Prospective multicenter	154	Quadripolar only	Quartet SJM	15.3	97.4%	* 2.7%	2.7%	0%	
Mehta ¹⁶	Prospective single center	40	Quadripolar only	Quartet SJM	6	95%	* 4.3%	3%	0%	
Sperzel ¹⁴	Prospective multicenter	75	Quadripolar only	Quartet SJM	15	94.6%	4.3%	4.3%	0%	

Published studies on performance and complications of CRT with a quadripolar LV lead. CMP: cardiomyopathy, Attain Medtronic: Attain Performa lead (Medtronic Ltd.), PNS: phrenic nerve stimulation, Quartet SJM: 1458Q, Quartet (St. Jude Medical). *: no percentage of all complications known, complications are divided into lead displacement and PNS requiring lead revision.

TABLE 2. Studies on comparison of response to CRT with a quadripolar LV lead (alternative vector or multipoint pacing) to conventional biventricular pacing.

First author	Design	n	Pacing configuration	Parameter(s)	Main result	Remarks
Jones ³⁶	Intra-operative	22	BIQ	Bioreadance measurement: CI	Large variations between BIQ electrodes within veins	Fixed AV delay
Asbach ³⁷	Intra-operative	16	BIQ vs. CONV	dP/dt _{max}	BIQ improves AHR: 31.3 vs. 28.2%, p<0.001	1 optimized AV delay per patient
Thibault ³⁹	Intra-operative	19	MPP vs. CONV	dP/dt _{max}	MPP with proximal and distal electrode: greatest benefit	1 optimized AV delay per patient
Pappone ⁴¹	Intra-operative	42	MPP vs. BIQ	SW (pressure-volume loops) and dP/dt _{max}	MPP improves AHR, SW: 27.2 vs. 19.4%, p=0.018, dP/dt: 15.9 vs. 13.5%, p<0.001	2 BIQ vs. 7 MPP settings, Fixed AV delay
Zanon ⁴²	Intra-operative	29	MPP vs. CONV	dP/dt _{max}	Average increase of best site with MPP (1231 ±267 mmHg/s) higher than CONV (1200 ±267 mmHg/s)	Fixed AV delay, multiple veins per patient
Cabrera Bueno ⁴⁷	Post-implantation	51	BIQ vs. CONV	Echo: CO	BIQ improves CO: 4.33 vs. 4.16l/min, p=.058	Optimized AV delay for each setting
Osca ³⁵	Post-implantation	27	BIQ vs. CONV	Trans thoracic impedance electrocardiography: CI, CO and SV	No significant difference BIQ & CONV	Optimized AV delay for each setting
Rinaldi ⁴⁰	Post-implantation	40	MPP vs. CONV	Echo, STE: peak radial strain CW-Doppler: VTI of LVOT	MPP increases peak strain and VTI, Strain: 18.3 vs. 9.3%, p<0.001, VTI: 13.5 vs. 10.9cm, p<0.01	VTI: 13 patients Fixed AV delay 8 MPP vs. 1 CONV setting
Rinaldi ⁴⁵	Post-implantation	41	MPP vs. CONV	Echo, TDI: Ts-SD	MPP decreases Ts-SD: 35.3±36.4 vs. 50.2 ±29.1ms, p<0.01	Fixed AV delay 8 MPP vs. 1 CONV setting
Calo ³⁴	Post-implantation and long-term outcome	22	BIQ vs. CONV	ECG: QRS-duration Echo: VTI, MPI, MR, EF, ESV, EDV and NYHA class at 6 months follow-up	BIQ higher VTI, MPI, less MR and shorter QRS-duration compared to CONV. No effect on long-term outcome	7 BIQ vs. 3 CONV setting, Fixed AV delay
Pappone ⁴⁶	Short-term outcome	43	MPP vs. CONV	Echo: EF, ESV, EDV and NYHA class at 3 months follow-up	MPP improves response: ΔESV: -21.0 vs. -12.6, p=0.03; ΔEF: +9.8 vs. +2.0%, p<0.001; ΔNYHA: -1.05 vs. -0.72, p=0.006	Optimal MPP configuration determined by SW CONV: distal or proximal electrode

Published studies on comparison of response to CRT with a quadripolar LV lead (alternative quadripolar pacing vector or multipoint pacing) to conventional biventricular pacing. AHR: acute hemodynamic response, BIQ: biventricular pacing with a quadripolar lead, BV: conventional biventricular pacing with a quadripolar lead, CI: cardiac index, CO: cardiac output, dP/dt_{max}: maximal rate of left ventricular pressure rise, LVOT: left ventricular outflow tract, MPI: myocardial performance index, MPP: multipoint pacing, MR: mitral regurgitation, STE: speckle tracking echocardiography, SV: stroke volume, SW: stroke work, TDI: tissue Doppler imaging, Ts-SD: standard deviation of time to peak contraction, VTI: velocity time integral.

OPTIMIZING LEAD PLACEMENT

The benefit of quadripolar leads lies in the additional pacing options. More pacing options facilitate placement in a stable position, while avoiding areas with fibrosis or PNS (central illustration). Several studies have demonstrated the benefit of finding the optimal site for LV lead positioning, in terms of acute hemodynamic benefit, echocardiographic reverse remodeling and long term clinical outcome (table 2).^{3, 17-19}

AVOIDING PHRENIC NERVE STIMULATION

As the left phrenic nerve is located close to the posterolateral side of the pericardium, phrenic nerve stimulation in the conventionally targeted mid-posterior and lateral positions is a common finding.²⁰ PNS due to LV pacing is seen in up to 13-33% of patients during CRT implantation with bipolar LV leads, with 10% requiring lead revision.^{20, 21} Although programming of the pacing stimulus may overcome PNS, lead placement can be restricted.²¹ Phrenic nerve involvement can also occur after implantation, due to lead dislodgement or intrathoracic displacement of the heart due to patient positioning.²¹ Hypothetically, PNS may occur due to a changed anatomic position of the heart after reverse remodeling. As summarized in table 1, the percentage of PNS requiring lead revision is between 0.0-0.3 percent among quadripolar leads. A large multicenter prospective study showed a lower prevalence of PNS requiring lead revision among quadripolar leads compared to bipolar leads.¹¹ A lower amount of lead revisions means even fewer possible complications due to a second intervention, which is an important clinical benefit.

CIRCUMVENTING SCAR TISSUE

Patients with ischemic cardiomyopathy are more frequent non-responders to CRT.²² Both scar tissue near the LV lead and total scar burden influence the response to CRT.¹² Pacing in a region of scar tissue can even deteriorate LV function, as proven by acute hemodynamic experiments and by long term follow-up.^{23, 24} Pacing in scarred regions results in slow or even absent electrical wave front propagation and reduces the effect of biventricular pacing. Avoiding lead placement in scarred regions is therefore an important determinant of response, which is directly related to the implantation procedure.²⁵ The quadripolar lead can aid in this process, whenever a successful lead position is limited by venous anatomy and results in the tip placed near scar tissue, the additional electrodes may offer important

alternatives. Forleo et al. found no differences in long-term volumetric and clinical response between ischemic and non-ischemic patients with quadripolar leads.²⁶ Their results could indicate that the increase of pacing options benefits response rate in ischemic patient. There was even a trend towards a higher decrease of end systolic volume in non-ischemic patients. Larger trials are needed to prove these results.

IMAGING GUIDED LEAD PLACEMENT

Two recent trials (i.e. TARGET and STARTER) proved the benefit of LV lead positioning of a bipolar lead while knowing the latest contracting segment (based on peak radial strain derived by speckle tracking echocardiography).^{3, 17} Both studies found an increased benefit of the echocardiographic strategy on survival and echocardiographic response. Even in the control group a large proportion of leads were placed concordant or adjacent. When lead positioning in both groups was compared to response, optimal placement was strongly associated with survival and response. Nevertheless, reaching the predefined target with bipolar leads can be difficult, as these trials showed that 10 to 15% of leads were placed remote from the intended area. Moreover, 7 to 23% of leads were placed apically, which was not part of the echocardiographic protocol. Quadripolar leads could facilitate imaging guided lead placement, increasing the chance to reach the intended target.

ELECTRO-ANATOMICAL GUIDED PLACEMENT

Delayed activated segments can also be found by determining the delay in electrical depolarization. The QLV-interval is used for this purpose, by determining the recorded timing of onset of the QRS-complex ('Q') on the ECG and the local depolarization at the LV lead electrode ('LV'). As an inter-individual parameter, QLV is related to acute response, reverse remodeling, and long term outcome.²⁷⁻²⁹ Patients with a long QLV-intervals (>95ms) were associated with an increase in reverse remodeling and quality of life.²⁷ Longer QLV-intervals also result in higher dP/dt_{max} , with a 10ms increase in QLV leading to 1.7-2.0% increase in dP/dt_{max} .^{28, 30} Zanon et al. confirmed the strong positive correlation of QLV and dP/dt_{max} within individual patients.²⁹ QLV could therefore be used in combination with quadripolar leads, as the electrode with the highest QLV can be selected for biventricular pacing. Although the difference in QLV within a single vein can be relatively small, the differences in dP/dt_{max} are significant.³¹ Figure 3 illustrates QLV within a vein for two separate patients using two different quadripolar leads.

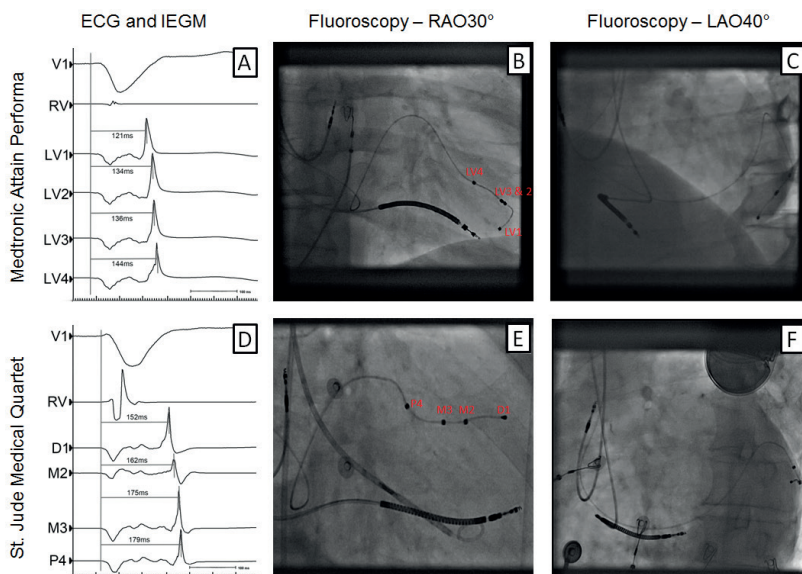


FIGURE 3. Electro-anatomical recordings of two quadripolar leads

A&D: ECG, IEGM of intrinsic rhythm, obtained with the Prucka EP system (GE Medical Systems, Milwaukee, WI, USA). B, C, E, and F: fluoroscopy images of two implantations of CRT with quadripolar leads. Images A, B and C represent a case with an implanted Medtronic Attain Performa S 4598, note the comparable QLV-interval of intrinsic rhythm of electrode LV2 and -3 (134 and 136ms respectively). The difference between the QLV-intervals of the St. Jude Medical Quartet lead (D, E and F) is notably larger (152, 162, 175, and 179ms).

Latest activated regions can also be mapped using electro-anatomic mapping (EAM) systems. Existing EAM systems have been used to find the latest activated region, using dedicated catheters within the coronary sinus and its side branches (figure 4).³² Areas with PNS can also be detected and therefore avoided during lead placement. The (acute) hemodynamic and clinical benefit of this method is unknown, but would be promising based on the results of studies on QLV and acute hemodynamic response.²⁹ Figure 4 is an excellent example of the benefits of quadripolar leads in combination with EAM, as the lead is wedged apically while the proximal electrode is positioned in the area with latest depolarization. Although accessibility by a thin guidewire used for EAM does not guarantee successful lead placement. Whether QLV or a similar parameter is the ideal tool for (quadripolar) lead positioning can be discussed. For a homogenous activation of the LV, the (very) last activated region is hypothetically suboptimal. Pacing the latest activated region will require more time to

depolarize the entire LV. Nevertheless, pacing in a ‘late’ activated region is beneficial to acute and long-term response, as proven by QLV.^{27, 29} Moreover, CRT depends on biventricular pacing, with fusion between RV- and LV-pacing. Rad et al. have shown that the order of activated regions due to RV-pacing can differ from intrinsic activation.³³ Therefore the delay between RV-pacing and LV-capture may be more important than QLV.

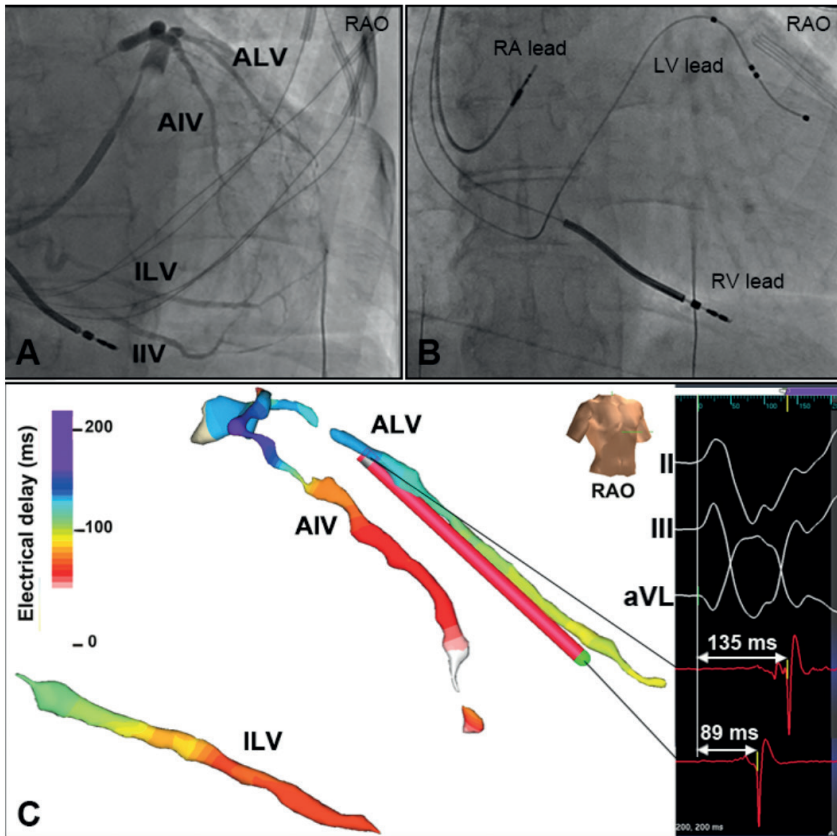


FIGURE 4. Electro-anatomical map of the coronary sinus with NavX ENSITE

A: Coronary venogram of a patient undergoing CRT implantation. B: X-ray of final LV lead placement. C: coronary venous electro-anatomical map during intrinsic ventricular activation together with the corresponding unipolar EGMs collected from the regions of earliest and latest activation. The coronary sinus and all side branches have been mapped. Connecting the LV lead to EnSite NavX allowed real-time visualization and navigation of the lead to the latest activated region in the electro-anatomic map. Note the large difference in local depolarization between proximal and distal sites in the ALV. The proximal electrode of the quadripolar lead was positioned in the area with latest depolarization. AIV: anterior inter-ventricular vein; ALV: antero-lateral vein; IIV: inferior inter-ventricular vein; ILV: infero-lateral vein; LV: left ventricular; RAO: right anterior oblique; RV: right ventricular; RA: right atrial. (Printed with permission of dr. K. Vernooy (MD, PhD), MUMC, Maastricht, the Netherlands).

OPTIMIZING PACING CONFIGURATION OF A QUADRIPOlar LEAD

Several studies have assessed the effects of optimizing pacing configurations of a quadripolar lead (table 2). Most studies focus on parameters for acute hemodynamic response, while only one reports results on short- or long term response. Calo et al. compared echocardiographic findings (e.g. velocity time integral (VTI) of the LV outflow tract) and QRS-duration, and found significant improvements of all parameters with optimized biventricular pacing using a quadripolar lead (BiQ) compared to conventional biventricular pacing using distal pacing vectors (CONV).³⁴ Conventional vectors were distal pacing vectors of the quadripolar lead, using a combination of electrode D1, M2 or the RV-coil, thus mimicking a standard bipolar lead. Two studies used non-invasive measurement of cardiac index to evaluate CRT with a quadripolar lead and found a widespread of response to tested pacing settings, but no significant differences between BiQ and CONV pacing.^{35,36} Studies on invasively measured hemodynamic response of CRT with quadripolar leads report apparent differences between pacing vectors. Asbach et al. found a significant increase of dp/dt_{max} in 12 out of 16 patients with BiQ versus CONV.³⁷ Shetty et al. used quadripolar leads to test differences in dp/dt_{max} within a coronary vein and between veins.³⁸ For individual patients, AHR within a vein varied between pacing electrodes. When patient data was combined, the overall difference between vectors was non-significant. Only one small study reported short term response of biventricular pacing using CRT with a quadripolar lead. Calo et al. optimized quadripolar pacing configurations using echocardiography in 22 patients. They found no differences in NYHA class or reverse remodelling (>15% decrease in LV end systolic volume) after 6 months, between 11 patients with optimized BiQ pacing and 11 patients with optimized CONV pacing.³⁴

OPTIMIZING MULTIPOINT PACING

Currently one manufacturer has a CRT-D device with MPP capability (Unify Quadra MP, St. Jude Medical). MPP is programmable as 'simultaneously' (minimal delay of 5ms) or with programmable inter left ventricular electrode delays (ILVD). Compared to implanting multiple LV leads, implanting a single quadripolar lead will not increase procedure duration

and fluoroscopy time. Several smaller studies recently published favourable results on the hemodynamic, electrical and mechanical response of MPP (table 2).³⁹⁻⁴² Rinaldi et al. used echocardiographic derived VTI of CW-Doppler of the left ventricular outflow tract.⁴⁰ VTI has a low signal-to-noise ratio and requires numerous iterations to make reliable estimations of LV-function.⁴³ Also a short and non-physiological AV delay (25ms) was used and some settings with long ILVD were compared (up to 80ms). This may have led to pacing in already depolarized myocardium, as the maximal spacing between two electrodes (47mm) combined with the conduction velocity (0.84m/s) of patients with dilated cardiomyopathy would lead to a theoretical maximum delay of 56ms.⁴⁴ However, myocardial fibrosis in between electrode positions may result in longer delays. Besides VTI, Rinaldi et al. compared peak radial strain derived by speckle tracking echocardiography and found higher values for MPP compared to CONV pacing (18.3 ± 7.4 vs. $9.3 \pm 5.3\%$, $p < 0.001$).⁴⁰ The same group published results of reduced dyssynchrony assessed with tissue Doppler imaging with MPP compared to conventional biventricular pacing.⁴⁵ However, eight non-randomized MPP settings were compared to only one conventional setting in both studies. Thereby the chance of defining outlying results of MPP as an optimum increased. MPP has been compared to conventional pacing with a quadripolar lead. However, in most cases MPP was compared to only one or two unifocal pacing vectors.^{39, 41} Pappone et al. compared pressure-volume loops obtained with MPP to CONV pacing and found significant increase with MPP.⁴¹ However, they compared a large number of MPP configurations (7) to a limited amount of conventional configurations (2). Thibault et al. reported heterogeneous effects of MPP, ranging from detrimental to beneficial, compared to conventional CRT. Zanon et al. used quadripolar LV leads and found a slight but significant increase in dp/dt_{\max} with MPP, compared to unifocal proximal and distal pacing.⁴² Although they repeated measurements, there was no comparison to baseline and physiological variation over time could therefore have influenced results. Only one follow-up study focused on the effects of MPP on echocardiographic response. Pappone et al. randomized 41 patients to conventional biventricular pacing or MPP.⁴⁶ The group receiving MPP had a higher percentage of echocardiographic responders after three months (76 vs. 50%). Ejection fraction improved and end-systolic volume was reduced compared to the conventional pacing group (table 2). The authors suggested that the favourable response could be attributed to the patients with ischemic cardiomyopathy, as MPP may have led to more homogenous electrical depolarization in ventricles with fibrotic tissue of these patients.

REMARKS ON REPORTED RESULTS

As can be appreciated from table 2, only a few studies directly compared BiQ to CONV.^{34, 35, 37, 47} The added benefit of quadripolar leads to standard bipolar leads on AHR needs further proving. Recent studies do show that AHR varies significantly between pacing vectors of a quadripolar lead, implying a patient specific approach to vector selection.^{36, 37} A quadripolar lead can therefore be beneficial, if stimulation at the additional electrodes is at least feasible. Both pacing- and PNS thresholds are as important as the benefit in AHR. Reports on available pacing vectors are variable. Asbach et al. reported an average of 9 out of 10 possible vectors, tested in 16 patients.³⁷ Unfortunately they didn't report specific cut-offs. Surprisingly, Sperzel et al. found that only 20% of patients had at least 9 possible pacing vectors without PNS and with good pacing threshold.¹⁴ 89% of patients had at least 3 (out of 10) possible vectors compared to 53% with 3 or more conventional vectors, with a cut-off for pacing threshold $\leq 2.5V$ and PNS $\geq 7.5V$.

Anodal capture is a confounder in results on pacing with quadripolar leads. Stimulation on an electrode pair (i.e. cathode and anode) is meant to depolarize myocardium at the cathodal electrode. However, with substantial output the anodal site could also be depolarized. Trolese et al. reported changes in QRS-width and -morphology using pacing vectors with a similar cathode and different anodes of the quadripolar lead.⁴⁸ The changes could be ascribed to anodal capture.⁴⁹ If anodal electrodes have low thresholds, intended bipolar stimulation could lead to dual site stimulation. This affects QRS-width as well as AHR and makes comparison between vectors problematic. Comparison of vectors with the RV-coil as anode could be a solution.

The absence of AV- and VV delay optimization is an important limitation of results on AHR. As AV- and VV delay optimization significantly influence AHR, published studies on hemodynamic assessment without optimization are difficult to interpret.⁵⁰ As can be appreciated from table 2, a large proportion of studies use a fixed AV- and/or VV delay. The increase of the hemodynamic improvement of the optimal pacing vector may be underestimated because a longer VV delay (with LV pre-activation) will be beneficial during LV pacing with the more basal electrodes of the quadripolar lead. Using different electrodes of a quadripolar lead or even multipoint pacing with a quadripolar lead would require intensive study protocols, with multiple AV- and/or VV delays for each vector. Protocols become even more time consuming when the comparison of a larger range of configurations requires iterations or curve-fitting to reduce the risk of bias.⁴³

Most studies on quadripolar leads primarily focus on MPP, neglecting optimal single site LV pacing. Animal experiments show that AHR of an optimal single pacing position could only be matched by adding a total of 6 pacing sites to a suboptimal pacing position.⁵¹ So, one optimally placed (quadripolar) lead is better than adding a pacing site. If the ideal pacing site is reached, which is even more likely by quadripolar leads, thoracoscopic epicardial placement or the emerging endocardial approach, an extra pacing site may be obsolete. Shetty et al. confirmed this hypothesis, as they found a significant increase of AHR while pacing a single endocardial site compared to MPP.⁵² Perhaps only a subset of patients would be eligible to respond to MPP. Unfortunately, none of the currently published studies were designed to identify markers for response to MPP. MPP is thought to depolarize the myocardium with a more homogenous electrical wave front, and could be beneficial in ventricles with heterogeneous conduction, for example due to fibrosis. This was confirmed in a group of CRT patients with posterolateral scar.⁵³ Another small study showed that 2 out of (only) 3 patients converted to responders with MPP, compared to conventional CRT.⁵⁴ Patient selection for MPP could be of interest, as MPP can also have detrimental effects on LV function.³⁹ Whether patients with heterogeneous conduction and/or previous myocardial infarction or simply non-responders are eligible for MPP is of interest.

The benefit of MPP depends on the location of the extra pacing site. The ideal location for an extra stimulus for MPP is unknown. Ploux et al. showed that pacing the latest activated site (during pacing with the previous implanted leads) is of incremental hemodynamic benefit.⁵¹ Implanting an additional lead at the latest electrical activated region during conventional biventricular pacing would be an interesting method for future patient trials. This concept is not feasible for quadripolar leads, as the electrode spacing and location is limited to one vein. Shetty et al. found no significant differences in AHR between MPP (with quadripolar leads) or multi-site pacing (with multiple LV leads), although their sample size was small (n=15).⁵² As shown by figure 3 and by Rad et al., the electrical delays along the optimal vein can be quite similar.³³ Stimulating two spots with relatively comparable electrical delays is probably not beneficial. It is therefore interesting to define the relation between electrical delays between quadripolar electrodes and the benefit to MPP. Pappone et al. found that the electrode pair with the largest anatomical spacing was optimal in 71% of patients, compared to the pair with the largest inter-electrode delay.⁴¹ An expected overlap between both strategies wasn't reported. Nevertheless it is an interesting result, as anatomical spacing merely resembles position while the electrical delay is a functional parameter.

ONGOING STUDIES

Two ongoing studies on MPP are the MultiPoint Pacing IDE study and the MORE CRT trial.^{55,56} The first is designed to include 506 patients with a CRT indication,⁵⁶ comparing the effects on response and complications of CRT with a quadripolar lead to CRT with a standard bipolar lead. The MORE-CRT trial is even larger, enrolling 1250 patients.⁵⁵ This, multicentre study will investigate the clinical effects of CRT with a quadripolar lead compared to bipolar lead. The effect of MPP on non-responders at six months follow-up will also be investigated.

FUTURE DIRECTIONS

Multipolar leads are currently restricted to four electrodes, possibly due to limitations in maximal lead diameter and device header size. Future developments could overcome these restrictions and open the door for hexa- or even octapolar leads. Additional electrodes increase the number of pacing options and will only increase the success rate of CRT implantation. Several short distanced dipoles for example (like the two middle electrodes in Medtronic quadripolar leads), could reduce the chance of PNS. Optimization however, becomes even more time consuming without a proper surrogate parameter (beside QLV). Whether multi-site pacing on more than two sites could be beneficial for a selection of patients is controversial. Firstly the benefit of one extra pacing site should be investigated thoroughly. The extra pacing sites can also be positioned in the coronary sinus, for left atrial sensing.⁵⁷ Left atrial sensing could obsolete the right atrial electrode in patients without atrial arrhythmia.

Lead positioning strategies could be optimized by incorporating results of imaging and electro-anatomic modalities. If scar tissue, delayed activation (either mechanical or electrical), PNS and pacing thresholds are incorporated in the venogram during implantation, an implanting physician could choose the optimal position and lead for the patient specific anatomy.^{32, 58} The quadripolar lead with a specific shape and distance between electrodes could then be selected, to achieve an optimal mid or basal position with more proximal electrodes, while distal electrodes are wedged near the apex. A heterogeneous choice of leads, as currently available, is therefore practical. Figure 4 displays a possible strategy, using EAM to guide the operator in choosing a lead with electrodes placed in the area with maximal electrical delay.

Optimization of CRT configuration is complicated by the additional electrodes and pacing options (e.g. MPP) of a quadripolar lead. Automated optimization algorithms such based on electrical delays could incorporate the electrode with longest QLV and acceptable pacing threshold without PNS for optimal quadripolar pacing configuration. However, the benefit of AV and VV delay optimization is debatable, as a meta-analysis of several optimization techniques found no apparent benefit.⁵⁹

CONCLUSION

The benefit of quadripolar leads over conventional bipolar leads has been underlined by recent trials. Quadripolar LV leads have lower complication rates and more pacing options, thereby reducing the frequency of PNS, circumventing fibrosis and facilitating reaching a predefined optimal position. Leads are available in various models and different electrode spacing, with an expected heterogeneity in use. Based on acute hemodynamic studies and a small randomized trial, quadripolar leads can improve acute and short-term response to CRT. Currently one manufacturer offers multipoint pacing, a pacing modality that can have benefit in certain cases. Its application is unclear, due to methodological shortcomings and contradictory results of recent studies, beside the unknown ideal substrate for MPP. Results of ongoing and future comparative studies on quadripolar leads regarding both acute hemodynamic response and long term outcome are warranted.

REFERENCES

1. Brignole M, Auricchio A, Baron-Esquivias G, Bordachar P, Boriani G, Breithardt OA, et al. 2013 ESC Guidelines on cardiac pacing and cardiac resynchronization therapy. *Eur Heart J*. 2013;34:2281-2329.
2. Russo AM, Stainback RF, Bailey SR, Epstein AE, Heidenreich PA, Jessup M, et al. ACCF/HRS/AHA/ASE/HFSA/SCAI/SCCT/SCMR 2013 appropriate use criteria for implantable cardioverter-defibrillators and cardiac resynchronization therapy. *J Am Coll Cardiol*. 2013;61:1318-68.
3. Khan FZ, Virdee MS, Palmer CR, Pugh PJ, O'Halloran D, Elsik M, et al. Targeted left ventricular lead placement to guide cardiac resynchronization therapy: the TARGET study: a randomized, controlled trial. *J Am Coll Cardiol*. 2012;59:1509-1518.
4. Saxon LA, Olshansky B, Volosin K, Steinberg JS, Lee BK, Tomassoni G, et al. Influence of left ventricular lead location on outcomes in the COMPANION study. *J Cardiovasc Electrophysiol*. 2009;20:764-8.
5. Singh JP, Klein HU, Huang DT, Reek S, Kuniss M, Quesada A, et al. Left ventricular lead position and clinical outcome in the multicenter automatic defibrillator implantation trial-cardiac resynchronization therapy (MADIT-CRT) trial. *Circulation*. 2011;123:1159-1166.
6. Biffi M, Zanon F, Bertaglia E, Padeletti L, Varbaro A, De Santo T, et al. Short-spaced dipole for managing phrenic nerve stimulation in patients with CRT: the "phrenic nerve mapping and stimulation EP" catheter study. *Heart rhythm : the official journal of the Heart Rhythm Society*. 2013;10:39-45.
7. Yang Z, Kirchhof N, Li S, Hine D, McVenes R. Effect of Steroid Elution on Electrical Performance and Tissue Responses in Quadripolar Left Ventricular Cardiac Vein Leads. *PACE*. 2015.
8. Bracke FA, Nathoe R, van Gelder BM. Cross-manufacturer mismatch between a quadripolar IS-4 lead and a defibrillator IS-4 port. *Heart rhythm : the official journal of the Heart Rhythm Society*. 2014;11:1226-8.
9. Behar JM, Bostock J, Zhu Li AP, Chin HM, Jubb S, Lent E, et al. Cardiac Resynchronization Therapy Delivered Via a Multipolar Left Ventricular Lead is Associated with Reduced Mortality and Elimination of Phrenic Nerve Stimulation: Long-Term Follow-Up from a Multicenter Registry. *J Cardiovasc Electrophysiol*. 2015;26:540-6.
10. Arias MA, Pachon M, Puchol A, Jimenez-Lopez J, Rodriguez-Padial L. Acute and mid-term outcomes of transvenous implant of a new left ventricular quadripolar lead versus bipolar leads for cardiac resynchronization therapy: results from a single-center prospective database. *Cardiol J*. 2012;19:470-8.

11. Crossley GH, Biffi M, Johnson B, Lin A, Gras D, Hussin A, et al. Performance of a novel left ventricular lead with short bipolar spacing for cardiac resynchronization therapy: primary results of the Attain Performa quadripolar left ventricular lead study. *Heart rhythm : the official journal of the Heart Rhythm Society*. 2015;12:751-8.
12. Ypenburg C, Schalij MJ, Bleeker GB, Steendijk P, Boersma E, Dibbets-Schneider P, et al. Impact of viability and scar tissue on response to cardiac resynchronization therapy in ischaemic heart failure patients. *Eur Heart J*. 2007;28:33-41.
13. Healey JS, Hohnloser SH, Exner DV, Birnie DH, Parkash R, Connolly SJ, et al. Cardiac resynchronization therapy in patients with permanent atrial fibrillation: results from the Resynchronization for Ambulatory Heart Failure Trial (RAFT). *Circ Heart Fail*. 2012;5:566-70.
14. Sperzel J, Danschel W, Gutleben KJ, Kranig W, Mortensen P, Connelly D, et al. First prospective, multi-centre clinical experience with a novel left ventricular quadripolar lead. *Europace*. 2012;14:365-72.
15. Forleo GB, Mantica M, Di Biase L, Panattoni G, Della Rocca DG, Papavasileiou LP, et al. Clinical and procedural outcome of patients implanted with a quadripolar left ventricular lead: early results of a prospective multicenter study. *Heart rhythm*. 2012;9:1822-8.
16. Mehta PA, Shetty AK, Squirrel M, Bostock J, Rinaldi CA. Elimination of phrenic nerve stimulation occurring during CRT: follow-up in patients implanted with a novel quadripolar pacing lead. *J Interv Cardiac Ep*. 2012;33:43-9.
17. Saba S, Marek J, Schwartzman D, Jain S, Adelstein E, White P, et al. Echocardiography-guided left ventricular lead placement for cardiac resynchronization therapy: results of the Speckle Tracking Assisted Resynchronization Therapy for Electrode Region trial. *Circ Heart Fail*. 2013;6:427-34.
18. Ypenburg C, van Bommel RJ, Delgado V, Mollema SA, Bleeker GB, Boersma E, et al. Optimal left ventricular lead position predicts reverse remodeling and survival after cardiac resynchronization therapy. *J Am Coll Cardiol*. 2008;52:1402-9.
19. Delnoy PP, Ottervanger JP, Luttkhuis HO, Vos DH, Elvan A, Ramdat Misier AR, et al. Pressure-volume loop analysis during implantation of biventricular pacemaker/cardiac resynchronization therapy device to optimize right and left ventricular pacing sites. *Eur Heart J*. 2009;30:797-804.
20. Seifert M, Schau T, Moeller V, Neuss M, Meyhoefer J, Butter C. Influence of pacing configurations, body mass index, and position of coronary sinus lead on frequency of phrenic nerve stimulation and pacing thresholds under cardiac resynchronization therapy. *Europace*. 2010;12:961-7.
21. Biffi M, Exner DV, Crossley GH, Ramza B, Couto B, Tomassoni G, et al. Occurrence of phrenic nerve stimulation in cardiac resynchronization therapy patients: the role of left ventricular lead type and placement site. *Europace*. 2012;15:77-82.

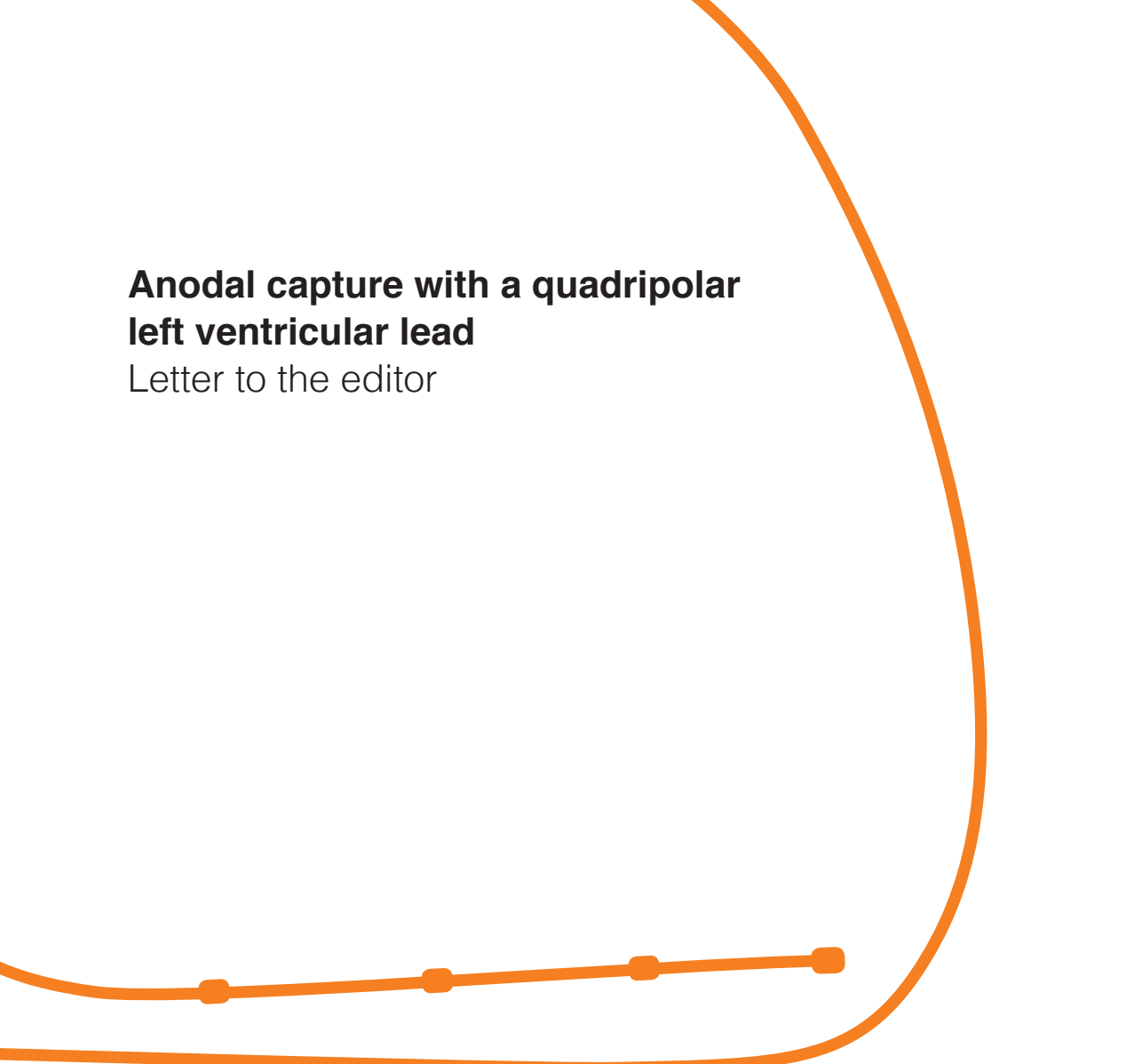
22. Shanks M, Delgado V, Ng AC, Auger D, Mooyaart EA, Bertini M, et al. Clinical and echocardiographic predictors of nonresponse to cardiac resynchronization therapy. *Am Heart J*. 2011;161:552-7.
23. Delgado V, van Bommel RJ, Bertini M, Borleffs CJ, Marsan NA, Arnold CT, et al. Relative merits of left ventricular dyssynchrony, left ventricular lead position, and myocardial scar to predict long-term survival of ischemic heart failure patients undergoing cardiac resynchronization therapy. *Circulation*. 2011;123:70-8.
24. de Roest GJ, Wu L, de Cock CC, Hendriks ML, Delnoy PP, van Rossum AC, et al. Scar tissue-guided left ventricular lead placement for cardiac resynchronization therapy in patients with ischemic cardiomyopathy: an acute pressure-volume loop study. *Am Heart J*. 2014;167:537-45.
25. Kydd AC, Khan FZ, Watson WD, Pugh PJ, Virdee MS, Dutka DP. Prognostic benefit of optimum left ventricular lead position in cardiac resynchronization therapy: follow-up of the TARGET Study Cohort. *J Am Coll Cardiol HF*. 2014;2:205-12.
26. Forleo GB, Di Biase L, Della Rocca DG, Panattoni G, Mantica M, Santamaria M, et al. Impact of previous myocardial infarction on outcomes of CRT patients implanted with a quadripolar left ventricular lead. Results from a multicentric prospective study. *Int J Cardiol*. 2012;160:145-6.
27. Gold MR, Birgersdotter-Green U, Singh JP, Ellenbogen KA, Yu Y, Meyer TE, et al. The relationship between ventricular electrical delay and left ventricular remodelling with cardiac resynchronization therapy. *Eur Heart J*. 2011;32:2516-2524.
28. Bogaard MD, Hesselink T, Meine M, Loh P, Hauer RN, Cramer MJ, et al. The ECG in cardiac resynchronization therapy: influence of left and right ventricular preactivation and relation to acute response. *J Cardiovasc Electrophysiol*. 2012;23:1237-45.
29. Zanon F, Baracca E, Pastore G, Fraccaro C, Roncon L, Aggio S, et al. Determination of the longest intrapatient left ventricular electrical delay may predict acute hemodynamic improvement in patients after cardiac resynchronization therapy. *Circ Arrhythm Electrophysiol*. 2014;7:377-83.
30. Gold MR, Leman RB, Wold N, Sturdivant JL, Yu Y. The effect of left ventricular electrical delay on the acute hemodynamic response with cardiac resynchronization therapy. *J Cardiac EP*. 2014;25:624-30.
31. van Gelder BM, Bracke FA. Acute hemodynamic effects of single- and dual-site left ventricular pacing employing a dual cathodal coronary sinus lead. *PACE*. 2015;38:558-64.
32. Rad MM, Blaauw Y, Dinh T, Pison L, Crijns HJ, Prinzen FW, et al. Left ventricular lead placement in the latest activated region guided by coronary venous electroanatomic mapping. *Europace*. 2015;17:84-93.

33. Mafi Rad M, Blaauw Y, Dinh T, Pison L, Crijns HJ, Prinzen FW, et al. Different regions of latest electrical activation during left bundle-branch block and right ventricular pacing in cardiac resynchronization therapy patients determined by coronary venous electro-anatomic mapping. *Eur J Heart Fail.* 2014;16:1214-22.
34. Calo L, Martino A, de Ruvo E, Minati M, Fratini S, Rebecchi M, et al. Acute echocardiographic optimization of multiple stimulation configurations of cardiac resynchronization therapy through quadripolar left ventricular pacing: a tailored approach. *Am Heart J.* 2014;167:546-54.
35. Osca J, Alonso P, Cano O, Sanchez JM, Tejada D, Andres A, et al. The use of quadripolar left ventricular leads improves the hemodynamic response to cardiac resynchronization therapy. *PACE.* 2015;38:326-33.
36. Jones MA, Khiani R, Foley P, Webster D, Qureshi N, Wong KC, et al. Inter- and Intra-vein Differences in Cardiac Output with Cardiac Resynchronization Pacing using a Multipolar LV Pacing Lead. *PACE.* 2014.
37. Asbach S, Hartmann M, Wengenmayer T, Graf E, Bode C, Biermann J. Vector selection of a quadripolar left ventricular pacing lead affects acute hemodynamic response to cardiac resynchronization therapy: a randomized cross-over trial. *PLoS one.* 2013;8:e67235.
38. Shetty AK, Duckett SG, Ma YL, Kapetanakis S, Ginks M, Bostock J, et al. The acute hemodynamic response to LV pacing within individual branches of the coronary sinus using a quadripolar lead. *Pacing Clin Electrophysiol.* 2012;35:196-203.
39. Thibault B, Dubuc M, Khairy P, Guerra PG, Macle L, Rivard L, et al. Acute haemodynamic comparison of multisite and biventricular pacing with a quadripolar left ventricular lead. *Europace.* 2013;15:984-991.
40. Rinaldi CA, Leclercq C, Kranig W, Kacet S, Betts T, Bordachar P, et al. Improvement in acute contractility and hemodynamics with multipoint pacing via a left ventricular quadripolar pacing lead. *J Interv Cardiac Ep.* 2014;40:75-80.
41. Pappone C, Calovic Z, Vicedomini G, Cuko A, McSpadden LC, Ryu K, et al. Multipoint left ventricular pacing improves acute hemodynamic response assessed with pressure-volume loops in cardiac resynchronization therapy patients. *Heart Rhythm.* 2014;11:394-401.
42. Zanon F, Baracca E, Pastore G, Marcantoni L, Fraccaro C, Lanza D, et al. Multipoint pacing by a left ventricular quadripolar lead improves the acute hemodynamic response to CRT compared with conventional biventricular pacing at any site. *Heart Rhythm.* 2015;12:975-81.

43. Sohaib SM, Whinnett ZI, Ellenbogen KA, Stellbrink C, Quinn TA, Bogaard MD, et al. Cardiac resynchronisation therapy optimisation strategies: systematic classification, detailed analysis, minimum standards and a roadmap for development and testing. *Int J Cardiol.* 2013;170:118-31.
44. Anderson KP, Walker R, Urie P, Ershler PR, Lux RL, Karwande SV. Myocardial electrical propagation in patients with idiopathic dilated cardiomyopathy. *J Clin Invest.* 1993;92:122-40.
45. Rinaldi CA, Kranig W, Leclercq C, Kacet S, Betts T, Bordachar P, et al. Acute effects of multisite left ventricular pacing on mechanical dyssynchrony in patients receiving cardiac resynchronization therapy. *J Card Fail.* 2013;19:731-738.
46. Pappone C, Calovic Z, Vicedomini G, Cuko A, McSpadden LC, Ryu K, et al. Multipoint left ventricular pacing in a single coronary sinus branch improves mid-term echocardiographic and clinical response to cardiac resynchronization therapy. *J Cardiovasc Electrophysiol.* 2015;26:58-63.
47. Cabrera Bueno F, Alzueta Rodriguez J, Olague de Ros J, Fernandez-Lozano I, Garcia Guerrero JJ, de la Concha JF, et al. Improvement in hemodynamic response using a quadripolar LV lead. *Pacing Clin Electrophysiol.* 2013;36:963-9.
48. Trolese L, Biermann J, Hartmann M, Schluermann F, Faber TS, Bode C, et al. Haemodynamic vector personalization of a quadripolar left ventricular lead used for cardiac resynchronization therapy: use of surface electrocardiogram and interventricular time delays. *Europace.* 2014;16:1476-81.
49. van Everdingen WM, van Gelder B, Meine M. Comment on the article by Trolese T et al. *Europace.* 2015;17:999.
50. Bogaard MD, Meine M, Tuinenburg AE, Maskara B, Loh P, Doevendans PA. Cardiac resynchronization therapy beyond nominal settings: who needs individual programming of the atrioventricular and interventricular delay? *Europace.* 2012;14:1746-1753.
51. Ploux S, Strik M, van Hunnik A, van Middendorp L, Kuiper M, Prinzen FW. Acute electrical and hemodynamic effects of multisite left ventricular pacing for cardiac resynchronization therapy in the dyssynchronous canine heart. *Heart Rhythm.* 2014;11:119-25.
52. Shetty AK, Sohal M, Chen Z, Ginks MR, Bostock J, Amraoui S, et al. A comparison of left ventricular endocardial, multisite, and multipolar epicardial cardiac resynchronization: an acute haemodynamic and electroanatomical study. *Europace.* 2014:873-879.
53. Ginks MR, Duckett SG, Kapetanakis S, Bostock J, Hamid S, Shetty A, et al. Multi-site left ventricular pacing as a potential treatment for patients with postero-lateral scar: insights from cardiac magnetic resonance imaging and invasive haemodynamic assessment. *Europace.* 2011;14:373-9.

54. Ginks MR, Shetty AK, Lambiase PD, Duckett SG, Bostock J, Peacock JL, et al. Benefits of endocardial and multisite pacing are dependent on the type of left ventricular electric activation pattern and presence of ischemic heart disease: insights from electroanatomic mapping. *Circulation Arrhythmia and electrophysiology*. 2012;5:889-97.
55. Boriani G. MOre REsponse on Cardiac Resynchronization Therapy with MultiPoint Pacing (MORE-CRT MPP). *ClinicalTrialsgov*. 2011;Identifier: NCT02006069.
56. Tomassoni G. MultiPoint Pacing IDE Study (MPP IDE). *ClinicalTrialsgov*. 2014;Identifier: NCT01786993.
57. Spinelli J, Zhu Q. Atrial pacing and sensing in cardiac resynchronization therapy. 2004.
58. Duckett SG, Ginks MR, Knowles BR, Ma Y, Shetty A, Bostock J, et al. Advanced image fusion to overlay coronary sinus anatomy with real-time fluoroscopy to facilitate left ventricular lead implantation in CRT. *PACE*. 2011;34:226-34.
59. Auger D, Hoke U, Bax JJ, Boersma E, Delgado V. Effect of atrioventricular and ventriculoventricular delay optimization on clinical and echocardiographic outcomes of patients treated with cardiac resynchronization therapy: a meta-analysis. *Am Heart J*. 2013;166:20-9.



A thick orange line starts at the top right, curves down and left, then curves back up and right, forming a large, open shape that frames the top and right sides of the page. A horizontal orange line with four square markers is positioned below the main title area.

Anodal capture with a quadripolar left ventricular lead

Letter to the editor

W.M. van Everdingen (MD)¹, Berry M. van Gelder (PhD)², M. Meine (MD, PhD)¹

¹ Department of Cardiology, University Medical Centre Utrecht, Utrecht, The Netherlands.

² Department of Cardiology, Catharina Ziekenhuis Eindhoven, Eindhoven, The Netherlands.

Adapted from: Europace. 2015 Jun;17(6):999.

The recent introduction of quadripolar leads for cardiac resynchronization therapy (CRT) raises the question which pacing vector is most beneficial to response and which parameter gives insight into the optimal vector. The study conducted by Trolese et al. is therefore of important value and unique in its kind.¹ The found correlation between maximal difference of the QRS-width (Δ QRS) and acute hemodynamic response (Δ LV-dP/dt_{max}) is an important finding to aid vector selection. However, their results give rise to questions.

Figure 1A of Trolese et al. shows an equal QRS morphology comparing M3M2 and M3P4 indicating cathodal stimulation from M3 and no effect of the anodal electrode. However, comparing D1M2 and D1P4 shows a clear difference in morphology. Because the cathodal electrode (D1) is the same in both configurations, this can be explained by anodal capture from either M2 or P4, implicating that in one of the configurations LV pacing is dual site and single site in the other. This will affect QRS-width as well as acute hemodynamic response and makes comparison between configurations problematic. The figure attached to this letter gives an example of changes in QRS-morphology with anodal capture (figure 1). Most probably there is also a typographical error in figure 1A of Trolese et al., regarding the QRS-width of baseline compared to D1M2.

Second, the change in QRS-morphology between vectors P4M2, P4RV, M3M2 and all preceding vectors in figure 1B of Trolese et al., suggest that the LV pacing wave front becomes less dominant (lead I less negative and lead V1 less positive) when the proximal electrodes are used. Electrodes M3 and P4 are possibly closer to the base of the ventricle, and would need pre-excitation (changes in interventricular (VV) delay) to depolarize a substantial part of the LV when pacing biventricular. Acute hemodynamic response of these vectors could be underestimated by a reduced contribution of LV depolarization by the LV pacing wave front. To show the true effect of LV pacing vectors on acute hemodynamic response, LV pre-excitation had to be programmed while pacing at proximal electrodes. Unfortunately, implementation of VV delays in the study protocol is sheer impossible, as it would result in long procedures.

Third, the analysis of Trolese et al. raise methodological questions. Although randomization of the pacing sequence and baseline measurements in-between pacing were performed,² outliers have large effect on findings, even more considering the small sample size (n=16).³ Repetition of measurements and curve-fitting with implementation of several AV delays could be a better approach, however leading to an undesired longer procedure. Increasing the sample size could also decrease the effects of outliers.

Lastly, based on above mentioned arguments and known intra-individual spread in correlation of interventricular delays and acute hemodynamic response, the conclusion that vector selection based on interventricular delay (IVD) is not supported, could be premature. Zanon et al. demonstrated that correlation of QLV-interval (comparable to IVD) and LV-dP/dt_{max} is quite variable between patients and strongly correlated intra-individually.⁴ We are however delighted by the articles published by Trolese and colleagues, as the introduction of quadripolar LV leads raise questions on optimal vector selection. However, the methodology and conclusions of their articles are up for debate.

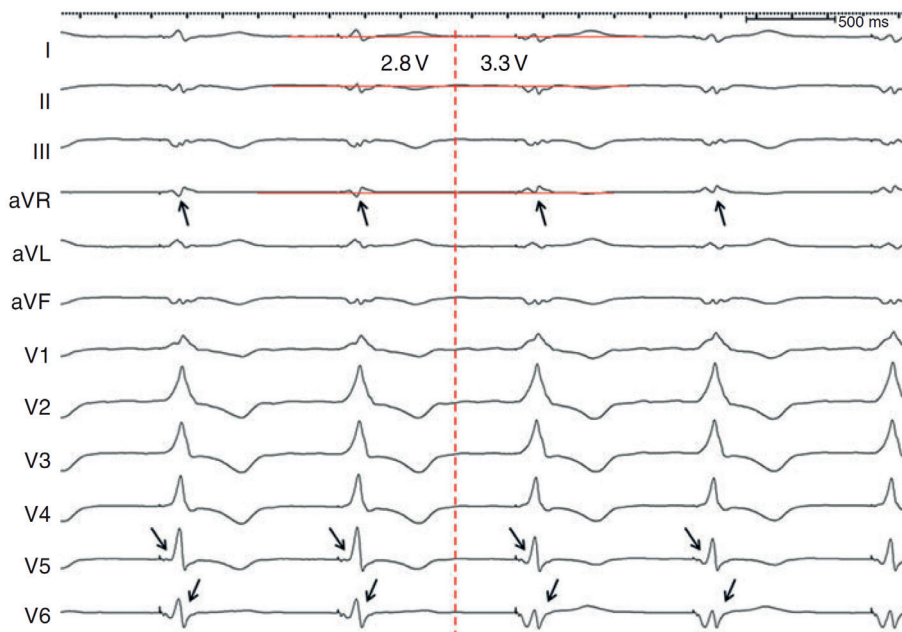


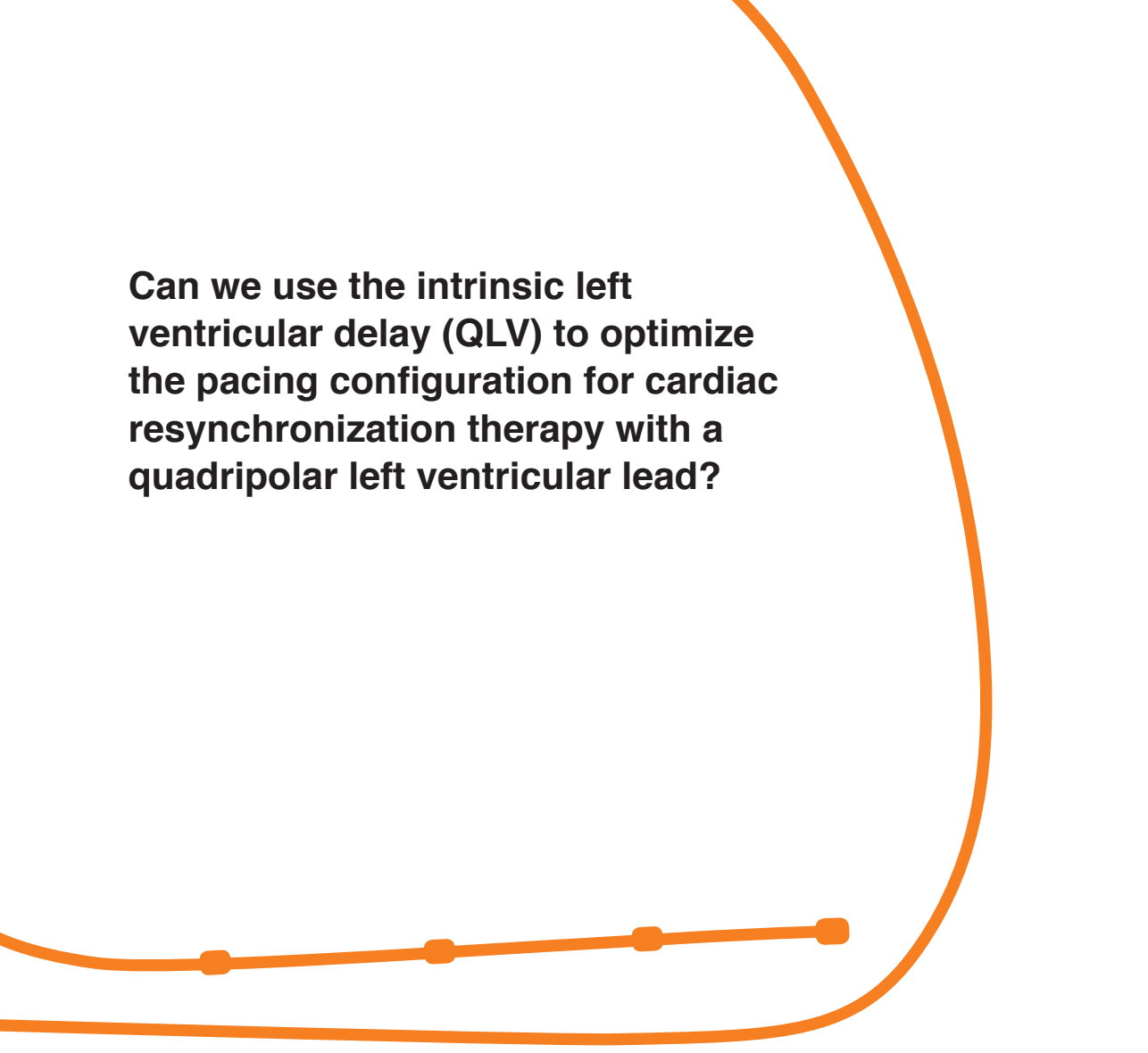
FIGURE 1. Stimulation on vector P4M3

Continuous ECG registration of stimulation on vector P4M3, with increased output from 2.8 to 3.3 Volt. Note the changes in QRS-morphology after increased output (especially lead I, II, aVR, V5 and V6), indicating anodal capture.

REFERENCES

1. Trolese L, Biermann J, Hartmann M, Schlurmann F, Faber TS, Bode C, et al. Haemodynamic vector personalization of a quadripolar left ventricular lead used for cardiac resynchronization therapy: use of surface electrocardiogram and interventricular time delays. *Europace*. 2014;16:1476-81.
2. Asbach S, Hartmann M, Wengenmayer T, Graf E, Bode C, Biermann J. Vector selection of a quadripolar left ventricular pacing lead affects acute hemodynamic response to cardiac resynchronization therapy: a randomized cross-over trial. *PLoS one*. 2013;8:e67235.
3. Sohaib SM, Whinnett ZI, Ellenbogen KA, Stellbrink C, Quinn TA, Bogaard MD, et al. Cardiac resynchronisation therapy optimisation strategies: systematic classification, detailed analysis, minimum standards and a roadmap for development and testing. *Int J Cardiol*. 2013;170:118-31.
4. Zanon F, Baracca E, Pastore G, Fracarro C, Roncon L, Aggio S, et al. Determination of the longest inpatient left ventricular electrical delay may predict acute hemodynamic improvement in patients after cardiac resynchronization therapy. *Circ Arrhythm Electrophysiol*. 2014;7:377-83.



A thick orange line starts from the top right, curves down and left, then continues horizontally across the middle of the page, and finally curves down and right towards the bottom right corner.

Can we use the intrinsic left ventricular delay (QLV) to optimize the pacing configuration for cardiac resynchronization therapy with a quadripolar left ventricular lead?

Wouter M. van Everdingen (MD)^{1*}, Alwin Zweerink (MD)^{2*}, Maarten J. Cramer (MD, PhD)¹, Pieter A. Doevendans (MD, PhD)¹, Uyên Châu Nguyễn (MD, MSc)^{3,4}, Albert C. van Rossum (MD, PhD)², Frits W. Prinzen (PhD)⁴, Kevin Vernooy (MD PhD)³, Cornelis P. Allaart (MD, PhD)², Mathias Meine (MD, PhD)¹

*: first two authors contributed equally to the manuscript

¹ Department of Cardiology, University Medical Center Utrecht, Utrecht, The Netherlands

² Department of Cardiology, and Institute for Cardiovascular Research (ICaR-VU), VU University Medical Center, Amsterdam, The Netherlands

³ Department of Cardiology, Maastricht University Medical Center, Maastricht, The Netherlands

⁴ Department of Physiology, CARIM, Maastricht University, Maastricht, The Netherlands

Under revision

ABSTRACT

Background: Previous studies indicated the importance of the intrinsic left ventricular (LV) electrical delay (“QLV”) for optimal benefit to cardiac resynchronization therapy (CRT). We investigated the use of QLV for achieving optimal acute hemodynamic response to CRT with a quadripolar LV lead.

Methods and results: Forty-eight heart failure patients with a left bundle branch block were prospectively enrolled (31 male, age: 66 ± 10 years, LV ejection fraction: $28\pm 8\%$, QRS duration: 176 ± 14 ms). Immediately after CRT implantation, invasive LV pressure-volume loops were recorded during biventricular pacing with each separate electrode at four atrioventricular delays. Acute CRT response, measured as change in stroke work ($\Delta\%$ SW) compared to intrinsic conduction, was related to intrinsic interval between Q on the electrocardiogram and LV sensing delay (QLV), normalized for QRS duration (QLV/QRSD), and electrode position. QLV/QRSD was $84\pm 9\%$ and variation between the four electrodes $9\pm 5\%$. $\Delta\%$ SW was $89\pm 64\%$ and varied by $39\pm 36\%$ between the electrodes. In univariate analysis, an anterolateral or lateral electrode position and a high QLV/QRSD had a significant association with a large $\Delta\%$ SW (all $p < 0.01$). In a combined model, only QLV/QRSD remained significantly associated with $\Delta\%$ SW ($p < 0.05$). However, a direct relation between QLV/QRSD and $\Delta\%$ SW was only seen in 24 patients, while 24 patients showed an inverse relation.

Conclusions: The large variation in acute hemodynamic response indicates that the choice of the stimulated electrode on a quadripolar lead is important. Although QLV/QRSD was associated with acute hemodynamic response at group level, it cannot be used to select the optimal electrode in the individual patient.

Key words: cardiac resynchronization therapy; stroke work; pressure-volume loop; quadripolar lead, optimization; electrical delay

INTRODUCTION

Cardiac resynchronization therapy (CRT) is a proven therapy for patients with heart failure and left ventricular (LV) conduction disorder, according to most recent international guidelines.¹ CRT improves prognosis, reduces mortality and morbidity, and induces reverse remodeling through electromechanical resynchronization.^{2, 3} Unfortunately, a substantial number of eligible patients (i.e. around 30-40%) show no significant response to CRT.⁴ An important cause of poor CRT response is a suboptimal placed LV lead.⁵ A suboptimal placed LV lead may hamper successful resynchronization, as the distally wedged pacing electrodes may be close to an infarcted region or remote from the electromechanical 'hotspot'.⁶ In order to reach this 'hotspot', quadripolar LV leads may be of beneficial use.⁷ As the tip of a quadripolar lead is often wedged in a tributary of the coronary sinus, its electrodes will span a range from apical to basal regions of the LV wall.⁸ Despite several studies on quadripolar leads,^{9, 10} the exact benefit of the additional pacing sites on LV function remains relatively unknown.⁸ Most studies only compared the benefit of the proximal electrodes to the distal electrode.^{9, 10} These studies were small, used non-invasive techniques to measure acute hemodynamic response with low signal to noise ratios, or a fixed atrioventricular (AV) delay.⁸ Moreover, non-invasive methods to select the optimal electrode of a quadripolar LV lead are lacking. Potential optimization methods are parameters of electrical delay derived from the ECG and/or intracardiac electrogram. The QLV interval is one of these electrical delays, defined by the delay between 'Q' on the surface ECG and local LV depolarization on the intracardiac electrogram at a given LV pacing site (figure 1).¹¹ The QLV may be normalized using the intrinsic QRS duration (QLV/QRSd).¹² A few studies reported that an apical and/or anterior LV lead position may be suboptimal for CRT response, while electrodes placed basal or mid-ventricular in a lateral position yield more favorable response.^{13, 14} However, these studies compared bipolar LV leads in different patients, without taking interpatient variability in consideration.

The hypothesis of this study is that biventricular pacing at a site with largest QLV/QRSd ratio provides the largest acute hemodynamic response. Therefore, the aim of the study was to associate the acute hemodynamic response of each electrode of the quadripolar LV lead was measured by invasive pressure-volume loops (PV-loops) with electrical and anatomical parameters.

METHODS AND MATERIALS

PATIENT COHORT

The observational Opticare-QLV study, was performed between 2014 and 2017 in three university medical center (University Medical Center Utrecht, Utrecht; VU University Medical Center, Amsterdam; and Maastricht University Medical Center, Maastricht; all in the Netherlands). A total of 51 consecutive patients planned for CRT implantation were included, with moderate to severe heart failure (i.e. NYHA class II or III), LV ejection fraction $\leq 35\%$, optimal pharmacological therapy, sinus rhythm, and a left bundle branch block (LBBB) according to Strauss criteria.¹⁵ Exclusion criteria were severe aortic valve stenosis, mechanical aortic valve replacement, and the presence of LV thrombus. All subjects gave written informed consent. The study was performed according to the Declaration of Helsinki and in agreement with the local medical ethics committees. As the data of this study is also used for future publications, the data, analytic methods, and study materials will not be made available to other researchers for purposes of reproducing the results or replicating the procedure.

CRT IMPLANTATION

All patients underwent electrocardiographic (ECG), echocardiographic examination and cardiac magnetic resonance imaging (CMR) prior to device implantation. CMR (or echocardiography) derived LV volumes were used to calibrate the conductance catheter-derived baseline volumes. CRT implantation was performed under local anesthesia. RV and right atrial (RA) leads were placed transvenously at conventional positions. The quadripolar LV lead (Quartet 1458Q, St. Jude Medical, Saint Paul, Minnesota, United States) was placed in one of the coronary veins overlying the LV free wall. A site in the lateral, antero- or posterolateral position was preferred. After electrophysiological measurements, the three leads were connected to a St. Jude Medical CRT-device.

ELECTROPHYSIOLOGICAL MEASUREMENTS

Electrophysiological (EP) measurements were performed using an on-site dedicated EP system. EP system settings of the three participating centers were matched to study protocols. The EP system was used to record simultaneous registrations of the twelve-lead surface ECG and the three implanted leads. Delays of specific pacing modalities were recorded and

delays between pacing artefacts and local depolarization at the leads were measured. For each electrode (i.e. D1, M2, M3, and P4), QLV was defined as the intrinsic conduction time from first Q on the surface ECG to local LV depolarization at the electrode of the quadripolar LV lead (QLV) (figure 1). The ratio between QLV and the intrinsic QRS duration was also calculated for each electrode (QLV/QRSD). We used QLV/QRSD to uniform results on conduction delay between patients. Next, RA pacing to RV sensing interval (RAp-RVs) was measured and used to calculate the patient specific AV delays. The delay between RV pacing to LV sensing interval (RVp-LVs) was measured as a parameter of paced interventricular conduction delay.

HEMODYNAMIC MEASUREMENTS

Directly after device implantation, a dedicated PV-loop conductance catheter (CD Leycom, Zoetermeer, The Netherlands) was inserted via the femoral artery and placed in the LV cavity. PV-loops were recorded for biventricular pacing with each individual electrode of the quadripolar lead, in-between baseline recordings during intrinsic conduction. The LV electrode was used as a cathode with the RV-coil as anode, resulting in four different pacing vectors. Only configurations without phrenic nerve stimulation close to the myocardial pacing threshold were used. For each electrode, four AV-delays were determined to approximate 20%, 40%, 60% and 80% of the patient's intrinsic AV conduction time (RAp-RVs interval). The interventricular delay was programmed to 40ms LV first, as LV pacing 40ms before RV pacing is favorable in 80% of CRT patients.¹⁶ The order in which the electrodes were tested was varied between patients. To keep heartrate constant, PV-loops were recorded during atrial pacing, with a frequency of 5-10 bpm above intrinsic rhythm. Recordings lasted 60 beats per pacing configuration, after excluding all inappropriate beats (i.e. extra systoles with one preceding and two subsequent beats). PV-loops during intrinsic conduction (i.e. RA pacing) were recorded for 30 beats at the same heart rate. The area of the PV-loop was used to calculate stroke work (SW). To account for baseline drift,¹⁷ the effect of biventricular pacing was quantified as change in SW, calculated as a %-change ($\Delta\%SW$) compared to the mean of the two adjoining baseline measurements. For each electrode, a parabolic curve was fitted to change in $\Delta\%SW$ obtained from the four AV delays (figure 1). The highest value of each parabolic curve was noted as the optimal change in $\Delta\%SW$ and corresponding AV-delay for the specific electrode.

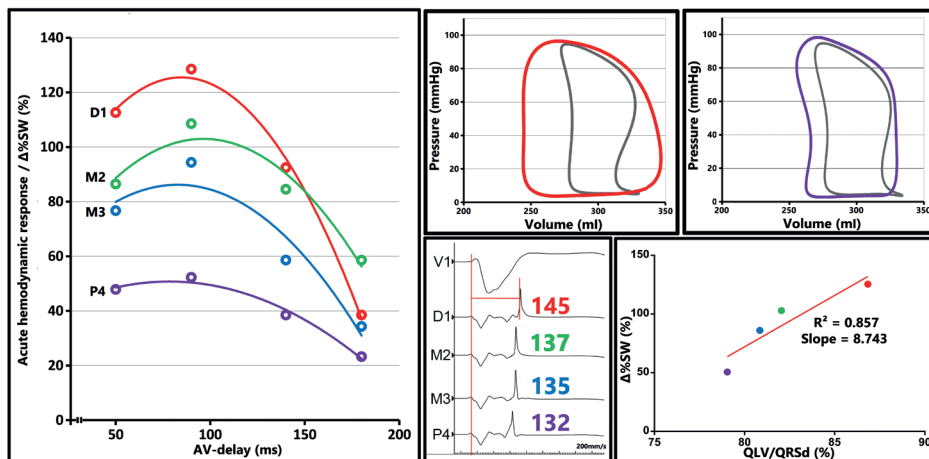


FIGURE 1. Method to determine the optimal pacing site of CRT with a quadripolar LV lead

The acute hemodynamic response is determined by calculating the increase in stroke work ($\Delta\%SW$) of pressure-volume (PV) loops of four atrioventricular (AV) delays and four electrodes compared to loops during right atrial pacing with intrinsic conduction (grey PV-loops). PV-loops of D1 (red) and M2 (green) are displayed in the upper right corner. For each tested AV-delay and electrode, $\Delta\%SW$ is plotted in the left panel. Delays are determined between Q on the surface ECG (V1) and local LV depolarization at the electrodes of the quadripolar lead (QLV) (middle lower panel). The QLV/QRSd ratio is plotted against $\Delta\%SW$ of each electrode at the optimal AV-delay, and a trendline is fitted. Electrode colors: D1: red, M2: green, M3: blue, P4: purple.

LEAD POSITION

After lead placement, fluoroscopy images were made in the left anterior oblique (LAO) 40° and in the in the right anterior oblique (RAO) 30° view to determine the specific position of each quadripolar LV lead electrode in the longitudinal direction (figure 2). On the RAO 30° view the distance between base of the LV and each electrode was divided by the distance between base and apex, in order to obtain the RAO-ratio (figure 2). The RAO-ratio was divided in three even groups, resulting in basal, mid, and apical positioned electrodes. For the LAO 40° view, the ventricle was divided in five equally sized regions overlying the LV free wall in the circumferential direction (i.e. anterior, anterolateral, lateral, posterolateral, and posterior).⁷

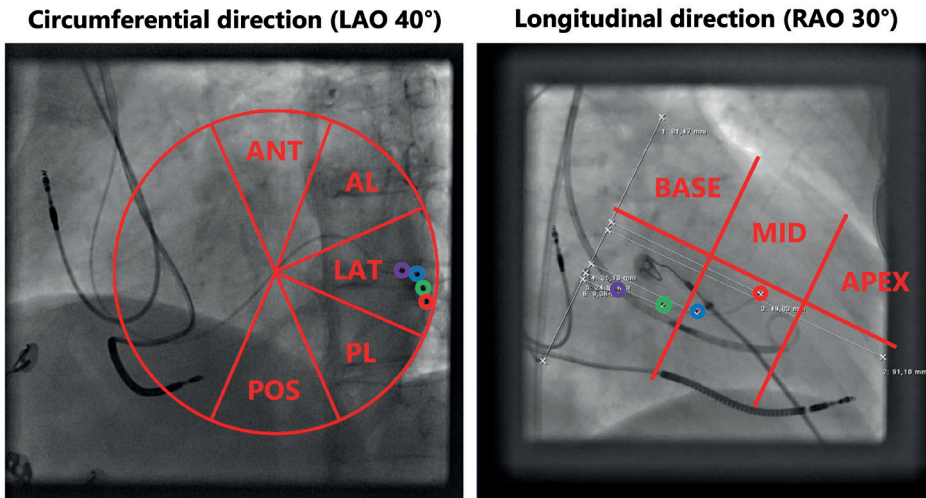


FIGURE 2. Anatomical position of the quadripolar LV lead electrodes

The quadripolar left ventricular (LV) lead and electrode position are determined using fluoroscopy in two views. In the circumferential direction, the left anterior oblique (LAO) 40° view was used to divide the LV in an anterior (ANT), anterolateral (AL), lateral (LAT), posterolateral (PL), and posterior segment (POS). In the longitudinal direction, the LV is divided in three evenly spaced segments based on the right anterior oblique (RAO) 30° view: base, mid and apex. The most distal electrode (D1) is red, the first mid electrode (M2) green, the second mid electrode (M3) blue and the proximal electrode (P4) purple.

STATISTICAL ANALYSIS

Statistical analysis was performed using SPSS statistics version 23 (IBM, Armonk, New York, USA). Data is presented as mean \pm standard deviation or median and interquartile range, based on normality of data. Of certain parameters, the variation between electrodes was calculated for each individual patient by subtracting the lowest value from the highest value. The average variation and standard deviation of the entire cohort were calculated with these values. To account for repeated measurements, differences in observed parameters between electrodes were compared in generalized estimated equation (GEE), with pairwise comparison. GEE's were also used to assess the value of expected predictors (i.e. electrode position in longitudinal and circumferential direction, RVp-LVs, QLV and QLV/QRSd ratio) of change in $\Delta\%$ SW on a group level. All parameters were tested separately, while both parameters on anatomical position were combined, after which each parameter with $p < 0.10$ was incorporated in a combined model. In case of significance of QLV and QLV/

QRSd, a single parameter was chosen based on the highest beta coefficient and p-value. The relation between hemodynamic response ($\Delta\%SW$) and QLV/QRSd of all four electrodes was calculated for each patient. A line was fitted to the four data points, of which the coefficient of determination and slope were noted (figure 1). Patients were divided in two groups based on the slope: patients with a positive slope and a negative slope. The average slope of all patients reflects the relation between QLV/QRSd and change in $\Delta\%SW$. The two groups were compared on baseline parameters using an independent T-test or Mann Whitney U test. A Chi-square test was used for categorical variables. A p-value below 0.05 was considered significant for the GEE in table 3. Due to the large number of comparisons, a p-value below 0.01 was considered significant for all remaining tests.

RESULTS

Fifty-one patients were included prospectively in the study, of which three were excluded from the analysis due to unreliable baseline PV-loops. Twenty-six patients were included in the University Medical Center Utrecht, sixteen in the VU University Medical Center and six in het Maastricht University Medical Center. Unacceptably high pacing thresholds precluded using electrode M2 in three patients, and electrode P4 in three other patients. Values in the remaining 48 patients and 186 electrodes were as follows: QLV: 140.2 ± 19.7 ms, QLV/QRSd: $79.9 \pm 9.2\%$, RVp-LVs: 146.4 ± 23.0 ms (table 1). In the longitudinal direction, distal electrodes (i.e. D1 and M2) were more often positioned apical, while the position of proximal electrodes (i.e. M3 and P4) was more often basal (table 2). In the LAO view, there were no significant differences in positioning of the electrodes. Overall, most electrodes were positioned in a lateral segment ($n=108$, 58%). There was no apparent resemblance between the bullseye of QLV/QRSd and acute hemodynamic response (figure 3). Large differences in QLV/QRSd were primarily seen in the anterolateral positioned electrodes, with higher values in the basal segment compared to the apical segment. $\Delta\%SW$ showed lower values in posterolateral and posterior positioned electrodes, while $\Delta\%dP/dt_{\max}$ was lowest in the posterior positioned electrodes. On average, QLV/QRSd of the distal electrode (D1) was significantly lower compared to the other three electrodes, although the variation between the electrodes was only $8.8 \pm 4.7\%$ (table 2). RVp-LVs delay showed larger and significant differences between all electrodes (RVp-LVs variation: 27.8 ± 13.2 ms), with

lowest values for the distal electrode, increasing towards the proximal electrode. The pacing threshold of electrode P4 was often higher, while phrenic nerve stimulation occurred less using this electrode. Despite these differences in electrical properties of the electrodes, no electrode consistently provided the largest increase in $\Delta\%SW$ (D1 in 17 (35%), M2 in 10 (21%), M3 in 6 (13%) and P4 in 15 (31%) patients). The mean acute hemodynamic response of biventricular pacing was 68.9 ± 59.3 for $\Delta\%SW$ and 13.3 ± 9.5 for $\Delta\%dP/dt_{max}$. The variation in $\Delta\%SW$ had a large distribution between patients (figure 4), mean variation $\Delta\%SW$ between the electrodes of a quadripolar lead was $38.8 \pm 36.4\%$, while $\Delta\%dP/dt_{max}$ had a variation of $4.9 \pm 2.9\%$ (supplementary figure 1).

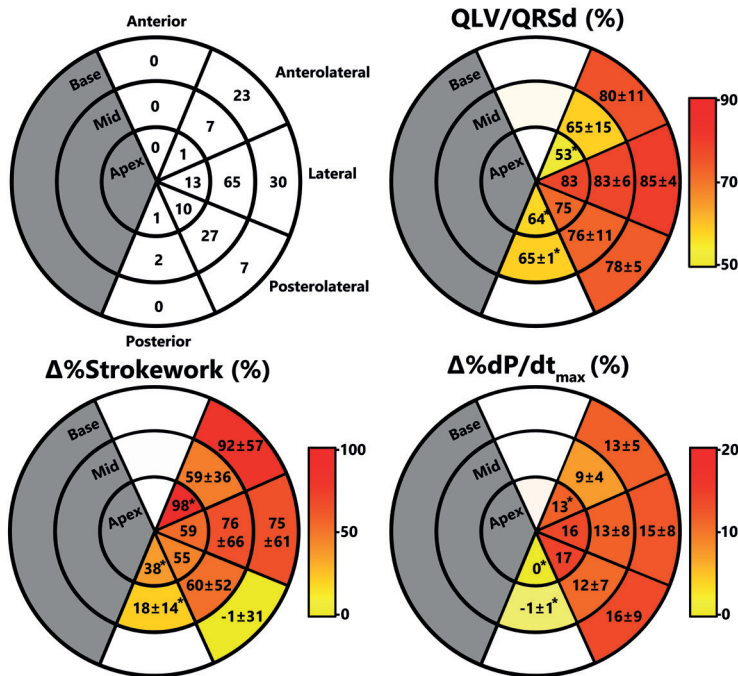


FIGURE 3. Anatomical representation of electrode position, electrical delay and hemodynamic response

The bullseye in the upper left corner displays the anatomical position of the 192 electrodes divided in 15 segments. The average and standard deviation of the QLV/QRSD of each segment are displayed in the upper right corner. Average acute hemodynamic response in percentage increase in stroke work and dP/dt_{max} of each segment are displayed in the lower two bullseyes. The one basal anterior electrode had no capture and therefore no hemodynamic values. *: values represent only 1 or 2 electrodes.

TABLE 1. Baseline characteristics

Parameter	Total cohort (n=48)	Direct relation QLV/QRSD- %SW (n=24)	Inverse relation QLV/ QRSD-%SW (n=24)	p-value
Age (years)	65.9±9.5	66.2±10.2	65.7±8.8	0.845
Sex (n, % of male)	31 (65%)	17 (71%)	14 (58%)	0.547
Type of cardiomyopathy (n, % of ICM)	13 (27%)	7 (29%)	10 (42%)	0.547
NYHA-class (n, %)				
II	33 (69%)	16 (67%)	17 (71%)	1.000
III	15 (31%)	8 (33%)	7 (29%)	
PR duration (ms)	182.8±31.3	186.6±33.7	179±28.8	0.403
QRS duration (ms)	175.6±13.6	174.2±12.6	176.9±14.6	0.504
Mean QLV (ms)	140.2±19.7	134.2±21.8	146.3±15.5	0.032
Mean QLV/QRSD (%)	79.9±9.2	77.1±11.5	82.7±4.9	0.034
QLV/QRSD variation (%)	8.8±4.7	8.0±3.8	9.6±5.5	0.227
Mean RVp-LVs (ms)	146.4±23.0	145.2±28.2	147.6±17.2	0.726
LV EDV (ml)	210.8±66.0	233.6±69.9	188.1±54.1	0.015
LV ESV (ml)	154.3±61.4	174.9±66.6	133.7±48.9	0.018
LV EF (%)	28.5±8.4	26.3±6.7	30.4±8.8	0.067
LV EDD (mm)	61.6±7.5	63.0±8.7	60.2±6.1	0.206
Creatinine	90.1±22.7	92.8±24.1	86.3±21.6	0.336
Log BNP	1.89±0.54	2.03±0.59	1.76±0.48	0.125
Medication (n, %)				
ACE-inhibitor or ATII-antagonist	47 (98%)	24 (100%)	23 (96%)	1.000
Beta-blocker	42 (88%)	22 (92%)	20 (83%)	0.724
Diuretic	32 (67%)	16 (67%)	16 (67%)	1.000
Aldosterone-antagonist	29 (60%)	11 (46%)	18 (75%)	0.075
Anticoagulant	30 (63%)	12 (50%)	18 (75%)	0.135
Comorbidities (n, %)				
Hypertension	17 (71%)	5 (21%)	12 (50%)	0.069
Renal failure	4 (17%)	1 (4%)	3 (13%)	0.609
Circumferential electrode position (n, %)				
Anterior	0	0	0	0.021
Anterolateral	31 (17%)	18 (20%)	13 (14%)	
Lateral	108 (58%)	44 (45%)	64 (68%)	
Posterolateral	44 (24%)	27 (29%)	17 (18%)	
Posterior	3 (2%)	3 (3%)	0	
Longitudinal electrode position (n, %)				
Basal	60 (32%)	28 (30%)	32 (34%)	0.053
Mid	101 (54%)	46 (50%)	55 (59%)	
Apical	25 (13%)	18 (20%)	7 (7%)	

Direct relation: patients with a direct relation between QLV/QRSD and change in stroke work ($\Delta\%$ SW). Inverted relation: patients with an inverse relation between QLV/QRSD and $\Delta\%$ SW. ACE: angiotensin converter enzyme, ATII: angiotensin receptor II, EDD: end-diastolic diameter, EDV: end-diastolic volume, ESV: end-systolic volume, ICM: ischemic cardiomyopathy, LV: left ventricular, LVEF: left ventricular ejection fraction, MI: myocardial infarction, n: number, NYHA-class: New York Heart Association functional class, QLV: Q to LV sensing delay, QLV/QRSD: ratio of QLV and QRS duration ratio.

Can we use the intrinsic left ventricular delay (QLV) to optimize the pacing configuration for cardiac resynchronization therapy with a quadripolar left ventricular lead?

TABLE 2. Electrode characteristics

Parameters (n=48)	D1 (n=48)	M2 (n=45)	M3 (n=48)	P4 (n=45)	p-value
Longitudinal position (n, %)					
Basal	0 (0%)	5 (10%)	22 (46%)	33 (73%)	<0.001
Mid	34 (71%)	34 (71%)	34 (48%)	10 (21%)	
Apical	14 (29%)	6 (13%)	3 (6%)	2 (4%)	
Circumferential position (n, %)					
Anterior	0	0	0	0	0.270
Anterolateral	4 (8%)	7 (16%)	8 (17%)	12 (25%)	
Lateral	27 (56%)	30 (67%)	28 (58%)	23 (51%)	
Posterolateral	17 (35%)	7 (16%)	11 (23%)	9 (20%)	
Posterior	0	1 (2%)	1 (2%)	1 (2%)	
Pacing threshold (V)	0.7 (0.3-1.8)	0.7 (0.4-2.2)	0.6 (0.4-1.8)	1.8 (0.5-5.2)*	<0.001
PNS threshold (V)	10.0 (2.0-10.0) [†]	10.0 (1.5-10.0)	10.0 (2.9-10)	10.0 (7.0 – 10.0) [†]	0.002
QLV (ms)	135.5±19.2*	142.1±20.2	141.9±21.1	144.3±20.0	<0.001
QLV/QRSd (%)	77.1±8.7*	80.6±9.7	80.8±10.0	82.1±9.8	<0.001
RVp-LVs (ms)	131.8±23.7*	144.9±23.9*	151.3±23.8*	158.1±24.5*	<0.001
Δ%SW (%)	67.4±55.0	74.4±55.4	70.9±64.4	63.1±63.2	0.011
Δ%dP/dt _{max} (%)	13.5±8.8	13.5±9.5	12.7±9.3	13.3±10.6	0.255

Mean and standard deviation with ± symbol, median and interquartile range between brackets. Phrenic nerve stimulation (PNS) thresholds were measured to a maximum of 10V. RVp-LVs: right ventricular pacing and left ventricular sensing interval. For other abbreviations, see table 1. *: p<0.001 compared to all other electrodes. †: p<0.01 between indicated electrodes.

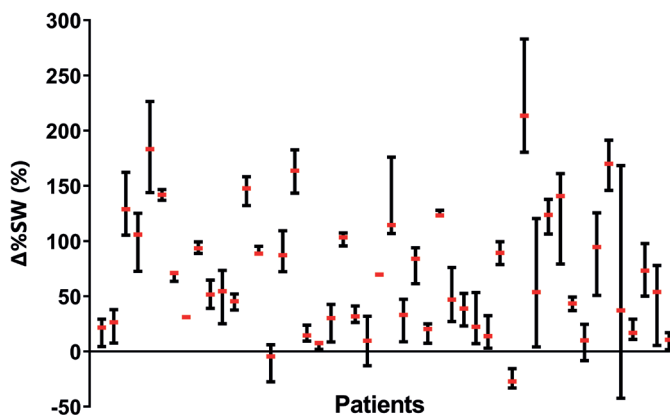


FIGURE 4. Change in stroke work per patient

Smallest, largest and median %-change in stroke work ($\Delta\%SW$) per patient. The red dashes depict the median, upper and lower bars the smallest and largest value obtained with one of the four electrodes of the quadripolar LV lead. Patients are ranked in the same order as figure 5; on the slope and direction of the R^2 .

RESULTS AT GROUP LEVEL

Biventricular pacing with the electrode of maximal QLV or QLV/QRSd tended to result towards a smaller increase of $\Delta\%SW$ compared to selecting the electrode with highest achievable $\Delta\%SW$ (67.8 ± 51.2 vs. 88.7 ± 63.8 %SW, $p=0.05$). The difference between biventricular pacing with the electrode with highest $RVp-LV_7$ was significant compared to the highest achievable $\Delta\%SW$ (67.8 ± 51.2 vs. 88.7 ± 63.8 %SW, $p<0.001$). A significant association between %SW and QLV/QRSd was observed at group level (table 3). This analysis showed that with each percent increase in QLV/QRSd, $\Delta\%SW$ increased with 0.9% in a single variable model and 0.8% in a combined model. A combined GEE model of anatomical position also showed a significant association between electrode position in the circumferential direction and $\Delta\%SW$ change. Electrodes in the anterolateral or lateral position were associated with $\sim 10\%$ higher $\Delta\%SW$ values compared to posterior and posterolateral positioned electrodes ($p<0.05$ for both comparisons). There was no association between change in $\Delta\%SW$ and electrode position in a longitudinal direction or $RVp-LV_7$. A combined GEE model of QLV/QRSd and electrode position in the circumferential direction showed a significant association of QLV/QRSd with change in $\Delta\%SW$, but no significant association of the electrode position.

TABLE 3. Prediction of change in %-change in stroke work

Single variable models (GEE) – electrical delays			
	B	SE (95% CI)	p-value
QLV	0.579	0.193 (0.202-0.956)	0.003
QLV/QRSd	0.934	0.332 (0.283-1.586)	0.005
RVp-LVs	0.076	0.245 (-0.404-0.556)	0.756
Combined model (GEE) – anatomical position			
	B	SE (95% CI)	p-value
Longitudinal position	.	.	.
Basal	-0.226	8.755 (-17.386-16.935)	0.979
Mid	4.157	7.109 (-9.776-18.090)	0.559
Apical	0*		
Circumferential position	.	.	.
Anterolateral	11.619	5.682 (0.483-22.755)	0.041
Lateral	9.068	4.543 (0.226-17.909)	0.044
Posterolateral or posterior	0*		
Combined model (GEE) – significant predictors			
	B	SE (95% CI)	p-value
QLV/QRSd	0.809	0.351 (0.121-1.497)	0.021
Circumferential position	.	.	.
Anterolateral	4.527	5.704 (-6.651-15.706)	0.427
Lateral	4.916	4.520 (-3.944-13.776)	0.227
Posterolateral or posterior	0*		

Single variable models show the results of the generalized estimated equation (GEE) of each parameter. The parameters with p-values <0.10 were combined in a final model (i.e. GEE). The categories posterolateral and posterior were combined, as there were only three electrodes positioned posterior. B: beta-coefficient. SE: standard error, CI: confidence interval. For other abbreviations: see table 1. *: set to zero because the parameter is redundant.

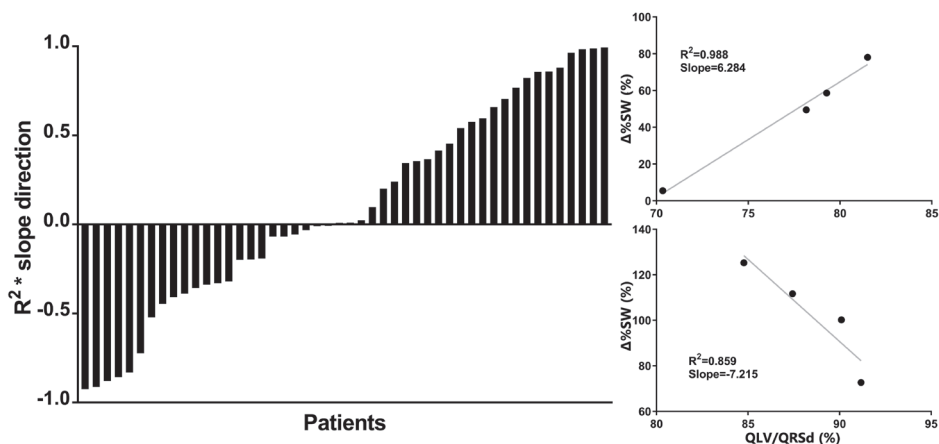


FIGURE 5. Distribution of the slope and coefficient of determination for $\Delta\%SW$ and $QLV/QRSd$

The slope direction multiplied by the coefficient of determination (R^2) of the trendline fitted to $QLV/QRSd$ and $\Delta\%SW$ for each patient. Values are arranged from lowest to highest value. There are 24 patients with a direct relation (positive slope) and 24 with an invert relation (negative slope). Examples of a direct relation (upper right panel) and an inverse relation (lower right panel) are shown on the right.

RESULTS FOR THE INDIVIDUAL PATIENT

Despite the significant relation between $QLV/QRSd$ and $\Delta\%SW$ at the group level described above, there was considerable heterogeneity in this relation in individual patients. The association between $\Delta\%SW$ and $QLV/QRSd$ had a direct relation (i.e. positive slope) for 24 patients but an inverse relation (i.e. negative slope) for the remaining 24 patients (figure 5). The R^2 tended to be higher in patients with a direct relation (0.570 ± 0.319), while it was lower for the patients with an inverse relation (0.377 ± 0.320 , $p=0.05$). These poorer correlations in case of an inverse relation may be explained by the smaller variation in $\Delta\%SW$ in the patients with inverse versus those with a direct relation (26.8 ± 20.0 vs. 50.8 ± 44.7 $\Delta\%SW$, $p=0.02$ (figure 4)). However mean $\Delta\%SW$ did not differ between patients with a direct ($67.8\Delta\%SW$) or inverse relation ($70.6\Delta\%SW$, $p=0.87$). Comparing baseline characteristics of patients with a direct and inverse $QLV/QRSd$ - $\Delta\%SW$ relation revealed no significant differences (table 1). However, QLV and $QLV/QRSd$ values tended to be lower, while LV end-diastolic and end-systolic volumes tended to be larger for patients with a direct relation. Accordingly, LV ejection fraction tended to be lower in patients with a direct $QLV/QRSd$ -

%SW relation. There tended to be more electrodes positioned in a posterolateral or posterior position in patients with a direct relation, while there was a trend towards more apically positioned electrodes in patients with an inverse QLV/QRSd-%SW relation.

DISCUSSION

The present study showed a statistically significant relation between intrinsic ventricular conduction time (QLV/QRSd) and acute hemodynamic response ($\Delta\%$ SW) at group level. However, only half of the patients showed a direct relation between QLV/QRSd and $\Delta\%$ SW, while the other half had an inverse relation. Therefore, QLV or QLV/QRSd may not predict the electrode of a quadripolar LV lead that provides the largest hemodynamic response at the individual level. There was also no association between the paced interventricular conduction time (RVp-LVs) and $\Delta\%$ SW. Nevertheless, anatomical position did reveal favorable sites for LV pacing, namely in the anterolateral or lateral position. Moreover, optimization of CRT with a quadripolar LV lead is important, as there was a large intra-individual variation in the acute hemodynamic response of the four electrodes.

THE OPTIMAL PACING SITE

Our results indicate a discrepancy between the optimal pacing site for the entire cohort and for the individual patient. While a longer QLV was significantly associated with a better hemodynamic response at group level, the relation between QLV and response ranged from strongly positive to inverse between individual patients. This discrepancy may be explained by several factors. Most leads were positioned in an area of pronounced delayed activation, with high QLV/QRSd values. Also, the variation in QLV between the four electrodes was relatively small. In animal studies it has been shown that, especially in a model of non-ischemic heart failure, there is a large region within the LV wall that, when paced, provides a significant hemodynamic effect.¹⁸ Therefore QLV/QRSd seems not predictive for the hemodynamic response within late activated areas, especially since some measurement variability has to be taken into account. In line with this idea is the observation that, patients with a direct relation tended to have lower QLV/QRSd values, potentially caused by suboptimally placed LV leads. This may imply that suboptimally placed leads may benefit more from selection of the pacing site with highest change in $\Delta\%$ SW. The weak

but significant association between QLV/QRSd and acute hemodynamic response on group level is of interest. The association indicates that pacing in a region with prolonged QLV/QRSd benefits acute hemodynamic response. However, it does not imply that increase in QLV/QRSd will automatically lead to an increase in stroke work in each patient. In contrast to our results, Zanon et al. found a strong direct relation between QLV and hemodynamic response, which was apparent in each patient.¹⁹ However, there are four main differences between their study and ours. Firstly, we used stroke work instead of dP/dt_{max} . While dP/dt_{max} is limited to pressure changes in the isovolumetric contraction phase, stroke work incorporates pressure and volume changes of the entire cardiac cycle.²⁰ Secondly, we only included patients with LBBB, as opposed to including also patients with intraventricular conduction delay and right bundle branch block.¹⁹ The latter had lower QLV values and a less favorable substrate for CRT response. Thirdly, we optimized the AV delay at each pacing configuration and programmed the interventricular pacing delay to 40ms LV first. A study of our own group showed that pacing the LV 40ms before the RV improved CRT response in 80% of all patients.¹⁶ Fourth and perhaps most important, while we only tested the four electrodes of a single quadripolar lead at a single target vein, Zanon et al. tested up to eleven pacing sites per patient in multiple cardiac veins, thereby including suboptimal sites with a short QLV. Thereby a large range of QLV values was obtained, larger than what is present in a single vein. The correlation between QLV and acute hemodynamic response seems driven by the shorter QLV values (<95ms), which are below the cut-off value for CRT response defined by Gold et al.¹¹ The lack of correlation between QLV/QRSd and hemodynamic response in a single vein is in line with results from the iSPOT study.²¹ QLV and QLV/QRSd may therefore be suitable parameters for lead placement in general, indicating the overall expected benefit, as it is a predictor for acute hemodynamic and long-term CRT response.^{11, 19} However, the QLV or QLV/QRSd cannot be used for selection of the optimal electrode of a quadripolar LV lead after lead placement in an already optimal area (i.e. anterolateral or lateral).

It could be argued that the lack of a clear QLV- $\Delta\%$ SW relation is due to the fact that not the delay during intrinsic activation, but that during RV pacing (a component of biventricular pacing) matters. Since the location of latest activated region often differs between RV pacing and LBBB activation,²² we also investigated the relation RVp-LVs delay with $\Delta\%$ SW. As the highest RVp-LVs value was frequently seen at the proximal electrode, while the electrode with highest change in acute hemodynamic response was heterogeneously distributed

between patients, RVp-LVs is also not suitable for optimization. Therefore, optimization of the pacing location within a quadripolar lead seems more complicated than merely selecting the latest activated site during LBBB or RV pacing. A rather good effect is already achieved when pacing at a relatively late activated region. An alternative hypothesis would be that the optimal LV pacing site is located at a region with fast LV free wall depolarization.²³ Such regions proved to be especially located at anterolateral or lateral sites, as has been shown previously.^{24, 25} These regions may overlap with areas which are late activated during intrinsic conduction, with prolonged QLV or QLV/QRSD. However, the actual 'hotspot' may differ, as the sites with largest QLV/QRSD values did not always produce the highest increase in $\Delta\%SW$.

ACUTE HEMODYNAMIC EFFECT

The effect of CRT on increase in stroke work was relatively large, however the findings are in line with results from earlier studies.^{9, 26} The relatively high $\Delta\%SW$ may be ascribed to patient selection (i.e. strict LBBB and relative low percentage of patients with ischemic cardiomyopathy) and optimization of the pacing configuration and AV delay, recruiting more of the potential substrate. The inter-individual difference in the benefit of CRT was large in our study population, which is in line with recent findings.²¹ Previous studies found more variation in dP/dt_{max} between patients or between different veins than pacing sites of a multipolar lead within a single vein.^{21, 27} However, our study showed a large intra-individual variation in $\Delta\%SW$ change of the four electrodes. Selecting the pacing site of a quadripolar lead is therefore important for acute hemodynamic response in a subset of patients. Optimization of CRT with a quadripolar LV lead using stroke work from PV-loops, would result a favorable long-term response in most patients.²⁰ The 20% increase in $\Delta\%SW$ cut-off value for response, defined by De Roest et al,²⁰ may result in nine (18%) non-responders for biventricular pacing with the distal electrode (i.e. conventional CRT) compared to only four patients (8%) for biventricular pacing with the optimal pacing configuration. Multi-point pacing may result in an even greater benefit,^{28, 29} which will be addressed in future work. QLV has also been associated with reverse remodeling and volumetric response to CRT.¹¹ The association of QLV/QRSD, SW and dP/dt_{max} with volumetric response in this patient cohort is of interest and will be investigated.

CLINICAL APPLICATION

Lead positioning is important for CRT response, as anterolateral and lateral positions resulted in relatively better response compared to posterolateral and posterior positions. The LV lead may preferably be placed in such a region, accompanied by considerable electrical delay, seen in high QLV/QRSd values. However, as QLV/QRSd (or RVp-LVs) is not capable of predicting the optimal electrode of a quadripolar lead after lead positioning in each individual patient, it should not be used for this purpose. The QLV/QRSd may therefore be used to select a vein for quadripolar LV lead placement, after which optimization of the pacing electrode should be dependent on functional assessment of CRT response. As not all clinicians have access to PV-loop measurements, future studies on alternative and preferably non-invasive methods to optimize CRT response are of interest.

LIMITATIONS

Although the sample size is relatively large for an invasive study and conducted in multiple centers, it is limited by the number of patients included. The strict inclusion criteria also reduced the number of eligible patients and prolonged the time period of inclusion. Three patients with underestimation of baseline function were excluded, as they showed PV-loops with crossing lines. Some of the patients that were included in the final analysis experienced underestimation of baseline stroke work, due to the fact that the shape of the loops was not rectangular but tailed, thereby reducing the area of the loop. This is a known phenomenon in conductance measurements for PV-loops in heart failure patients. Therefore, the absolute value of $\Delta\%SW$ increase may be overestimated, but due to the repeated measurement design (i.e. each patient serves as its own control), it is possible to compare different settings within each patient. Although the study methodology was complex and the distribution of patients over the three centers was uneven, baseline characteristics were comparable between centers, as well as the relationship between QLV/QRSd and $\Delta\%SW$. Our methods may have a different result in patients with intraventricular conduction delay, as optimization may have a bigger impact in patients with a less favorable substrate for CRT. The current protocol with various AV-delays and pacing settings was time-consuming. Therefore, the interventricular delay was fixed at an offset of 40ms LV first, because such an offset is favorable in most CRT patients.¹⁶ Whether the acute hemodynamic response obtained in each patient correlates to an improved long-term prognosis is debatable. However, changes in dP/dt_{max} are unable to predict reverse remodeling,³⁰ while changes in SW are associated with favorable volumetric response.²⁰

CONCLUSIONS

There are large intra-individual variations in acute hemodynamic CRT response between electrodes of a quadripolar LV lead, indicating the benefit of patient specific optimization. Although QLV/QRSd had a significant association with acute hemodynamic CRT response at group level, QLV/QRSd was not usable to predict the electrode of a quadripolar LV lead with highest hemodynamic response for the individual patient. Therefore, optimization of the pacing configuration of CRT with a quadripolar LV lead should rely on functional assessment of cardiac function, instead of local electrical delay.

REFERENCES

1. Russo AM, Stainback RF, Bailey SR, Epstein AE, Heidenreich PA, Jessup M, et al. ACCF/HRS/AHA/ASE/HFSA/SCAI/SCCT/SCMR 2013 appropriate use criteria for implantable cardioverter-defibrillators and cardiac resynchronization therapy. *J Am Coll Cardiol*. 2013;61:1318-68.
2. Cleland JG, Daubert JC, Erdmann E, Freemantle N, Gras D, Kappenberger L, et al. The effect of cardiac resynchronization on morbidity and mortality in heart failure. *N Engl J Med*. 2005;352:1539-49.
3. Ghio S, Freemantle N, Scelsi L, Serio A, Magrini G, Pasotti M, et al. Long-term left ventricular reverse remodelling with cardiac resynchronization therapy: results from the CARE-HF trial. *Eur J Heart Fail*. 2009;11:480-8.
4. Wilkoff BL, Fauchier L, Stiles MK, Morillo CA, Al-Khatib SM, Almendral J, et al. 2015 HRS/EHRA/APHRS/SOLAECE expert consensus statement on optimal implantable cardioverter-defibrillator programming and testing. *Europace*. 2016;18:159-83.
5. Khan FZ, Virdee MS, Palmer CR, Pugh PJ, O'Halloran D, Elsik M, et al. Targeted left ventricular lead placement to guide cardiac resynchronization therapy: the TARGET study: a randomized, controlled trial. *J Am Coll Cardiol*. 2012;59:1509-1518.
6. Abu Daya H, Alam MB, Adelstein E, Schwartzman D, Jain S, Marek J, et al. Echocardiography-guided left ventricular lead placement for cardiac resynchronization therapy in ischemic vs nonischemic cardiomyopathy patients. *Heart Rhythm*. 2014;11:614-9.
7. Bogaard MD, Doevendans PA, Leenders GE, Loh P, Hauer RN, van Wessel H, et al. Can optimization of pacing settings compensate for a non-optimal left ventricular pacing site? *Europace*. 2010;12:1262-9.
8. van Everdingen WM, Cramer MJ, Doevendans PA, Meine M. Quadripolar Leads in Cardiac Resynchronization Therapy. *J Am Coll EP*. 2015:225-237.
9. Pappone C, Calovic Z, Vicedomini G, Cuko A, McSpadden LC, Ryu K, et al. Multipoint left ventricular pacing improves acute hemodynamic response assessed with pressure-volume loops in cardiac resynchronization therapy patients. *Heart Rhythm*. 2014;11:394-401.
10. Thibault B, Dubuc M, Khairy P, Guerra PG, Macle L, Rivard L, et al. Acute haemodynamic comparison of multisite and biventricular pacing with a quadripolar left ventricular lead. *Europace*. 2013;15:984-91.

11. Gold MR, Birgersdotter-Green U, Singh JP, Ellenbogen KA, Yu Y, Meyer TE, et al. The relationship between ventricular electrical delay and left ventricular remodelling with cardiac resynchronization therapy. *Eur Heart J*. 2011;32:2516-2524.
12. Singh JP, Fan D, Heist EK, Alabiad CR, Taub C, Reddy V, et al. Left ventricular lead electrical delay predicts response to cardiac resynchronization therapy. *Heart Rhythm*. 2006;3:1285-92.
13. Singh JP, Klein HU, Huang DT, Reek S, Kuniss M, Quesada A, et al. Left ventricular lead position and clinical outcome in the multicenter automatic defibrillator implantation trial-cardiac resynchronization therapy (MADIT-CRT) trial. *Circulation*. 2011;123:1159-66.
14. Kronborg MB, Johansen JB, Riahi S, Petersen HH, Haarbo J, Jorgensen OD, et al. An anterior left ventricular lead position is associated with increased mortality and non-response in cardiac resynchronization therapy. *Int J Cardiol*. 2016;222:157-62.
15. Strauss DG, Selvester RH, Wagner GS. Defining left bundle branch block in the era of cardiac resynchronization therapy. *Am J Cardiol*. 2011;107:927-34.
16. Bogaard MD, Meine M, Tuinenburg AE, Maskara B, Loh P, Doevendans PA. Cardiac resynchronization therapy beyond nominal settings: who needs individual programming of the atrioventricular and interventricular delay? *Europace*. 2012;14:1746-53.
17. Sohaib SM, Whinnett ZI, Ellenbogen KA, Stellbrink C, Quinn TA, Bogaard MD, et al. Cardiac resynchronisation therapy optimisation strategies: systematic classification, detailed analysis, minimum standards and a roadmap for development and testing. *Int J Cardiol*. 2013;170:118-31.
18. Helm RH, Byrne M, Helm PA, Daya SK, Osman NF, Tunin R, et al. Three-dimensional mapping of optimal left ventricular pacing site for cardiac resynchronization. *Circulation*. 2007;115:953-61.
19. Zanon F, Baracca E, Pastore G, Fraccaro C, Roncon L, Aggio S, et al. Determination of the longest inpatient left ventricular electrical delay may predict acute hemodynamic improvement in patients after cardiac resynchronization therapy. *Circ Arrhythm Electrophysiol*. 2014;7:377-83.
20. de Roest GJ, Allaart CP, Kleijn SA, Delnoy PP, Wu L, Hendriks ML, et al. Prediction of long-term outcome of cardiac resynchronization therapy by acute pressure-volume loop measurements. *Eur J Heart Fail*. 2013;15:299-307.
21. Sterlinski M, Sokal A, Lenarczyk R, Van Heuverswyn F, Rinaldi CA, Vanderheyden M, et al. In Heart Failure Patients with Left Bundle Branch Block Single Lead MultiSpot Left Ventricular Pacing Does Not Improve Acute Hemodynamic Response To Conventional Biventricular Pacing. A Multicenter Prospective, Interventional, Non-Randomized Study. *PLoS one*. 2016;11:e0154024.

22. Mafi Rad M, Blaauw Y, Dinh T, Pison L, Crijns HJ, Prinzen FW, et al. Different regions of latest electrical activation during left bundle-branch block and right ventricular pacing in cardiac resynchronization therapy patients determined by coronary venous electro-anatomic mapping. *Eur J Heart Fail.* 2014;16:1214-22.
23. Pluijmer M, Bovendeerd PH, Lumens J, Vernooij K, Prinzen FW, Delhaas T. New insights from a computational model on the relation between pacing site and CRT response. *Europace.* 2016;18:iv94-iv103.
24. Saxon LA, Olshansky B, Volosin K, Steinberg JS, Lee BK, Tomassoni G, et al. Influence of left ventricular lead location on outcomes in the COMPANION study. *J Cardiovasc Electrophysiol.* 2009;20:764-8.
25. Thebault C, Donal E, Meunier C, Gervais R, Gerritse B, Gold MR, et al. Sites of left and right ventricular lead implantation and response to cardiac resynchronization therapy observations from the REVERSE trial. *Eur Heart J.* 2012;33:2662-71.
26. de Roest GJ, Wu L, de Cock CC, Delnoy PP, Hendriks ML, van Rossum AC, et al. Bifocal left ventricular stimulation or the optimal left ventricular stimulation site in cardiac resynchronization therapy: a pressure-volume loop study. *Europace.* 2016;18:1030-7.
27. Shetty AK, Duckett SG, Ma YL, Kapetanakis S, Ginks M, Bostock J, et al. The acute hemodynamic response to LV pacing within individual branches of the coronary sinus using a quadripolar lead. *Pacing Clin Electrophysiol.* 2012;35:196-203.
28. Pappone C, Calovic Z, Vicedomini G, Cuko A, McSpadden LC, Ryu K, et al. Improving cardiac resynchronization therapy response with multipoint left ventricular pacing: Twelve-month follow-up study. *Heart Rhythm.* 2015;12:1250-8.
29. Zanon F, Marcantoni L, Baracca E, Pastore G, Lanza D, Fraccaro C, et al. Optimization of left ventricular pacing site plus multipoint pacing improves remodeling and clinical response to cardiac resynchronization therapy at 1 year. *Heart Rhythm.* 2016;13:1644-51.
30. Bogaard MD, Houthuizen P, Bracke FA, Doevendans PA, Prinzen FW, Meine M, et al. Baseline left ventricular dP/dtmax rather than the acute improvement in dP/dtmax predicts clinical outcome in patients with cardiac resynchronization therapy. *Eur J Heart Fail.* 2011;13:1126-32.

SUPPLEMENTAL MATERIAL

SUPPLEMENTARY RESULTS

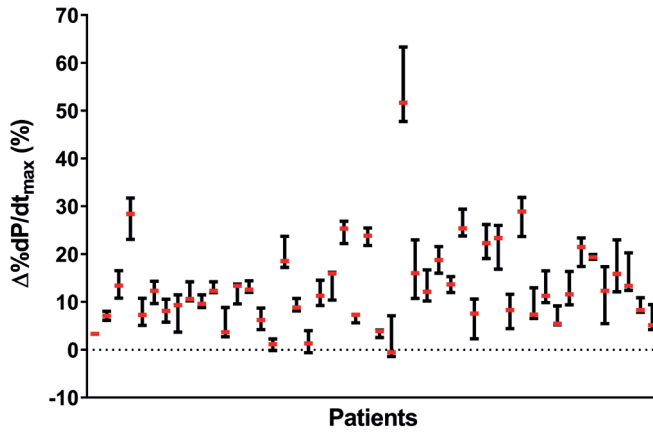
RESULTS FOR DP/dt_{MAX}

$\Delta\%dP/dt_{max}$ had a variation between electrodes of $4.9\pm 2.9\%$ (supplementary figure 1). In the GEE, higher QLV/QRSd values were not associated with changes in $\Delta\%dP/dt_{max}$. There was also no significant association of QLV or RVp-LVs with $\Delta\%dP/dt_{max}$. Neither was there an association with the electrode position in either the longitudinal or circumferential direction (supplementary table 1).

SUPPLEMENTARY TABLE 1. Prediction of change in %-change in dP/dt_{max}

Single variable models (GEE)			
	B	SE (95% CI)	p-value
QLV	-0.075	0.045 (-0.163-0.014)	0.100
QLV/QRSd	-0.003	0.030 (-0.061-0.014)	0.906
RVp-LVs	-0.001	0.016 (-0.033-0.002)	0.961
Combined model (GEE) anatomical position			
Longitudinal position			
Basal	0.925	0.734 (-0.525-2.375)	0.211
Mid	0.456	0.587 (-0.694-1.605)	0.437
Apical	0*		
Circumferential position			
Anterolateral	1.196	1.297 (-3.838-1.247)	0.318
Lateral	-0.735	0.738 (-2.183-0.712)	0.319
Posterolateral or posterior	0*		

The single variable models depict the results of the generalized estimated equation of separate each parameter. B: beta-coefficient. SE: standard error, CI: confidence interval. For other abbreviations: see table 1. *: set to zero because the parameter is redundant.

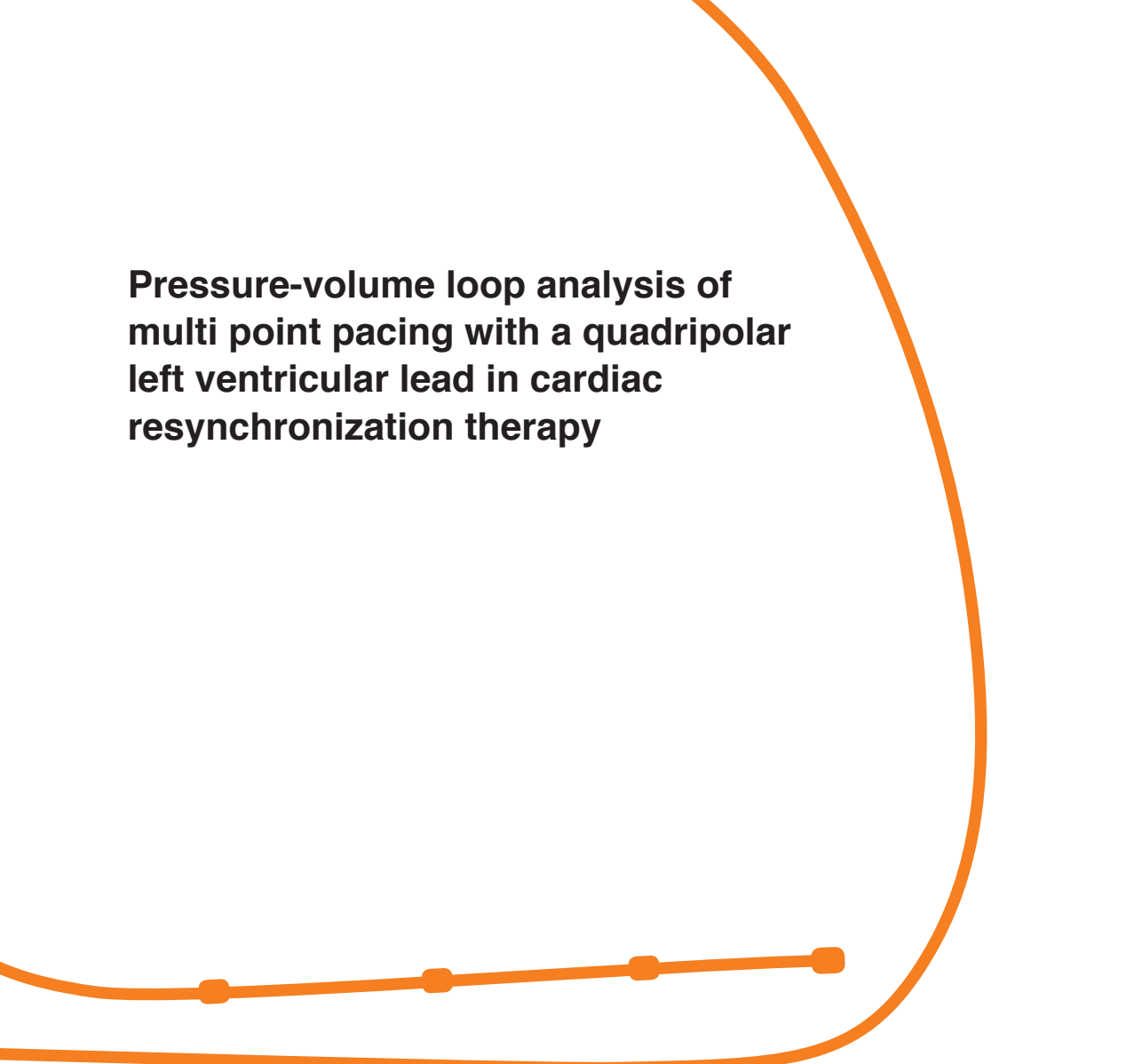


SUPPLEMENTARY FIGURE 1. Acute hemodynamic response (dP/dt_{max}) per patient

Smallest, largest and median %-change in dP/dt_{max} ($\Delta\%dP/dt_{max}$) per patient. The red dashes depict the median, upper and lower bars the smallest and largest value obtained with one of the four electrodes of the quadripolar LV lead. Patients are ranked in the same order as figure 4 and 5.

Can We Use the Intrinsic Left Ventricular Delay (QLV) to Optimize the Pacing Configuration for Cardiac Resynchronization Therapy with a Quadripolar Left Ventricular Lead?



A thick orange line starts from the top right, curves down and left, then curves back up and right, forming a large, open shape that frames the title. A horizontal orange line with four circular markers is positioned below the title.

Pressure-volume loop analysis of multi point pacing with a quadripolar left ventricular lead in cardiac resynchronization therapy

Wouter M. van Everdingen (MD)¹, Alwin Zweerink (MD)², Odette A.E. Salden (MD)¹, Maarten J. Cramer (MD, PhD)¹, Pieter A. Doevendans (MD, PhD)¹, Elien B. Engels (PhD)³, Albert C. van Rossum (MD, PhD)², Frits W. Prinzen (PhD)³, Kevin Vernooij (MD, PhD)⁴, Cornelis P. Allaart (MD, PhD)², Mathias Meine (MD, PhD)¹

¹ Department of Cardiology, University Medical Center Utrecht, Utrecht, The Netherlands

² Department of Cardiology, and Institute for Cardiovascular Research (ICaR-VU), VU University Medical Center, Amsterdam, The Netherlands

³ Department of Physiology, CARIM, Maastricht University, Maastricht, The Netherlands

⁴ Department of Cardiology, Maastricht University Medical Center, Maastricht, The Netherlands

Under revision

ABSTRACT

Background: Multi-point pacing (MPP) with a quadripolar left ventricular (LV) lead may increase response to cardiac resynchronization therapy (CRT).

Objectives: This study aimed to compare MPP to optimal biventricular pacing with a quadripolar LV lead and find factors associated with hemodynamic response to MPP.

Methods: Heart failure patients with a left bundle branch block underwent CRT implantation. Q to local LV sensing interval (QLV), corrected for QRS duration (QLV/QRSD) was measured. Invasive pressure-volume loops were assessed during four biventricular pacing settings and three MPP settings, using four atrioventricular delays. Hemodynamic response was defined as change in stroke work ($\Delta\%SW$) compared to baseline measurements during intrinsic conduction. $\Delta\%SW$ of MPP was compared to conventional biventricular using the distal electrode (BIV-CONV) and the electrode with highest change in $\Delta\%SW$ (BIV-OPT).

Results: Forty-three patients were analyzed (66 ± 10 years, 63% males, 30% ischemic cardiomyopathy (ICM), LV ejection fraction (LVEF) $29\pm 8\%$, and QRS-duration 175 ± 13 ms. QLV/QRSD was $84\pm 8\%$ and variation between LV electrodes $9\pm 5\%$. Compared to BIV-CONV, MPP showed a significant higher increase of SW ($\Delta\%SW +15\pm 35\%$, $p<0.05$) with a large interindividual variation. There was no significant difference in $\Delta\%SW$ with MPP compared to BIV-OPT ($-5\pm 24\%$, $p=0.19$). Male gender and low LVEF were associated with increase in $\Delta\%SW$ due to MPP vs. BIV-OPT in multivariate analysis, while ICM was only associated in univariate analysis.

Conclusion: Optimization of the pacing site of a quadripolar LV lead is more important than to program MPP. However, specific subgroups (i.e. males and low LVEF) do benefit substantially from MPP.

INTRODUCTION

Cardiac resynchronization therapy (CRT) is an established therapy for patients with heart failure and left ventricular (LV) conduction delay.¹ CRT aims to improve LV hemodynamic function by electromechanical resynchronization of LV contraction. Unfortunately, a considerable (30-40%) proportion of patients are considered non-responders to CRT.² Non-response has several causes, of which a suboptimal LV lead position is an important contributor.³ A suboptimal placed LV lead may reduce the effect of biventricular pacing on efficient electromechanical resynchronization.⁴ Several strategies have been suggested to optimize LV lead position, such as guided LV lead positioning, endocardial pacing, and multi-site pacing (i.e. LV pacing in more than one vein) or multi-point pacing.⁴⁻⁶ Multi-point pacing (MPP) implies pacing the LV free wall with two pacing stimuli, delivered by a single quadripolar LV lead. MPP might lead to a more homogeneous electromechanical activation and subsequently an additional improvement in LV function.^{7,8} MPP is proven to be beneficial compared to conventional biventricular pacing in terms of acute hemodynamic response, functional improvement and reverse remodeling.^{5,9-11} Although these results are promising, most studies did not compare MPP to the most optimal setting of biventricular pacing, as obtained with a quadripolar LV lead (BIV-OPT). Moreover, hemodynamic response of MPP varies among patients,¹² suggesting that patient specific differences (e.g. presence of ischemic cardiomyopathy or a low myocardial conduction velocity between electrodes) and/or therapy delivery (e.g. lead position) are factors contributing to the effect of MPP. The aim of this study was to compare the acute hemodynamic response of MPP, measured by invasive pressure-volume (PV) loops, to biventricular pacing using the electrode of quadripolar LV lead with highest increase in hemodynamic function. Patient characteristics, electrocardiographic and electro-anatomical parameters are correlated with MPP response. The hypothesis of this study is that patients with ischemic cardiomyopathy or those with an low myocardial conduction velocity between electrodes of a quadripolar LV lead will benefit to MPP, as the additional pacing site may cause a faster and/or more homogeneous depolarization of the LV.

METHODS AND MATERIALS

PATIENT COHORT

The Opticare-QLV trial is a multicenter observational study, which was performed in three university medical centers (University Medical Center Utrecht; VU University Medical Center, Amsterdam; and Maastricht University Medical Center, Maastricht; all in the Netherlands). Fifty-one patients planned for CRT implantation were prospectively enrolled. Inclusion criteria were moderate to severe heart failure (i.e. NYHA class II or III), LV ejection fraction $\leq 35\%$, optimal pharmacological therapy, sinus rhythm, and a left bundle branch block (LBBB) according to Strauss criteria.¹³ Exclusion criteria were presence of LV thrombus, severe aortic valve stenosis, or a mechanical aortic valve replacement. The study was performed according to the Declaration of Helsinki and in agreement with the local medical ethics committees. All subjects gave written informed consent.

BASELINE CHARACTERISTICS

Prior to implantation baseline characteristics were collected, among which laboratory tests (creatinine and BNP-levels), age, gender, NYHA functional class, PR interval, QRS duration, and QRS morphology. All patients underwent an echocardiographic examination and cardiac magnetic resonance imaging (CMR) before CRT implantation. Derived LV volumes were used to calibrate the conductance catheter-derived volumes. Type of cardiomyopathy was classified as dilated (DCM) or ischemic (ICM) using the definition of Felker et al.¹⁴ Patients with history of myocardial infarction or revascularization (CABG or PCI), with $\geq 75\%$ stenosis of left main or proximal LAD, or with $\geq 75\%$ stenosis of two or more epicardial vessels were categorized as ICM.

CRT IMPLANTATION

CRT implantation was performed under local anesthesia. The right atrial (RA) and right ventricular (RV) leads were placed transvenously at conventional positions. The quadripolar LV lead (Quartet 1458Q, St. Jude Medical, St. Paul, Minnesota, United States) was placed transvenously in one of the coronary veins overlying the LV free wall. An anterolateral, lateral, or posterolateral position was preferred. After electrophysiological measurements, the three leads were connected to a St. Jude Medical CRT-device.

ELECTROPHYSIOLOGICAL MEASUREMENTS

Electrophysiological (EP) measurements were performed using an on-site dedicated EP system. EP system settings (i.e. filter settings, gain, sampling frequency) of the three participating centers were matched to study protocols. Using the EP system, simultaneous registrations of the twelve-lead surface ECG and the three implanted leads were recorded. Temporary pacing was used to measure delays of specific pacing settings between electrodes, among which the Q on the surface ECG to LV sensing delay (QLV) and the ratio between QLV, QRS duration (QLV/QRSD) and local myocardial conduction velocity. Conduction time was measured as the pacing to sensing intervals between the four electrodes during LV only pacing with each separate electrode. The distances between the electrodes were used to obtain the conduction velocity. Conduction velocity below 0.70 m/s was considered 'slow', while all other values were considered normal.¹⁵

TABLE 1. Pacing configurations

Biventricular pacing (BIV)	Multi-point pacing (MPP)
LV-D1 – 40ms – RV	LV-D1 – 5ms – LV-P4 – 35ms – RV
LV-M2 – 40ms – RV	LV-D1 – 35ms – LV-P4 – 5ms – RV
LV-M3 – 40ms – RV	LV-P4 – 35ms – LV-D1 – 5ms – RV
LV-P4 – 40ms – RV	

All pacing configurations were tested with four atrioventricular delays. In case of non-capture or phrenic nerve stimulation, a different electrode pair with largest inter-electrode distance was used for MPP. LV: left ventricular, LV-D1: LV pacing with electrode D1, LV-M2: LV pacing with electrode M2, LV-M3: LV pacing with electrode M3, LV-P4: LV pacing with electrode P4, RV: right ventricular

HEMODYNAMIC MEASUREMENTS AND PACING PROTOCOL

Next, a dedicated PV-loop conductance catheter (CD Leycom, Zoetermeer, The Netherlands) was placed in the LV cavity after right femoral artery access. For all pacing settings, including MPP, the RV coil was used as anode and the interventricular delay between first LV pacing site and RV was kept constant at 40ms LV first (table 1). Biventricular pacing was performed with each quadripolar electrode separately as LV pacing site. MPP was programmed in three settings: 1) distal and proximal simultaneously (i.e. 5ms delay), 2) distal followed by proximal with a 35ms delay and 3) proximal followed by distal with a 35ms delay. The observed conduction delay between the two electrodes used for MPP was above 35ms in

all cases. MPP was conducted with the electrodes with the largest anatomical distance (e.g. usually D1 and P4) or any other combination with acceptable pacing thresholds and without phrenic nerve stimulation.

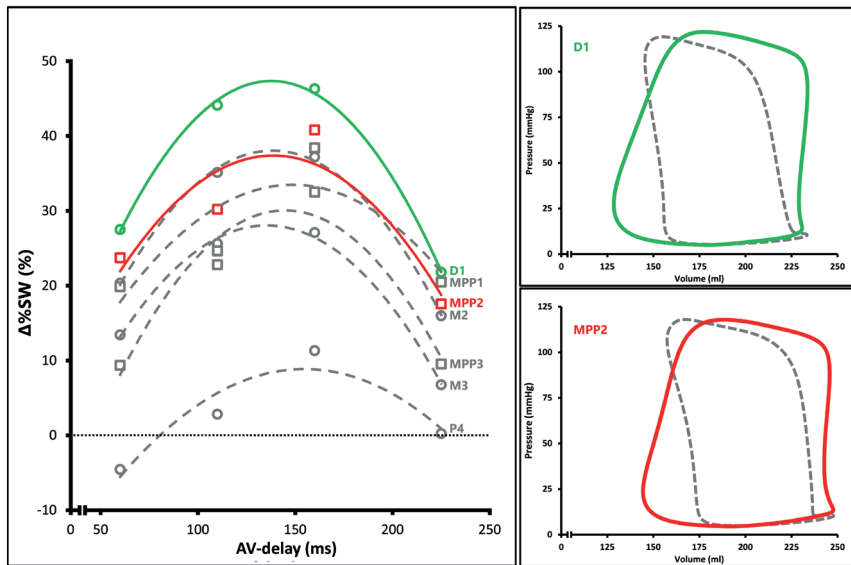


FIGURE 1. Optimization method based on pressure-volume loops

Left panel: Optimization curves during all pacing modes in one patient. broken lines represent parabolic lines fitted through the measured changes in stroke work compared to intrinsic conduction) during four atrioventricular (AV) delays. Results from biventricular pacing configurations are shown by circles and those from multi-point pacing (MPP) configurations by squares. In this patient biventricular pacing with D1 (green) was the optimal BIV configuration and MPP with D1-P4 with 35ms delay between both pacing stimuli (MPP2, red) the best MPP configuration. The corresponding pressure-volume (PV) loops are displayed in the right panels, broken lines representing PV loops of intrinsic conduction (right atrial pacing).

For each pacing mode, atrioventricular (AV) delays of 80%, 60%, 40% and 20% of the patient's intrinsic atrioventricular conduction (i.e. RA pacing to RV sensing delay) were used. PV-loops were recorded during pacing 5 to 10 bpm above intrinsic rhythm, for 60 beats during pacing settings and for 30 beats during baseline references of right atrial pacing. Stroke work (SW) was calculated as the surface of the recorded PV-loops. The change in SW ($\Delta\%SW$) of each pacing setting was calculated compared to the adjacent baseline references. The $\Delta\%SW$ of the four different AV delays of a single pacing configuration was plotted and a 2nd order polynomial line was fitted. The peak of the parabola was used as

maximal increase in $\Delta\%SW$ of the specific pacing setting (figure 1). The same method was used for the maximal value of the first derivative of LV pressure (dP/dt_{\max}). This method reduces measurement variability and allows for reliable estimation of the optimal AV delay and maximal achievable increase in stroke work.¹⁶ Patients were excluded from the final analysis if the PV-loop during baseline measurements showed crossing sections and large end-diastolic tails. The loops are the result of poor measurement of volume changes and lead to underestimation of stroke work during intrinsic LBBB. Underestimation of baseline values leads to unreliable high increases in $\Delta\%SW$, as the PV-loops often increase to normal shape during biventricular pacing.

Response to MPP was defined as the change in $\Delta\%SW$ compared to either conventional biventricular pacing using the most distal electrode (BIV-CONV), or as change in $\Delta\%SW$ compared to biventricular pacing with the electrode of the quadripolar lead with highest change in $\Delta\%SW$ (BIV-OPT).

LEAD POSITION

After lead placement, fluoroscopy images were made in the left anterior oblique (LAO) 40° and in the in the right anterior oblique (RAO) 30° angle to determine the specific position of each quadripolar LV lead electrode. The LV was divided in six segments in the circumferential direction (septal, anterior, anterolateral, lateral, posterolateral, and posterior) on the LAO view and in three segments (basal, mid, and apical) on the RAO view.¹⁷

STATISTICAL ANALYSIS

Statistical analysis was performed using SPSS (SPSS statistics 23.0, IBM, New York, USA). Patients were classified with a benefit of MPP if $\Delta\%SW$ of MPP was higher than $\Delta\%SW$ of BIV-OPT, the remaining patients were classified as those without benefit of MPP. The univariate relation of predictors for change in $\Delta\%SW$ due to MPP were analyzed using linear regression, both for change compared to BIV and compared to BIV-OPT. Univariate predictors with a p-value <0.10 were tested in a multivariate analysis. The relation of variables with response to MPP was analyzed using a T-test or Mann-Whitney U-test, dependent on normality of data, or a Chi-Square test in case of categorical variables. The optimal AV delays and hemodynamic effect of pacing strategies analyzed with a paired T-test or Wilcoxon signed rank test, depending on normality of data. Mean \pm standard deviation or median and interquartile range are given, depending on normality of data. A p-value below 0.05 was considered significant for all tests.

RESULTS

Fifty-one patients were included in the study, of whom eight were excluded from this analysis. Three of the excluded patients had considerable underestimation of the PV-loop during intrinsic rhythm. Two patients did not receive MPP due to a technical error during the pacing protocol. Three more patients were excluded due to large baseline drift of SW measurements between biventricular pacing and the MPP pacing configurations.

In the remaining 43 patients there were 63% male ($n=27$) and 30% ($n=13$) with an ischemic etiology of heart failure (table 2). PR duration was 183 ± 32 ms, QRS duration was 175 ± 13 ms. QLV of the electrode with highest value was 147 ± 16 ms, with a QLV/QRSD ratio of $84\pm 8\%$. LV dimensions were enlarged (end-diastolic volume 208 ± 62 ml, LV end-systolic volume 154 ± 56 ml), and systolic function was impaired (LV ejection fraction $29\pm 8\%$). CMR images were available in 40 patients, of whom 8 had evidence of delayed enhancement. There was no statistical significant difference in the amount of patients with scar, nor in scar size, between patients with and without a positive effect of MPP compared to BIV-OPT.

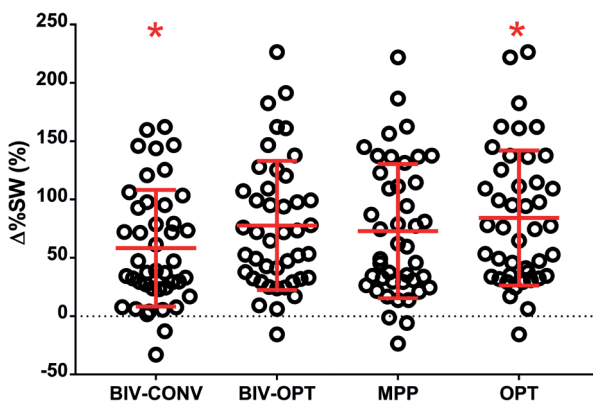


FIGURE 2. Acute hemodynamic effect of four optimization strategies

Acute hemodynamic effect in percentage change of stroke work ($\Delta\%SW$) of biventricular pacing with the distal electrode (BIV-CONV), with the optimal electrode (BIV-OPT), multi-point pacing (MPP) or the optimal setting (OPT). The optimal setting is either MPP or BIV-OPT. *: statistically significant increase in $\Delta\%SW$ compared to all other strategies in a paired t-test ($p < 0.01$).

TABLE 2. Baseline characteristics

Parameter	Analyzed patients (n=43)	Patients without benefit of MPP (n=26)	Patients with benefit of MPP (n=17)	p-value
Age	66±10	66±10	65±9	0.750
Sex (n, % of male)	27 (63%)	13 (50%)	14 (82%)	0.032
Cardiomyopathy (n, % of ICM)	11 (26%)	6 (23%)	5 (29%)	0.642
Scar (n, %)	8 (19%)	6 (24%)	2 (13%)	0.414
Scar size* (%)	9 (2-19)	9 (4-16)	11 (1-20)	1.000
NYHA-class (n, %)				
II	29 (67%)	18 (69%)	12 (71%)	0.722
III	14 (33%)	8 (31%)	5 (29%)	
PR duration (ms)	183±32	181±24	185±41	0.717
QRS duration (ms)	175±13	173±14	177±12	0.280
Max QLV (ms)	147±16	146±17	148±15	0.691
Max QLV/QRSd (%)	84±8	85±9	84±5	0.624
QLV/QRSd variation (%)	9±5	10±5	8±4	0.187
Conduction velocity (m/s)	0.60±0.20	0.67±0.28	0.51±0.12	0.014
LV EDV (ml)	209±62	191±43	235±77	0.044
LV ESV (ml)	151±57	134±39	178±70	0.029
LV EF (%)	29±8	31±9	26±6	0.031
Creatinine (µmol/L)	87±21	84±24	92±15	0.218
Log BNP	1.85±0.49	1.8±0.41	1.99±0.60	0.212
Medication (n, %)				
ACE-inhibitor or ATII-antagonist	42 (98%)	26 (100%)	16 (94%)	0.211
Beta-blocker	36 (84%)	20 (77%)	15 (88%)	0.351
Diuretics	30 (70%)	16 (62%)	13 (76%)	0.307
Aldosterone-antagonists	25 (58%)	16 (62%)	11 (65%)	0.834
Anti-coagulants	27 (43%)	13 (50%)	13 (76%)	0.083
Comorbidities (n, %)				
Hypertension	15 (35%)	12 (46%)	3 (18%)	0.055
Renal dysfunction	3 (7%)	1 (4%)	2 (12%)	0.820
Circumferential electrode position (n, %)				
Anterior	0	0	0	0.152
Anterolateral	31 (19%)	22 (22%)	9 (14%)	
Lateral	96 (58%)	52 (51%)	44 (67%)	
Posterolateral	37 (22%)	24 (24%)	13 (20%)	
Posterior	3 (2%)	3 (3%)	0	
Longitudinal electrode position (n, %)				
Basal	55 (33%)	34 (34%)	21 (32%)	0.124
Mid	89 (53%)	49 (49%)	50 (76%)	
Apical	23 (14%)	18 (18%)	5 (8%)	

Multi-point pacing (MPP) responders and non-responders are defined by a positive or negative change in stroke work (Δ SW) between biventricular pacing with the electrode with highest change in Δ SW and highest increase in Δ SW with MPP. The p-value of the comparison of patients with a benefit and those without a benefit of MPP compared to BIV-OPT is depicted in the last column. ACE: angiotensin converter enzyme, ATII: angiotensin receptor II, BIV-OPT: optimal change in Δ SW with biventricular pacing, EDD: end-diastolic diameter, EDV: end-diastolic volume, ESV: end-systolic volume, EF: ejection fraction, ICM: ischemic cardiomyopathy, Log-BNP: 10th logarithmic conversion of Brain Natriuretic Peptide, LV: left ventricular, NYHA-class: New York Heart Association functional class, SW: stroke work, QLV: Q to LV sensing delay. QLV/QRSd: ratio between QLV and intrinsic QRS duration. *: scar size in patients with scar on late gadolinium enhanced images.

During biventricular pacing, the largest $\Delta\%SW$ was achieved with electrode D1 in fifteen (35%), M2 in eight (19%), M3 in five (12%) and P4 in fifteen (35%) patients. MPP was applied using electrode D1 and M3 in three patients (7%) and with D1 and P4 in all other patients. Thirty-one (72%) patients showed a larger $\Delta\%SW$ during MPP than during BIV-CONV pacing and seventeen (40%) showed a larger $\Delta\%SW$ during MPP than during BIV-OPT (table 3 and figure 2). MPP increased $\Delta\%SW$ significantly ($+15\pm 35\%$, $p<0.05$) as compared to BIV-CONV pacing, but there was no significant change between MPP and BIV-OPT ($-5\pm 24\%$, $p=0.19$). The $\Delta\%SW$ due to MPP compared to BIV-OPT was heterogeneous, being larger than 10% in sixteen patients, larger than 10% in nine patients and eighteen patients showing a decrease in $\Delta\%SW$ larger than 10%. A heterogeneous effect was also seen for changes in $\%dP/dt_{\max}$ (figure 3). There was a large variation in response to MPP compared to BIV-OPT (figure 4). $\Delta\%dP/dt_{\max}$ of MPP was not significantly different from BIV-CONV ($-0.2\pm 4.0\%$, $p=0.71$), whereas it was significantly lower for MPP compared to BIV-OPT (-1.8 ± 3.8 , $p<0.01$). There were no significant differences in the AV delay with highest change in $\Delta\%SW$ between pacing configurations. The optimal AV delay for BIV-CONV was: $133\pm 43\text{ms}$, BIV-OPT: $120\pm 37\text{ms}$, MPP: $129\pm 36\text{ms}$ (BIV-CONV vs. BIV-OPT: $p=0.15$, BIV-CONV vs. MPP: $p=0.17$, BIV-OPT vs. MPP $p=0.65$).

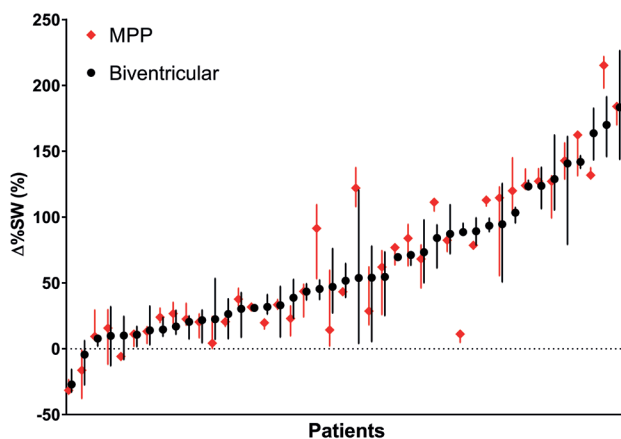


FIGURE 3. Acute hemodynamic effect of biventricular pacing and multi-point pacing per patient

Change in stroke work ($\Delta\%SW$) of biventricular pacing (black circles) and multi-point pacing (MPP) (red diamonds). The symbols depicts the median value of the four BIV settings and of the three MPP settings, while lowest and highest values of BIV and MPP are displayed by bars. $\Delta\%SW$: percentage change in stroke work as compared to reference measurements. Patients are sorted by the mean increase in $\Delta\%SW$ during biventricular pacing.

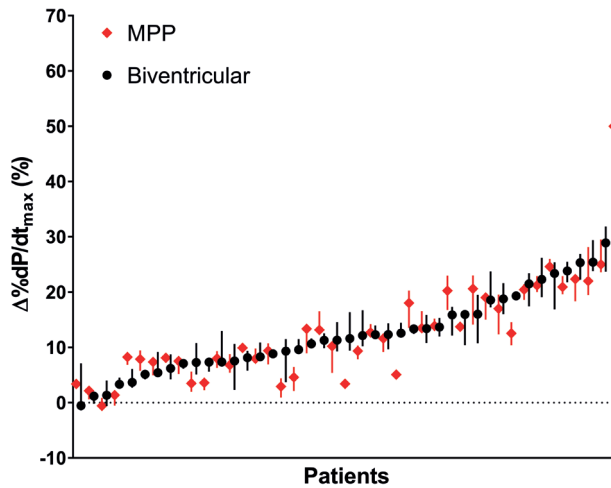


FIGURE 4. Change in dP/dt_{max} of biventricular site pacing and multi-point pacing per patient

Change in $\%dP/dt_{max}$ of biventricular pacing (black circles) and multi-point pacing (MPP) (red diamonds) is given. The medians of four BIV settings and three MPP settings are displayed by the symbol, while lowest and highest value are displayed by bars. $\%dP/dt_{max}$: percentage change in maximal rate of LV pressure rise.

TABLE 3. Effect of pacing strategies on acute hemodynamic response

Strategy	All patients (n=43)	Patients without benefit of MPP (n=26)	Patients with benefit of MPP (n=17)	p-value
BIV-CONV ($\Delta\%SW$)	58±50	55±53	64±46	0.568
BIV-OPT ($\Delta\%SW$)	78±55	78±59	78±50	0.960
MPP ($\Delta\%SW$)	73±58	59±56	94±56	0.035
Differences				
BIV-OPT vs. BIV-CONV ($\Delta\%SW$)	19±27 [†]	25±5 [†]	14±29*	0.170
MPP vs. BIV-CONV ($\Delta\%SW$)	15±35*	5±32	30±34 [†]	0.012
MPP vs. BIV-OPT ($\Delta\%SW$)	-5±24	-19±18 [†]	16±15 [†]	<0.001

Multi-point pacing (MPP) responders and non-responders are defined by a positive or negative change in stroke work ($\Delta\%SW$) between biventricular pacing with the electrode with highest change in $\Delta\%SW$ and highest increase in $\Delta\%SW$ with MPP. In the last column, the p-value is depicted for the comparison of MPP responders and non-responders. $\Delta\%SW$: percentage change in stroke work. BIV: biventricular pacing with the distal electrode (D1) of the quadripolar left ventricular lead, BIV-OPT: biventricular pacing with the electrode with highest change in $\Delta\%SW$, MPP: multi-point pacing. Effects between groups were compared with a Mann-Whitney U test and corresponding p-values are shown in the rightmost column. Effects within a group were compared with a Wilcoxon signed rank test, with: *: p<0.05 between two strategies. †: p<0.001 between two strategies.

Patients with a positive effect of MPP compared to BIV-OPT were more often male, had larger LV end-diastolic and end-systolic volume, a lower LV ejection fraction, and lower myocardial conduction velocity (table 2). Male patients and those with ICM also had a larger $\Delta\%SW$ of MPP vs. BIV-OPT (figure 5). Increase in $\Delta\%SW$ tended to be higher for those with low conduction speed ($p=0.055$). Patients with a positive response to MPP vs. BIV-OPT tended to have distal electrodes (D1) in a mid-position (15 mid and 2 apical), while patients with a negative response had a more evenly distributed D1 position (16 mid and 10 apical, $p=0.056$). Univariate analysis of linear regression showed significant association of LV ejection fraction, type of cardiomyopathy and sex with change in $\Delta\%SW$ of MPP vs. BIV-OPT (table 4). End-diastolic volume, QRS duration, QLV/QRSD, scar size and conduction velocity were not associated with change in $\Delta\%SW$ of MPP vs. BIV-OPT. Multivariate analysis confirmed that LV ejection fraction and male sex were independent predictors for hemodynamic response of MPP compared to BIV-OPT, while type of cardiomyopathy was not included in the model.

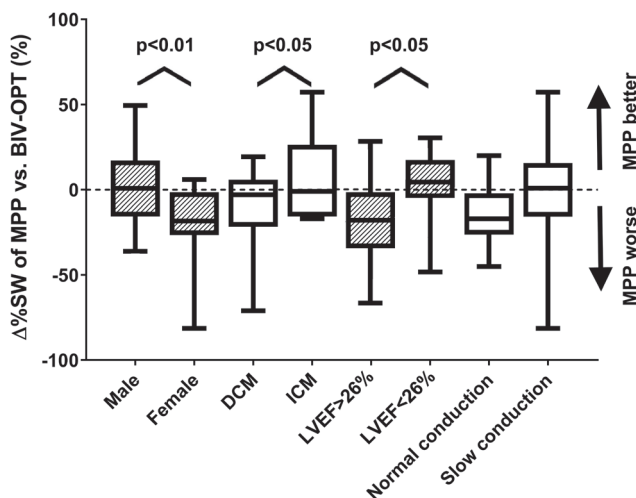


FIGURE 5. Response to MPP vs. BIV-OPT for four categorical variables

%-Change in stroke work ($\Delta\%SW$) of multi-point pacing (MPP) vs. optimal biventricular pacing with one of the electrodes of the quadripolar lead (BIV-OPT). Conduction speed is categorized in fast ($\geq 0.7m/s$) and slow ($< 0.7m/s$) myocardial conduction between the electrodes of a quadripolar lead. DCM: dilated cardiomyopathy. For other abbreviations, see table 1. *: $p < 0.05$ for a Mann-Whitney U-test between indicated categories, †: $p < 0.01$ between indicated categories.

TABLE 4. Univariate and multivariate models for predictors of response to MPP vs. BIV-OPT

Univariate analysis				
	B	SE	R	p-value
Sex (male)	19.16	6.95	0.40	0.009
Cardiomyopathy (ICM)	17.05	7.95	0.32	0.038
Scar size (%)	0.03	0.71	0.01	0.970
LV EDV (ml)	0.06	0.06	0.16	0.306
LV EF (%)	-0.95	0.42	0.33	0.030
Conduction velocity (m/s)	-0.17	0.16	0.17	0.293
QLV/QRSd (%)	3.12	47.1	0.01	0.948
QRS duration (ms)	-0.07	0.28	0.04	0.793
Multivariate analysis				
	B	SE	R	p-value
Sex (male)	17.59	6.72	0.40	0.012
LV EF (%)	-0.83	0.40	0.49	0.042
Cardiomyopathy (ICM)	.	.	.	0.184

Univariate analysis depicts the values of linear regression of the specific parameter and change in $\Delta\%SW$ between MPP and biventricular pacing with the electrode with highest change in $\Delta\%SW$ (BIV-OPT). Multivariate forward analysis incorporates the parameters with a $p < 0.10$ in the univariate analyses. R value of the multivariate analysis indicates the R value of the model with incorporation of that parameter. Sex was incorporated first, LV EF second. B: beta-coefficient, SE: standard error, R: correlation coefficient. For other abbreviations, see table 2.

DISCUSSION

The acute hemodynamic response of MPP compared to biventricular pacing with the distal electrode (BIV-CONV) showed a significant improvement. The effect of MPP compared to the optimal configuration of a quadripolar LV lead (BIV-OPT) showed no overall benefit. These findings indicate that optimization of the LV site for biventricular pacing with a quadripolar lead is of primary importance. MPP may have additional benefit in a sub-selection of patients, specifically males and those having a low LV ejection fraction.

THE EFFECT OF MULTI-POINT PACING

While MPP was beneficial compared to conventional CRT, we found a heterogeneous and non-significant hemodynamic effect of MPP compared to CRT with the optimal configuration of a quadripolar LV lead. As we optimized the atrioventricular delay and tested each pacing site of a quadripolar LV lead for biventricular pacing, the additional effect of MPP compared to BIV-OPT was low in our study. Our results are however comparable to a study in which atrioventricular delay optimization was used and all biventricular pacing sites were compared to MPP.¹⁸ While some studies also indicate that response to MPP is heterogeneous among patients,^{12,18} Zanon et al. found a small but significant increase in acute hemodynamic response (i.e. dP/dt_{max}) with MPP compared to unifocal LV paced sites in all patients.⁵ We used both SW and dP/dt_{max} and found a variation in the effect of MPP with both indices (figure 2 and 3). Pappone et al. also used stroke work derived from pressure-volume loops and showed that the best of seven MPP settings improved hemodynamic function more than biventricular pacing with only the distal or proximal electrode of a quadripolar LV lead.⁹ These findings are in line with our results, as we found that MPP resulted in higher $\Delta\%SW$ benefit than BIV-CONV. As we found no benefit of three MPP settings compared to four BIV settings, a single optimized pacing site may be ideal for CRT. The presence of an ideal location for biventricular pacing which cannot be improved by multiple LV pacing sites has been put forward by Ploux et al.⁷ Finding the optimal biventricular pacing configuration is of primary importance. Although we still need tools to select the optimal biventricular pacing configuration, one well-placed lead is potentially better than adding extra pacing sites to a suboptimal placed lead. Generally, patients benefit most from an optimized single LV pacing site, but some benefit from MPP. The effect of LV pacing site optimization is therefore heterogeneous and requires a patient tailored approach.

PREDICTING MPP RESPONSE

Specific subsets of patients might benefit of MPP, as we observed that especially male patients and those with lower ejection fraction benefited from MPP. Gender was the strongest predictor in the multivariate analysis, possibly because males more often had ICM (50% vs. 13%, $p=0.17$) and larger hearts (LV EDV: 223 ± 68 vs. 184 ± 42 ml, $p<0.05$). The additional electrical wave front of MPP may lead to a more homogeneous and/or faster depolarization of the enlarged LV free wall. Also, differences in cardiac size have shown to modify the effect of QRS duration on CRT response.^{19,20} Although LV EDV was higher

in MPP responders, LV EDV did not have an association with the percentage change in $\Delta\%SW$ of MPP vs. BIV-OPT in our study. MPP could also be beneficial in ventricles with heterogeneous conduction, potentially caused by myocardial fibrosis. The direct effect of scar burden on the hemodynamic benefit of MPP was shown in computer simulations.²¹ These results were confirmed in a patient study with posterolateral scar,²² and in patients with ICM in general in several other studies.^{18,23,24} Sohal et al. observed that only non-LBBB patients converted from hemodynamic non-responders with conventional CRT to multi-site pacing responders.²⁴ This may partly be explained by the prevalence of ICM which is higher in non-LBBB patients resulting in a more heterogeneous conduction of the left ventricle.²⁵ As we only included patients with a 'strict' LBBB using Strauss criteria,¹³ the prevalence of patients with substantial myocardial scar in our study was relatively low. Implementation of our methods in CRT candidates without strict LBBB is of interest, as the scar burden is potentially larger in these patients.^{21,26}

We used the electrodes with largest inter-electrode distance for MPP, which were the most valuable electrodes for MPP in prior studies.^{11,12} As the effect of MPP with a quadripolar LV lead may be dependent on the electrode spacing, the effect of inter-electrode distance and the number of electrodes on an LV lead are also of interest for future work. Several manufacturers, including the one used in this study, have developed quadripolar leads with varying electrode spacing. Larger electrode spacing may facilitate a better distribution of electrodes over the LV wall. Nonetheless, the effective electrode spacing is limited by the coronary venous anatomy. Large electrode spacing may result in non-capture in case of short tributary branches. We already observed non-capture on the proximal electrode in three patients with the electrode spacing (i.e. 47mm) of the current quadripolar lead.

MPP might be used to further optimize hemodynamic response in subgroups of patients. However, in the current patient population (i.e. strict LBBB), only one patient converted from non-responder with BIV-OPT to a responder with MPP using the 20% increase in $\Delta\%SW$ cut-off value defined by De Roest et al. ($\Delta\%SW$ of BIV-OPT: 9%, MPP: 29%).²⁷ However, three patients became a non-responder with MPP, while they were classified as responder to BIV-OPT. Physicians should therefore first test the acute effect of biventricular pacing with each separate electrode of the quadripolar lead. MPP may then be implemented if the benefit of biventricular pacing is lower than desired, especially in patients with an ischemic etiology of heart failure, male patients and those with very low LV ejection fraction. Nevertheless, MPP should not be programmed blindly, as it can have a detrimental effect on

hemodynamic response. The hemodynamic effect of MPP should therefore always be tested, moreover as it increases battery drainage. As PV-loop recordings are not standard clinical practice, testing of the hemodynamic effect of MPP should be performed by, preferably non-invasive, assessment of cardiac function such as the plethysmographic method of Kyriacou et al.²⁸

LIMITATIONS

There are some limitations to take into account. Owing to the use of invasive measurements the sample size of this study is relatively small and the time period of inclusion relatively long. The strict LBBB criteria resulted in a selection of patients with a class I indication for CRT and a low number of patients with ICM.²⁹ The results regarding patients with ICM should therefore be interpreted with caution. Patients with ICM and pronounced areas of scar were therefore prone to be excluded, while they might benefit more from MPP. Although patients with ICM often had only small areas of myocardial scar, the etiology of heart failure in these patients is different from DCM. Pressure-volume loop analysis with various AV-delays and pacing modes was time-consuming. The study protocol was therefore shortened by the use of a fixed offset of 40ms LV first. The interventricular delay might have influenced results, although an offset of 40ms is preferable in most CRT patients.³⁰ Due to the implantation protocol, most LV leads were placed in a favorable segment (i.e. anterolateral, lateral or posterolateral). The intra- and inter-individual differences between studied parameters was therefore relatively small, although it also reflects clinical practice. Pressure-volume loop analysis of MPP was always performed after biventricular pacing modes and therefore not randomized. Although randomization is preferred to reduce bias by baseline drift of the catheter, pacing configurations were performed in a fixed order to reduce programming errors. Nevertheless, the effect of baseline drift was compensated by the repeated reference measurements before and after each BIV or MPP pacing configuration. Furthermore, to minimize the effect that excessive baseline drift might have on the results, three patients with considerable drift between BIV modes and MPP were excluded from the analysis.

CONCLUSION

In patients with typical LBBB, the acute hemodynamic response of MPP compared to biventricular pacing with the distal electrode showed a significant improvement. The effect of MPP compared to the optimal configuration of a quadripolar LV lead showed no overall benefit. Therefore, optimization of the LV site for biventricular pacing with a quadripolar lead is of primary importance. Nevertheless, MPP may have additional benefit in a specific sub-selection of patients.

REFERENCES

1. Brignole M, Auricchio A, Baron-Esquivias G et al. 2013 ESC Guidelines on cardiac pacing and cardiac resynchronization therapy. *Eur Heart J* 2013;34:2281-2329.
2. Wilkoff BL, Fauchier L, Stiles MK et al. 2015 HRS/EHRA/APHRS/SOLAECE expert consensus statement on optimal implantable cardioverter-defibrillator programming and testing. *Europace* 2016;18:159-83.
3. Mullens W, Grimm RA, Verga T et al. Insights from a cardiac resynchronization optimization clinic as part of a heart failure disease management program. *J Am Coll Cardiol* 2009;53:765-73.
4. Khan FZ, Virdee MS, Palmer CR et al. Targeted left ventricular lead placement to guide cardiac resynchronization therapy: the TARGET study: a randomized, controlled trial. *J Am Coll Cardiol* 2012;59:1509-1518.
5. Zanon F, Baracca E, Pastore G et al. Multipoint pacing by a left ventricular quadripolar lead improves the acute hemodynamic response to CRT compared with conventional biventricular pacing at any site. *Heart Rhythm* 2015;12:975-81.
6. Shetty AK, Sohal M, Chen Z et al. A comparison of left ventricular endocardial, multisite, and multipolar epicardial cardiac resynchronization: an acute haemodynamic and electroanatomical study. *Europace* 2014:873-879.
7. Ploux S, Strik M, van Hunnik A, van Middendorp L, Kuiper M, Prinzen FW. Acute electrical and hemodynamic effects of multisite left ventricular pacing for cardiac resynchronization therapy in the dyssynchronous canine heart. *Heart rhythm* 2014;11:119-25.
8. van Everdingen WM, Cramer MJ, Doevendans PA, Meine M. Quadripolar Leads in Cardiac Resynchronization Therapy. *J Am Coll EP* 2015:225-237.
9. Pappone C, Calovic Z, Vicedomini G et al. Multipoint left ventricular pacing improves acute hemodynamic response assessed with pressure-volume loops in cardiac resynchronization therapy patients. *Heart Rhythm* 2014;11:394-401.
10. Zanon F, Marcantoni L, Baracca E et al. Optimization of left ventricular pacing site plus multipoint pacing improves remodeling and clinical response to cardiac resynchronization therapy at 1 year. *Heart Rhythm* 2016;13:1644-51.
11. Pappone C, Calovic Z, Vicedomini G et al. Multipoint left ventricular pacing in a single coronary sinus branch improves mid-term echocardiographic and clinical response to cardiac resynchronization therapy. *J Cardiovasc Electrophysiol* 2015;26:58-63.

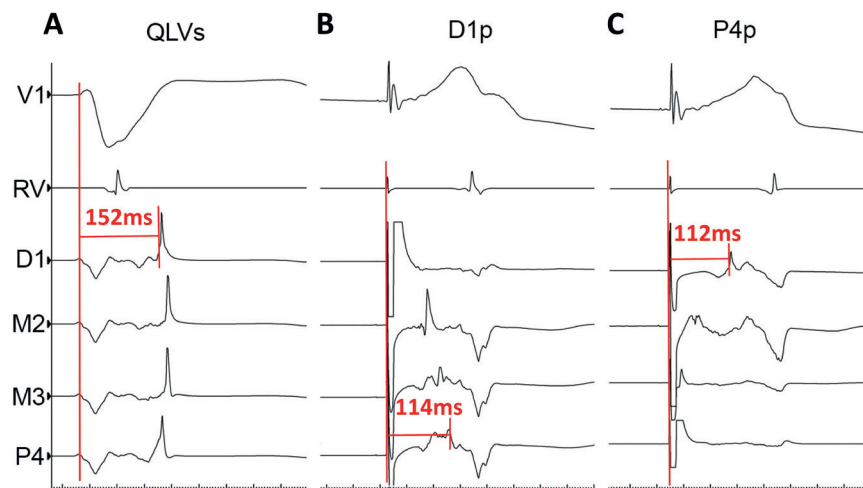
12. Thibault B, Dubuc M, Khairy P et al. Acute haemodynamic comparison of multisite and biventricular pacing with a quadripolar left ventricular lead. *Europace* 2013;15:984-91.
13. Strauss DG, Selvester RH, Wagner GS. Defining left bundle branch block in the era of cardiac resynchronization therapy. *Am J Cardiol* 2011;107:927-34.
14. Felker GM, Shaw LK, O'Connor CM. A standardized definition of ischemic cardiomyopathy for use in clinical research. *J Am Coll Cardiol* 2002;39:210-8.
15. Anderson KP, Walker R, Urie P, Ershler PR, Lux RL, Karwande SV. Myocardial electrical propagation in patients with idiopathic dilated cardiomyopathy. *J Clin Invest* 1993;92:122-40.
16. Sohaib SM, Whinnett ZI, Ellenbogen KA et al. Cardiac resynchronisation therapy optimisation strategies: systematic classification, detailed analysis, minimum standards and a roadmap for development and testing. *Int J Cardiol* 2013;170:118-31.
17. Bogaard MD, Doevendans PA, Leenders GE et al. Can optimization of pacing settings compensate for a non-optimal left ventricular pacing site? *Europace* 2010;12:1262-9.
18. Sterlinski M, Sokal A, Lenarczyk R et al. In Heart Failure Patients with Left Bundle Branch Block Single Lead MultiSpot Left Ventricular Pacing Does Not Improve Acute Hemodynamic Response To Conventional Biventricular Pacing. A Multicenter Prospective, Interventional, Non-Randomized Study. *PloS one* 2016;11:e0154024.
19. Varma N, J. L, He J, Niebauer M, Manne M, Tchou P. Sex-Specific Response to Cardiac Resynchronization Therapy. *J Am Coll EP* 2017;3:844-853.
20. Zweerink A, Wu L, de Roest GJ et al. Improved patient selection for cardiac resynchronization therapy by normalization of QRS duration to left ventricular dimension. *Europace* 2017;19:1508-1513.
21. Niederer SA, Shetty AK, Plank G et al. Biophysical modeling to simulate the response to multisite left ventricular stimulation using a quadripolar pacing lead. *Pacing Clin Electrophysiol* 2012;35:204-14.
22. Ginks MR, Duckett SG, Kapetanakis S et al. Multi-site left ventricular pacing as a potential treatment for patients with postero-lateral scar: insights from cardiac magnetic resonance imaging and invasive haemodynamic assessment. *Europace* 2011;14:373-9.
23. Ginks MR, Shetty AK, Lambiase PD et al. Benefits of endocardial and multisite pacing are dependent on the type of left ventricular electric activation pattern and presence of ischemic heart disease: insights from electroanatomic mapping. *Circulation Arrhythmia and electrophysiology* 2012;5:889-97.

24. Sohal M, Shetty A, Niederer S et al. Mechanistic insights into the benefits of multisite pacing in cardiac resynchronization therapy: The importance of electrical substrate and rate of left ventricular activation. *Heart Rhythm* 2015;12:2449-57.
25. Zareba W, Klein H, Cygankiewicz I et al. Effectiveness of Cardiac Resynchronization Therapy by QRS Morphology in the Multicenter Automatic Defibrillator Implantation Trial-Cardiac Resynchronization Therapy (MADIT-CRT). *Circulation* 2011;123:1061-72.
26. Derval N, Duchateau J, Mahida S et al. Distinctive Left Ventricular Activations Associated With ECG Pattern in Heart Failure Patients. *Circ Arrhythm Electrophysiol* 2017;10.
27. deRoest GJ, Allaart CP, Kleijn SA et al. Prediction of long-term outcome of cardiac resynchronization therapy by acute pressure-volume loop measurements. *Eur J Heart Fail* 2013;15:299-307.
28. Kyriacou A, Pabari PA, Whinnett ZI et al. Fully automatable, reproducible, noninvasive simple plethysmographic optimization: proof of concept and potential for implantability. *Pacing Clin Electrophysiol* 2012;35:948-60.
29. Russo AM, Stainback RF, Bailey SR et al. ACCF/HRS/AHA/ASE/HFSA/SCAI/SCCT/SCMR 2013 appropriate use criteria for implantable cardioverter-defibrillators and cardiac resynchronization therapy. *J Am Coll Cardiol* 2013;61:1318-68.
30. Bogaard MD, Meine M, Tuinenburg AE, Maskara B, Loh P, Doevendans PA. Cardiac resynchronization therapy beyond nominal settings: who needs individual programming of the atrioventricular and interventricular delay? *Europace* 2012;14:1746-53.

SUPPLEMENTAL MATERIAL

SUPPLEMENTAL METHODS

Measurement of myocardial conduction velocity was performed using the proximal and distal electrodes of the quadripolar left ventricular (LV) lead. LV only pacing with a short AV delay (20ms) was performed and intracardiac electrograms (IEGMs) were recorded. The interval between pacing artefact and local depolarization was measured from one end to the other by pacing at the proximal electrode and sensing at the distal electrode, and vice versa (supplemental figure 1). Time intervals were averaged and divided by the electrode distance measured on fluoroscopy. The right anterior oblique view offers a good approximation of the inter electrode distance. The distance between the mid electrodes (10mm) was used as a reference.



SUPPLEMENTAL FIGURE 1.

Patient example of electrophysiological recordings of intrinsic conduction during left bundle branch block (A), left ventricular (LV) only pacing with electrode D1 (B) and LV only pacing with electrode P4 (C). Time interval between Q in surface electrode V1 and local left ventricular depolarization on the intracardiac electrogram of D1 is measured as QLV. QLV is corrected by QRS duration to acquire QLV/QRSd. The time interval between LV only pacing with D1 and local depolarization in P4 and vice versa are measured in B and C. The two time intervals are averaged and divided by the electrode spacing to obtain conduction velocity.



AV optimization in CRT with quadripolar leads: should we optimize every pacing configuration including multi point pacing?

Wouter M. van Everdingen (MD)¹, Alwin Zweerink (MD)²,
Odette A.E. Salden (MD)¹, Maarten J. Cramer (MD, PhD)¹,
Pieter A. Doevendans (MD, PhD)¹, Albert C. van Rossum (MD, PhD)²,
Frits W. Prinzen (PhD)⁴, Kevin Vernooy (MD, PhD)³, Cornelis P. Allaart (MD, PhD)²,
Mathias Meine (MD, PhD)¹

¹ Department of Cardiology, University Medical Center Utrecht, Utrecht, The Netherlands

² Department of Cardiology, and Institute for Cardiovascular Research (ICaR-VU),
VU University Medical Center, Amsterdam, The Netherlands

³ Department of Cardiology, Maastricht University Medical Center, Maastricht, The Netherlands

⁴ Department of Physiology, CARIM, Maastricht University, Maastricht, The Netherlands

Submitted

INTRODUCTION

Cardiac resynchronization therapy (CRT) is an effective treatment for patients with advanced systolic heart failure and left ventricular (LV) electrical conduction delay.¹ CRT aims to improve LV function with biventricular pacing leading to electromechanical resynchronization.² CRT may thereby induce reverse remodelling, and may lead to improvements in functional status, exercise tolerance, and subsequently in morbidity and mortality.¹ These effects are however not seen in all CRT patients, as a considerable amount of patients do not respond significantly.³ Non-response to CRT is partly attributed to suboptimal device programming,⁴ which can be optimized using the atrioventricular (AV) delay. The AV delay influences several intracardiac mechanisms that directly impact LV filling, among which atrioventricular interaction is best known.⁵ The AV delay also affects intra- and interventricular interaction,^{5,6} and optimization may lead to fusion of intrinsic conduction with either LV and/or right ventricular (RV) pacing.⁷ Optimization of the AV delay can increase acute hemodynamic performance.⁸ Numerous AV delay optimization methods have been proposed, with variable results.⁹ While algorithms using invasive optimization methods may be more reliable, non-invasive methods are more feasible for implementation in clinical practice.^{8,9} A relatively easy, fast and non-invasive method is the use of intracardiac electrograms (IEGM) to define the AV delay based on measured conduction intervals.¹⁰ Although IEGM-based algorithms to optimize the AV delay are already included in current devices, they lack proper physiological support and are at best non-inferior to echocardiographic optimization methods.⁹ Moreover, it is unknown whether different LV pacing configurations of a quadripolar lead require different AV delays to achieve the maximum potential of CRT.

This study aims to define an AV delay optimization method for CRT with a quadripolar left ventricular LV lead based on intrinsic conduction intervals. Patient specific optimal AV delays are determined using pressure-volume (PV) loop analysis, obtained invasively directly after CRT implantation. The optimal AV delay during multiple pacing configurations of a quadripolar LV lead are compared.

METHODS

This study is part of the Opticare-QLV trial, a multicentre observational study performed in three university medical centres in the Netherlands (University Medical Center Utrecht; VU University Medical Center, Amsterdam; and Maastricht University Medical Center, Maastricht), designed to investigate the benefits of quadripolar LV leads in CRT by invasive PV loop analysis. In total, 51 consecutive patients with moderate to severe heart failure (NYHA class II or III), LV ejection fraction $\leq 35\%$, sinus rhythm, optimal medical therapy, and a left bundle branch block (LBBB) according to the Strauss criteria were included.¹¹ Exclusion criteria were severe aortic valve stenosis, aortic valve replacement, or the presence of LV thrombus. All patients gave written informed consent. The study was performed according to the Declaration of Helsinki and in agreement with the local medical ethics committees.

STUDY PROTOCOL

An ECG was recorded prior to implantation for all patients, of which PR interval, P wave duration, QRS duration, and QRS morphology were noted. Patients also underwent echocardiography and cardiac magnetic resonance (CMR) imaging prior to device implantation. CMR or echocardiography derived LV volumes were used to calibrate the conductance catheter-derived baseline volumes. CRT implantation was performed under local anaesthesia. RV and right atrial (RA) leads were placed transvenously at conventional positions. The quadripolar LV lead was aimed at a tributary of the coronary sinus overlying the LV free wall at an anterolateral, lateral or posterolateral site. After electrophysiological measurements, the three leads were connected to a CRT device.

ELECTROPHYSIOLOGICAL MEASUREMENTS

Electrophysiological measurements were performed using an on-site dedicated system. The electrophysiological system was connected to the surface ECG and the implanted pacemakers leads to obtain simultaneous recordings. Delays of specific pacing modalities were recorded and delays between pacing spikes and local depolarization were measured. For each patient, the RA sensing to RVs interval (RAs-RVs) and RA pacing to RV sensing interval (RAp-RVs) was measured. For each quadripolar lead electrode, the Q on surface ECG to local LV depolarization (QLV), QLV normalized for intrinsic QRS duration (QLV/QRSD), and RV pacing to LV sensing interval (RVp-LVs), was measured.

HEMODYNAMIC MEASUREMENTS

Directly after device implantation, a dedicated PV loop conductance catheter (CD Leycom, Zoetermeer, The Netherlands) was inserted via the femoral artery and placed in the LV cavity. PV-loops were recorded for CRT with four paced AV delays during four biventricular pacing settings (BIV, i.e. RV and with one of the four electrodes of the quadripolar LV lead) and three multi-point pacing settings (MPP). The paced AV delay was set to approximate 80%, 60%, 40% and 20% of the RAp-RVs interval. The protocol was limited to atrial pacing, to stabilize cardiac rhythm. The interventricular (VV) delay was kept constant at 40ms LV-first. PV-loops of pacing configurations were recorded for 60 beats and 5 to 10 bpm above intrinsic rhythm, after excluding all inappropriate beats (i.e. extra systoles and two subsequent beats). PV loops during intrinsic conduction (i.e. RA pacing) were recorded as baseline measurements before and after each biventricular pacing run for a period of 30 beats. Change in stroke work (SW) of pacing configurations was calculated as a percentage change ($\Delta\%SW$) compared to the mean of the two adjoining baseline measurements. This method allows for reliable assessment of the effects of CRT, by correction of potential baseline drift.¹² For each BIV and MPP setting, a parabolic curve was fitted to the four data points (figure 1). All fitted curves with a physiological plausible shape (i.e. downward opening with a determinable maximum) and a coefficient of determination (R^2) ≥ 0.7 were used for further analysis. Of these curves, the maximal increase in $\Delta\%SW$ and corresponding AV delay were determined. For each patient, the maximal $\Delta\%SW$ and corresponding AV delay (AV_{OPT}) was compared to $\Delta\%SW$ based on a fixed AV delay of 120ms, 130ms, 160ms and 180ms, determined in the fitted curve. Lastly, the change in $\Delta\%SW$ based on 50% of the RAp-RVs delay ($AV_{50\%}$) was calculated using the coordinates of the fitted optimization curve (figure 2).

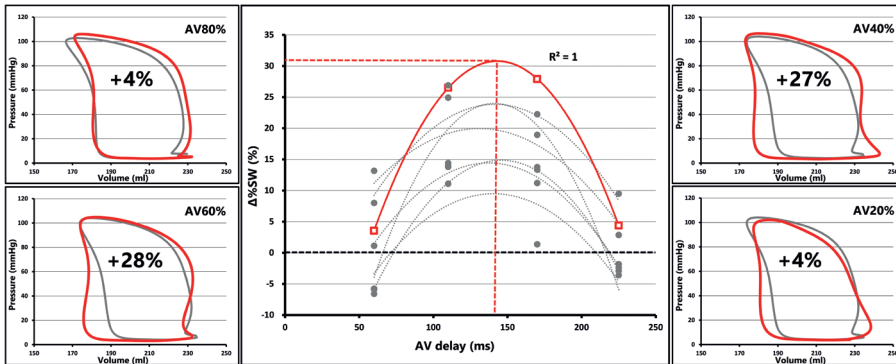


FIGURE 1. Method to determine the optimal AV delay

Example of pressure-volume (PV) loops of four atrioventricular (AV) delays of one pacing configuration using electrode D1. The percentage increase in stroke work ($\Delta\%SW$) of pacing (red loops) is calculated using the reference loops (grey loops) of right atrial pacing with intrinsic conduction. The results are plotted in a graph, and a 2nd order polynomial line is fitted to the four data points (red parabola). The maximal increase in $\Delta\%SW$ and corresponding AV delay are noted. The same is repeated for the remaining six configurations (grey dots and grey dotted curves), resulting in a total of four biventricular pacing configurations and three multi-point pacing configurations.

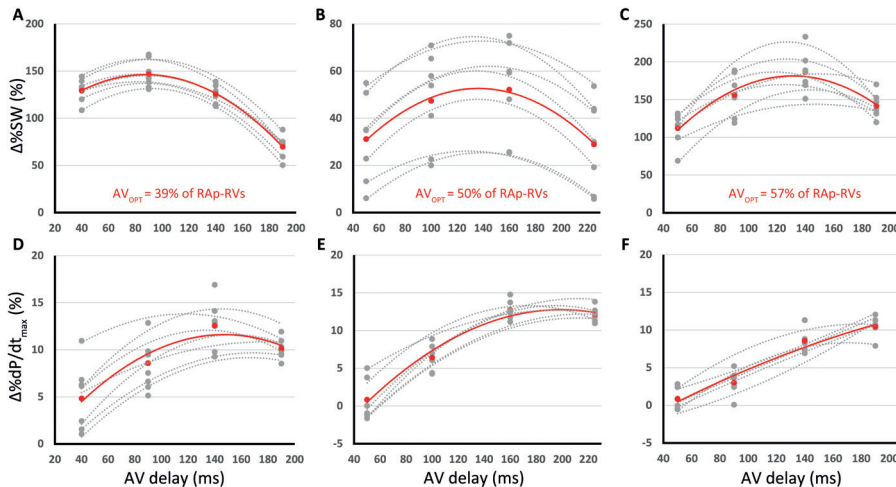


FIGURE 2. Example of atrioventricular delay optimization

Change in stroke work ($\Delta\%SW$) in the upper panels (A, B and C) and $\Delta\%dP/dt_{max}$ in the lower panels for three cases (D, E and F). For each case, up to seven pacing configurations (single and multi-point) were tested using four atrioventricular (AV) delays, which are represented by grey dots. The average of all measurements is indicated with black dots. A 2nd order polynomial curve was fitted for each set: pacing configurations (grey dotted curves), average (black dotted curve) and maximum (red solid curve).

STATISTICAL ANALYSIS

Statistical analysis was performed using SPSS (SPSS statistics 23.0, IBM, New York, USA). Mean and standard deviation or median and interquartile range are given depending on normality of data. The difference in baseline characteristics between patients included and excluded in the study was analysed using a T-test or Mann-Whitney U-test, dependent on normality of data, or a Chi-Square test in case of categorical variables. Subgroups were compared using similar tests. Optimal AV delays per pacing setting, for SW and dP/dt_{max} for BIV and MPP, and increase in $\Delta\%SW$ of each AV-optimization strategy were compared using paired T-tests. The optimal AV delay per setting was compared with a Pearson correlation coefficient and intra-class correlation coefficient. The univariate relation of predictors for the optimal AV delay were analysed with linear regression analysis. Univariate predictors with a p-value <0.10 were tested in a multivariate linear regression analysis. A p-value below 0.05 was considered significant for all tests.

RESULTS

Fifty-one patients were included in the main study, of which 44 were used for the present analysis. Reasons for exclusion were: unreliable baseline loops ($n=3$), AV optimization curves without a physiological plausible curve or curves with a low ($R^2<0.7$) coefficient of determination ($n=4$). Patients excluded from the analysis had worse diastolic function, with statistically significant higher E/E' , while left atria tended to be larger (table 1). In patients included in the final analysis, the paced AV delay with maximal increase in $\Delta\%SW$ was 128 ± 32 ms, while the intra-individual variation was 30 ± 14 ms. Paired t-tests showed that there were no statistically significant differences in the optimal AV delay between electrodes (D1: 134 ± 32 ms, M2: 125 ± 29 ms, M3: 123 ± 23 ms, P4: 123 ± 24 ms, all p =non-significant). There was also no difference in the optimal AV delay between biventricular pacing (126 ± 26 ms) and MPP (126 ± 21 ms, $p=0.29$). Correlation of the optimal AV delay between the pacing configurations was high (table 2). Intra-class correlation coefficient for average measures of the optimal AV delay was 0.64 (0.45-0.78, $p<0.001$). Examples of AV delay optimization for three patients are depicted in figure 2. The optimal AV delay led to an increase in $\Delta\%SW$ of $104\pm 76\%$. The AV delay with maximal increase in $\Delta\%dP/dt_{max}$ was longer compared to the optimal AV delay for $\Delta\%SW$ (160 ± 33 vs. 128 ± 32 ms $p<0.001$). AV optimization led to a mean increase in $\Delta\%dP/dt_{max}$ of $16\pm 11\%$ as compared to intrinsic conduction.

TABLE 1. Baseline characteristics of study population and excluded subjects

	Study population (n=44)	Excluded subjects (n=7)	p-value
Age (years)	66±10	69±5	0.320
Sex (% male)	28 (63%)	4 (57%)	0.741
NYHA class (n, %)			
II	29 (66%)	5 (71%)	0.774
III	15 (34%)	2 (29%)	
Type of CMP (n, %)			
DCM	28 (63%)	4 (57%)	0.741
ICM	16 (36%)	3 (43%)	
P-wave duration (ms)	123.5±12.7	122.0±18.8	0.776
PR interval (ms)	184.0±31.5	179.1±25.4	0.694
QRS duration (ms)	175.1±13.8	178.5±9.9	0.535
QLV/QRSd (%)	83.5±9.5	87.9±4.3	0.246
LV EDV (ml)	198 (169-241)	240 (184-304)	0.268
LV ESV (ml)	148 (106-172)	180 (136-252)	0.234
LV EF (%)	28.9±8.4	23.4±6.5	0.105
E/A ratio	0.65 (0.49-0.99)	1.30 (0.72-1.50)	0.118
E/E'	12.2 (10.1-16.0)	18.4 (13.7-27.1)	0.042
LA size (ml/m ²)	35.7 (28.2-41.2)	40.8 (35.1-60.2)	0.052
¹⁰ log BNP (pmol/L)	1.87±0.56	2.15±0.47	0.219
Creatinine (μmol/L)	90.4±23.5	100.6±41.2	0.549
RAp-RVs (ms)	274.3±49.1	273.6±23.4	0.970
RAs-RVs (ms)	201.9±31.4	202.1±47.4	0.985
QLV _{max} (ms)	146.2±19.7	156.9±11.8	0.172
QLV/QRSd (%)	83.5±9.5	87.9±4.3	0.246
RVp-LVs _{max} (ms)	157.6±24.9	173.9±23.0	0.112
Optimal AV delay for SW (ms)	128.0±32.2	126.8±59.6*	0.940
Optimal AV delay for dP/dt _{max} (ms)	159.5±33.0	158.7±23.1	0.950

LV volumes and ejection fraction are based on echocardiography. CMP: cardiomyopathy, DCM: dilated cardiomyopathy, ICM: ischemic cardiomyopathy, EDV: end-diastolic volume, ESV: end-systolic volume, EF: ejection fraction, LA: left atrial, LV: left ventricular, NYHA: New York Heart Association, RAp-RVs: right atrial pacing to right ventricular sensing interval, RAs-RVs: right atrial sensing to right ventricular sensing interval, QLV_{max}: maximal delay between Q on surface ECG and LV depolarization, QLV/QRSd: ratio between QLV and intrinsic QRS duration, RVp-LVs_{max}: maximal conduction interval between right ventricular pacing to left ventricular sensing. *: some patients were excluded because of unreliable baseline loops and still showed AV optimization curves with a physiological shape and R²>0.7.

TABLE 2. Correlation of optimal atrioventricular delays between pacing configurations

	BIV1	BIV2	BIV3	BIV4	MPP1	MPP2	MPP3
BIV1		.690*	.872*	.763*	.833*	.895*	.668*
BIV2	.690*		.878*	.806*	.885*	.836*	.732*
BIV3	.872*	.878*		.785*	.951*	.925*	.796*
BIV4	.763*	.806*	.785*		.916*	.871*	.791*
MPP1	.833*	.885*	.951*	.916*		.940*	.850*
MPP2	.895*	.836*	.925*	.871*	.940*		.498 [†]
MPP3	.668*	.732*	.796*	.791*	.850*	.498 [†]	

Matrix of Pearson correlation coefficients of the optimal atrioventricular delays for each pacing configuration. BIV1 to -4 are biventricular pacing configurations with one of the quadripolar electrodes. MPP1 to -3 are multi-point pacing configurations. *: $p < 0.001$, [†]: $p < 0.05$.

CONDUCTION INTERVALS AND OPTIMAL AV TIMING

A longer optimal paced AV delay was observed in patients with prolonged PR-interval (>200 ms) compared to patients with a normal PR-interval (154 ± 32 ms vs. 118 ± 27 ms, $p = 0.001$, figure 3). Male patients) tended to have longer AV delays compared to females (135 ± 32 vs. 117 ± 31 ms, $p = 0.08$). Patients with a NYHA functional class II also tended to have longer optimal AV delays compared to those NYHA III patients (135 ± 31 ms vs. 115 ± 33 ms, $p = 0.05$). The correlation of ECG derived parameters (i.e. P-wave duration and PR-interval) with the optimal AV delay were all statistically significant (figure 4). The same accounted for the intracardiac electrogram derived parameters (i.e. RAp-RVs and RAs-RVs). Univariate linear regression showed that several parameters of conduction delay (RAp-RVs, RAs-RVs, P-wave duration, PR interval and QLV/QRSD) were significantly related to the optimal AV delay (table 3). The strongest relation was seen between RAp-RVs and AV_{OPT} . The optimal AV delay was $47 \pm 9\%$ of the RAp-RVs delay and 4 ± 29 ms longer than P-wave duration. The optimal AV delay can be more precisely calculated using the equation: $AV_{OPT} = 1.15 * RAp-RVs - 186$ ms. The multivariate linear regression analysis showed that only RAp-RVs remained associated with the optimal AV delay ($R: 0.69$, $p < 0.001$).

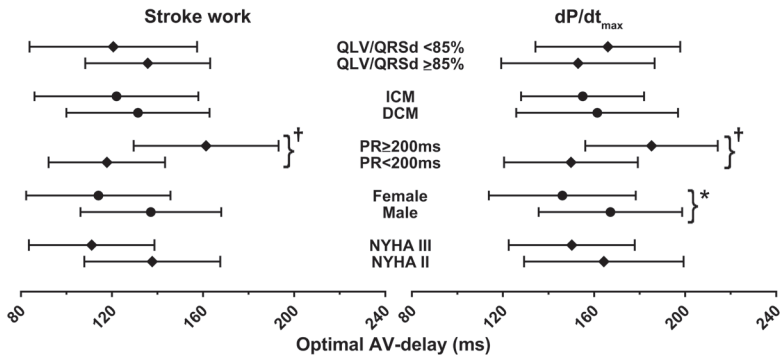


FIGURE 3. Optimal atrioventricular delay of specific subgroups

Atrioventricular (AV) delay with optimal hemodynamic response measured as change in stroke work and dP/dt_{max} . Categories include the ratio between Q to left ventricular sensing delay and QRS duration ratio (QLV/QRSD), type of cardiomyopathy: dilated cardiomyopathy (DCM) and ischemic cardiomyopathy (ICM), PR interval above or below the cut-off value for 1st degree AV block (i.e. 200ms), gender, and type of New York Heart Association (NYHA) functional class. Statistical significant difference with *: $p < 0.05$, †: $p < 0.002$.

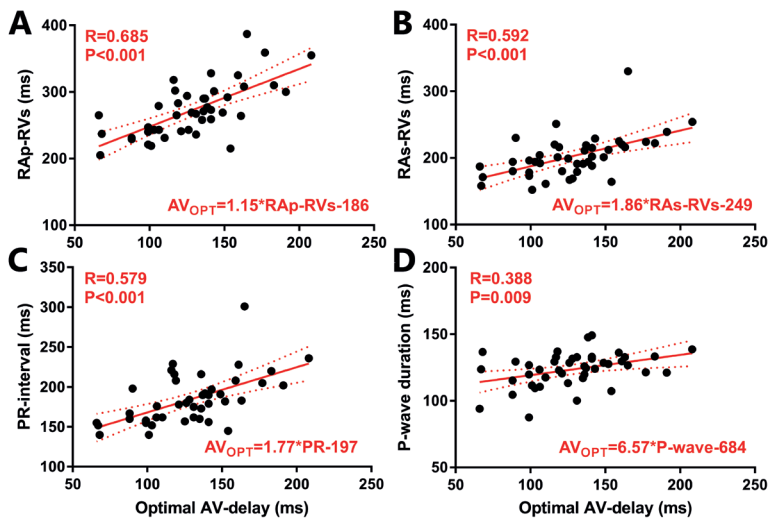


FIGURE 4. Correlation plots of parameters with the optimal AV delay based on stroke work

Correlation of A) right atrial pacing to right ventricular sensing delay (RAP-RVs), B) right atrial sensing to right ventricular sensing delay (RAS-RVs), C) PR interval, and D) P-wave duration with the optimal atrioventricular (AV) delay based on maximal percentage change in stroke work. The correlation coefficient (R), p-value (P) are given for each plot, as well as the equation of the fitline between the predictor and the optimal AV delay. The outlier in panel B and D is caused by a patient with severe atrioventricular conduction delay.

TABLE 3. Univariate and multivariate relation of predictors for the optimal AV delay

Variable	Univariate			Multivariate		
	B (SD)	R	p-value	B (SD)	R	p-value
RAp-RVs (ms)	0.55 (0.09)	0.69	<0.001	0.54 (0.09)	0.69	<0.001
RAs-RVs (ms)	0.60 (0.13)	0.59	<0.001	-	-	0.977
P-wave duration (ms)	0.99 (0.36)	0.39	0.009	-	-	0.167
PR interval (ms)	0.59 (0.13)	0.58	<0.001	-	-	0.190
QRS duration (ms)	-0.09 (0.36)	0.04	0.800	-	-	-
QLV (ms)	-0.43 (0.24)	0.26	0.087	-	-	-
QLV/QRSd (%)	-1.01 (0.50)	0.30	0.049	-	-	0.343
RVp-LVs (ms)	-0.05 (0.20)	0.04	0.797	-	-	-

B: Beta coefficient, SD: standard deviation, R: correlation coefficient. For other abbreviations see table 1.

HEMODYNAMIC RESPONSE

Compared to the other strategies, the change in $\Delta\%SW$ with $AV_{50\%}$ ($98\pm 74\%$) was closest to the maximal benefit achievable. The patient specific effect $AV_{50\%}$ showed heterogeneous results, with a considerable amount of patients with an over- or underestimation of the optimal AV delay (figure 5). Nevertheless, only a four patients with normal PR conduction (PR interval: 156ms) required much shorter AV delays and showed a difference in $\Delta\%SW$ of $>10\%$ between $AV_{50\%}$ and AV_{OPT} . However, the benefit of $AV_{50\%}$ was small and not significantly different compared to fixed delays of 120ms ($96\pm 73\%$, $p=0.29$) or 130ms ($95\pm 72\%$, $p=0.08$). Nevertheless, pacing at longer AV delays (i.e. 160ms, 180ms, and at 70% of RAp-RVs) showed significantly lower $\Delta\%SW$ values ($85\pm 66\%$, $73\pm 61\%$, $73\pm 63\%$ respectively, $p<0.005$ compared to $AV_{50\%}$, AV_{120ms} and AV_{130ms}).

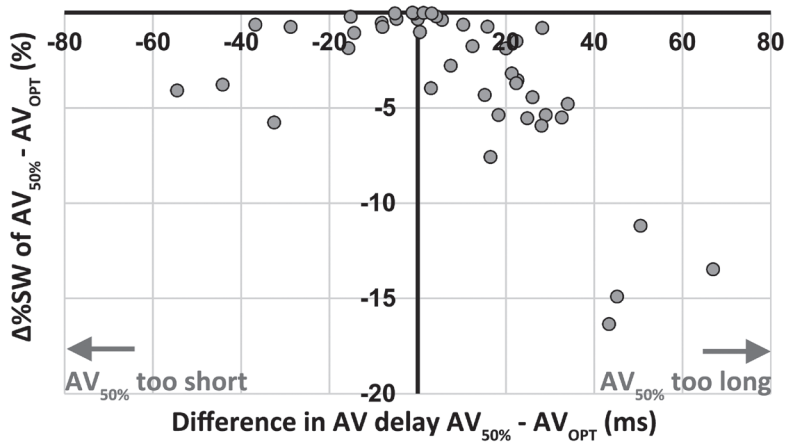


FIGURE 5. Difference in stroke work and atrioventricular delay of $AV_{50\%}$ vs AV_{OPT}

The patient specific effect of an atrioventricular (AV) delay based 50% of the right atrial pacing to right ventricular sensing interval ($AV_{50\%}$) compared to the optimal AV delay (AV_{OPT}). Difference between $AV_{50\%}$ and AV_{OPT} on change in stroke work ($\Delta\%SW$) and the AV delay is given.

DISCUSSION

Conduction intervals derived from the intracardiac electrogram can be used to estimate the AV delay with optimal hemodynamic response in patients with CRT. The mean optimal AV delay was dependent on intrinsic conduction delays, and corresponded with ~50% of the RAp-RVs delay. Therefore, an AV delay based on 50% of the RAp-RVs interval can be used to optimize the AV delay, to achieve an almost optimal, patient specific, effect in hemodynamic response. The AV delay with optimal hemodynamic benefit is similar for all pacing configurations of a quadripolar LV lead, advocating optimization of a single setting before comparison of all possible pacing sites and MPP.

AV DELAY OPTIMIZATION: PATIENT SPECIFIC OR FIXED?

To our knowledge, this is the first study on atrioventricular delay optimization in CRT with quadripolar LV leads using PV-loop analysis. Our study showed that the optimal paced AV delay is approximately 130ms determined by $\Delta\%SW$ and approximately 160ms by LV dP/dt_{max} , which is shorter than earlier results of our group (i.e. optimal paced AV delay with

LV dP/dt_{\max} of 180ms).⁸ The difference between RAs-RVs and RAp-RVs was ~70ms in this study and implementation of the AV_{50%} algorithm would result in an optimal sensed AV delay 35ms shorter than the paced AV delay (i.e. ~100ms). The sensed AV delay would be shorter compared to values found in previous studies (i.e. SMART-AV: 120ms) and work of our own group (i.e. 130ms).^{8,9} However, those results were based on LV dP/dt_{\max} , which only reflects the rate of LV pressure changes in the isovolumetric contraction phase. LV dP/dt_{\max} is highest at fusion of intrinsic conduction and ventricular pacing, which occurs at relative long AV delays,⁸ despite reduced diastolic filling properties. Results on PV-loops incorporate information on pressure and volume changes throughout the entire cardiac cycle, and thus include the systolic and diastolic performance. Shortening of the AV delay during CRT will lead to an increase in preload, as shown by Jones et al.,¹³ which is directly visualized in a PV-loop. The effect of increased preload is reflected by the shorter optimal AV delays found with $\Delta\%SW$ compared to dP/dt_{\max} . Some patients in our study benefited in terms of $\Delta\%SW$ with rather short AV delays. These short AV delays will decrease the effect of intrinsic conduction on ventricular activation, which indicates that interventricular interaction due to LV and RV pacing is more important in some patients. These heterogeneous effects, even in a cohort of patients with LBBB, show that there is no 'one size fits all' method for AV optimization. The observation that the optimal AV delay is close to 50% of RAp-RVs indicates that filling parameters may be important. Since absolute values of the optimal AV delay are longer for patients with prolonged PR intervals, optimized atrioventricular filling seems more important than fusion of intrinsic conduction and LV and RV pacing in most patients. The mean AV delay for RV pacing in our study (50% of RAp-RVs + 40ms = 177ms) was also shorter than the intrinsic PR interval (184ms). The association between PR interval and optimal AV delay may be ascribed to conduction delay in the atria, requiring a longer interval between complete atrial activation and contraction and ventricular activation. This is supported by the association between P wave duration and the optimal AV delay. As seen in prior studies,⁸ a trend towards a longer PR interval is seen in men compared to women. Men have larger hearts compared to women, indicating that cardiac size influences optimal AV timing. The effect of CRT in patients with prolonged PR interval is of interest, as a benefit was found in a sub analysis of the COMPANION trial and in a sub-analysis of non-LBBB patients in the MADIT-CRT.^{14, 15} In these sub analyses, patients with a prolonged PR interval benefited more from CRT in terms of reduced heart failure hospitalizations and mortality.¹⁶

COMPARISON TO CURRENT DEVICE ALGORITHMS

All CRT devices have built in algorithms for AV delay optimization based on intracardiac electrograms. Patients may benefit more from CRT with the AV_{50%} method, as current algorithms do not shorten the AV delay far enough. Current methods, such as QuickOpt (St. Jude Medical, St. Paul, Minnesota, USA), rely on a fixed sum of several milliseconds on measured P-wave duration (i.e. 80ms if P-wave duration <100ms and 110ms if P-wave duration >100ms). In our study population, QuickOpt would result in relatively long paced AV delays (i.e. 205±10ms). Moreover, the increase with 30ms based on a P-wave duration above 100ms is not physiological.¹² The Adaptiv-CRT algorithm of Medtronic (Minneapolis, Minnesota, USA) implements LV only pacing and uses an AV delay at 70% of the RAp-RVs delay or RAp-RVs -40ms (i.e. whichever is shorter, and the paced AV delay never exceeds 180ms), for fusion with intrinsic conduction. Adaptiv-CRT has been proven to be effective on clinical outcome and echocardiographic response.^{10, 17} The Adaptiv-CRT algorithm is different for patients with a RAp-RVs interval above or below 270ms (or 250ms in other Medtronic devices). However, the optimal AV delay in the 24 patients with RAp-RVs ≤270ms in our study was significantly shorter compared to Adaptiv-CRT (i.e. 111ms vs. Adaptiv-CRT: 168ms). The AV optimization method described by Gold et al. most closely resembles the AV_{50%} strategy, as it also uses a fraction of measured pacing intervals between atria and ventricles.¹⁸ Nevertheless, the resulting paced AV delays of Gold et al. were longer (i.e. 208±62ms) than ours. The difference between prior mentioned optimization algorithms and our results suggest that LV dP/dt_{max} measurements were used for these algorithms.

LIMITATIONS

There are some limitations to take into account. The AV delay was optimized directly after device implantation, and translation of these results to AV delay optimization after evidence of reverse remodeling is unknown. The benefit of patient specific AV delay optimization on long-term benefit of CRT is controversial. There is no clear benefit of any chosen strategy compared to fixed AV delays.¹⁹ Nevertheless, increase in $\Delta\%SW$ is known to predict long-term CRT response,²⁰ and every percentage of increase in $\Delta\%SW$ may potentially improve the patient's prognosis. Measurements were performed at rest, which may influence optimal AV timing. Exercise and thereby increased sympathetic drive leads to an increase in hemodynamic function, an increased heart rate and relative shorter diastolic phase compared to the systolic phase. AV delay optimization was performed with a fixed VV

delay of 40ms LV first because previous studies showed that LV pre-activation produces the highest hemodynamic response.⁸ To avoid programming errors, the pacing protocols were applied in a fixed order and were therefore non-randomized. As the implemented optimization protocol was time consuming and to stabilize heart rhythm, only optimization of the paced AV delay was performed. However, CRT patients are generally in sinus rhythm, and ventricular pacing after atrial sensing is more common in clinical practice. Although there was no significant benefit of an IEGM based method compared to fixed AV delays, this study might have been underpowered to find a significant difference between strategies.

CONCLUSION

A paced AV delay optimization strategy based on 50% of the intrinsic AV conduction interval is closest to the maximal achievable and patient specific acute hemodynamic effect. As the AV delay for optimal hemodynamic response is similar between pacing configurations of a quadripolar LV lead in a single patient, optimization is only necessary for one pacing configuration.

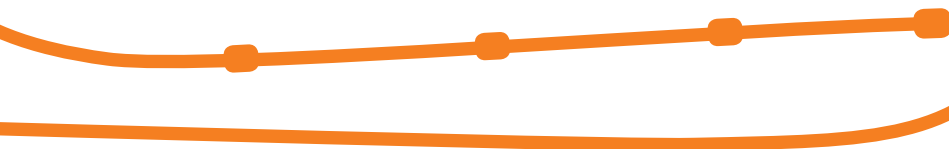
REFERENCES

1. Cleland JG, Abraham WT, Linde C, Gold MR, Young JB, Claude Daubert J, et al. An individual patient meta-analysis of five randomized trials assessing the effects of cardiac resynchronization therapy on morbidity and mortality in patients with symptomatic heart failure. *Eur Heart J*. 2013;34:3547-56.
2. Prinzen FW, Vernoooy K, De Boeck BW, Delhaas T. Mechano-energetics of the asynchronous and resynchronized heart. *Heart Fail Rev*. 2011;16:215-24.
3. Daubert JC, Saxon L, Adamson PB, Auricchio A, Berger RD, Beshai JF, et al. 2012 EHRA/HRS expert consensus statement on cardiac resynchronization therapy in heart failure: implant and follow-up recommendations and management. *Europace*. 2012;14:1236-86.
4. Mullens W, Grimm RA, Verga T, Dresing T, Starling RC, Wilkoff BL, et al. Insights from a cardiac resynchronization optimization clinic as part of a heart failure disease management program. *J Am Coll Cardiol*. 2009;53:765-73.
5. Auricchio A, Ding J, Spinelli JC, Kramer AP, Salo RW, Hoersch W, et al. Cardiac resynchronization therapy restores optimal atrioventricular mechanical timing in heart failure patients with ventricular conduction delay. *J Am Coll Cardiol*. 2002;39:1163-9.
6. Sweeney MO, Prinzen FW. Ventricular pump function and pacing: physiological and clinical integration. *Circ Arrhythm Electrophysiol*. 2008;1:127-39.
7. Vernoooy K, Verbeek XA, Cornelussen RN, Dijkman B, Crijns HJ, Arts T, et al. Calculation of effective VV interval facilitates optimization of AV delay and VV interval in cardiac resynchronization therapy. *Heart Rhythm*. 2007;4:75-82.
8. Bogaard MD, Meine M, Tuinenburg AE, Maskara B, Loh P, Doevendans PA. Cardiac resynchronization therapy beyond nominal settings: who needs individual programming of the atrioventricular and interventricular delay? *Europace*. 2012;14:1746-53.
9. Ellenbogen KA, Gold MR, Meyer TE, Fernandez Lozano I, Mittal S, Waggoner AD, et al. Primary results from the SmartDelay determined AV optimization: a comparison to other AV delay methods used in cardiac resynchronization therapy (SMART-AV) trial: a randomized trial comparing empirical, echocardiography-guided, and algorithmic atrioventricular delay programming in cardiac resynchronization therapy. *Circulation*. 2010;122:2660-8.
10. Singh JP, Abraham WT, Chung ES, Rogers T, Sambelashvili A, Coles JA, Jr., et al. Clinical response with adaptive CRT algorithm compared with CRT with echocardiography-optimized atrioventricular delay: a retrospective analysis of multicentre trials. *Europace*. 2013;15:1622-8.

11. Strauss DG, Selvester RH, Wagner GS. Defining left bundle branch block in the era of cardiac resynchronization therapy. *Am J Cardiol.* 2011;107:927-34.
12. Sohaib SM, Whinnett ZI, Ellenbogen KA, Stellbrink C, Quinn TA, Bogaard MD, et al. Cardiac resynchronisation therapy optimisation strategies: systematic classification, detailed analysis, minimum standards and a roadmap for development and testing. *Int J Cardiol.* 2013;170:118-31.
13. Jones S, Lumens J, Sohaib SM, Finegold JA, Kanagaratnam P, Tanner M, et al. Cardiac resynchronization therapy: mechanisms of action and scope for further improvement in cardiac function. *Europace.* 2016.
14. Olshansky B, Day JD, Sullivan RM, Yong P, Galle E, Steinberg JS. Does cardiac resynchronization therapy provide unrecognized benefit in patients with prolonged PR intervals? The impact of restoring atrioventricular synchrony: an analysis from the COMPANION Trial. *Heart Rhythm.* 2012;9:34-9.
15. Kutuyifa V, Stockburger M, Daubert JP, Holmqvist F, Olshansky B, Schuger C, et al. PR interval identifies clinical response in patients with non-left bundle branch block: a Multicenter Automatic Defibrillator Implantation Trial-Cardiac Resynchronization Therapy substudy. *Circ Arrhythm Electrophysiol.* 2014;7:645-51.
16. Rickard J, Karim M, Baranowski B, Cantillon D, Spragg D, Tang WHW, et al. Effect of PR interval prolongation on long-term outcomes in patients with left bundle branch block vs non-left bundle branch block morphologies undergoing cardiac resynchronization therapy. *Heart Rhythm.* 2017;14:1523-1528.
17. Burns KV, Gage RM, Curtin AE, Gorcsan J, 3rd, Bank AJ. Left ventricular-only pacing in heart failure patients with normal atrioventricular conduction improves global function and left ventricular regional mechanics compared with biventricular pacing: an adaptive cardiac resynchronization therapy sub-study. *Eur J Heart Fail.* 2017.
18. Gold MR, Niazi I, Giudici M, Leman RB, Sturdivant JL, Kim MH, et al. A prospective comparison of AV delay programming methods for hemodynamic optimization during cardiac resynchronization therapy. *J Cardiovasc Electrophysiol.* 2007;18:490-6.
19. Auger D, Hoke U, Bax JJ, Boersma E, Delgado V. Effect of atrioventricular and ventriculoventricular delay optimization on clinical and echocardiographic outcomes of patients treated with cardiac resynchronization therapy: a meta-analysis. *Am Heart J.* 2013;166:20-9.
20. de Roest GJ, Allaart CP, Kleijn SA, Delnoy PP, Wu L, Hendriks ML, et al. Prediction of long-term outcome of cardiac resynchronization therapy by acute pressure-volume loop measurements. *Eur J Heart Fail.* 2013;15:299-307.



General discussion



GENERAL DISCUSSION

In this thesis, multiple strategies to optimize the efficacy of cardiac resynchronization therapy (CRT) are described. Strategies based on prediction of CRT response and optimization of device implantation and device optimization are discussed separately. In the first part, the use of parameters of mechanical dyssynchrony and discoordination for prediction of response to CRT are described. These parameters were obtained with several strain imaging techniques, which showed apparent differences even if obtained in the same patient. Strain imaging techniques based on CMR had the highest predictive value, while the clinically more feasible technique of STE performed reasonable. In the second part, the effect of RV dysfunction on prediction of CRT response with parameters of mechanical dyssynchrony was assessed using patient data and computer models. RV dysfunction complicates prediction by diminishing the effect of CRT, while the effect on mechanical dyssynchrony was relatively small. In the third part of the thesis, optimization of CRT with a quadripolar LV lead is described. The benefits of a quadripolar LV are reviewed in chapter 9. The pitfall of anodal capture with a quadripolar LV lead is described in chapter 10. In chapter 11 we show that promising electrogram-derived parameters fail to designate the optimal electrode of a quadripolar LV lead in the individual patient. Despite this finding, quadripolar leads may increase the acute response to CRT, although this requires invasive hemodynamic testing. MPP may further improve response to CRT. We found no overall benefit in acute hemodynamic response compared to optimized biventricular pacing with a quadripolar lead, although some subgroups may improve (chapter 12). Optimization of the atrioventricular (AV) delay may also improve response to CRT improved by fusion of intrinsic left bundle branch block (LBBB) activation and ventricular pacing using a patient specific optimized AV delay, as shown in chapter 13.

ECHOCARDIOGRAPHIC PARAMETERS FOR PREDICTION OF CRT RESPONSE

The first part of the thesis showed that mechanical dyssynchrony and discoordination can be assessed using imaging techniques such as speckle tracking echocardiography, as evaluated in chapter 2 to 4, or cardiac magnetic resonance imaging (CMR) using tagging or feature tracking (chapter 5 and 6). These techniques use dedicated software algorithms, which are commercially available through several vendors. Differences between STE software

packages of several vendors were observed (chapter 3 and 4). These differences are also seen between strain imaging techniques, and our work has shown that CMR based images have higher comparability than STE (chapter 5). However, CMR tagging, feature tracking and STE were all capable of predicting volumetric response to CRT (chapter 6).

Echocardiography is an important diagnostic tool for physicians, it is easily applicable and may provide information on cardiac status. With this bedside tool, information on valvular function, RV and LV dimensions, systolic and diastolic function are relatively easily obtained (chapter 2). However, a more complicated issue is the use of echocardiographic parameters of mechanical dyssynchrony for prediction of response to CRT. While results of the first multi-center trial (PROSPECT) on response prediction with parameters of mechanical dyssynchrony were rather disappointing,¹ single center studies with positive results keep appearing.²⁻⁴ There are multiple factors attributed to the neutral outcome of the PROSPECT study. Firstly, the analysis of dyssynchrony parameters was conducted in multiple labs, introducing bias in the measurement. Next, multiple parameters were tested, which were mostly based in timing of certain events. And lastly, most parameters were based on tissue Doppler imaging, which is more sensitive to noise compared to STE.⁵ Finally, the use of parameters based on timing of peaks has been questioned; instead measures of mechanical discoordination appear to be better predictors of CRT response.^{2, 6} The MARC study is the first multi-center study in which all echocardiograms were analyzed with STE by a dedicated core lab for assessment of parameters of mechanical dyssynchrony and discoordination.⁷ Despite the implementation of a core lab, implementation of these parameters remained difficult. Echocardiographic images were obtained with either of two ultrasound machine vendors, requiring vendor-specific STE software.⁸ Images could also be analyzed by a third, vendor-independent software package. However, the effect of this specific package on quantification of mechanical dyssynchrony and discoordination parameters was unknown. The dyssynchrony and discoordination parameters used in the MARC study were therefore based on visual assessment (i.e. apical rocking and septal flash) and the interval between onset of LV and RV ejection, known as the interventricular mechanical delay (IVMD).⁷ Although these parameters also showed positive results in other large studies (i.e. apical rocking),⁹ they are not included in current CRT guidelines.^{10, 11} In order to persuade clinicians defining the guidelines, dyssynchrony and discoordination parameters need to be reliable, with low test re-test measurement variability. Although we found apparent similarities in septal strain patterns between two STE software packages (i.e. GE EchoPac and Philips QLAB) in chapter

3, in chapter 4 we have shown that this is not the case for three commonly used vendors of STE software. Between analyses provided by these vendors significant differences in values of mechanical dyssynchrony parameters were observed, even when implemented in the same patient. It should be recognized that the aforementioned study (chapter 3) was performed in 2013, while the study in chapter 4 was performed in 2016. STE software is constantly under development, partly due to the standardization task force of the echocardiographic societies,¹² and new versions may result in different strain values, which are hopefully more comparable between vendors. A more recently performed and more extensive study showed significant results between seven vendors.¹³ Because it is not known what vendor should be regarded as the gold standard, we compared results of speckle tracking performed by one vendor (i.e. TomTec 2DCPA) with CMR techniques; CMR tagging and CMR feature tracking. CMR tagging is considered a gold-standard for strain measurements (chapter 5 and 6). While CMR Feature tracking showed fair comparability with CMR tagging, agreement between STE and CMR tagging derived strains/dyssynchrony was overall poor. This may be ascribed to several differences between the techniques, elucidated in chapter 5. While the amplitude was the main difference in chapter 3, differences were seen in amplitude and timing of events in chapter 5. Nevertheless, both CMR based techniques and STE were capable of predicting response in the same patient population (chapter 6). Especially the categorization of septal strain patterns and the septal strain value at aortic valve closure proved to be good predictors of CRT response. These two parameters both reflect the septal discoordination due to LBBB, as the amount of septal rebound stretch (SRSsept, which is primarily seen in type 1 and 2 LBBB septal strain patterns) directly influences the end-systolic strain value of the septum (ESSsep). It was surprising that SRSsept performed significantly poorer, as SRSsept is directly affected by myocardial viability and subsequently correlates with reduced CRT response. ESSsep values of patients with lower myocardial viability might resemble those of potential CRT responders, with reduced values close to zero per cent circumferential shortening.¹⁴ Our cohort consisted of patients with a low scar burden, and we therefore could not evaluate the effect of scar on ESSsep. These results should therefore be validated in larger cohorts, ideally in patients with a considerable myocardial scar burden.

The direction of myocardial strain used for assessment of dyssynchrony and discoordination should be based on experience, observed results, and the implemented imaging technique. Most CMR based studies use circumferential strain,^{15, 16} while STE is primarily based on longitudinal strain.^{17, 18} We found a poor correlation between CMR tagging and STE in

parameters based on circumferential strain. However, the predictive value of circumferential strain parameters derived by STE was rather high. Lumens et al. even used radial strain to assess the systolic shortening index (SSI) and found a predictive value when used in combination with electrocardiographic parameters.² Nevertheless, longitudinal strain of the interventricular septum is more convenient, as even in patients with dilated hearts due to heart failure, the septum is easily visualized with adequate image quality.

Studies like our own (chapter 3 to 6) are a first step to understanding of the discrepancies between techniques on mechanical dyssynchrony and discoordination. Most software packages for strain imaging are not tested for purposes outside the scope for which they are made available. They lack validation in disease states such as dyssynchronous heart failure. Although a clinician always has the final verdict, differences in results between vendors may lead to misdiagnosis. A well-made decision is becoming increasingly complicated with the pace of current developments. Therefore, validation of current and new versions of medical imaging software is crucial. Validation of algorithms should first focus on biophysiological models of heart failure and dyssynchrony.¹⁹ These models may test the capability of different software packages to detect predetermined changes in dyssynchrony. With phantom models and computer-generated images of dyssynchrony, similar results should be obtained. After validation in these models, a head-to-head comparison can be made, similar to our approach in chapter 3. Only after successful validation of the technique in large patient studies, may new tools be made available for clinical decision making.

COMPUTER MODELLING OF CARDIAC FUNCTION, INFLUENCE OF RV ON CRT

Response to CRT may be influenced by right ventricular (RV) function. As the right ventricle is a complex chamber and the influence of the right ventricle is difficult to interpret by current imaging techniques, computer modelling may aid in the understanding. In chapter 7 a combination of computer modelling and patient data was used to understand the effect of RV function on parameters of mechanical dyssynchrony and CRT response. We found that poor RV function may decrease CRT response, while it has only a small effect on the amount of dyssynchrony. RV dysfunction may therefore complicate prediction of response to CRT (chapter 8) and should be assessed before CRT implantation.

Intra- and interventricular interaction of dyssynchronous heart failure is difficult to understand. Patient data in this field is complex, hampering understanding of the physiological interaction

of CRT with the heart. Computer modelling may elucidate these interactions (chapter 7). In line with chapter 8, Niederer et al. used a computer model to understand the effect of multi-site pacing and the interaction with LV scar.²⁰ Models may also aid in the understanding of issues raised by (strain) imaging.²¹ The specific model used for computer modelling depends on the hypothesis. Complex 3D models of anatomy, activation and function are possible, but sometimes a more simplified model suffices. We used the CircAdapt model, to answer the question whether RV function interacts with LV dyssynchrony and the prediction of CRT response. As shown in chapter 8, RV dysfunction has almost no influence on the amount of LV dyssynchrony in LBBB simulations, while LV dysfunction does. However, both RV and LV dysfunction influence the potential effect of CRT on changes in LV contractile function. RV dysfunction, measured as RV fractional area change (RVFAC), may therefore complicate prediction of CRT response. It should therefore be taken into account beside assessment of mechanical dyssynchrony. However, a recent meta-analysis has shown that no parameter of RV dysfunction was able to predict CRT response.²² RVFAC tended to predict changes in LV ejection fraction, but the association was non-significant. The use of changes in LV ejection fraction as parameter for CRT response, instead of LV end-systolic volume, may have affected the results. Nevertheless, conflicting evidence is apparent in this field,²³⁻²⁵ which may also be attributed to the mixed group of patients with RV dysfunction. While all CRT patients have LV dysfunction, with possible backward failure causing RV failure, RV failure may also be a co-existent. With current imaging techniques, it is difficult to dissect both pathophysiological conditions.

CRT OPTIMIZATION STRATEGIES

SELECTION OF PACING ELECTRODE ON QUADRIPOLE LEAD

The first step in optimization of CRT is optimization of the LV lead position (figure 1). After optimization of the LV lead position, a quadripolar LV lead facilitates additional pacing options and sites compared to bipolar leads. The latter is especially helpful in case of non-capture or phrenic nerve stimulation on one of the electrodes, and these leads have even shown to improve long-term response.²⁶⁻²⁸ Similar to earlier studies,^{29, 30} we found a large intra-individual variation in acute hemodynamic response between electrodes of a quadripolar LV lead. This necessitates parameters which aid in the selection of the optimal pacing site of CRT with a quadripolar LV lead. A promising parameter for optimization

of the LV lead position (i.e. QLV or QLV/QRSd) has been evaluated in this thesis (chapter 11).³¹ Although the QLV is able to predict long-term response,³² and may be used to find an optimal LV area for biventricular pacing,³¹ we found that it cannot be used to define the optimal pacing electrode of a quadripolar LV lead. If a quadripolar LV lead is placed in an area with sufficient conduction delay, QLV of all four electrodes will be prolonged while differences in hemodynamic response may vary between electrodes. However, Thomas Edison (1847-1931) once said “Just because something doesn’t do what you planned it to do, doesn’t mean it’s useless.” This applies for QLV and QLV/QRSd, as these parameters may still be indicators of expected CRT response,³³ although they do not predict the pacing site with highest acute hemodynamic response of a quadripolar LV lead. Moreover, the optimal pacing area may be relatively large in LBBB, as shown by animal experiments.³⁴ Although the QLV and QLV/QRSd may be more global indicators of optimal areas for LV pacing,^{31, 33, 35} after lead placement the QLV cannot be used to select the optimal pacing site of the quadripolar LV lead. When optimizing the pacing site of a quadripolar lead, anodal capture may occur if an electrode of the quadripolar lead is selected as anode. Anodal capture may influence results in studies on acute hemodynamic response. By using the RV coil as node, anodal capture is unlikely to occur.

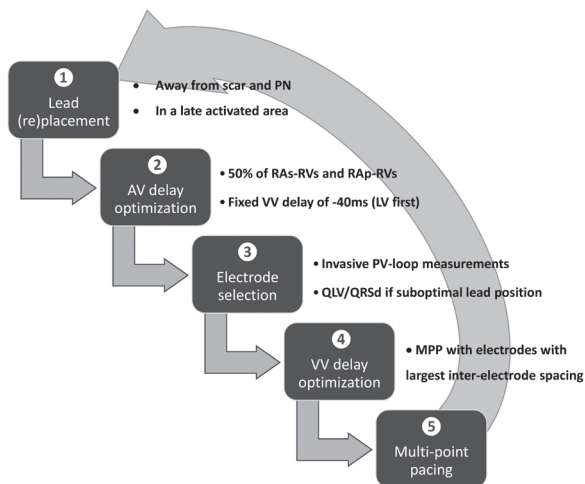


FIGURE 1. CRT device optimization roadmap

Roadmap for optimization of CRT with a quadripolar LV lead. AV: atrioventricular, VV: interventricular, MPP: multi-point pacing, PN: phrenic nerve, RAs-RVs: right atrial sensing to right ventricular sensing interval, RAP-RVs: right atrial pacing to right ventricular sensing interval, PV: pressure-volume, QLV/QRSd: Q to LV sensing interval divided by the intrinsic QRS duration.

Other non-invasive methods to select the optimal LV lead electrode may use a combination of electrical, pathophysiological and/or mechanical characteristics. While the influence of pacing near scar tissue is known,^{36,37} the optimal pacing site in patients without considerable scar tissue may be large.³⁴ Although the association of LV pacing in regions with considerably electrical and/or mechanical delay and CRT response is strong,^{31, 33, 38, 39} it may be partly coincidental.⁴⁰ Areas of late activation during LBBB and areas for optimal LV pacing may accidentally overlap, as the optimal pacing site causing fast LV depolarization may be unrelated to the latest electrically activated area during intrinsic conduction.⁴⁰ However, trials with pre-procedural imaging to distinguish optimal sites with parameters of mechanical dyssynchrony show positive results.^{38,41} These trials used speckle tracking echocardiography guided lead implantation and showed positive effects on reverse remodeling and outcome in patient with concordant lead positions.⁴¹⁻⁴³ Nevertheless, these results are possibly driven by avoiding infarcted segments by exclusion of regions with low strain amplitudes.^{14, 44} The LV lead was therefore never targeted in an area of myocardial scar, which was an important determinant in sub-analysis of the TARGET and STARTER trial.^{41, 45} Although these trials show positive results, so far no method is universally advised for targeted LV lead placement. This is possibly caused by the relatively high measurement variability seen in strain imaging. Differences in assessment of mechanical dyssynchrony were observed between three widely used STE software packages (chapter 3 and 4). Moreover, our results from chapter 5 show that the specific strain imaging technique (e.g. CMR tagging or speckle tracking echocardiography) used to measure timing of delayed activation (e.g. TTP_{max}) is relevant. Furthermore, as most electrodes of a single quadripolar lead will be in or near the same segment, it is difficult to distinguish an optimal site with the coarse layout of segments obtained with these techniques.

CRT DEVICE OPTIMIZATION

After LV lead placement, multiple device settings are programmable to attenuate the effect of CRT. Classically these are AV and VV timing, but more recently electrode selection of the quadripolar LV lead and also MPP has become available, thus increasing the number of options considerably. These programming options may all increase CRT response. We studied the effect of multi-point pacing (MPP) and found that especially male patients, those with ischemic cardiomyopathy (ICM) and low LV ejection fraction more often respond to

MPP (chapter 12). Although we included a sub-selection of CRT patients (i.e. strict LBBB according to Strauss)⁴⁶ with relatively low scar burden, this finding is in line with several other modelling and clinical studies.^{20, 47, 48} The effect of MPP in the Opticare-QLV study was relatively small compared to other MPP studies.^{49, 50} The limited effect may be ascribed to the acute hemodynamic response of conventional biventricular pacing with a quadripolar LV lead, which was already relatively high in our study. Firstly, because we optimized biventricular pacing and secondly due to the inclusion of patients with a favorable substrate for CRT response (i.e. LBBB). Clinicians should therefore take caution when implementing MPP in these patients, and the effect should be evaluated by assessment of cardiac function. Moreover, as MPP also increases battery drainage and reduces device longevity,⁵¹ the clinical effect should be noteworthy in order to justify the use of MPP. It is also unknown whether we should test MPP directly after implantation or after a period without sufficient reverse remodeling (i.e. watch and wait). A large multi-center study on the effect of MPP in CRT non-responders (the More-CRT study) which may answer this question, is currently ongoing.⁵² It will be especially interesting to investigate the effect of MPP in patients with a less favorable substrate for CRT response. Patients with non-specific intraventricular conduction delay (i.e. non-LBBB) have more heterogeneous conduction and activation of the LV,⁵³ a larger scar burden, and may benefit from multiple pacing sites for fast depolarization of the LV free wall.²⁰ A study with pressure-volume loop analysis evaluating the effect of MPP in these patients would be of value, as these patients are often non-responders to CRT. Increasing the effect of CRT in these sub-populations may widen the applicability of CRT, as the number of implantations in these patients is decreasing since the implementation of new and stricter guidelines.⁵⁴

Atrioventricular delay (AV) timing influences the acute hemodynamic response of CRT. Specific conduction delays, either measured on the ECG or the intracardiac electrogram, may be used to define the optimal AV delay. We found that implementation of a paced AV delay based on a fraction (50%) of the intrinsic right atrial pacing to right ventricular sensing delay (RAp-RVs), may improve acute hemodynamic response. As most patients get ventricular pacing after atrial sensing, the sensed AV delay is more important for clinical practice. Implementation of a sensed AV delay, calculated with 50% of the right atrial sensing to right ventricular sensing delay (RAs-RVs) seems reasonable. This delay would be approximately 35ms shorter compared to the RAp-RVs delay in our study (chapter 13), which is in accordance with earlier work.⁵⁵ The acute response of an AV delay based on

50% of RAp-RVs was closest to the maximal increase in stroke work achievable. However, it is not significantly better compared to a fixed delay of 120 or 130ms. These findings are in line with our current knowledge on AV delay optimization, which all show non-inferiority of AV optimization strategies compared to fixed delays.⁵⁵ Despite many different optimization tools, the beneficial effect on long-term prognosis does not exceed that achieved with fixed AV delays.⁵⁶ However, our results do question the current algorithms of device manufacturers. While some are based on a subtraction of a certain amount of milliseconds from measured intrinsic conduction intervals (i.e. QuickOPT, St. Jude Medical, Saint Paul, USA), others use relative large percentages which result in long AV delays (i.e. Adaptiv-CRT, Medtronic, Minneapolis, USA).⁵⁷ The AV delay needs to be short enough for LV (pre-)activation to depolarize the LV free wall before arrival of the RV pacing wave front or intrinsic conduction. Moreover, an AV delay comparable to our optimization strategy facilitated optimal hemodynamic response in previous work of our group.⁵⁸ The response was facilitated by optimal fusion of ventricular pacing, leading to a more homogeneous electrical depolarization of the LV.⁵⁸ Current device algorithms may be improved by implementation of our AV delay optimization strategy. The effects of AV delay optimization should however first be tested in larger studies, focused on long-term effects.

ROADMAP FOR CRT DEVICE OPTIMIZATION

Considering all these (novel) options for CRT device optimization, a physician needs a roadmap after implantation of CRT with a quadripolar LV lead (figure 1). AV delay optimization should have first priority, as it is a major contributor to CRT response.⁵⁹ The optimal AV delay is also similar for the four electrodes of the quadripolar LV lead and MPP, as observed in chapter 13. AV delay optimization may therefore be conducted with any of the quadripolar lead electrodes, using a fixed VV delay of -40ms (LV first), as most patients will benefit from LV pre-activation.⁵⁵ The intrinsic conduction intervals may be used to calculate the patient specific optimal AV delay. An AV delay 50% of RAp-RVs for right atrial pacing and 50% of RAs-RVs for right atrial sensing may be programmed. Secondly, the specific electrode of the quadripolar lead may be selected. Optimization of the pacing site is currently limited to invasive measurements of hemodynamic function, but may be replaced by non-invasive equivalents. Non-invasive tools maybe helpful in patients with suboptimal lead positioning (i.e. posterolateral or posterior) and relatively low QLV/QRSd ($\leq 75\%$). In these patients the electrode with highest QLV/QRSd potentially increases hemodynamic

function most. If the highest increase in hemodynamic function is insufficient to warrant CRT response, further steps may be taken. Although not evaluated in our studies, VV delay optimization is one of the following options.⁵⁵ VV delay optimization directly influences ventricular interaction, in which an offset of -40ms (LV-first) is considered optimal in most patients.⁵⁵ However, this offset may not be favorable in all patients and moreover these data are based on LV dP/dt_{\max} instead of stroke work. Fourth, MPP could be considered. Especially in male patients, patients with ischemic cardiomyopathy and those with poor LV function, MPP could have a beneficial effect compared to biventricular pacing. MPP should be programmed with the electrodes with the largest inter-electrode spacing, to gain maximal effect of the additional pacing site.^{50, 60} If all above mentioned fail to substantiate a benefit of CRT, a different lead position may be considered.

FUTURE PERSPECTIVE

GUIDED LEAD PLACEMENT

As mentioned, pre-implantation derived information may guide optimal LV lead placement during CRT implantation. Targeting the LV lead away from scar tissue is perhaps the most important aspect of LV lead implantation.^{36,45} Scar identification is relatively easily through CMR with delayed gadolinium enhancement. Typically, CMR images are described by the radiologist, mentioning scar burden and location. Scar location can be visualized in a bulls-eye plot, to facilitate the translation of the segmental distribution to fluoroscopy images of coronary venous anatomy during CRT implantation. The implanting physician needs to make a cerebral fusion of these images. Despite the talent and intellect of an electrophysiologist, this situation remains suboptimal. Therefore, multiple groups, including our own, are working on systems to fuse characteristics of CMR images with live fluoroscopy images.⁶¹⁻⁶³ By fusing images containing information on scar location and burden, areas of latest mechanical or electrical activation and/or the location of the phrenic nerve, the cardiologist may be guided towards the target location (figure 2). The cardiologist may avoid veins which are close to the phrenic nerve, or areas without capture, as these suboptimal areas are directly visible. Targeted lead placement with live visualization will potentially increase response to CRT. Beside improving the therapeutic effect of CRT, the procedure time may also be reduced, as fruitless attempts resulting in phrenic nerve stimulation or pacing in areas of fibrosis may be circumvented. Faster implantations mean less radiation exposure, less chance of complications, reduced time consumption, and thus an improvement in cost-effectiveness. Most important, the patient may benefit directly by a more effective implementation of CRT.⁴¹

In order to enhance the effect of CRT in the individual patient, imaging data may be even used in a biophysiological computer model. By integrating patient specific information on fibrosis, anatomy and contractility, we might be able to predict the effect of CRT for the individual patient.⁶⁴ This may aid in patient selection and therapy optimization, evaluating potential effects for the individual patient. In combination with visualization of the coronary venous system with contrast enhanced images from CT or CMR, the hemodynamic effect of a different lead position may also be evaluated in a computer model. This is even feasible before implantation, creating a predefined roadmap for the cardiologist.⁴⁰ These aspects may be fused with X-ray imaging during CRT implantation, to guide the cardiologist to the target

region.⁶⁵ Although further research is required before implementation of computer models with live images during implantation, this thesis aids in the quest for optimal use of CRT.

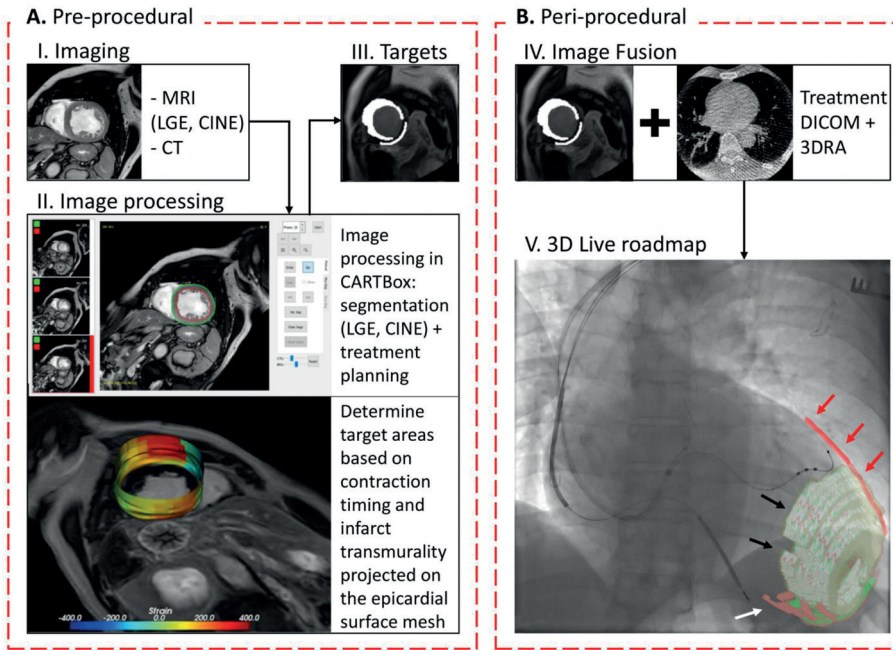


FIGURE 2. Image fusion for CRT device implantation

Image fusion of pre-operative acquired cardiac MRI and CT with 3D rotational fluoroscopy. Panel A depicts the procedural steps for image fusion, including acquisition of cardiac MRI for visualization of scar and delayed contraction and CT for identification of the left phrenic nerve (I). Image processing in the CARTBox software (II) and creation of treatment files (III) are also shown. Panel B depicts the actual image fusion of the treatment file with live fluoroscopy during CRT implantation. The target area (red and green area) is visualized by a white arrow, the region of scar (light green area) with black arrows, and lastly the phrenic nerve (red line) with red arrows. 3DRA: 3D rotational angiography; CINE: Cine MRI, CRT: cardiac resynchronization therapy, LGE: late gadolinium enhancement. Figure printed with permission of H.T. van den Broek.

REFERENCES

1. Chung ES, Katra RP, Ghio S, Bax J, Gerritse B, Hilpisch K, et al. Cardiac resynchronization therapy may benefit patients with left ventricular ejection fraction >35%: a PROSPECT trial substudy. *Eur J Heart Fail.* 2010;12:581-7.
2. Lumens J, Tayal B, Walmsley J, Delgado-Montero A, Huntjens PR, Schwartzman D, et al. Differentiating Electromechanical From Non-Electrical Substrates of Mechanical Discoordination to Identify Responders to Cardiac Resynchronization Therapy. *Circ Cardiovasc Imaging.* 2015;8:e003744.
3. Risum N, Tayal B, Hansen TF, Bruun NE, Jensen MT, Lauridsen TK, et al. Identification of Typical Left Bundle Branch Block Contraction by Strain Echocardiography Is Additive to Electrocardiography in Prediction of Long-Term Outcome After Cardiac Resynchronization Therapy. *J Am Coll Cardiol.* 2015;66:631-41.
4. Van't Sant J, Ter Horst IA, Wijers SC, Mast TP, Leenders GE, Doevendans PA, et al. Measurements of electrical and mechanical dyssynchrony are both essential to improve prediction of CRT response. *J Electrocardiol.* 2015;48:601-8.
5. Teske AJ, De Boeck BW, Melman PG, Sieswerda GT, Doevendans PA, Cramer MJ. Echocardiographic quantification of myocardial function using tissue deformation imaging, a guide to image acquisition and analysis using tissue Doppler and speckle tracking. *Cardiovasc Ultrasound.* 2007;5:27.
6. Kirn B, Jansen A, Bracke F, van Gelder B, Arts T, Prinzen FW. Mechanical discoordination rather than dyssynchrony predicts reverse remodeling upon cardiac resynchronization. *Am J Physiol Heart Circ Physiol.* 2008;295:H640-6.
7. Maass AH, Vernooij K, Wijers SC, van 't Sant J, Cramer MJ, Meine M, et al. Refining success of cardiac resynchronization therapy using a simple score predicting the amount of reverse ventricular remodelling: results from the Markers and Response to CRT (MARC) study. *Europace.* 2017.
8. Negishi K, Lucas S, Negishi T, Hamilton J, Marwick TH. What is the primary source of discordance in strain measurement between vendors: imaging or analysis? *Ultrasound Med Biol.* 2013;39:714-20.
9. Stankovic I, Prinz C, Ciarka A, Daraban AM, Kotrc M, Aaronson M, et al. Relationship of visually assessed apical rocking and septal flash to response and long-term survival following cardiac resynchronization therapy (PREDICT-CRT). *Eur Heart J Cardiovasc Imaging.* 2016;17:262-9.

10. Ponikowski P, Voors AA, Anker SD, Bueno H, Cleland JG, Coats AJ, et al. 2016 ESC Guidelines for the diagnosis and treatment of acute and chronic heart failure: The Task Force for the diagnosis and treatment of acute and chronic heart failure of the European Society of Cardiology (ESC). Developed with the special contribution of the Heart Failure Association (HFA) of the ESC. *Eur J Heart Fail.* 2016;18:891-975.
11. Russo AM, Stainback RF, Bailey SR, Epstein AE, Heidenreich PA, Jessup M, et al. ACCF/HRS/AHA/ASE/HFSA/SCAI/SCCT/SCMR 2013 appropriate use criteria for implantable cardioverter-defibrillators and cardiac resynchronization therapy: a report of the American College of Cardiology Foundation appropriate use criteria task force, Heart Rhythm Society, American Heart Association, American Society of Echocardiography, Heart Failure Society of America, Society for Cardiovascular Angiography and Interventions, Society of Cardiovascular Computed Tomography, and Society for Cardiovascular Magnetic Resonance. *J Am Coll Cardiol.* 2013;61:1318-68.
12. Voigt JU, Pedrizzetti G, Lysyansky P, Marwick TH, Houle H, Baumann R, et al. Definitions for a common standard for 2D speckle tracking echocardiography: consensus document of the EACVI/ASE/Industry Task Force to standardize deformation imaging. *J Am Soc Echocardiogr.* 2015;28:183-93.
13. Farsalinos KE, Daraban AM, Unlu S, Thomas JD, Badano LP, Voigt JU. Head-to-Head Comparison of Global Longitudinal Strain Measurements among Nine Different Vendors: The EACVI/ASE Inter-Vendor Comparison Study. *J Am Soc Echocardiogr.* 2015;28:1171-1181, e2.
14. Kydd AC, Khan F, Gopalan D, Ring L, Rana BS, Virdee MS, et al. Utility of speckle tracking echocardiography to characterize dysfunctional myocardium in patients with ischemic cardiomyopathy referred for cardiac resynchronization therapy. *Echocardiography.* 2014;31:736-43.
15. Bilchick KC, Dimaano V, Wu KC, Helm RH, Weiss RG, Lima JA, et al. Cardiac magnetic resonance assessment of dyssynchrony and myocardial scar predicts function class improvement following cardiac resynchronization therapy. *J Am Coll Cardiol Img.* 2008;1:561-8.
16. Zwanenburg JJ, Gotte MJ, Kuijter JP, Heethaar RM, van Rossum AC, Marcus JT. Timing of cardiac contraction in humans mapped by high-temporal-resolution MRI tagging: early onset and late peak of shortening in lateral wall. *Am J Physiol Heart Circ Physiol.* 2004;286:H1872-80.
17. Leenders GE, De Boeck BW, Teske AJ, Meine M, Bogaard MD, Prinzen FW, et al. Septal rebound stretch is a strong predictor of outcome after cardiac resynchronization therapy. *J Card Fail.* 2012;18:404-12.

18. Risum N, Jons C, Olsen NT, Fritz-Hansen T, Bruun NE, Hojgaard MV, et al. Simple regional strain pattern analysis to predict response to cardiac resynchronization therapy: rationale, initial results, and advantages. *Am Heart J*. 2012;163:697-704.
19. D'Hooge J, Barbosa D, Gao H, Claus P, Prater D, Hamilton J, et al. Two-dimensional speckle tracking echocardiography: standardization efforts based on synthetic ultrasound data. *Eur Heart J Cardiovasc Imaging*. 2016;17:693-701.
20. Niederer SA, Shetty AK, Plank G, Bostock J, Razavi R, Smith NP, et al. Biophysical modeling to simulate the response to multisite left ventricular stimulation using a quadripolar pacing lead. *Pacing Clin Electrophysiol*. 2012;35:204-14.
21. Lumens J, Leenders GE, Cramer MJ, De Boeck BW, Doevendans PA, Prinzen FW, et al. Mechanistic evaluation of echocardiographic dyssynchrony indices: patient data combined with multiscale computer simulations. *Circ Cardiovasc Imaging*. 2012;5:491-9.
22. Sharma A, Bax JJ, Vallakati A, Goel S, Lavie CJ, Kassotis J, et al. Meta-Analysis of the Relation of Baseline Right Ventricular Function to Response to Cardiac Resynchronization Therapy. *Am J Cardiol*. 2016;117:1315-21.
23. Leong DP, Hoke U, Delgado V, Auger D, Witkowski T, Thijssen J, et al. Right ventricular function and survival following cardiac resynchronisation therapy. *Heart*. 2013;99:722-8.
24. de Groote P, Millaire A, Foucher-Hossein C, Nugue O, Marchandise X, Ducloux G, et al. Right ventricular ejection fraction is an independent predictor of survival in patients with moderate heart failure. *J Am Coll Cardiol*. 1998;32:948-54.
25. Bernard A, Donal E, Leclercq C, Ollivier R, Schnell F, de Place C, et al. Impact of right ventricular contractility on left ventricular dyssynchrony in patients with chronic systolic heart failure. *Int J Cardiol*. 2011;148:289-94.
26. Pappone C, Calovic Z, Vicedomini G, Cuko A, McSpadden LC, Ryu K, et al. Improving cardiac resynchronization therapy response with multipoint left ventricular pacing: Twelve-month follow-up study. *Heart Rhythm*. 2015;12:1250-8.
27. Zanon F, Marcantoni L, Baracca E, Pastore G, Lanza D, Fraccaro C, et al. Optimization of left ventricular pacing site plus multipoint pacing improves remodeling and clinical response to cardiac resynchronization therapy at 1 year. *Heart Rhythm*. 2016;13:1644-51.
28. Leyva F, Zegard A, Qiu T, Acquaye E, Ferrante G, Walton J, et al. Cardiac Resynchronization Therapy Using Quadripolar Versus Non-Quadripolar Left Ventricular Leads Programmed to Biventricular Pacing With Single-Site Left Ventricular Pacing: Impact on Survival and Heart Failure Hospitalization. *J Am Heart Assoc*. 2017;6.

29. Asbach S, Hartmann M, Wengenmayer T, Graf E, Bode C, Biermann J. Vector selection of a quadripolar left ventricular pacing lead affects acute hemodynamic response to cardiac resynchronization therapy: a randomized cross-over trial. *PLoS one*. 2013;8:e67235.
30. Cabrera Bueno F, Alzueta Rodriguez J, Olague de Ros J, Fernandez-Lozano I, Garcia Guerrero JJ, de la Concha JF, et al. Improvement in hemodynamic response using a quadripolar LV lead. *Pacing Clin Electrophysiol*. 2013;36:963-9.
31. Zanon F, Baracca E, Pastore G, Fraccaro C, Roncon L, Aggio S, et al. Determination of the longest intrapatient left ventricular electrical delay may predict acute hemodynamic improvement in patients after cardiac resynchronization therapy. *Circ Arrhythm Electrophysiol*. 2014;7:377-83.
32. Gold MR, Birgersdotter-Green U, Singh JP, Ellenbogen KA, Yu Y, Meyer TE, et al. The relationship between ventricular electrical delay and left ventricular remodelling with cardiac resynchronization therapy. *Eur Heart J*. 2011;32:2516-2524.
33. Singh JP, Fan D, Heist EK, Alabiad CR, Taub C, Reddy V, et al. Left ventricular lead electrical delay predicts response to cardiac resynchronization therapy. *Heart Rhythm*. 2006;3:1285-92.
34. Helm RH, Byrne M, Helm PA, Daya SK, Osman NF, Tunin R, et al. Three-dimensional mapping of optimal left ventricular pacing site for cardiac resynchronization. *Circulation*. 2007;115:953-61.
35. Rad MM, Blaauw Y, Dinh T, Pison L, Crijns HJ, Prinzen FW, et al. Left ventricular lead placement in the latest activated region guided by coronary venous electroanatomic mapping. *Europace*. 2015;17:84-93.
36. Ypenburg C, SchaliJ MJ, Bleeker GB, Steendijk P, Boersma E, Dibbets-Schneider P, et al. Impact of viability and scar tissue on response to cardiac resynchronization therapy in ischaemic heart failure patients. *Eur Heart J*. 2007;28:33-41.
37. de Roest GJ, Wu L, de Cock CC, Hendriks ML, Delnoy PP, van Rossum AC, et al. Scar tissue-guided left ventricular lead placement for cardiac resynchronization therapy in patients with ischemic cardiomyopathy: an acute pressure-volume loop study. *Am Heart J*. 2014;167:537-45.
38. Saba S, Marek J, Schwartzman D, Jain S, Adelstein E, White P, et al. Echocardiography-guided left ventricular lead placement for cardiac resynchronization therapy: results of the Speckle Tracking Assisted Resynchronization Therapy for Electrode Region trial. *Circ Heart Fail*. 2013;6:427-34.
39. Ypenburg C, van Bommel RJ, Delgado V, Mollema SA, Bleeker GB, Boersma E, et al. Optimal left ventricular lead position predicts reverse remodeling and survival after cardiac resynchronization therapy. *J Am Coll Cardiol*. 2008;52:1402-9.
40. Pluijmert M, Bovendeerd PH, Lumens J, Vernooy K, Prinzen FW, Delhaas T. New insights from a computational model on the relation between pacing site and CRT response. *Europace*. 2016;18:iv94-iv103.

41. Kydd AC, Khan FZ, Watson WD, Pugh PJ, Virdee MS, Dutka DP. Prognostic benefit of optimum left ventricular lead position in cardiac resynchronization therapy: follow-up of the TARGET Study Cohort (Targeted Left Ventricular Lead Placement to guide Cardiac Resynchronization Therapy). *JACC Heart Failure*. 2014;2:205-12.
42. Khan FZ, Virdee MS, Palmer CR, Pugh PJ, O'Halloran D, Elsik M, et al. Targeted left ventricular lead placement to guide cardiac resynchronization therapy: the TARGET study: a randomized, controlled trial. *J Am Coll Cardiol*. 2012;59:1509-1518.
43. Mele D, Nardoza M, Malagu M, Leonetti E, Fragale C, Rondinella A, et al. Left Ventricular Lead Position Guided by Parametric Strain Echocardiography Improves Response to Cardiac Resynchronization Therapy. *J Am Soc Echocardiogr*. 2017.
44. Daya HA, Alam MB, Adelstein E, Schwartzman D, Jain S, Marek J, et al. Echocardiography-guided left ventricular lead placement for cardiac resynchronization therapy in ischemic vs nonischemic cardiomyopathy patients. *Heart Rhythm*. 2014.
45. Abu Daya H, Alam MB, Adelstein E, Schwartzman D, Jain S, Marek J, et al. Echocardiography-guided left ventricular lead placement for cardiac resynchronization therapy in ischemic vs nonischemic cardiomyopathy patients. *Heart Rhythm*. 2014;11:614-9.
46. Strauss DG, Selvester RH, Wagner GS. Defining left bundle branch block in the era of cardiac resynchronization therapy. *Am J Cardiol*. 2011;107:927-34.
47. Sterlinski M, Sokal A, Lenarczyk R, Van Heuverswyn F, Rinaldi CA, Vanderheyden M, et al. In Heart Failure Patients with Left Bundle Branch Block Single Lead MultiSpot Left Ventricular Pacing Does Not Improve Acute Hemodynamic Response To Conventional Biventricular Pacing. A Multicenter Prospective, Interventional, Non-Randomized Study. *PLoS one*. 2016;11:e0154024.
48. Sohal M, Shetty A, Niederer S, Lee A, Chen Z, Jackson T, et al. Mechanistic insights into the benefits of multisite pacing in cardiac resynchronization therapy: The importance of electrical substrate and rate of left ventricular activation. *Heart Rhythm*. 2015;12:2449-57.
49. Zanon F, Baracca E, Pastore G, Marcantoni L, Fraccaro C, Lanza D, et al. Multipoint pacing by a left ventricular quadripolar lead improves the acute hemodynamic response to CRT compared with conventional biventricular pacing at any site. *Heart Rhythm*. 2015;12:975-81.
50. Pappone C, Calovic Z, Vicedomini G, Cuko A, McSpadden LC, Ryu K, et al. Multipoint left ventricular pacing improves acute hemodynamic response assessed with pressure-volume loops in cardiac resynchronization therapy patients. *Heart Rhythm*. 2014;11:394-401.
51. Akerstrom F, Narvaez I, Puchol A, Pachon M, Martin-Sierra C, Rodriguez-Manero M, et al. Estimation of the effects of multipoint pacing on battery longevity in routine clinical practice. *Europace*. 2017.

52. Leclercq C. More rEponse on Cardiac Resynchronization Therapy With MultiPoint Pacing (MORE-CRT MPP). *ClinicalTrials.gov*. 2013;NCT02006069.
53. Derval N, Duchateau J, Mahida S, Eschali r R, Sacher F, Lumens J, et al. Distinctive Left Ventricular Activations Associated With ECG Pattern in Heart Failure Patients. *Circ Arrhythm Electrophysiol*. 2017;10.
54. Lyons KJ, Ezekowitz JA, Liang L, Heidenreich PA, Yancy CW, DeVore AD, et al. Impact of Current Versus Previous Cardiac Resynchronization Therapy Guidelines on the Proportion of Patients With Heart Failure Eligible for Therapy. *JACC Heart Failure*. 2017;5:388-392.
55. Bogaard MD, Meine M, Tuinenburg AE, Maskara B, Loh P, Doevendans PA. Cardiac resynchronization therapy beyond nominal settings: who needs individual programming of the atrioventricular and interventricular delay? *Europace*. 2012;14:1746-53.
56. Auger D, Hoke U, Bax JJ, Boersma E, Delgado V. Effect of atrioventricular and ventriculoventricular delay optimization on clinical and echocardiographic outcomes of patients treated with cardiac resynchronization therapy: a meta-analysis. *Am Heart J*. 2013;166:20-9.
57. Burns KV, Gage RM, Curtin AE, Gorcsan J, 3rd, Bank AJ. Left ventricular-only pacing in heart failure patients with normal atrioventricular conduction improves global function and left ventricular regional mechanics compared with biventricular pacing: an adaptive cardiac resynchronization therapy sub-study. *Eur J Heart Fail*. 2017.
58. Ter Horst IAH, Bogaard MD, Tuinenburg AE, Mast TP, de Boer TP, Doevendans P, et al. The concept of triple wavefront fusion during biventricular pacing: Using the EGM to produce the best acute hemodynamic improvement in CRT. *Pacing Clin Electrophysiol*. 2017;40:873-882.
59. Jones S, Lumens J, Sohaib SM, Finegold JA, Kanagaratnam P, Tanner M, et al. Cardiac resynchronization therapy: mechanisms of action and scope for further improvement in cardiac function. *Europace*. 2016.
60. Thibault B, Dubuc M, Khairy P, Guerra PG, Macle L, Rivard L, et al. Acute haemodynamic comparison of multisite and biventricular pacing with a quadripolar left ventricular lead. *Europace*. 2013;15:984-91.
61. Mounthey P, Behar JM, Toth D, Panayiotou M, Reiml S, Jolly MP, et al. A Planning and Guidance Platform for Cardiac Resynchronization Therapy. *IEEE Trans Med Imaging*. 2017.
62. Behar JM, Claridge S, Jackson T, Sieniewicz B, Porter B, Webb J, et al. The role of multi modality imaging in selecting patients and guiding lead placement for the delivery of cardiac resynchronization therapy. *Expert Rev Cardiovasc Ther*. 2017;15:93-107.

63. Nguyen UC, Mafi-Rad M, Aben JP, Smulders MW, Engels EB, van Stipdonk AM, et al. A novel approach for left ventricular lead placement in cardiac resynchronization therapy: Intraprocedural integration of coronary venous electroanatomic mapping with delayed enhancement cardiac magnetic resonance imaging. *Heart Rhythm*. 2017;14:110-119.
64. Pluijmert M, Lumens J, Potse M, Delhaas T, Auricchio A, Prinzen FW. Computer Modelling for Better Diagnosis and Therapy of Patients by Cardiac Resynchronisation Therapy. *Arrhythm Electrophysiol Rev*. 2015;4:62-7.
65. Behar JM, Mountney P, Toth D, Reiml S, Panayiotou M, Brost A, et al. Real-Time X-MRI-Guided Left Ventricular Lead Implantation for Targeted Delivery of Cardiac Resynchronization Therapy. *J Am Coll EP*. 2017;3:803-814.



Appendix

- I Nederlandse samenvatting
- II List of abbreviations
- III List of publications
- IV Dankwoord
- V Curriculum vitae

NEDERLANDSE SAMENVATTING

Cardiale resynchronisatie therapie (CRT) heeft een positieve effectiviteit op kwaliteit van leven, morbiditeit en mortaliteit.^{1, 2} Helaas heeft een substantieel deel van de patiënten die een CRT-implantatie hebben ondergaan, onvoldoende baat van de therapie.³ Er zijn verschillende strategieën om de effectiviteit van de therapie te vergroten. Enerzijds kan men de patiënten met een grote kans op een goed effect op voorhand selecteren. Hierdoor vermindert het aantal onnodige ingrepen, wordt de kosteneffectiviteit vergroot en kan schaarse en dure academische zorg beter worden ingezet. Wellicht nog belangrijker, patiënten krijgen hierdoor geen onnodige zorg met kans op schade door complicaties tijdens de ingreep of schade door de therapie zelf.⁴ Anderzijds kan men de effectiviteit van de therapie vergroten, door de toepassing te verbeteren en het effect op de pompfunctie te verhogen. De effectiviteit kan verbeterd worden door de plaatsing en het gebruik van de linkerkamer draad te optimaliseren. Tevens zijn de instellingen van het CRT-apparaat te optimaliseren, ten einde de samenwerking van de verschillende hartkamers en wanden van linkerhartkamer te verbeteren. Dit proefschrift heeft zowel betrekking op de selectie van patiënten, op de plaatsing van de linkerkamerdraad, als op de instellingen van het CRT-apparaat.

PATIËNTEN SELECTIE VOOR CRT

De juiste patiënten voor CRT kunnen geselecteerd worden met parameters die de elektrische en/of mechanische dyssynchronie of discoördinatie meetbaar maken. In de huidige internationale cardiologische richtlijnen worden voornamelijk elektrische parameters gebruikt afkomstig van het ECG, waaronder de QRS breedte en morfologie.^{5, 6} Om de selectie criteria te verbeteren kunnen parameters van mechanische dyssynchronie en discoördinatie worden toegevoegd.⁷ Parameters van mechanische dyssynchronie en discoördinatie kunnen in beeld worden gebracht met medische beeldvormende technieken, zoals magnetische resonantie beeldvorming (MRI) en echocardiografie. In hoofdstuk 2 geven we een overzicht van de mogelijkheden van echocardiografie bij de klinische toepassing van CRT. De mechanische dyssynchronie parameters worden uiteengezet, alsmede hun sterktes en zwaktes. Een grote multicenter studie naar dyssynchronie parameters liet zien dat deze parameters van onvoldoende nut zijn voor selectie.⁸ Discoördinatie parameters zijn, in tegenstelling tot de op timing gebaseerde dyssynchronie parameters, gebaseerd op fracties

of percentages van inefficiënte myocardiale beweging. Deze parameters zijn veelbelovend gebleken in monocenter studies.^{7, 9} De toepassing van deze parameters laat echter op zich wachten. Enerzijds kan dat komen door verschillen in de absolute waarden wanneer deze parameters worden onderzocht met verschillende systemen voor echocardiografie. In dit proefschrift zijn verschillende systemen onderzocht die gebruik maken van het spikkel patroon van een echocardiogram om de beweging van de verschillende delen van de hartspier te volgen. Deze techniek heet 'speckle tracking echocardiografie'. Drie veel gebruikte computersystemen om de hoeveelheid beweging c.q. discoördinatie te volgen zijn geanalyseerd. De beweging in het interventriculaire septum gaf opvallende verschillen tussen twee systemen in een kleine studie (hoofdstuk 3). Het indelen in typische septale bewegingspatronen gaf echter goede overeenkomsten. Deze bevindingen konden niet gereproduceerd worden in de nieuwste software versies (hoofdstuk 4). Er werden in een grotere groep patiënten belangrijke verschillen gezien tussen drie veelgebruikte systemen. Er waren tevens grote verschillen in afkapwaarden van parameters voor het voorspellen van CRT-respons. Het is belangrijk dat deze systemen een betere overeenkomst laten zien, omdat de grote verschillen de translatie van deze techniek naar de kliniek bemoeilijkt. In een andere studie zijn de dyssynchronie en discoördinatie parameters gemeten met twee MRI-technieken (MRI tagging en MRI feature tracking) en vergeleken met speckle tracking echocardiografie. De MRI-technieken bleken bij het meten van dyssynchronie en discoördinatie een betere overeenkomst met elkaar te hebben (hoofdstuk 5). Desondanks waren alle drie de technieken in staat om CRT-respons te voorspellen met een parameter gebaseerd op de eind-systolische rek van het septum (hoofdstuk 6). Tevens presteerde de indeling in typische septale bewegingspatronen goed met alle drie de technieken.

In hoofdstuk 7 wordt de toepassing van computermodellen bij het begrijpen van beeldvorming van de rechterhartkamer functie en pathologie beschreven. De rechterhartkamer is een complexe hartkamer, zowel qua structuur als functie. De complexe interactie van de verschillende hartkamers en dyssynchronie en discoördinatie bij het linkerbundeltakblok kan beter begrepen worden met behulp van computersimulaties. Deze kennis is toegepast in hoofdstuk 8, waar de invloed van de rechterhartkamer op het voorspellen van CRT-respons is onderzocht. Dysfunctie van de rechterhartkamer bleek de kans op CRT-respons te verminderen, maar had relatief weinig invloed op de hoeveelheid discoördinatie in het septum. Daarom kan de maat voor systolische septale discoördinatie (SRSsept) niet gebruikt worden om CRT-respons te voorspellen in patiënten met ernstig falen van de rechterhartkamer.

Echocardiografische beoordeling van de pompfunctie van de rechterhartkamer is derhalve belangrijk bij het selecteren van patiënten voor CRT.

PLAATSING VAN DE LINKERKAMERDRAAD

CRT maakt gebruik van drie draden, met naast de twee draden in de rechterboezem en rechterkamer een draad om de linkerhartkamer. Uit meerdere grootschalige onderzoeken naar de werking en effectiviteit van CRT is bekend dat de ligging van de linkerkamerdraad belangrijk is.¹⁰⁻¹² De linkerkamerdraad is dan ook de draad die voor vroege activatie zorgt van de, tijdens het linkerbundeltakblok laat geactiveerde, linkerkamer vrije wand. Het resynchroniseren heeft vooral betrekking op het weer gelijktijdig laten samentrekken van het interventriculaire septum en de linkerkamer vrije wand. Zoals gezegd heeft de plek waar de draad geplaatst een groot effect op de effectiviteit van CRT.^{13, 14} De linkerkamerdraad plaatsing is echter beperkt door de coronaire veneuze anatomie. De cardioloog kan met de conventionele endovasculaire benadering alleen de gebieden bereiken waar een linkerkamerdraad in een coronaire vene is te plaatsen. Ondanks dat dit de meest gebruikte techniek is, blijft het een proces van mogelijkheden en beperkingen. Met de standaard bipolaire linkerkamerdraden was het mogelijk om slechts met twee elektroden aan het distale uiteinde van de draad het hart elektrisch te prikkelen. Wanneer deze elektroden, na een lange procedure, dichtbij of in geïnfarceerd weefsel geplaatst zijn, is CRT niet effectief.^{15, 16} Tevens kan draadplaatsing beperkt worden door de zenuw naar het middenrif (nervus phrenicus sinistra). Indien de draad dicht bij de nervus phrenicus ligt, kan deze elektrisch geprikkeld raken ten tijde van CRT. Hierdoor krijgt een patiënt hikjes met de snelheid van zijn of haar hartfrequentie. Ook deze situatie is onacceptabel en benodigd een nieuwe draadplaatsing. Tenslotte bestaat er bewijs dat elke patiënt een zogeheten 'optimale plek' heeft voor de linkerkamerdraad. Dit is waarschijnlijk het gebied met aantoonbaar late elektrische activatie tijdens het linkerbundeltakblok en dientengevolge late contractie.¹⁷ Als de linkerkamer hier gestimuleerd wordt is het effect op de pompfunctie het grootst.

Sinds enkele jaren zijn er door meerdere fabrikanten draden op de markt gebracht met meerdere elektrodes. Deze quadripolaire (vierpolige) linkerkamerdraden hebben verspreid over het uiteinde van de draad vier elektroden liggen. In hoofdstuk 9 van dit proefschrift worden de verschillende quadripolaire draden uitgelicht. In dit hoofdstuk concluderen we dat de additionele elektroden een belangrijke meerwaarde zijn voor CRT. De drie eerdergenoemde belangrijke aspecten van linkerkamerdraad plaatsing, plaatsing in een

doelgebied, weg van infarct en de nervus phrenicus, zijn gemakkelijker te bereiken. Meerdere onderzoeken werden bekeken, welke allen een meerwaarde vonden van de quadripolaire linkerkamerdraad. Zowel op het aantal succesvolle draad plaatsingen, acute hemodynamische effect en de gevolgen op de lange termijn. Er zijn echter ook nog een aantal onduidelijkheden. Zo zijn er weinig onderzoeken uitgevoerd die gericht gekeken hebben naar de meerwaarde van de extra elektroden op de pompfunctie ten opzichte van de standaard bipolaire draad. Daarnaast is het onbekend welke elektrode de meest gunstige effecten heeft voor de individuele patiënt. Het is belangrijk om te weten of de quadripolaire draden niet alleen de implantatie vergemakkelijken, maar ook hoe we de patiënt zoveel mogelijk baat kunnen geven. Met het oog op patiëntgerichte zorg zijn we in 2014 begonnen aan de Opticare-QLV studie. Een studie naar de optimalisatie van cardiale resynchronisatie therapie met quadripolaire linker ventrikel draden. In hoofdstukken 11 tot en met 13 staan de resultaten van dit onderzoek beschreven. In vier jaar tijd hebben we in drie academische centra in Nederland 51 patiënten onderzocht. Direct na CRT implantatie werd het hemodynamisch effect op de linkerkamerfunctie van de vier elektroden gemeten met invasieve druk-volume curves. Hierbij is ons duidelijk geworden dat de acute hemodynamische effecten van CRT met quadripolaire draden sterk variëren tussen de patiënten. Sommige patiënten lieten een klein effect zien van CRT, anderen een zeer groot. Het verschil in effect van de vier elektroden was per patiënt ook divers. Bij sommige patiënten was er weinig verschil, bij anderen was dit verschil groot. Op voorhand is dit effect niet te voorspellen. Welke elektrode de patiënt het meeste baat geeft, bleek ook een moeilijke puzzel. Na lang passen en meten, bleek een veelbelovende parameter niet het juiste puzzelstuk. In eerdere onderzoeken was de intrinsieke geleidingsvertraging van Q op het oppervlakte electrocardiogram naar de lokale depolarisatie bij de linkerkamerdraad elektrode (QLV) geassocieerd met acuut hemodynamisch respons.^{18, 19} Draad plaatsing in een gebied met een zo groot mogelijke vertraging of lang QLV-interval, zou de hemodynamische respons vergroten. Dit bleek in ons onderzoek niet zo te zijn. In slechts de helft van de patiënten was er een direct verband tussen QLV en hemodynamische respons. Deze patiënten bleken vaker een minder gunstige draadpositie te hebben, met lagere QLV-waarden. De patiënten zonder een directe relatie waren niet op voorhand aan te wijzen. Op groepsniveau was er wel een relatie tussen QLV, gecorrigeerd voor de intrinsieke QRS duur, en hemodynamische respons. Concluderend kunnen we zeggen dat het belangrijk is om de draad in een gebied met een lang QLV-interval te plaatsen, maar dat de elektrode met de beste hemodynamische respons niet te selecteren is op basis van het QLV.

CRT-INSTELLINGEN

Naast het selecteren van een optimale elektrode, biedt een quadripolaire draad ook de mogelijkheid tot multi-point pacing (MPP). Met MPP kunnen twee elektroden van dezelfde quadripolaire draad tegelijkertijd of met een kleine tijdsvertraging de linkerkamer elektrisch prikkelen. MPP zou de snelheid en homogeniteit van de depolarisatie van de linkerkamer vrije wand kunnen verbeteren. Meerdere onderzoeken zijn positief over het effect van MPP op de effectiviteit van CRT.^{20, 21} Omdat er in de methodiek van de eerdere onderzoeken beperkingen zaten, is het effect van MPP onderzocht in hoofdstuk 12. Drie verschillende MPP-instellingen werden vergeleken met vier instellingen van 'conventioneel' CRT. Conventioneel CRT betekent dat er een van de vier elektroden van de quadripolaire draad wordt gebruikt voor stimulering van de linkerkamer vrije wand. Het gemiddelde effect van MPP op de acute hemodynamische respons ten opzichte van de beste conventionele instelling was negatief, alhoewel niet significant. Sommige patiënten verbeterden met MPP ten opzichte van de beste conventionele instelling, anderen verslechterden. De verschillen tussen MPP en conventioneel CRT waren vaak gering, en slechts in sommige gevallen groot. Er zijn geen complicaties van MPP bekend. Echter, aangezien MPP een negatief effect heeft op de levensduur van de batterij van het CRT-apparaat, is het belangrijk dat MPP een bewezen meerwaarde heeft. Vooral mannen, patiënten met een ischemische oorzaak van het hartfalen en patiënten met een slechtere linkerkamer pompfunctie hadden meer baat van MPP ten opzichte van conventioneel CRT. In deze patiënten kan het effect van MPP gemeten worden, indien conventioneel CRT onvoldoende verbetering geeft ten opzichte van de situatie zonder CRT.

Een andere instelling die direct effect heeft op de hemodynamische functie is het atrioventriculaire (AV) interval. Tussen het registreren van atriale activatie (of atriale stimulatie) en het elektrisch stimuleren van de hartkamers, wordt een interval geprogrammeerd: het AV-interval. Ondanks dat de bewijsvoering voor optimalisatie strategieën voor het AV-interval tekortschiet,²² hebben alle fabrikanten van CRT-apparaten ingebouwde algoritmen voor dit doel. Deze algoritmen zijn vaak niet of onvoldoende op fysiologische bewijsvoering gebaseerd. Omdat er in het Opticare-QLV onderzoek vier atrioventriculaire intervallen getest zijn per elektrode, is het optimale interval per patiënt te bepalen. Dit interval is namelijk patiënt specifiek en kan bij de juiste instelling tot een verbetering van de acute hemodynamische respons leiden.^{23, 24} In ons onderzoek tonen we aan dat een eenvoudig algoritme gebaseerd op patiënt specifieke intrinsieke intervallen leidt tot goede resultaten.

Dit algoritme is gebaseerd op een AV-interval gebaseerd op 50% van het tijdsinterval tussen stimulering in de boezem en depolarisatie van de rechterkamer electrode. Het algoritme evenaart de maximale hoeveelheid acute hemodynamische respons als beste, al is het verschil met een standaard instelling van 120ms niet statistisch significant en ook niet relevant. Het effect van een patiënt specifieke instelling zal echter in een ander cohort geverifieerd moeten worden. Omdat in dit onderzoek alleen atriale 'pacing' is onderzocht en het CRT-apparaat bij de meeste patiënten op het intrinsieke sinusritme zal reageren, moet het algoritme ook gecontroleerd worden voor atriale 'sensing'. Dat de variatie in optimaal AV-interval niet significant varieert per patiënt was echter een opvallende bevinding in ons onderzoek. Hierdoor kan het patiënt-specifieke optimale AV-interval voor één elektrode berekend worden, en hoeft dit niet per stimuleringsplek bepaald te worden.

REFERENTIES

1. Cleland JG, Daubert JC, Erdmann E, Freemantle N, Gras D, Kappenberger L, et al. Long-term effects of cardiac resynchronization therapy on mortality in heart failure [the Cardiac Resynchronization-Heart Failure (CARE-HF) trial extension phase]. *Eur Heart J*. 2006;27:1928-32.
2. Goldenberg I, Kutyifa V, Klein HU, Cannom DS, Brown MW, Dan A, et al. Survival with cardiac-resynchronization therapy in mild heart failure. *N Engl J Med*. 2014;370:1694-701.
3. Wilkoff BL, Fauchier L, Stiles MK, Morillo CA, Al-Khatib SM, Almendral J, et al. 2015 HRS/EHRA/APHRS/SOLAECE expert consensus statement on optimal implantable cardioverter-defibrillator programming and testing. *Europace*. 2016;18:159-83.
4. Perkiomaki JS, Ruwald AC, Kutyifa V, Ruwald MH, McNitt S, Polonsky B, et al. Risk factors and the effect of cardiac resynchronization therapy on cardiac and non-cardiac mortality in MADIT-CRT. *Europace*. 2015;17:1816-22.
5. Russo AM, Stainback RF, Bailey SR, Epstein AE, Heidenreich PA, Jessup M, et al. ACCF/HRS/AHA/ASE/HFSA/SCAI/SCCT/SCMR 2013 appropriate use criteria for implantable cardioverter-defibrillators and cardiac resynchronization therapy. *J Am Coll Cardiol*. 2013;61:1318-68.
6. Ponikowski P, Voors AA, Anker SD, Bueno H, Cleland JG, Coats AJ, et al. 2016 ESC Guidelines for the diagnosis and treatment of acute and chronic heart failure: The Task Force for the diagnosis and treatment of acute and chronic heart failure of the European Society of Cardiology (ESC). Developed with the special contribution of the Heart Failure Association (HFA) of the ESC. *Eur J Heart Fail*. 2016;18:891-975.
7. Lumens J, Tayal B, Walmsley J, Delgado-Montero A, Huntjens PR, Schwartzman D, et al. Differentiating Electromechanical From Non-Electrical Substrates of Mechanical Discoordination to Identify Responders to Cardiac Resynchronization Therapy. *Circ Cardiovasc Imaging*. 2015;8:e003744.
8. Chung ES, Leon AR, Tavazzi L, Sun JP, Nihoyannopoulos P, Merlino J, et al. Results of the Predictors of Response to CRT (PROSPECT) trial. *Circulation*. 2008;117:2608-16.
9. Leenders GE, De Boeck BW, Teske AJ, Meine M, Bogaard MD, Prinzen FW, et al. Septal rebound stretch is a strong predictor of outcome after cardiac resynchronization therapy. *J Card Fail*. 2012;18:404-12.
10. Saxon LA, Olshansky B, Volosin K, Steinberg JS, Lee BK, Tomassoni G, et al. Influence of left ventricular lead location on outcomes in the COMPANION study. *J Cardiovasc Electrophysiol*. 2009;20:764-8.

11. Singh JP, Klein HU, Huang DT, Reek S, Kuniss M, Quesada A, et al. Left ventricular lead position and clinical outcome in the multicenter automatic defibrillator implantation trial-cardiac resynchronization therapy (MADIT-CRT) trial. *Circulation*. 2011;123:1159-66.
12. Thebault C, Donal E, Meunier C, Gervais R, Gerritse B, Gold MR, et al. Sites of left and right ventricular lead implantation and response to cardiac resynchronization therapy observations from the REVERSE trial. *Eur Heart J*. 2012;33:2662-71.
13. Kydd AC, Khan FZ, Watson WD, Pugh PJ, Virdee MS, Dutka DP. Prognostic benefit of optimum left ventricular lead position in cardiac resynchronization therapy: follow-up of the TARGET Study Cohort (Targeted Left Ventricular Lead Placement to guide Cardiac Resynchronization Therapy). *JACC Heart Failure*. 2014;2:205-12.
14. Khan FZ, Virdee MS, Palmer CR, Pugh PJ, O'Halloran D, Elsik M, et al. Targeted left ventricular lead placement to guide cardiac resynchronization therapy: the TARGET study: a randomized, controlled trial. *J Am Coll Cardiol*. 2012;59:1509-1518.
15. Ypenburg C, Schalijs MJ, Bleeker GB, Steendijk P, Boersma E, Dibbets-Schneider P, et al. Impact of viability and scar tissue on response to cardiac resynchronization therapy in ischaemic heart failure patients. *Eur Heart J*. 2007;28:33-41.
16. Khan FZ, Virdee MS, Read PA, Pugh PJ, O'Halloran D, Fahey M, et al. Effect of low-amplitude two-dimensional radial strain at left ventricular pacing sites on response to cardiac resynchronization therapy. *J Am Soc Echocardiogr*. 2010;23:1168-76.
17. Saba S, Marek J, Schwartzman D, Jain S, Adelstein E, White P, et al. Echocardiography-guided left ventricular lead placement for cardiac resynchronization therapy: results of the Speckle Tracking Assisted Resynchronization Therapy for Electrode Region trial. *Circ Heart Fail*. 2013;6:427-34.
18. Zanon F, Baracca E, Pastore G, Fraccaro C, Roncon L, Aggio S, et al. Determination of the longest inpatient left ventricular electrical delay may predict acute hemodynamic improvement in patients after cardiac resynchronization therapy. *Circ Arrhythm Electrophysiol*. 2014;7:377-83.
19. Singh JP, Fan D, Heist EK, Alabiad CR, Taub C, Reddy V, et al. Left ventricular lead electrical delay predicts response to cardiac resynchronization therapy. *Heart Rhythm*. 2006;3:1285-92.
20. Pappone C, Calovic Z, Vicedomini G, Cuko A, McSpadden LC, Ryu K, et al. Improving cardiac resynchronization therapy response with multipoint left ventricular pacing: Twelve-month follow-up study. *Heart Rhythm*. 2015;12:1250-8.
21. Zanon F, Baracca E, Pastore G, Marcantoni L, Fraccaro C, Lanza D, et al. Multipoint pacing by a left ventricular quadripolar lead improves the acute hemodynamic response to CRT compared with conventional biventricular pacing at any site. *Heart Rhythm*. 2015;12:975-81.

22. Auger D, Hoke U, Bax JJ, Boersma E, Delgado V. Effect of atrioventricular and ventriculoventricular delay optimization on clinical and echocardiographic outcomes of patients treated with cardiac resynchronization therapy: a meta-analysis. *Am Heart J*. 2013;166:20-9.
23. Bogaard MD, Meine M, Tuinenburg AE, Maskara B, Loh P, Doevendans PA. Cardiac resynchronization therapy beyond nominal settings: who needs individual programming of the atrioventricular and interventricular delay? *Europace*. 2012;14:1746-53.
24. Ter Horst IAH, Bogaard MD, Tuinenburg AE, Mast TP, de Boer TP, Doevendans P, et al. The concept of triple wavefront fusion during biventricular pacing: Using the EGM to produce the best acute hemodynamic improvement in CRT. *Pacing Clin Electrophysiol*. 2017.



LIST OF ABBREVIATIONS

$\Delta\%dP/dt_{\max}$:	percentage change in maximal rate of pressure rise
$\Delta\%SW$:	percentage change in stroke work
2D:	two dimensional
2DS-RV:	right ventricular free wall peak strain
3D:	three dimensional
3DE:	three dimensional echocardiography
AHR:	acute hemodynamic response
AP4CH or 4CH:	apical four chamber view
ARVC:	arrhythmogenic right ventricular cardiomyopathy
ASE:	American Society of Echocardiography
AV:	atrioventricular
AVC	strain: strain value at aortic valve closure
AVC:	aortic valve closure
BiQ:	biventricular pacing with a quadripolar lead
BIV-CONV:	biventricular pacing with the distal electrode of a quadripolar lead;
BIV-OPT:	biventricular pacing with the electrode with highest increase in stroke work, of a quadripolar lead;
B-mode:	brightness mode
CHD:	congenital heart defect
CMR:	cardiac magnetic resonance imaging
CMR-FT:	cardiac magnetic resonance feature tracking
CMR-TAG:	cardiac magnetic resonance myocardial tagging
CONV:	conventional biventricular pacing with a bipolar lead or distal pacing vector of a quadripolar lead (i.e. tip electrode)
COV:	coefficient of variation
CRT:	cardiac resynchronization therapy
CSPAMM:	complementary spatial modulation of magnetization
CURE:	circumferential uniformity ratio estimates
DCM:	dilated cardiomyopathy
EACVI:	European Association of Cardiovascular Imaging
EAM:	electro-anatomical map

ECG:	electrocardiogram
ESV:	end-systolic volume
GE:	General Electric
GEE:	generalized estimated equation
ICC:	intra-class correlation coefficient
ICM:	ischemic cardiomyopathy
IEGM:	intracardiac electrogram
ILVD:	inter left ventricular delay
ISF_{LV} :	internal stretch factor of all left ventricular segments
$ISF_{sep-lat}$:	internal stretch factor of septum and lateral wall
IVMD:	interventricular mechanical dyssynchrony
L_0 :	reference length
LAO:	left anterior oblique
LBBB:	left bundle branch block
LBBB-1:	double-peaked systolic shortening
LBBB-2:	early pre-ejection shortening peak followed by prominent systolic stretching
LBBB-3:	pseudonormal shortening with a late-systolic shortening peak followed by less pronounced end-systolic stretch
LV:	left ventricular <i>or</i> left ventricle
LVEDV:	left ventricular end-diastolic volume
LVEDV:	left ventricular end-diastolic volume
LVEF:	left ventricular ejection fraction
LVESV:	left ventricular end-systolic volume
MARC:	Markers and Response to Cardiac Resynchronization Therapy
MPP:	multi-point pacing
MRI:	magnetic resonance imaging
NYHA:	New York Heart Association
Onset-delay:	time delay between onset of shortening of septal and lateral wall
Peak-delay:	septal to lateral wall delay of time to maximal peak shortening
PNS:	phrenic nerve stimulation
PV:	pressure-volume
PV-loop:	pressure volume loop

QLV/QRSd:	ratio between Q on surface ECG to LV sensing interval and QRS duration
QLV:	Q-wave (on ECG) to LV depolarization (on IEGM) interval
R:	correlation coefficient
R ² :	coefficient of determination
RA:	right atrial
RAO:	right anterior oblique
RAp-RVs:	right atrial pacing to right ventricular sensing interval
ROI:	region of interest
RV:	right ventricular <i>or</i> right ventricle
RVEDA:	right ventricular end-diastolic area
RVESA:	right ventricular end-systolic area
RVFAC:	right ventricular fractional area change
RVp-LVs:	right ventricular pacing to left ventricular sensing interval
SL-delay:	septal to lateral wall delay
SRS:	septal rebound stretch
SRSsept:	systolic rebound stretch of the septum
SS:	systolic strain
SSFP:	steady-state free-precession
SSI:	systolic stretch index
STE:	speckle tracking echocardiography
Strain-SL:	time-to-peak strain between septum and LV lateral wall
SW:	stroke work
TAPSE:	tricuspid annular plane systolic excursion
TE:	echo time
TR:	repetition time
TRPG:	tricuspid regurgitation peak gradient
TTP:	time to peak strain
TTP _{first} :	time to first peak
TTP _{max} :	time to maximal peak
TTP _{SD} :	standard deviation of time to peak max of all segments
VTI:	velocity time integral
VV:	interventricular



LIST OF PUBLICATIONS

van Everdingen WM, Maass AH, Vernooy K, Meine M, Allaart CP, De Lange FJ, Teske AJ, Geelhoed B, Rienstra M, Van Gelder IC, Vos MA, Cramer MJ. Comparison of strain parameters in dyssynchronous heart failure between speckle tracking echocardiography vendor systems. *Cardiovasc Ultrasound*. 2017;15(1):25

van Everdingen WM, Zweerink A, Nijveldt R, Salden OAE, Meine M, Maass AH, Vernooy K, De Lange FJ, van Rossum AC, Croisille P, Clarysse P, Geelhoed B, Rienstra M, Van Gelder IC, Vos MA, Allaart CP, Cramer MJ. Comparison of strain imaging techniques in CRT candidates: CMR tagging, CMR feature tracking and speckle tracking echocardiography. *Int J Cardiovasc Imaging*. 2017 Oct 17. [Epub ahead of print]

Walmsley J, **van Everdingen WM**, Cramer MJ, Prinzen FW, Delhaas T, Lumens J. Combining computer modelling and cardiac imaging to understand right ventricular pump function. *Cardiovascular Research*. 2017;113(12):1486-1498.

van Everdingen WM, Walmsley J, Cramer MJ, van Hagen I, De Boeck BWL, Meine M, Delhaas T, Doevendans PA, Prinzen FW, Lumens J, Leenders GE. Echocardiographic Prediction of Cardiac Resynchronization Therapy Response Requires Analysis of Both Mechanical Dyssynchrony and Right Ventricular Function: A Combined Analysis of Patient Data and Computer Simulations. *J Am Soc Echocardiogr*. 2017;30(10):1012-1020.

Stams TRG, Dunnink A, **van Everdingen WM**, Beekman HDM, van der Nagel R, Kok B, Bierhuizen MFA, Cramer MJ, Meine M, Vos MA. Deleterious acute and chronic effects of bradycardic right ventricular apex pacing: consequences for arrhythmic outcome. *Basic Res Cardiol*. 2017;112(4):46.

van Everdingen WM, Lodewijks PCA, van Assen T, Counselling athletes with cardiac arrhythmias and conduction abnormalities based on the AHA/ACC recommendations. *Blog article – BJSM*. 2016 Nov

van Assen T, **van Everdingen WM**, Lodewijks PCA. Counseling athletes with hypertrophic cardiomyopathy; a difficult task for the sports physician. *Blog article – BJSM*. 2016 Oct

van Everdingen WM, Schipper JC, van 't Sant J, Ramdat Misier K, Meine M, Cramer MJ. Echocardiography and cardiac resynchronisation therapy, friends or foes? *Neth Heart J*. 2016;24(1):25-38.

van 't Sant J, Mast TP, Bos MM, Ter Horst IA, **van Everdingen WM**, Meine M, Cramer MJ. Echo response and clinical outcome in CRT patients. *Neth Heart J*. 2016 Jan;24(1):47-55.

van 't Sant J, Fiolet AT, ter Horst IA, Cramer MJ, Mastenbroek MH, **van Everdingen WM**, Mast TP, Doevendans PA, Versteeg H, Meine M. Volumetric Response beyond Six Months of Cardiac Resynchronization Therapy and Clinical Outcome. *PLoS One*. 2015 May 1;10(5)

van Everdingen WM, Cramer MJ, Doevendans PA, Meine M. Quadripolar Leads in Cardiac Resynchronization Therapy. *J Am Coll EP*. 2015:225-237.

van Everdingen WM, van Gelder B, Meine M. Comment on the article by Trolese T et al. *Europace*. 2015;17(6):999.

van Deursen CJ, Wecke L, **van Everdingen WM**, Ståhlberg M, Janssen MH, Braunschweig F, Bergfeldt L, Crijns HJ, Vernooy K, Prinzen FW. Vectorcardiography for optimization of stimulation intervals in cardiac resynchronization therapy. *J Cardiovasc Transl Res*. 2015;8(2):128-37.

van Everdingen WM, Paiman ML, van Deursen CJ, Cramer MJ, Vernooy K, Delhaas T, Prinzen FW. Comparison of septal strain patterns in dyssynchronous heart failure between speckle tracking echocardiography vendor systems. *J Electrocardiol*. 2015;48(4):609-16

DANKWOORD

En dan het deel wat waarschijnlijk de meeste aandacht zal krijgen, het dankwoord. Promoveren doet niemand alleen, daar is een team voor nodig. Een team dat geolied samenwerkt om studies op te zetten, patiënten te includeren, data te analyseren en om papers te schrijven. Dat team heb ik gevonden in het UMC Utrecht, maar ook zeker daar buiten. Dit proefschrift is een voorbeeld van samenwerking tussen vooraanstaande universitair medische centra in Nederland, met vooropstaand de prettige samenwerking met het VU universitair medisch centrum en het Maastrichtse Universitair Medisch Centrum. In de MARC studie hebben we naast het VUMC en het MUMC+, succesvol samengewerkt met het UMCG te Groningen, AMC te Amsterdam en het MST te Enschede. Dat trans-universitaire samenwerkingsverband is ook duidelijk herkenbaar in het duo van promotoren, afkomstig van de universiteiten van Utrecht en Maastricht.

Prof. dr. Prinzen, beste **Frits**, ik noem je als eerste. Mede omdat in chronologisch opzicht jij de eerste bent die me op het promotie-pad heeft gestuurd. In 2012 begon ik met een afstudeeronderzoek bij de afdeling fysiologie van de Universiteit van Maastricht. Ondanks dat er in Maastricht een promotietraject tot de mogelijkheden behoorde, heeft degene die als laatst genoemd wordt ervoor gezorgd dat ik naar midden Nederland verkaste. Dat heeft zeker niet aan jouw laagdrempelige en betrokken houding, open en kritische blik, 24/7 bereikbaarheid, snelle en stimulerende reflecties op manuscripten en gezellige samenwerking gelegen. Daarom ben ik des te verheugd dat je als 2^e promotor alsnog onderdeel bent geworden van mijn promotieteam. Frits, bedankt!

Prof. dr. Doevendans, beste **Pieter**, als professor en afdelingshoofd van de cardiologie van het grote UMCU keek ik in het begin tegen je op. Dat doe ik na 3.5 jaar in het UMC Utrecht nog steeds, maar dan op een heel andere manier. Ondanks dat je rol veelal op de achtergrond was, ben je altijd belangrijk geweest tijdens het proces. De nuchtere periodieke overleggen waren altijd 'to the point'. Een prestatie van formaat om dit voor zo velen promovendi te kunnen zijn. Tussentijds was er ook nog ruimte voor lange tochten op de racefiets (naar Rome in 2016 en naar Barcelona in 2017) met goede gesprekken onderweg en een blikje cola in Orvieto. Het aantal ballen dat jij hoog houdt zou een jongleur doen verbazen. Dank voor de mogelijkheid om te promoveren binnen de cardiologie in het UMC Utrecht. Pieter, bedankt!

Dr. Meine, beste **Mathias**, jij bent een begrip binnen de elektrofysiologie. Jouw encyclopedische kennis van studies op het gebied van cardiale devices, tot aan de meest obscure inclusiecriteria aan toe is fenomenaal. Je herkent praktisch elke lead en device op een X-thorax, kent alle criteria voor het LBTB en voor een Duitser heb je bovendien prachtige humor. Het is dat je elk jaar ouder wordt volgens de kalender, maar bij jou is het geestelijke klokje gestopt na de 30. Dat blijkt uit de continue perfectionering van je ski-jumps, waarbij het achterwaarts skiën op de zwarte piste om je techniek te verbeteren mij met stomheid heeft geslagen. Aan jou valt niet te tippen. Ook niet aan je ondernemingszin, welke er toe heeft geleid dat we binnen de CRT onderzoekswereld twee prachtige studies hebben opgezet. Je hebt me de vrijheid gegeven om het onderzoek op te zetten, maar hield altijd focus, "op die papers". Mathias, bedankt!

Dr. Cramer, beste **Maarten Jan**, jij hebt me op aanraden van Yves America (waarvoor dank!) uit het Rijnstate Ziekenhuis in Arnhem opgepikt om te komen promoveren in Utrecht. Dat begon op z'n zachts gezegd een beetje vreemd, ons eerste overleg was aan een ziekenhuisbed waar je in opgenomen lag. Gelukkig heeft je enorme drive gecompenseerd voor je tijdelijke gebrek aan Hb en ben je wonderwel weer op de been. Jij bent de aanjager van zovele samenwerkingen en onderzoeksideeën. In het begin waren die ideeën soms zo talrijk, dat ik bij moest komen van je woorden-waterval. Zonder jouw tomeloze energie, overvloed aan complimenten, en je kwaliteiten als netwerker en bruggebouwer was ik niet waar ik nu ben. Maarten Jan, bedankt!

De leescommissie, onder aanvoering van **prof. dr. Birgitta Velthuis**, met **prof. dr. Arno Hoes** en **prof dr. Willem Suyker**, dank voor het kritisch beoordelen van mijn proefschrift. De leescommissie wordt verder opgeluisterd door twee biomedische ingenieurs uit Maastricht. **Prof. dr. Tammo Delhaas**, dank voor de constructieve feedback op manuscripten en beoordeling van het proefschrift. **Dr. Joost Lumens**, ook jij dank voor de beoordeling van het proefschrift, dank voor je expertise en het CircAdapt model dat zo mooi aansloot op onze klinische waarnemingen.

Om een bepaalde volgorde aan te houden, eerst de collega's van buiten Utrecht. De belangrijkste was **Alwin Zweerink**, die later aan bod zal komen als paranimf. Zonder je co-promotor, **Cor Allaart**, waren we nooit samen aan het Opticare avontuur begonnen. Cor,

dank voor je hulp bij alle stukken, de de studie metingen, overleggen en gesprekken bij een hapje eten. Zonder jullie was Opticare geen succes geworden. Jullie (inmiddels ex-)collega **Robin Nijveldt** wil ik ook graag de revue laten passeren, mede dankzij zijn ervaring op cardiac imaging zijn er twee mooie papers geschreven. Robin, tot in Nijmegen!

In het MUMC+ heeft het studieteam onder aanvoering van **Kevin Vernooy** voor de broodnodige extra inclusies gezorgd. **Elien Engels en Uyen Chau Nguyen** hebben menig frustratie momentje gehad om de studie ook in Maastricht op te starten. Na twee uur implanteren is een uur toekijken hoe er lusjes gedraaid worden op een computerscherm redelijk eentonig. **Justin Luermans**, dank voor je geduld bij de PV-loop metingen, helemaal wanneer er iets misging met fragiele kabeltjes of als de PV-loop metingen herhaald moesten worden.

Het gehele MARC studie team wil ik bedanken voor de mogelijkheden die ik heb gekregen om mee te werken aan de verzameling en analyse van data en vooral het uitwerken van twee sub-analyses. **Alexander Maass, Frederik de Lange, Marc Vos, Bastiaan Geelhoed, Michiel Rienstra, Isabelle van Gelder**, allen bedankt!

Dan mag ik uiteraard de Fransen niet vergeten die hun tagging software in bruikleen hebben gegeven aan het VU. **Pierre Croisille** et **Patrick Clarysse**, merci! **Arco**, jij mag ook niet ontbreken, als strain-professor heb je je steentje bijgedragen, dank voor je input en de hulp bij het maken, analyseren en interpreteren van die eigenzinnige straincurves.

Mijn co-auteurs op de prachtige papers over de rechterhartkamer wil ook bedanken voor hun samenwerking. **John Walmsley**, dankzij je grondige blik, sterke commentaar in rebuttals en prachtige schrijfstijl hebben we twee mooie papers geschreven. Dankzij **Joost Lumens** z'n model en input en **Tammo Delhaas** z'n scherpe blik zijn beide stukken geperfectioneerd. Iris van Hagen, ook dank je voorbereidende werk. **Geert**, fietsmaatje en kamergenoot op weg naar Barça en Rome, zowel op de fiets als op wetenschappelijk gebied ben je een machine; geen teken van vermoeidheid, altijd scherp en met de juiste cadans op weg. Zowel richting Barcelona als met het RV manuscript wist je de juiste route uit te stippelen en zijn we, met soms een kleine detour, op ons doel afgegaan.

Elektrofysiologen, wat zijn jullie een prettig team om in mee te werken. Een mooie samenstelling van diverse karakters, samenkomend door een enorme gedrevenheid om het werk, de zorg voor het elektrisch zieke hart, te perfectioneren. **Jeroen**, je eerlijkheid en praktische instelling zijn een mooie karaktereigenschap en zal ik proberen te evenaren. **Anton**, kenner van bijna alles (koffie, auto's, zelfrijdende robotballen, Frankrijk en natuurlijk CRT-D's), ik ga de lange gesprekken en je wijsheid missen. Dank voor je hulp bij het vinden, includeren en opereren van studiepatiënten! **Peter**, dank voor je kundigheid tijdens de EFO overdrachten en verhalen tijdens de EFO BBQ's. **Rutger**, dank voor de gesprekken over onze grootste hobby, jammer dat we niet ooit samen een rondje hebben gefietst. Ook dank aan alle andere cardiologen van het UMC voor de soepele samenwerking, en speciaal **Folkert Meijboom** voor de hulp bij het leren interpreteren van de echocardiografie.

Ex-mierennestgenoten, jullie hebben 3.5 jaar promoveren tot een feest gemaakt. De combinatie van allerlei karakters en functies was een genot. Te beginnen met twee fellows, **Nick** en **Jurjan**, die continu met hun rug naar het bureau zaten en onder invloed van vele dharkans® de mooiste humor door de kamer slingerden. Nick, dat jij elektrofysioloog in het UMC bent geworden is meer dan terecht. Jammer dat je van onze kamer wegpromoveerde naar het hoekje bij Peter. Geniet van je hobby's (ableren en fietsen) en van de periodieke del met mayo. Jur, met je plek in Den Haag heb je geen reistijdswinst gekregen, maar wel een eigen plek als cardioloog. Al zou je misschien veel tijd kunnen winnen door je ellenlange telefonische consulten over de bluetooth koptelefoon in de auto naar huis te voeren. Vergeet niet af en toe lekker te zeiken. **Cas**, jou noem ik aan het einde, nog even geduld. De combi van psychologen en artsen in het nest was wellicht preventief bedoeld. **Mirjam**, je hebt vast je mooie gezin vast al verder uitgebreid, een mooie baan gekregen en nog vele Raccoon liedjes meegezongen. **Ivy**, dank voor de vele gezellige gesprekken. Ik heb respect voor je discipline, wie reist er elke keer voor dag en dauw naar het UMC en begint om 7 uur met werken (behalve Mathias)? **Samir**, ook jij mag hier de revue passeren, al verkaste je al snel naar een verdieping hoger. Dank voor de gesprekken over de jacht(honden), de streken van je zootjes en de perikelen op de afdeling. Ook **Moniek** was een aanwinst voor het nest, je paste er zo tussen, je bent een gezellige dame en nu vast hoogzwanger, veel plezier met je grotere gezin. **Erik** hikte er ook nog even tussendoor en vermaakt zich nu in Rotterdam. **Wil**, man van verbouwingen, van katheters en Polen, draaiende op een mengsel van saté en friet, hopelijk komen je artikelen snel online nu je huis af is. Dan nog twee dames die elk hun

eigen draai aan het nest gaven. **Iris** door permanent in rapper-bontjas, verhuuld achter stapels papier, op zeven computerschermen tegelijkertijd te werken. Je wist al snel wat je wilde, dat bewonder ik (kon ik dat zelf maar), en vond je droombaan in Best. **Odetta**, retteketet, spervuur aan geluiden en woorden, je vindt vast en zeker een manier om ze allemaal op papier te krijgen. De laatste (schrijf)maanden zijn door jou een klein feest geworden.

Zonder ondersteuning van het EFO-secretariaat was ik nooit op tijd klaar geweest. **Cornelie, Emely, Linda, Joyce, Veronique, Fenna en Marlies**, jullie enthousiasme, taartmomenten, luisterende oren en geklets is de cement die de EFO bij elkaar houdt. Dank voor al jullie hulp, ik ga jullie missen! Ook **Ingrid** (met het plannen van alle agenda's en ondersteuning bij de jungle die promoveren is), **Sylvia, Tamara en Jantine**, dank voor de hulp.

Alle medewerkers van de HCK, en met nadruk angry **Bert**, dank voor jullie geduld. Door de ellenlange metingen moesten jullie veelal zuchten als ik HCK1 binnen wandelde, maar desalniettemin waren jullie tot na sluitingstijd bereid om je voor het goede doel in te zetten. **Echografisten, Elly, Elly, Ineke en Jeanette**, dank voor jullie geduld bij het leren en maken van echo's. Ook de echografisten van het Rijnstate (vooral **Bob en Maarten**), dank voor het wegwijs maken in de wereld van de echocardiografie.

Device technici, Hans, Rolf, Maaïke, Niels, Casper, dank voor de ondersteuning tijdens de implantaties en follow-up van de studie patiënten.

Heren en dame van St. Jude, of nu Abbott, dank voor de ondersteuning, de medewerking en flexibiliteit. **Rob, Anna** en vooral **Jos** (voorkomen van hypoglycemische coma's met Snelle Jelles): dank!

Arts-onderzoekers, uit het **Q, Stratenum** en de **Villa**, dank voor de borrels, uitjes en weekendjes. **Einar** en **Bas** voor jullie humor op de fiets, broodnodig om 10 uur fietsen te doorstaan, vooral als er ook onderweg gestopt(!) moet worden om te drinken... Laat het dan iets met druivuh zijn. Succes in Oslo! **Lennart**, praktisch m'n buurman in Arnhem, dank voor de lifts naar Utrecht. Generaal **René** en z'n ongezoeten mening en leger technische geneeskunde studenten, **Mira** (en het legendarische filmpje voor Iris), **Thomas** (stiekem net zo kritisch als de tor, vooral op strain, succes met het lopen van de Jan Knippenberg Memorial),

Jetske (dank voor het voorbereidende werk als dakpan en bij de MARC studie), **Peter Paul** (allemandsvriend), **Dirk** (durka-durka, remember Papendal en dan vooral de vrijdagochtend, Rome, en organisator van het legendarische Sofia-weekend), **Wouter G** (mede-radioloog in spé, jouw boekje komt er wel). **Thijs**, aka Hans, dank voor je prachtige (lange) verhalen en ietwat grove, Franse stripjes. **Marloes**, wat een gezellige en eerlijke dame ben jij, dank voor de lol tijdens het promoveren en in bijzonder het ESC in Rome.

Frebus en Paul, mannen van CART-Tech, succes met het uitbouwen van jullie bedrijf en het opzetten van nieuwe studies. Met jullie creativiteit en gedrevenheid zit het wel goed, op naar een product dat wordt gebruikt bij alle CRT implantaties!

Jet, Albert, David en anderen bij de medische fysiologie, dank voor de samenwerking op experimenteel gebied. Het was een leuke uitdaging om te pionieren met echo's bij trouwe viervoeters.

Aan de studenten die ik heb mogen begeleiden: **Sophie, Diana, Karan, Dirk-Jan** en **Saniyé**, dank voor jullie inzet. Al heeft het niet altijd tot publicaties mogen leiden, jullie hebben een hoop werk verzet en voor gezelligheid gezorgd.

Dames en heren van de sportgeneeskunde, **Donna, Karin, Wout, Frank, Gijs, Prabath, Tijmen** en **secretaresses**, dank voor het warme welkom en de mogelijkheid om dit prachtige discipline te beoefenen. Het is niet mijn uiteindelijke keuze geworden, maar dat heeft alles behalve aan jullie gelegen. Wat zijn jullie een fijn team om in te mogen werken!

Bonobo's, vrienden, jullie zijn een heerlijke afleiding naast het werk en naast goede borrelgenoten ook mooie reismaatjes. Ik kijk al maanden uit naar onze volgende bestemming (?) in april, waar we onze trip naar Jordanië gaan overklassen.

Diemse boys, op jullie kan ik bouwen. Al sinds de basisschool (**Mark**) en middelbare school (**Wouter en Ruben**) zijn we maatjes, hopelijk gaan we nog vaak weekendjes samen weg. In de toekomst hopelijk met jullie lieve aanhang, **Felia, Marijke** en **Santi**.

N.F.C., fietsvrienden, dank voor de nodige kilometers op de fiets, weekendjes en vergeet niet de zak aardappels, blikjes, toeters, bloemetjes tijdens mijn bachelor weekend. Hopelijk gaan we hele wat meer colletjes beklimmen nu ik in de regio blijf.

Ook mijn lieve familie wil bedanken, mijn ouders **Wil** en **Laurens**, die me altijd steunen, en me mijn eigen weg laten bewandelen, dank! **Stefan**, **Marieke** en **Meike**, dank voor de gezelligheid. **Stef**, hopelijk hardlopen we nog aardig wat kilometers samen. **Laura** en **Yarl**, onze reisbuddies naar Amerika, fijn om een zus en zwager-in-spé te hebben die zo op één golfengte zitten. Ook mijn schoonouders, **Lilian** en **Toon**, wil ik danken voor hun steun, met goede gesprekken in combinatie met menig herfstbokje. Tenslotte mijn lieve **opa** en **oma**, dank voor de gezellige familiemomenten en voelbare waardering.

Dan op een na laatst, de twee paranimfen. Zoals gezegd is dit boekje tot stand gekomen door een geoliede samenwerking met het VU, mijn promotiebuddy **Alwin Zweerink** heeft met zijn vele 2^e of gedeelde auteursplekken een groot stempel gedrukt op de inhoud. Zonder dat het op voorhand zo bedoeld was hebben we een hoop samen onderzocht. Je nuchtere blik, voorliefde voor crossmotoren, gele racewagens en stampot kan ik waarderen. Naast modder omploegen in de regio Zutphen heb je belachelijk veel geschreven. Jouw boekje gaat waarschijnlijk dikker worden dan deze! En **Cas**, das Körper, het nest heeft niet alleen jou en Marloes samengebracht, maar ook ons kantoorhuwelijk gesmeed. In die 3.5 jaar hebben we menig sportmoment niet ongezien beleefd (de tourcomputer), een hoop congressen en trainingen samen bezocht, en een hoop lol beleefd. Het is niet gek dat zoveel mensen met je weglopen, jij bent een topper (afgezien van je clubliefde). Hopelijk komen we elkaar nog vaak tegen!

En dan tot slot, de meest belangrijke persoon in mijn leven. Lieve **Lianke**, doordat jij er altijd voor mij bent, en je (soms bijna teveel) wegcijfert, heb ik dit promotietraject kunnen afronden. Al heb je geen letter op papier gezet, dit boekje heb jij ook voor elkaar gebokst. Als mijn levenspartner sta je altijd voor me klaar, tijdens de dalen en tijdens hoogtepunten. Met als grootste hoogtepunt ons huwelijk, een dag die alles was wat we ervan voorgesteld hadden en misschien wel meer. Laat dat een mooie voorbode zijn voor de rest van ons leven!

CURRICULUM VITAE

Wouter Maria van Everdingen was born May 9th 1987 in the hospital of Zevenaar. As the middle of three children, he was raised by his father Laurens and mother Wil in Didam. After graduation from high school he moved to Enschede to study Technical Medicine at the University of Twente. With a bachelor degree in his pocket he moved to Maastricht. There he studied the 'AKO-master' and became a medical doctor and clinical scientist. In the final year of the master a research project at the department of physiology of prof. Prinzen sparked the ambition to start a PhD. In between studying he met his future wife Lianke Opdam, who convinced him to move to Arnhem first. A year as resident for the department of cardiology in the Rijnstate hospital in Arnhem followed. During this year he was offered the opportunity to start a PhD at the UMC Utrecht. This book is the result of four years work at the department of cardiology, with a sidestep as resident sports medicine. In between research he found time to cycle, but most of all to marry in June 2016. Together with his wife he lives in Arnhem. He will start training to become a radiologist in the Radboud UMC in Nijmegen in February 2018.

